RUHR-UNIVERSITÄT BOCHUM

Wolfgang Lieske

Impact of polymer constitution on the hydro-mechanical behaviour of modified bentonite for the application in geotechnical and geoenvironmental engineering

Bochum 2022

Heft 72

Schriftenreihe des Lehrstuhls für
Bodenmechanik, Grundbau und Umweltgeotechnik

Herausgeber: Torsten Wichtmann

ISSN 2699-1020

Wolfgang Lieske Impact of polymer constitution on modified bentonite

72

ISSN 2699-1020

Ruhr-Universität Bochum
Schriftenreihe Bodenmechanik, Grundbau und Umweltgeotechnik
Heft 72

Herausgeber:
Prof. Dr.-Ing. habil. Torsten Wichtmann
Ruhr-Universität Bochum
Fakultät für Bau- und Umweltingenieurwissenschaften
Lehrstuhl für Bodenmechanik, Grundbau und Umweltgeotechnik
44801 Bochum
Telefon: 0234/ 3226135
Telefax: 0234/ 3214236
Internet: www.bgu.ruhr-uni-bochum.de

ISSN 2699-1020

Impact of polymer constitution on the hydro-mechanical behaviour of modified bentonite for the application in geotechnical and geoenvironmental engineering

Dissertation

as a requirement for the degree of
Doktor-Ingenieur (Dr.-Ing.)

at the Faculty of
Civil and Environmental Engineering
Ruhr-Universität Bochum

by
Wolfgang Lieske, M.Sc.

Reviewers
Prof. Dr.-Ing. habil. Torsten Wichtmann
Prof. Dr.-Ing. habil. Achim Hettler
Prof. Dr. ir. Gemmina Di Emidio

Preface of the editor

The improvement of the properties of bentonite by the addition of water-soluble polymers becomes increasingly popular in geotechnical and geoenvironmental engineering. However, the large variety of available polymers impedes the choice of a suitable polymer for a certain application, considering that the knowledge on the effect of certain polymer properties on the behaviour of the polymer-modified bentonite is limited.

In his dissertation Wolfgang Lieske has systematically investigated, analysed and described the influence of the charge and molecular weight of the polymers as well as the mixing and post-mixing treatment methods on various properties (plasticity, compressibility, soil water retention, swelling pressure, permeability) of the modified bentonite. Cationic, non-ionic and anionic polymers were tested with different molecular weights and charge densities. The unusual appearance and behaviour of the polymer-bentonite mixtures necessitated the development of special testing devices, the modification of established testing procedures and for some types of polymers the application of post-treatment procedures like drying and grinding to obtain a soil-like material. Based on investigations of the microstructure and theoretical considerations regarding the complex interaction between the polymer chains and the clay particles or aggregates the macromechanically observed behaviour of the polymer-modified bentonite could be linked to micromechanics.

The research work of Wolfgang Lieske has significantly enhanced the knowledge on the influence of the polymer properties on the behaviour of polymer-modified bentonite. The large influence of the mixing procedure and post-mixing treatment found in this study is of particular importance for practical applications. The results of the experimental study will form the basis for the development of recommendations regarding the appropriate choice of polymers for certain geotechnical and geoenvironmental applications. Furthermore, future research regarding a quick classification of polymers for such applications, the influence of the polymer concentration in the mixture and the durability of the polymers in long-term applications can perfectly base upon the findings of the current study.

This research has been done in the framework of the project SCHA 675/21-1 “Multiscale investigations on the structure and hydro-mechanical properties of clay-polymer composites”. The funding of German Research Council (DFG) is gratefully acknowledged.

Torsten Wichtmann

Vorwort des Verfassers

Die vorliegende Arbeit entstand während meiner Tätigkeit als wissenschaftlicher Mitarbeiter am Lehrstuhl für Grundbau, Boden- und Felsmechanik und Leitung von Herrn Prof. Dr.-Ing. habil. Tom Schanz und ab dem Jahr 2019 am Lehrstuhl für Bodenmechanik, Grundbau und Umweltgeotechnik unter Leitung von Prof. Dr.-Ing. habil. Torsten Wichtmann.

Mein besonderer Dank gilt dabei den beiden Lehrstuhlinhabern, unter deren Anleitung diese Arbeit angefertigt wurde. Prof. Schanz hat durch seine breite fachliche Expertise, seinen Enthusiasmus und seine inspirierende Art meine Begeisterung für die Forschung und insbesondere für die Bodenmechanik geweckt. Die Jahre unter seiner Leitung waren prägend für meine berufliche und persönliche Entwicklung, nicht zuletzt wegen der vielen intensiven Gespräche und Möglichkeiten, die er mir durch sein persönliches Engagement eröffnete. Sein plötzlicher und viel zu früher Tod ist ein großer Verlust, der mich noch immer bewegt. Mein Dank gilt Prof. Torsten Wichtmann, der als neuer Lehrstuhlinhaber bereitwillig meine Betreuung übernommen hat. Seine Geduld, sein Interesse und sein Vertrauen in meine Arbeit haben es erst möglich gemacht, meine Dissertation erfolgreich abzuschließen. Seine offene und allseits interessierte Art ermöglichten es, dass die im Rahmen meiner Arbeit entwickelten Ideen am Lehrstuhl fortgeführt werden können.

Ich danke Herrn Prof. Dr.-Ing. habil. Marc Wichern für die Übernahme des Vorsitzes und Prof. Dr.-Ing. habil. Achim Hettler für die Übernahme des Koreferats. Die Anmerkungen zur Arbeit und der intensive Austausch mit Prof. Hettler waren lehrreich und nicht nur aus bodenmechanischer Sicht interessant.

Special thanks go to Dr. ir. Gemmina Di Emidio for acting as a reviewer for my thesis and for her support over the past years, which goes far beyond that. Her motivating personality, her generous support, and her competence in the field of polymer modification had a decisive influence on my work. The extensive exchange during a research stay and numerous discussions gave me vital input for my work.

Bedanken möchte ich mich bei den Postdocs des Lehrstuhls, insbesondere bei Dr.-Ing. Wiebke Baille und Dr.-Ing. Diethard König, deren Türen für mich immer offenstanden. Sie haben mir inbesondere in der schwierigen Zeit nach dem Tod von Prof. Schanz durch ihr Engagement und ihre Expertise geholfen meine Forschung erfolgreich fortzuführen und mich in außergewöhnlicher Weise unterstützt.

Die Arbeit wurde von der Deutschen Forschungsgemeinschaft (DFG) als Verbundprojekt in Zusammenarbeit mit dem Kompetenzzentrum für Materialfeuchte am Karlsruher Institut für Technologie gefördert. An dieser Stelle möchte ich mich bei Frau Dr. Hanna Viefhaus für die Initiierung des Projekts und die entscheidenden Vorarbeiten sowie bei Frau apl. Prof. Dr. Katja Emmerich, Frau Dr. Annett Steudel und Herrn Dr. Frank Friedrich für die fruchtbare Zusammenarbeit und die lehrreiche Unterstützung auf dem Gebiet der Ton-Mineralogie bedanken.

Die vorliegende Dissertation basiert auf einem umfangreichen experimentellen Programm. Die Durchführung war nur möglich durch die tatkräftige Mitwirkung der Labormitarbeiter Herr Skubisch und Herr Müller sowie der Studentinnen Kristin Ader, Anika Erkes, Joanna Herrmann und Alischa Albared, denen ich für ihre Arbeit danken möchte.

Unter Berücksichtigung der Zeit als studentische Hilfskraft war ich fast 10 Jahre lang mit dem Lehrstuhl verbunden, in denen mich viele Kollegen begleitet haben. Dank Euch wird diese Zeit für mich immer unvergesslich bleiben. Zahlreiche Diskussionen, Mittagessen und Betriebsausflüge machten die Zeit sowohl fachlich als auch zwischenmenschlich zu einem besonderen Abschnitt meines Lebens, der mich fachlich, aber auch persönlich geprägt hat.

Zu guter letzter gilt mein größter Dank meiner Frau Svenja und unseren drei Töchtern Paula, Jule und Ylvie, die mich in unbeschreiblicher Weise unterstützt haben. Für die Geduld, den Verzicht und die zahlreichen Ermunterungen danke ich Euch von Herzen.

Wolfgang Lieske

Abstract

Water-soluble polymers are of growing importance in the field of geotechnical engineering. These types of polymers are used to generate suctions in the field of experimental unsaturated soil mechanics, to replace or improve the properties of bentonite in supporting fluids, and to modify clay for use in barriers, to name just a few applications. The polymer modification of clay is based on various mechanisms that differ significantly depending on the nature of the polymer. To date, there is a lack of detailed knowledge about the relationship between the properties of the polymer used, the expected effects of the polymer and the resulting hydro-mechanical behaviour of a modified clay, which is why the modification of clay is primarily carried out empirically.

The present work addresses the influence of polymer properties on the hydro-mechanical behaviour of modified bentonite. This issue was addressed based on an analysis of the physico-chemical properties of the two raw materials, polymer and bentonite, before starting the experimental investigation of mixtures. Basic concepts of polymer chemistry were applied to geotechnical and soil mechanical applications, such as the penetration of viscous fluids into granular media and the relationship between polymer concentration, molecular weight, and osmotic pressure.

In the experimental programme, a natural sodium bentonite (MX80) was modified by wet mixing with polyacrylamides of different charge properties and molecular weights. The material was examined both directly after mixing and after an subsequent drying and grinding process in order to investigate the influence of such treatment. The experimental investigations include the determination of adsorption isotherms, plasticity properties, one-dimensional compression behaviour and water retention properties. The experimental results were complemented by investigation of the microfabric. The results were discussed in terms of the influence of polymer properties on the surface properties of the modified clay and the effect of bridging by polymers.

Anionic polymers were investigated in an experimental programme adapted to these polymers. The swelling pressure of different dry blended polymer-bentonite mixtures was determined in a permeability cell developed as part of the work, followed by permeability tests with deionised water and a 0.05 mol/l $CaCl_2$ solution. The increase in swelling pressure and decrease in permeability observed during the experiments after addition of polymers were discussed using a conceptual model in which the polymer is present as concentrated polymer spots embedded in macropores of the clay matrix.

Kurzfassung

Wasserlösliche Polymere sind auf dem Gebiet der Geotechnik von wachsender Bedeutung. Diese Art von Polymeren werden zur Erzeugung von Saugspannungen im Bereich der experimentellen teilgesättigten Bodenmechanik, als Ersatz oder zur Verbesserung der Eigenschaften von Bentonit in Stützflüssigkeiten und zur Modifizierung von Ton für den Einsatz in Abdichtungen verwendet, um nur einige Anwendungen zu nennen. Die Modifikation von Ton mittels Polymeren basiert dabei auf verschiedenen Mechanismen, die sich nach Beschaffenheit des Polymers deutlich unterscheiden. Bisher fehlt es an detaillierten Kenntnissen über die Beziehung zwischen den Eigenschaften des verwendeten Polymers, den zu erwartenden Effekten des Polymers und den daraus resultierenden hydro-mechanischen Verhalten eines modifizierten Tons, weshalb die Modifikation von Ton meist empirisch erfolgt.

Die vorliegende Arbeit befasst sich mit dem Einfluss von Polymereigenschaften auf das hydro-mechanische Verhalten von modifiziertem Bentonit. Diese Frage wurde basierend auf einer Analyse der physikalisch-chemischen Eigenschaften der beiden Ausgangsmaterialien und einer experimentellen Untersuchung von unterschiedlichen Mischungen behandelt. Grundlegende Konzepte der Polymerchemie wurden auf geotechnische und bodenmechanische Probleme übertragen, wie z.B. das Eindringen viskoser Flüssigkeiten in granulare Medien und die Beziehung zwischen Polymerkonzentration, Molekulargewicht und osmotischem Druck.

Im experimentellen Programm wurde ein natürlicher Natrium Bentonit (MX80) durch Nassmischung mit Polyacrylamiden unterschiedlicher Ladungseigenschaften und Molekülgewichten modifiziert. Das Material wurde teilweise direkt nach dem Mischen und teilweise nach einem anschließenden Trocknen und Mahlen untersucht, um den Einfluss einer derartigen Aufbereitung zu untersuchen. Die experimentellen Untersuchungen umfassen die Bestimmung der Adsorptionsisothermen, der Plastizitätseigenschaften, des eindimensionalen Kompressionsverhaltens und der Wasserretentionseigenschaften. Die experimentellen Ergebnisse wurden durch Untersuchung der Mikrostruktur ergänzt. Die Ergebnisse wurden im Hinblick auf den Einfluss der Polymereigenschaften auf die Oberflächeneigenschaften des modifizierten Tons und den Effekt von Polymerbrücken diskutiert.

Anionische Polymere wurden in einem auf diese Polymere angepasstem experimentellen Programm untersucht. In einer im Rahmen der Arbeit entwickelte Permeabilitätszelle wurde der Quelldruck verschiedener trocken gemischter Polymer-Bentonit Gemische bes-

timmt, gefolgt von Durchlässigkeitsversuchen mit deionisierten Wasser und einer 0.05 mol/l $CaCl_2$ Lösung. Der im Rahmen der Versuche beobachtete Anstieg des Quelldrucks und die Abnahme der Permeabilität nach Zugabe von Polymeren wurden anhand eines konzeptionellen Modells erörtert, in dem das Polymer als konzentrierter Polymerspots vorliegt, die in Makroporen der Tonmatrix eingebettet sind.

Contents

List of Figures

List of Tables

1 Introduction

1.1 Background

The term polymer describes long-chained macromolecules composed of several repeat units. From this general definition, the term polymer includes a broad field of natural molecules such as the human DNA, plant fibres, bacterial as well as a huge variation of synthetic products which are omnipresent in the natural and man-made environment (Israelachvili, 2015).

Polymers can be found in numerous geotechnical and geoenvironmental applications. Solid polymers such as plastics are used in their various forms often with a long tradition and broad experience in use. They are utilized as part of technical products, for instance as distance pieces, covers and sealing tapes. Geotextiles and geomembranes, manufactured from polymeric raw materials, are used in reinforcement and sealing applications, often found with a better life cycle assessment than conventional methods for ground improvement (Heerten, 2012). Shredded waste tires are used as a recycling material to improve retention behaviour and other soil properties (Edil, 2007).

In the last decades, water-soluble polymers have been used to produce highly viscous liquids to modify pore fluids or to modify the surface properties of soil solids. This type of polymer is fundamentally different from polymers in the form of plastics, which are not discussed further in this thesis.

Water-soluble polymers were introduced to replace bentonite or to improve its performance, e.g. in support fluids (Lam et al., 2015), to modify bentonites for the use in clay-based barriers (Schanz et al., 2004; Di Emidio et al., 2017) and as conditioners in mechanised tunnelling (Zumsteg et al., 2013, 2014), to name a few. In addition, several innovations can be found in the literature such as the use of polymers as binders, often motivated by the demand for a sustainable and environmentally friendly (i.e. renewable and lower CO_2 footprint) alternative to cement-based stabilisation agents (Muguda et al., 2017). Additionally, the use of polymers to control suction in the field of unsaturated soil

testing needs to be mentioned (Delage et al., 1998; Tripathy et al., 2011; Lieske et al., 2020 (a.)).

However, most of the geotechnical applications using water-soluble polymers are based on the adaption of techniques previously used in other disciplines. For example, the use of polymers to apply suction has long been known in the context of biology (Lagerwerff et al., 1961; Zur, 1966). Polymer solutions to replace bentonite suspensions have been used to enhance oil recovery since the 1960s (Sorbie, 1991), and the modification of clay by polymers has been the subject of intensive research in colloid chemistry and mineralogy for years (Theng, 2012). The term colloid describes particles whose behaviour is widely dictated by surface forces rather than gravity due to their small size. Although there is a certain experience in utilising water-soluble polymers, the direct transfer of previous results obtained in other scientific disciplines into geotechnical and geoenvironmental research and application is challenging.

The relevant scales of investigation are not consistent for the different research disciplines and therefore the transferability of results is limited. In colloid chemistry, for example, the modification of smectite surfaces and the intercalation behaviour of polymers in the interlayers of smectite particles have been intensively investigated (Theng, 2012). However, this does not allow for conclusions to be drawn with respect to the hydro-mechanical behaviour of modified bentonites as effects of structure at a larger scale need to be taken into account in addition to interactions at colloid level. For soil-mechanical applications, a much more integral investigation of materials becomes necessary. In addition, studies in colloid science mainly deal with highly diluted polymer solutions, and such conditions are of little practical relevance in geotechnical engineering. It is widely accepted that there are significant differences in the interaction of diluted, semi-diluted and concentrated polymer solutions with charged solids such as smectite minerals (Fleer et al., 1988).

A further crucial challenge is posed by the polymers themselves. Polymers are available in a very wide range of properties. While technically relevant properties of insoluble solid polymer materials (e.g. plastics) can be adequately described by common mechanical properties like strength and stiffness, such parameters are less relevant to describe a polymer in solution and to capture its relevant properties for the polymer-clay interaction. In the field of colloid science, linear polymers are therefore often categorised regarding ionic charge (positive, negative, neutral), polarity (polar, non-polar), and molar mass, whereas the latter equates to the length of the particular polymer chains for a linear polymer (Ward, 1981; Theng, 2012).

Figure 1.1 gives insight into the huge bandwidth of polymeric properties encountered in geotechnical and geoenvironmental studies. Here, τ represents the global charge of the polymer and M the molecular weight. The lower limit of the molecular weight is the transition to oligomers, molecules which in principle also consist of repeat units. However, due to their significantly fewer number of repeat units oligomers in solution show properties more close to an ideal solution. The blue markers represent polymers used for the control of suction in unsaturated soil mechanics testing (Lieske et al., 2020 (a.)).

The green markers show the properties of polymers used for the modification of cohesive soils. The data set shows the significant variation in polymer properties, but these have not

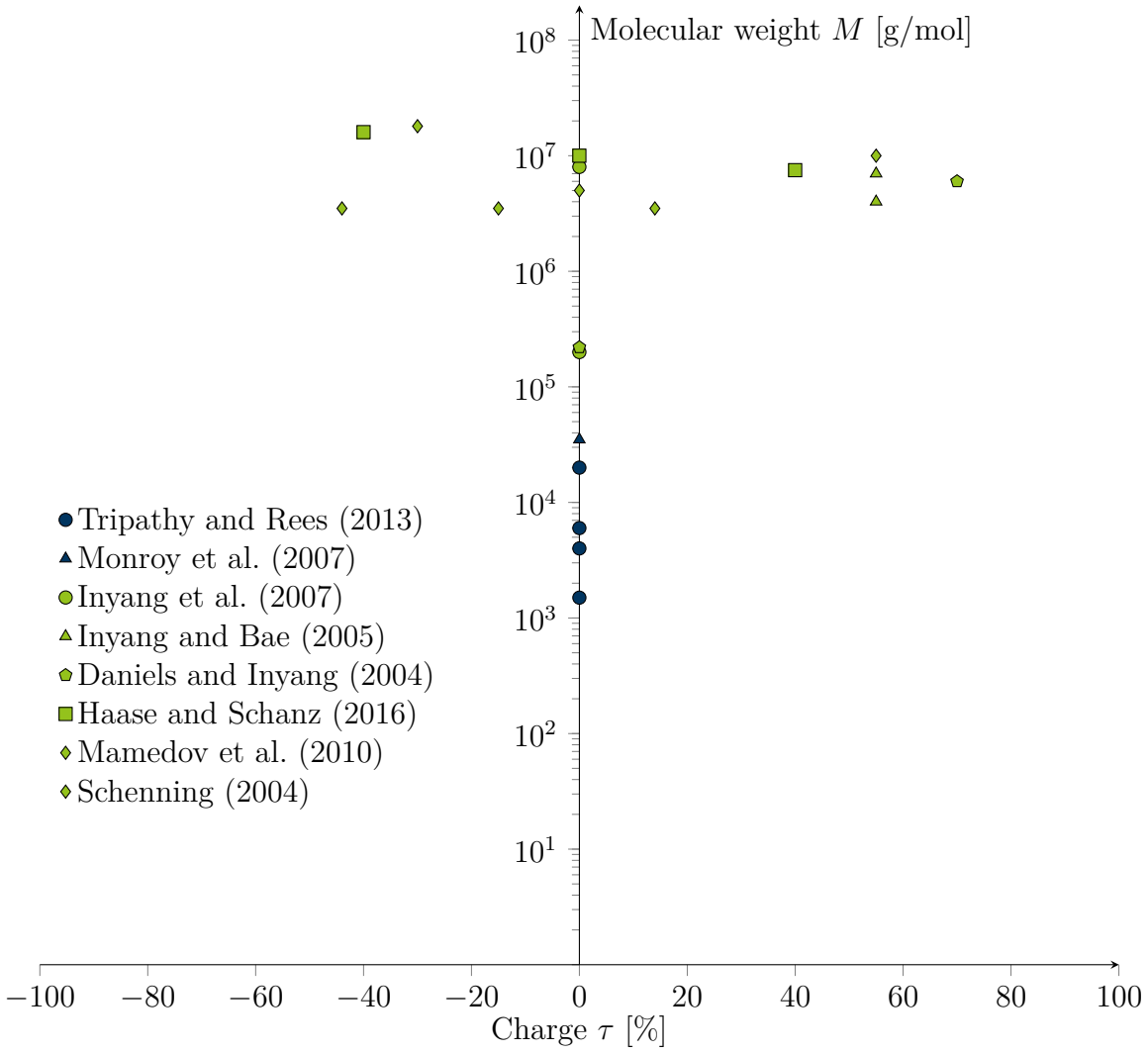

Figure 1.1: Molecular weight and charge properties of polymers used in some recent studies on polymer modification

been explicitly associated with differences in the behaviour of the modified soil. Although the diagram has been heavily simplified, i.e. monomer characteristics and polarity have not been taken into account, the wide range of polymers used becomes obvious. Based on the current state of research there is no clear and systematic basis for a classification of suitable polymers for geotechnical and geoenvironmental applications. Instead, their suitability for a given task is tested by 'trial and error'. Although some significant progress has been made in this way, the predicition of the effect of different polymers on the soil behaviour is still a challenge.

These difficulties for a well-directed application of polymers in geotechnical engineering are mainly caused by the great variety of possible polymers, the missing understanding of their behaviour and the effects of boundary conditions in the various geotechnical applications on the polymer-clay interaction. These problems so far limit the systematic use of polymers as a versatile additive in geotechnics.

1.2 Objectives

The general objective of the current study is to investigate the impact of different polymer characteristics on the hydro-mechanical behaviour of modified bentonite. In this sense, the present work follows the work of Haase (2017), who used a cationic, a non-ionic and an anionic polymer (polyacrylamide) to modify different clays, namely a natural calcium (Calcigel) and sodium/calcium (MX80) bentonite as well as a natural kaolin (Spergau kaolin). The polymer-clay-interaction was studied on different scales by experiments regarding the adsorption behaviour and the hydro-mechanical behaviour, as well as by microstructural investigations. The focus of this work was set on the effect of overall polymer charge (cationic, anionic, noionic) on the different clay types.

In contrast to Haase (2017), this work is dedicated to different polymer properties and how these properties relate to the hydro-mechanical behaviour of a modified bentonite and the mixing and modification process. Emphasis of the work is directed more towards the polymer and therefore basic aspects of polymer chemistry will be addressed in detail. Synthetic polyacrylamides were chosen as this family of polymers is available in a wide range of properties. The polymers used for the modification of the clay are of different charge, charge density and molecular weight. The clay used is a natural bentonite with high smectite content (MX80). This type of clay has been used due to its great importance in geotechnical engineering and especially in geoenvironmental engineering.

The objectives of the study that arise from this are as follows:

- Outline fundamental characteristics of polymers in solution
- Study the impact of polymer characterisics on the behaviour of polymers in solution
- Study the impact of polymer characteristics on the interaction with charged bentonite surfaces on the microscale
- Experimentally investigate the hydro-mechanical behaviour of modified bentonite with special focus on the impact of polymer characteristics on the macroscale
- Interpretation of the results with focus on the influence of the polymer constitution on the behaviour of the modified clay

1.3 Layout of the thesis

The first part of the thesis is dedicated to the theoretical background of linear polymers, clays and polymer-enhanced soils. The basic terminology for the description of polymers is given and the basic properties of flexible linear polymers in solution are presented. The aim is to establish a relationship between the polymer properties and the behaviour of polymer solutions. This is vital to identify the importance of polymer properties on mixing conditions as well as polymer-clay interaction and, thus, to correctly interpret the observations made on the macroscale. Doing so, typical properties of polymer solutions (e.g. viscosity and osmotic pressure) will be investigated and the influence of the polymer constitution on these properties will be shown by means of applications in soil mechanics. This part is followed by an introduction to clay mineralogy, clay fabric and bentonite. Basic properties of bentonite and its sensitivity to environmental conditions are discussed as it is often the motivation for polymer modification. This part which also deals with microfabric, mineral characteristics and polymer-clay interaction will give insight into the different levels of polymer-modification i.e., surface modification, intercalation, bridging and pore fluid alteration.

The second part of the thesis deals with the experimental investigations of the materials, the results and their interpretation. At first, all the materials used are described and characterised. Subsequently, the experimental techniques used are explained in detail. Since the differently charged polymers are relatively specific in their polymer-clay interactions, these are each examined in separate chapters. A short introduction is given at the beginning of each chapter, followed by the experimental results and the interpretations

of findings. The experimental investigations are always adapted to the corresponding polymers. The chapters conclude with a summary of the results and their relevance. An overall summary is provided at the end of the thesis, which also takes a look at open questions and the resulting follow-up investigations.

2 Basic properties of flexible linear chain polymers in solution

2.1 General

Knowledge of the specific properties of polymers in solution is crucial for a deeper insight into the complex mechanisms of polymer-clay interaction, especially with respect to the sensitivity of this interaction to mixing conditions and the influence of polymer properties on the hydro-mechanical behaviour of modified soils. A concise discussion of relevant aspects will therefore be given in this chapter with focus on linear polymers, which are the primary subject of this work. The general term "polymer" as used in this chapter will therefore refer to "linear polymers", i.e. properties related to polymers in the following sections will specifically address linear polymer chains, not the entire category of water-soluble polymers.

The first step is to introduce the basic structure of linear polymers and their volumetric behaviour under varying boundary conditions. Subsequently, some widely used polymers are presented with respect to their geotechnical relevance and their use beyond geotechnical engineering. The second part of this chapter deals with two properties of polymer solutions (osmotic pressure, viscosity), which differ significantly from those of typical ideal solutions and Newtonian fluids (such as water). Relevant properties of selected polymers important for geotechnical applications are discussed in the context of polymer chemistry, classical soil mechanics and selected macroscopic observations. The content of the chapter 'Osmotic pressure in polymer solutions' has already been published by the author and reference is made to the respective paper (Lieske et al., 2020 (a.)).

2.2 Polymers and their behaviour in solution

2.2.1 Architecture and flexibility of polymers

Polymer is a general term for macromolecules consisting of several repeat units. In their non-connected state, these repeating units are called monomers. A pearl necklace as shown in Figure 2.1 can illustrate the simple case of a linear polymer chain. Each bead represents a repeat unit which is of the same type in case of homopolymers, or a combination of different types of repeat units in case of copolymers. Monomers which are not linked to a polymer are low molecular weight molecules. Since the monomers may undergo some chemical modifications during polymer formation, the repeating units may not be the same as the monomer. The nature and chemical character of the repeating units can be found in huge variations and also the synthesis of polymers is possible in a variety of arrangements according to technical possibilities.

Figure 2.2 shows a segment of a polyacrylamide polymer chain. The polymer backbone (main chain) is composed of carbon molecules (gray) linked by covalent bonds (shared electrons). Along the side of the polymer main chain molecules are located that are called functional groups. In case of a polyacrylamide homopolymer the functional group is composed of a carbon-ion and one oxigen (red) and a primary amino group (nitrogen =

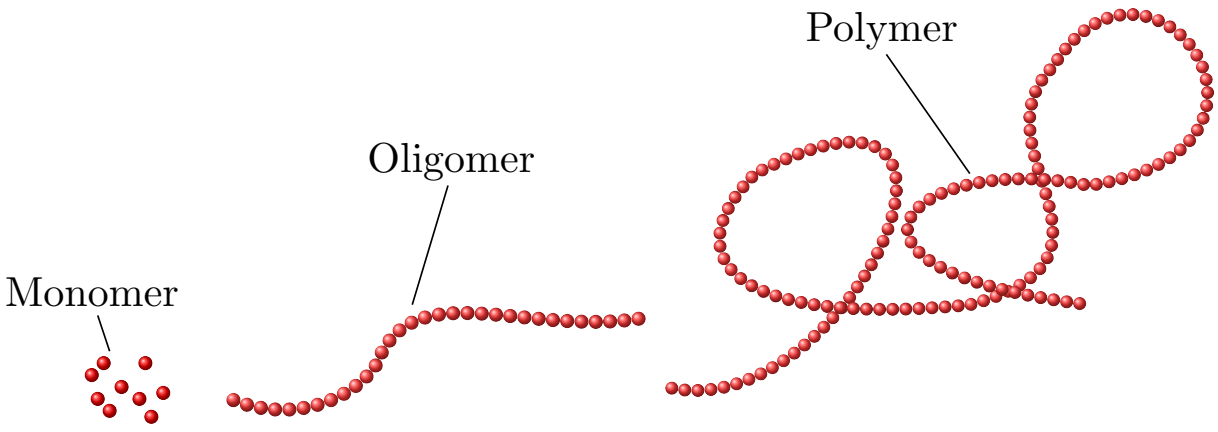

Figure 2.1: Schematic representation of a single monomer, an unbranched oligomer and a linear polymer

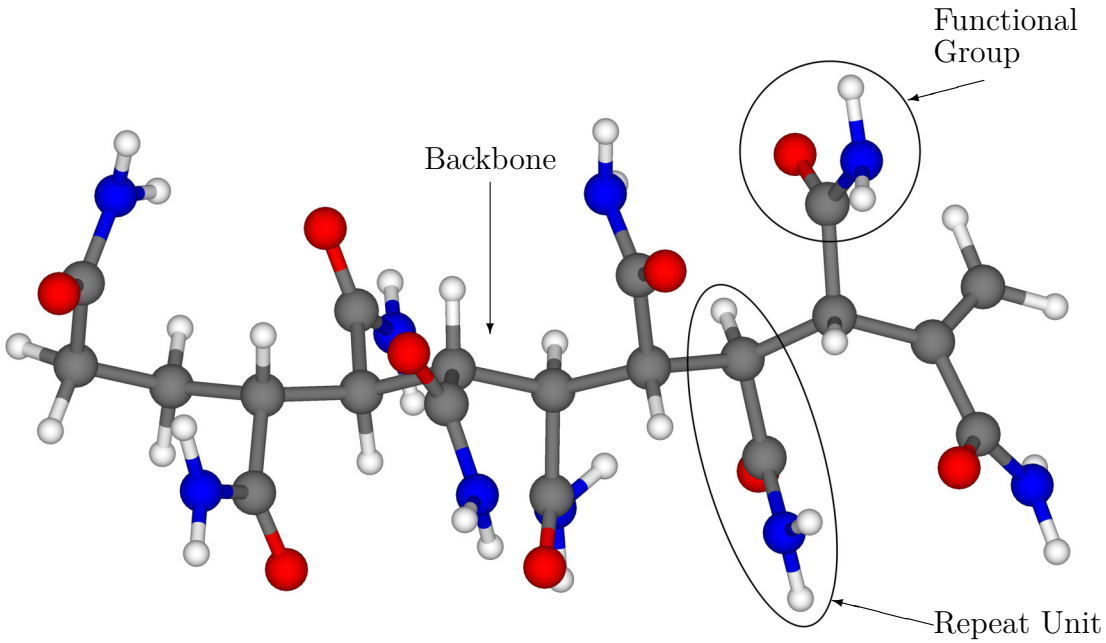

Figure 2.2: Segment of a polyacrylamid polymer chain

blue, hydrogen = white). Depending on the nature of the repeating units these functional groups can have different size and complexity.

Polymer chains commonly feature flexibility when dissolved in an appropriate solvent. Flexibility is a key feature of these types of polymers, as it controls not only the interaction between two neighbor molecules but also an intreraction between different parts of a polymer chain. However, flexibility depends upon the chemical boundary conditions and the architecture of the polymer. For the sake of completeness, rigid rod-like polymers should also be mentioned here, which form another non-flexible class of polymers. However, since water soluble unbranched flexible polymers (i.e. polar linear polymer chains) are most commonly used to modify mineral surfaces (Theng, 2012), the rod-like polymers will not be considered in the following.

Flexibility also gives rise to the marked difference in behaviour between polymer solutions and ideal solutions. Contrary to molecules such as dissolved salts and oligomers, flexible polymers in solution change their shape to adopt an energy-optimal state depending on the boundary conditions. Oligomers, which are also a sequence of monomers, do not show the typical properties of polymers in solution due to their short chains and the resulting missing ability to adopt different conformations. In contrast to the very long polymer chains, intramolecular interaction is relatively low compared to intermolecular interaction. Oligomers in solution therefore show properties closer to ideal solutions.

An adjustment of morphology of some isolated polymers in solution as a consequence of a change in pH value is demonstrated in Figure 2.3 (Szilagyi et al., 2014). The photographs taken with an atomic-force microscope show the sensitivity of the polymer (poly-2-vinylpyridine) to changes in the pH value of the solvent. While the polymer chain is strongly unwound at a pH value of 3.89, the slight increase to a pH value of 4.24 leads to an extreme coiled morphology of the polymer chain. This change in shape of a polymer is accompanied by a significant alteration of properties such as osmotic pressure, viscosity, and adsorption characteristics which are relevant for engineering applications (Israelachvili, 2015).

Polymers can be found in a solid state (amorphous or crystalline), in a gel-like, highly viscous liquid form or as a diluted solution (Teraoka, 2002; Israelachvili, 2015). Depending

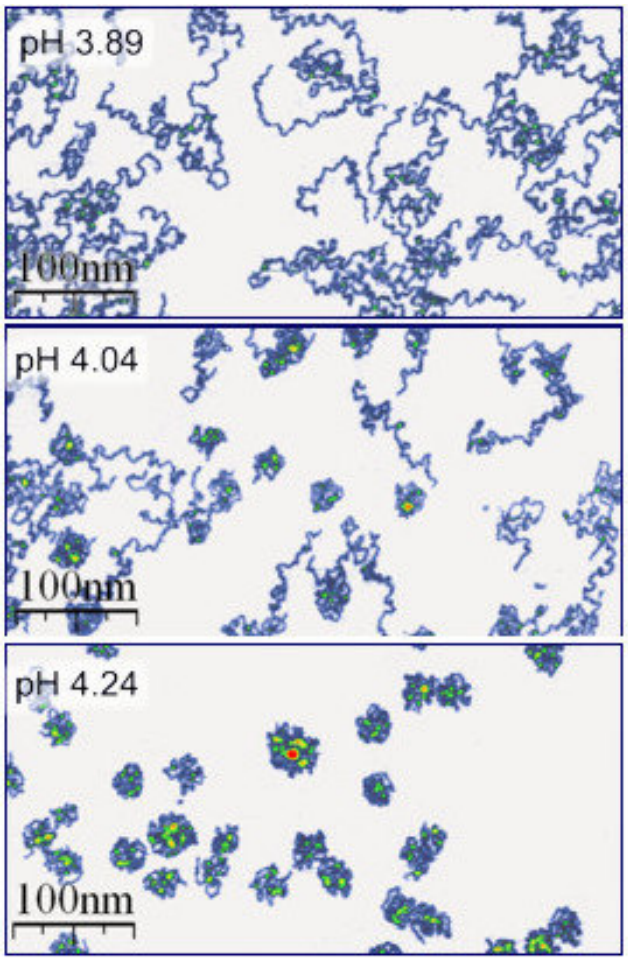

Figure 2.3: Poly(2-vinylpyridine)-molecules analysed using an atomic force microscope (AFM) (Roiter and Minko, 2005)

on the number of molecules per volume of a solvent, the governing interactions between individual polymers and within a polymer chain can strongly differ. Likewise, these interactions within and between polymer chains are affected by boundary conditions such as pH value, temperature, dissolved ions, to name a few (Fleer et al., 1988; Szilagyi et al., 2014; Israelachvili, 2015). However, the extent to which this depends on boundary conditions is strongly influenced by the chemical nature of the polymer.

The flexibility of the polymer chain also gives rise to a variable volume occupied by the single polymer. In polymer chemistry, flexible polymers are commonly described as random coils with a variable coil size. The radius of gyration (R_g) is a measure for the dimensions of a single polymer molecule or polymer coil in an ideal solution, also termed as theta solvent, where there are no interactions between the polymer segments and the solvent. However, in real solutions there might be interactions between solvent and polymer causing the polymer to expand or shrink. Figure 2.4 shows the relation between solvent quality and respective volume occupied by a single polymer chain. The radius of gyration for a theta solvent is proportional to the number of monomers (n) with the exponent 0.5. By contrast, in good and poor solvents attractive or repulsive forces cause the coils to arrange in a denser (globule) or more uncoiled (expanded coil) state (Israelachvili, 2015). The radius of the polymer chain in a poor solvent (R) scales with the exponent 0.33, while the radius in a good solvent (also called a Flory solvent)(R_F) scales with the exponent 0.6.

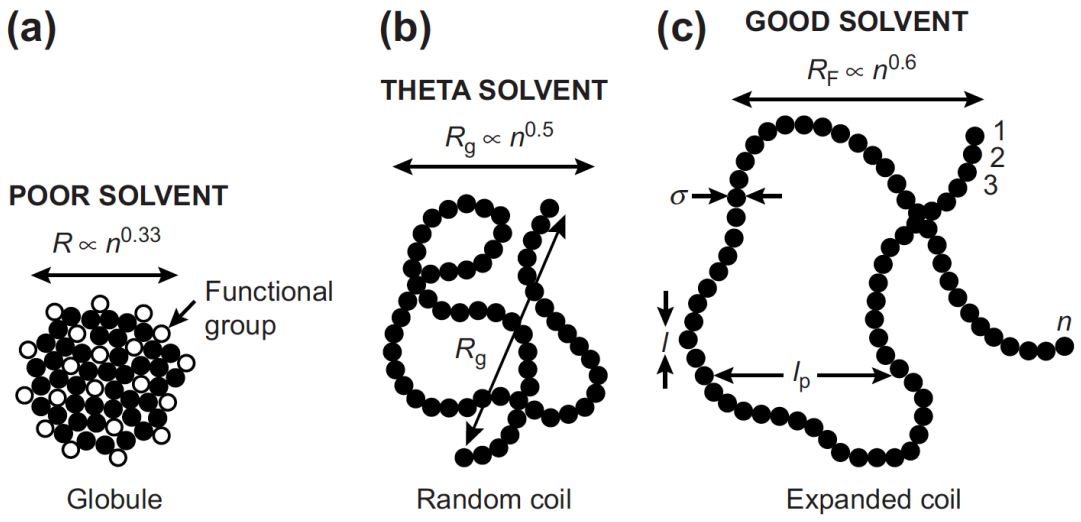

Figure 2.4: Different states of polymers chains in solution: polymer in (a.) poor solvent (b.), theta solvent, (c.) good solvent (Israelachvili, 2015)

2.2.2 Classification of polymers

Polymer chains can interact with charged and non-charged mineral surfaces and some types of polymers are even able to intercalate into the interlayer of clay minerals. Polymers, which were not bound in the soil matrix can move along an osmotic or hydraulic gradient by advective or diffusive flux within the porous environment of a soil structure (Tripathy et al., 2011; Scalia et al., 2014; Verst et al., 2022). However, since the flexible polymer chains will alter their morphology depending on the boundary conditions, the mobility of polymers in a porous soil structure depend on the type of polymer, the chemical environment and the mineralogical composition of the respective soil (Chauveteau et al., 1984).

In order to understand and compare experimental results obtained from tests conducted with polymers in the field of geotechnical engineering, a certain classification of the polymers is necessary. Typically the grain size distribution, the Atterberg limits and the minimum and maximum void ratio are used in soil mechanics to characterize fine-grained and non-cohesive soils, respectively (Mitchell et al., 2005). In contrast to soils, which are likewise available with a significant variety in mineralogy, grain size distribution and grain shape, there is yet no robust system for characterisation of polymers in geotechnics.

In the following section, some basic parameters known from polymer science for the description and classification of polymers are presented.

Ionicity describes the proportion of charged repeat units in a polymer chain when occurring as a copolymer. The properties of charged polymers depend strongly on the proportion of charged components in a polymer chain (Dobrynin and Rubinstein, 2005).

The molecular weight describes the mass of the individual polymer chain. When comparing two polymers composed of the same type of repeating unit, a higher molecular weight of the polymer corresponds to a longer polymer chain, i.e. a larger number of repeating units per polymer chain. The number of repeating units per chain is termed degree of polymerisation (Teraoka, 2002).

In most cases, polymers are not present as a multitude of similar chains, but rather as a mixture of polymer chains of different lengths (Munk et al., 1980; Ward, 1981). Therefore, the molecular weight of a polymer should be considered as a mean value. More in detail, there are different definitions of the molecular weight, e.g. the number average molecular weight (M_n) or the weight average molecular weight (M_w) (Ward, 1981). However, for several applications, the molecular weight is back-calculated based

on empirical correlations that rely on macroscopic observations such as viscosity or osmotic pressure (Munk et al., 1980; Ward, 1981).

Functional groups of a polymer chain can be of different sizes and different complexities and they determine the lateral dimensions of the polymer. For soil mechanical applications the structure and the size of the functional groups of a polymer are crucial. For instance: the intercalability, i.e. the possibility of penetration between the unit layers of clay minerals, depends on the nature of the functional groups (Bergaya et al., 2006).

However, the description of polymers in geotechnical studies has so far mostly been based on charge properties (Ashmawy et al., 2002; Di Emidio, 2010; Razakamanantsoa et al., 2014; Haase, 2017), the type of functional groups (Di Emidio, 2010; Tian et al., 2016; Mazzieri et al., 2010; Scalia et al., 2014; Haase, 2017) and the molecular weight of the polymers used (Inyang and Bae, 2005; Scalia et al., 2014; Haase, 2017).

2.3 Frequently encountered polymers in geotechnics and environmental geotechnics

Polymers are produced in a large number of variations and from a wide variety of raw materials. Accordingly, there is a very large number of available polymers with different properties (e.g. charge properties, molecular weights und chemical nature of repeating units). For geotechnical applications, polymers have to satisfy several requirements. On the one hand, the used polymer must be suitable to obtain the desired improvement or soil property. On the other hand, polymer stability with respect to the application and sustainability as well as environmental compatibility of the polymer and economic aspects need to be satisfied. In the following, a brief summary of water-soluble polymers frequently encountered in geotechnical applications is given and their use beyond the geotechnical applications is presented. A complete overview of the wide field of polymers would be beyond the scope of this work and reference is made to respective literature (Teraoka, 2002; Theng, 2012; Israelachvili, 2015).

Polymers can firstly be divided into biopolymers (often referred to as natural polymers) and polymers made from petroleum derivatives. The raw materials for the synthesis of biopolymers are obtained from renewable raw materials or produced directly by microorganisms cultivated specifically for this purpose (microbial polymers). Bio-polymers are commonly attributed to a more sustainable production and lower prices. However, the

term biopolymer in this context must be distinguished from the property of biodegradability, i.e. potential degradation by bacteria. This property can apply both to polymers produced from petroleum derivatives (Prambauer et al., 2019). Polymers obtained from petroleum derivatives provide other advantages such as good batch-to-batch uniformity and predictable, or in other words tailor-made properties such as mechanical properties and rate of degradation (Lu et al., 2009; Doppalapudi et al., 2014). Like biopolymers, petroleum-based polymers are degraded when subjected to thermal, chemical and biological impacts (Yu et al., 1979; Doppalapudi et al., 2014). However, in several applications it remains unclear to which extent the degradation will occur under boundary conditions relevant in geotechnical engineering (e.g. moderate temperature and pressure regimes, low chemical potential). Studies further indicate that some degradation products of synthetic polymers are toxic (Smith et al., 1997). A comprehensive review on biodegradable polymers (bio-polymers and petroleum based-polymers) is given in Doppalapudi et al. (2014).

A polymer that has long been known in soil mechanics is polyethylene glycol (PEG). PEGs with a very high molecular weight larger than about 20 000 g/mol are known as Polyethylene oxide (PEO). The chemical formulation is (HO-$(CH_2CH_2O)_n$-H) (Hasse et al., 1995). This highly water-soluble non-ionic polymer is used to apply a chemical gradient in unsaturated soil mechanics (Lieske et al., 2020 (a.)). A comprehensive discussion of this topic can be found in Section 2.4. Inyang and Bae (2004) further used PEO to improve the water retention behaviour of montmorillonite in barrier systems. In colloid science, PEG is used as a flocculation agent. The main effect of this polymer has been identified in interparticle bridging and in alteration of clay surfaces and interlayers (Gregory and Barany, 2011; Theng, 2012). Kang and Bate (2016) indicated a stiffer material behaviour and an increase in shear wave velocity of kaolin fly ash mixtures modified with PEO, which was reasoned by additional strength caused by inter-particle bridges. Beyond that, Anderson et al. (2010) describe that PEGs are suitable to prevent swelling during oil recovery actions. However, in the context of drilling fluids, unlike for the modification of clay, the polymer is not mixed directly with the soil. Further, PEGs are widely used in cosmetic products, medicines and cleaning products (Israelachvili, 2015).

Microbial produced polymers such as xanthan and guar gum have recently gained significant attention in geotechnical engineering. These polymers belong to the group of polysaccharides. They can be produced in a sustainable and cheap way and are therefore promoted as an alternative binder, in particular for developing countries (Chang et al., 2015). Due to their complex molecule structure, these polymers have a low degree of

flexibility (Sorbie, 1991). Several studies demonstrated the potential of these polymers to improve strength properties of soils. For instance, Muguda et al. (2017) showed that the increase in unconfined compression strength of a modified soil mixed at proctor water content (70 % sand, 16 % clay, 10 % gravel, 4 % silt) after adding 2% biopolymer and drying for 7 days was higher than after addition of 8% cement. Likewise, Chang and Cho (2019) showed a significant impact of biopolymer on sand-clay mixtures. Higher ductility was found in bio-polymer-stabilized soil samples compared to cement-stabilized specimens (Lee et al., 2019). Yong and Mourato (1990) used xanthan to modify the rheology of kaolin suspensions. The study gives evidence that the anionic groups of the polymer are able to bind to the positively charged edges of the kaolin particles and induce an additional strength, comparable to the bonding found in structured clays (Pusch and Yong, 2006). Long before these kinds of polymers were used to modify soil properties, they were utilised in drilling fluids (Sorbie, 1991) and in the food industry. In the latter, they are used, for example, to control the consistency of sauces such as mayonnaise (Thomareisa and Chatziantoniou, 2011).

Carboxymethyl cellulose (CMC) is another polysaccharide, but unlike xanthan and guar gum, it is not produced microbially but is synthesised from cellulose. The polymer chain is negatively charged. This polymer has been used as a substitute for bentonite in supporting fluids (Jefferis and Lam, 2013). However, one of the most prominent applications of CMC in the frame of geotechnical engineering is a modified bentonite referred to as 'hyper-clay' introduced in Di Emidio (2010). This polymer-enhanced bentonite has widely been investigated in terms of membrane behaviour, hydraulic conductivity under aggressive boundary conditions and wetting-drying behaviour (De Camillis et al., 2017) and is therefore intended for the use in hydraulic barriers. CMC is, like other biopolymers, used in food industry, cosmetics and biomedical applications. Additionally, it is used in paper production (Di Emidio, 2010).

Polyacrylates, polyacrylamides and copolymers of acrylamide and acrylate describe a common group of usually linear chain polymers with varying charge properties and chain lengths synthesised from petroleum derivatives. These chains are thinner and thus more flexible than chains from polysaccharides formed by sugar rings, as their repeat units are much smaller. These polymers were used in support fluids (mostly as negatively charged co-polymer) to replace bentonite suspensions (Lam et al., 2015; Verst et al., 2022). Polyacrylamides have further a long tradition to be used for soil conditioning. Already in the 1950's Monsanto introduced the product 'Krilium', which was used to control soil structure. Further, polyacrylamides were used as flocculation agents and to modify

clays for geoenvironmental applications (Theng, 2012; Haase and Schanz, 2015; Haase, 2017). Due to teir ability to floc colloids, polyacrylamids are widely used in wastewater treatment. Beyond that, cross-linked poylacrylamides, in which polymer chains have been linked by chemical modification, were frequently encountered as super-adsorbent polymers (SAP). As superadsorbers, these polymers are used in many different ways, for example as a binding agent in diapers. Even though the polymer polyacrylamide is not considered hazardous, the respective monomer acrylamide is considered carcinogenic.

Some other polymers that have been used in geotechnical studies, however, have played a minor role so far and should be mentioned for the sake of completeness. Chitosan is a polymer synthesised from exoscelleton of shellfish (e.g. crabs). Like xanthan and guar gum, this polymer has a low degree of flexibility. Positively charged chitosan is used to modify clay (Theng, 2012). Kang and Bate (2016) show the potential of chitosan to improve the strength of kaolin-fly ash mixtures but the effect was less pronounced than it has been observed for PEO.

2.4 Osmotic pressure in polymer solutions

Osmotic pressure describes a difference in chemical potential along a concentration gradient. This pressure corresponds to the difference in hydro-static level between a solution and a solvent in burettes, separated with a semi-permeable membrane. Driven by a chemical gradient, there is a pursuit to balance the potential of the solution. As the semi-permeable membrane prevents diffusion of the dissolved substances into the pure solvent, the solvent penetrates further into the solution and leads to differential fluid levels. In the frame of soil mechanics or more specifically unsaturated soil testing, this osmotic pressure is synonymously termed osmotic suction.

The osmotic suctions of salt solutions (ideal solutions) is commonly calculated using the simplified van't Hoff's law (Equation (2.1)). Steuter et al. (1981) stated that the osmotic suction of ideal solutions is directly a function of the number of molecules in solution and therefore, a linear relationship persists between concentration and osmotic suction for salt solutions based on Equation (2.1), where π [MPa] is the osmotic pressure, c [g/ml] is the concentration, R [8.314 J/mol K] is the gas constant, and T [K] is the temperature.

$$\pi = RTc \tag{2.1}$$

In contrast, polymer solutions exhibit non-linear suction-concentration relationships and hence an application of van't Hoff's law to calculate suctions of polymer-water mixtures is very limited. The difference between the osmotic pressure of an ideal solution (i.e. salt solution) and a polymer solution is visualisised in Figure 2.5. The increase of concentration in an ideal solution (blue line) is directly linked to an increase of the osmotic pressure, as the water potential increases with the number of interacting molecules in the solution. By contrast, polymers assemble a huge number of molecules in a single chain. Thus, polymer solutions (green line) yield lower osmotic pressures at low concentrations, as number of interacting molecules is lower.

In order to include the thermodynamicly effects of polymers in solution, the Flory-Huggins virial expression (Equation (2.2)) has been proposed (Orofino and Flory, 1957). In Equation (2.2), M_n [g/mol] is the number average molar mass and A_2 [$\mathrm{mol\,cm^3\,g^{-2}}$] and A_3 [$\mathrm{mol\,cm^6\,g^{-3}}$] are virial coefficients.

$$\left(\frac{\pi}{c}\right)_{c=0} = RT\left(\frac{1}{M_n} + A_2 \cdot c + A_3 \cdot c^2 ...\right) \tag{2.2}$$

The virial coefficients are a measure of the thermodynamically active volume occupied by a single macromolecule and the polymer-solvent interaction. In a good solvent, the volume occupied by polymer chains is higher than that in a poor solvent (Fleer et al., 1988). Theoretical derivations of the virial coefficients are given by Casassa (1972) and Orofino and Flory (1957). However, in practical applications the virial coefficients are commonly experimentally determined or derived from semi-empirical approaches.

For instance, based on the measured suctions of several PEGs from various experimental techniques, such as laser-light scattering, isopiestic methods, and membrane osmometry, Hasse et al. (1995) proposed Equations (2.3) and (2.4) for calculating the virial coefficients, where T [K] is the actual temperature and the theta temperature T_Θ [K] is a polymer characteristic [$T_{\Theta,PEG} = 375.5$ K].

$$A_2 = 2.49\left(\frac{1}{T} - \frac{1}{T_\Theta}\right) \tag{2.3}$$

$$A_3 = 29.3\left(\frac{1}{T} - \frac{1}{T_\Theta}\right) \tag{2.4}$$

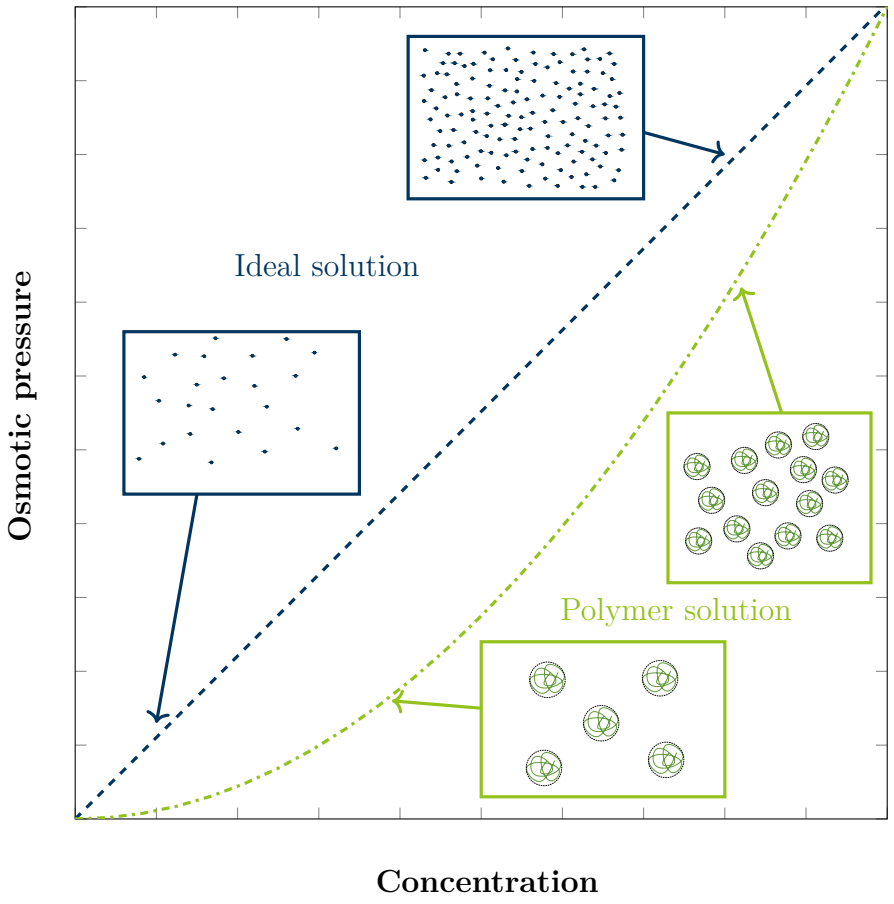

Figure 2.5: Schematic diagram of the development of osmotic pressure as a function of concentration for a polymer solution and an ideal solution

2.4.1 Utilisation of PEG-polymers to apply suction in unsaturated soil mechanics

In unsaturated soil mechanics polymer solutions, or more in detail Polyethylenglycol (PEG) solutions, are used to apply an osmotic gradient on the soil-water system. This technique, commonly termed osmotic technique (Zur, 1966), was frequently used in the laboratory for establishing the water retention curves of fine-grained soils (Williams and Shaykewich, 1969; Fleureau et al., 1993; Delage et al., 1998; Fleureau et al., 2002; Tripathy et al., 2014). The technique has been used to study the hydro-mechanical behaviour of swelling soils by several researchers (Kassiff and Ben Shalom, 1971; Cuisinier and Masrouri, 2005).

Using this technique, a very high magnitude of suction can be applied within a reasonable

time. Studies in the past have shown that suction up to 10 MPa can be applied using the osmotic technique (Delage et al., 1998) that far exceeds the maximum applied suction of 1.5 MPa in pressure plate and pressure membrane tests.

Kaufmann (1973), Money (1989), Delage et al. (1998), and Tripathy and Rees (2013) have established relationships between concentration and suction of several PEGs based on the results from various measurement techniques. For quick determination of suctions of PEG solutions, the Brix index values from refractometer measurements have also been used by some researchers (Tripathy and Rees, 2013; Delage et al., 1998). Although much effort has been devoted to measure and predict suctions of PEGs, accuracies of these predictions are limited due to the inadequate consideration of polymer characteristics (i.e. molar mass) (Tripathy et al., 2011; Monroy et al., 2007).

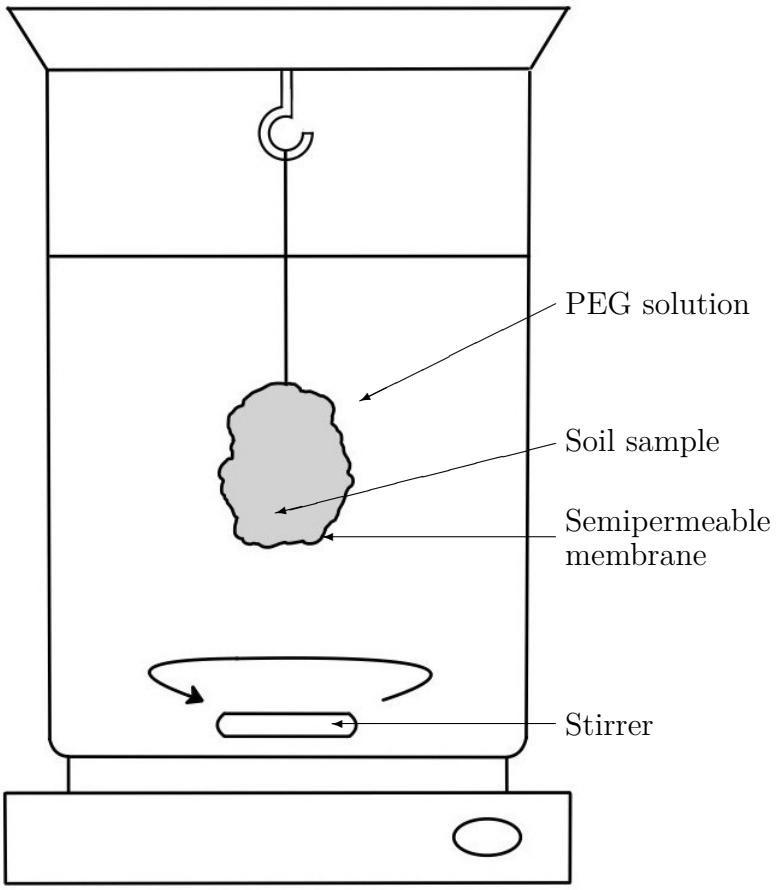

Figure 2.6: Test setup for the determination of water retention behaviour using the osmotic method

Previous studies have shown very good agreements between results from osmotic, pressure plate, and pressure membrane tests for a variety of soils (Tripathy et al., 2014; Delage and Cui, 2008; Zur, 1966). The magnitudes of suction imposed in soil samples during osmotic tests and for known applied suctions have been verified by high capacity tensiometer measurements (Delage and Cui, 2008; Monroy et al., 2007; Slatter et al., 2000; Dineen and Burland, 1995). These studies have shown that the membrane effect (i.e., interaction between PEG and semi-permeable membrane) generally causes a reduction in suction imposed and it depends upon the type of semipermeable membrane and the PEG type used. Delage et al. (1998) stated that suction measurements in case of vapour equilibrium technique (VET) involve vapour phase equilibrium process, whereas the osmotic technique used to impose suction in soils involves the water phase continuity between the soil sample and PEG solution. Therefore, a difference between the imposed and measured suctions in case of soils is related to the osmotic component of the suction. Tripathy et al. (2014) noted that an equilibrium between ion concentration on both sides of the semipermeable membrane may be lacking in case of clays and therefore, the osmotic technique may not always impose the desired matrix suction in soils.

An assessment of suction imposed in a soil sample requires the suction of the PEG used as a reference and hence correct estimations of suction of PEGs becomes extremely crucial for laboratory testing of unsaturated soils. Suctions of PEG solutions can be determined using various techniques, such as freezing-point depression, membrane osmometry, chilled-mirror dew-point, vapor pressure osmometry, thermocouple psychrometry, vapour equilibrium, osmotic tensiometer, laser-light scattering, and high suction probe (Tripathy and Rees, 2013; Monroy et al., 2007; Delage et al., 1998; Kaufmann, 1973; Peck and Rabbidge, 1968; Lagerwerff et al., 1961). Comparison of suction measurements from some of these techniques have been reported in the literature (Tripathy and Rees, 2013). The measurement accuracies and applicability of some of the techniques have been reported to be poorer at high concentrations and temperatures (Lagerwerff et al., 1961; Kaufmann, 1973). Hasse et al. (1995) suggested that the reliability of various techniques depends upon the concentration and molar mass of PEGs for which suction is determined and therefore combinations of different techniques may be adopted. However, for unsaturated soil testing chilled-mirror hygrometer, vapour equilibrium technique and high suction probe are the most common methods to determine suction of soil samples and PEG-solutions. Further, the independent measurement of generated soil suction through high capacity tensiometer is limited to suctions below 2 MPa.

Based on experimental investigations Delage et al. (1998) introduced Equation (2.5) to calculate the suction of a PEG solution. The unit of c* in Equation (2.5) is in g of PEG per g of water.

$$\pi = 11(c^*)^2 \tag{2.5}$$

By contrast to the Flory-Huggins approach, Equation (2.5) does not consider the impact of the molecular weight. Further, Equation (2.5) uses concentration c* in terms of g_{PEG}/g_{water} whereas the Flory-Huggins expression considers the concentration c as mass of PEG per volume of mixture and therefore also includes the concentration dependent density of a PEG-solution.

2.4.2 Simplified approach to calculate suction

Even though the osmotic method has widely been used in unsaturated soil testing and some semi-empirical approaches exist to calculate suction of PEG-solutions, these approaches do not consider the impact of the polymer characteristics in an appropriate manner.

Therefore, a simplified approach was derived in Lieske et al. (2020 (a.)) for the sake to include polymer characteristics in the calculation of the osmotic suction of a polymer solution. The Flory-Huggins virial expression (Equation (2.2)) was modified by replacing the virial coefficients in Equation (2.2) by a single empirical coefficient, Γ [mol cm^{3}g^{-2}], that represents the conjugate effects of PEG-water interaction. Equation (2.6) presents the modified Flory-Huggins virial expression.

$$\pi = RTc^* \left(\frac{1}{\mathrm{M}_n} + \Gamma \cdot c^* \right) \tag{2.6}$$

Equation (2.6) provides a linear distribution of the experimental results in a normalized suction (π/c^*)-c^* plot, where c^* is the concentration in g of PEG per ml of water (Figure 2.7). The interaction coefficient (Γ) can be determined through linear regression. That is, the gradient of π/c^* versus c^* plot yields the value of Γ. As c* $\approx$ c for c $\sim$ 0, the intersection of the linear regression on the π/c^* axis provides RT/M_n. The latter can be used to verify the actual average molar mass of PEGs.

The application of Equation (2.6) has several advantages over the empirical relationships suggested by various researchers in the past (Kaufmann, 1973; Money, 1989; Tripathy

et al., 2011) in that (i) the method is unit balanced, (ii) enables to verify the actual molar mass, (iii) ensures a precise prediction of suction since both polymer concentration and polymer molecular weight are taken into account.

Suctions of various PEGs reported by Tripathy and Rees (2013), Monroy et al. (2007) and Kaufmann (1973), were used to determine the values of average molecular mass of the PEGs and the associated interaction coefficient Γ (Table 2.1). The reported suctions by these studies are corresponding to various molar mass of PEGs, measurement techniques, temperatures, and different ranges of PEG concentration.

Molar mass (M_n) and interaction coefficient (Γ)

The measured suctions of various PEGs reported by Tripathy and Rees (2013), Monroy et al. (2007), and Kaufmann (1973) are plotted in π/c^*-c^* space in Figure 2.7. Best-fitting of the data presented in Figure 2.7 enables determining the values of M_n and Γ. Near linear relationships were noted with very high R^2 values in all cases considered. The values of M_n and Γ obtained from these plots are shown in Table 2.1.

The calculated values of M_n based on Tripathy and Rees (2013)'s data for PEGs 1500, 4000, and 6000 emphasized the applicability of the suggested procedure in which cases good agreements can be noted between the designated and calculated molar mass of the PEGs (Table 2.1). The same trend can be observed for the M_n values calculated based on Monroy et al. (2007)'s data. A significant difference is noted between the calculated and the designated molar mass for PEG 20 000 reported by Tripathy and Rees (2013) in which case, the calculated M_n is found to be smaller than the designated value. Similarly, differences are also noted between the calculated and the designated molar mass for PEG 6000 reported by Kaufmann (1973). In this case, the calculated M_n based on psychrometer tests is found to be smaller, whereas that calculated based on vapour pressure osmometry is found to be greater than the designated molar mass. Hasse et al. (1995) have also noted deviations from manufacturers specifications of the average molar masses of PEGs.

Examination of the reported data considered in the current study indicated that a strong correlation exists between the calculated M_n and Γ for various PEGs, as shown in Figure 2.8. Equation (2.7) allows a direct calculation of the interaction coefficient for a known value of M_n.

$$\Gamma = 2\,M_n \cdot 10^{-8} + 0.0037 \tag{2.7}$$

Table 2.1: Designated molar mass and calculated molar mass based on experimental data (shown as measured M_n) and the interaction coefficients for various reported PEGs.

Designated molar mass	Measurement technique	T [°C]	c^* $[g_{PEG}/ml_{H_2O}]$	$RT{\cdot}M_n^{-1}$ $RT{\cdot}M_n^{-1}$	Measured M_n	$\Gamma \cdot 10^{-3}$ $[mol\,cm^3\,g^{-2}]$	R^2 [-]	
1 500	Chilled-mirrow hygrometer	25	0.096-1.092	1.6041	1 544	0.00375	0.9901	Tripathy and Rees (2013)
4 000			0.097-1.099	0.6463	3 833	0.00378	0.9927	
6 000			0.096-1.091	0.4389	5 645	0.00380	0.9937	
20 000			0.096-1.090	0.1771	13 990	0.00390	0.9933	
6 000	Psychrometer	25	0.100-0.401	0.6110	4 055	0.00391	0.9968	Kaufmann (1973)
6 000	Vapour pressure osmometer	25	0.100-0.401	0.1426	17 374	0.00415	0.9993	
35 000	IC Tensiometer	25[a]	0.049-0.250	0.0641	38 652	0.00447	0.9716	Monroy et al. (2007)

[a] Temperature assumed

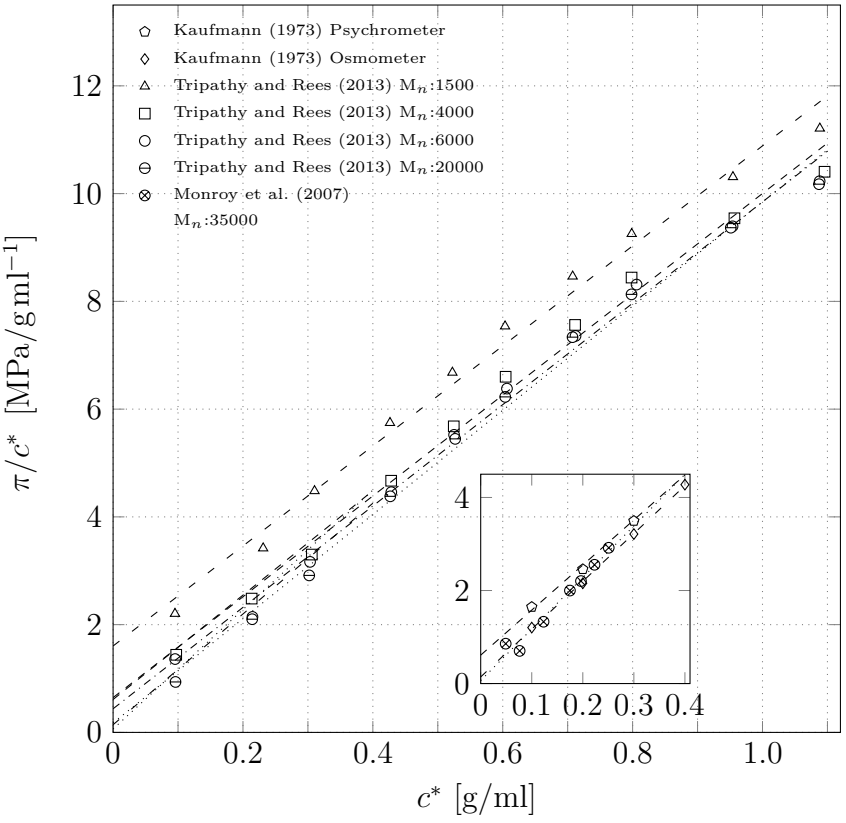

Figure 2.7: c* versus π/c* plot based on experimental data reported in the literature

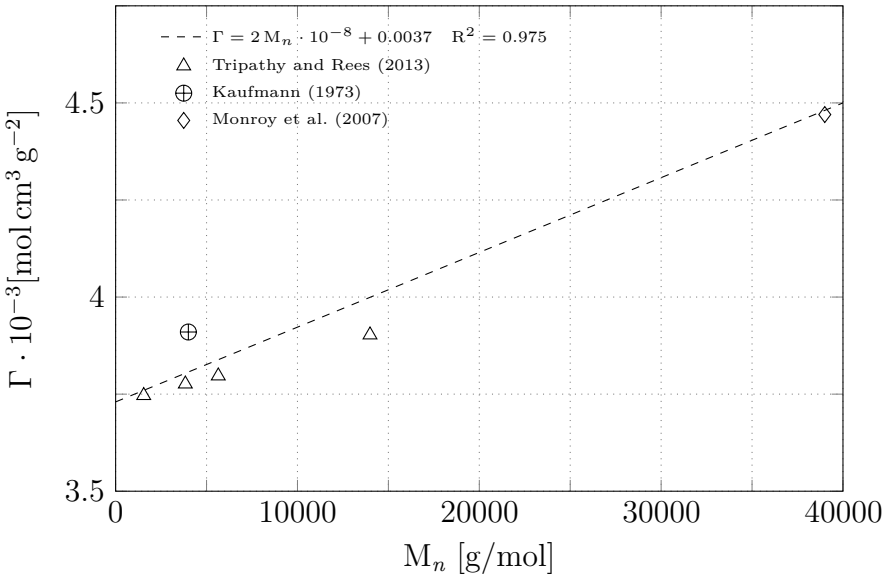

Figure 2.8: Interaction coefficient (Γ) as a function of the number average molar mass (M_n)

Application of the suggested method

The proposed modified Flory-Huggins approach introduced in Equation 2.6 can be used to establish c*-π relationships for any PEG based on the known value of M_n. As seen in Table 2.1, variations between the designated and actual values of M_n may be expected for specific cases. Therefore, it is advisable to determine the actual values of M_n based on experimental data. For this purpose, few concentrations and the corresponding suctions for any PEG are experimentally calibrated using the available technique and the data may be plotted in the π/c*-c* space for determining the actual value of M_n (see Figure 2.7). In the case of non-availability of experimental data, manufacturer's information on M_n may be considered. The interaction coefficient Γ can be determined from Equation (2.7). The suction for any concentration can then be calculated from Equation (2.6).

Figures 2.9 and 2.10 show comparisons of experimental data and calculated concentration-suction relationships for various PEGs. For the experimental data in Figures 2.9 and 2.10, the concentrations of the PEGs were calculated by converting the actual reported concentration units to the desired unit in this study (Tripathy and Rees, 2013). The calculated concentration-suction relationships presented in Figures 2.9 and 2.10 are based on three different approaches: (i) the approach suggested in this study (Equations (2.6) and (2.7)), (ii) Hasse et al. (1995)'s approach using Equations (2.2) to (2.4), and (iii) the widely used empirical relationship proposed by Delage et al. (1998) (Equation 2.5). In all cases the values M_n determined by linear regression were used and the values of Γ were calculated using Equation (2.7). The values of coefficient of determination based on experimental and calculated suctions are shown in the legends of Figures 2.9 and 2.10 for all the approaches.

Figure 2.9 show that in general, the calculated concentration-suction relationship based on Equation (2.5) shows a tendency to remain below the experimental data for low concentrations, whereas it lies above the experimental data for lower M_n PEGs indicating an overestimation of the calculated suctions. For higher M_n PEGs, Equation (2.5) yields similar results as from the suggested approach. In contrast, the Flory-Huggins approach using the virial coefficients suggested by Hasse et al. (1995) (Equations 2.2 to 2.4) shows poorer agreement with the experimental data sets considered in this study for all cases. The concentration-suction relationship from the approach suggested in this study shows very good agreement with the experimental data. The measured suction versus calculated suction values (from Equation 2.6) for various PEGs are presented in Figure 2.10. Figure 2.10 shows very good agreement between the measured and calculated suctions for a large

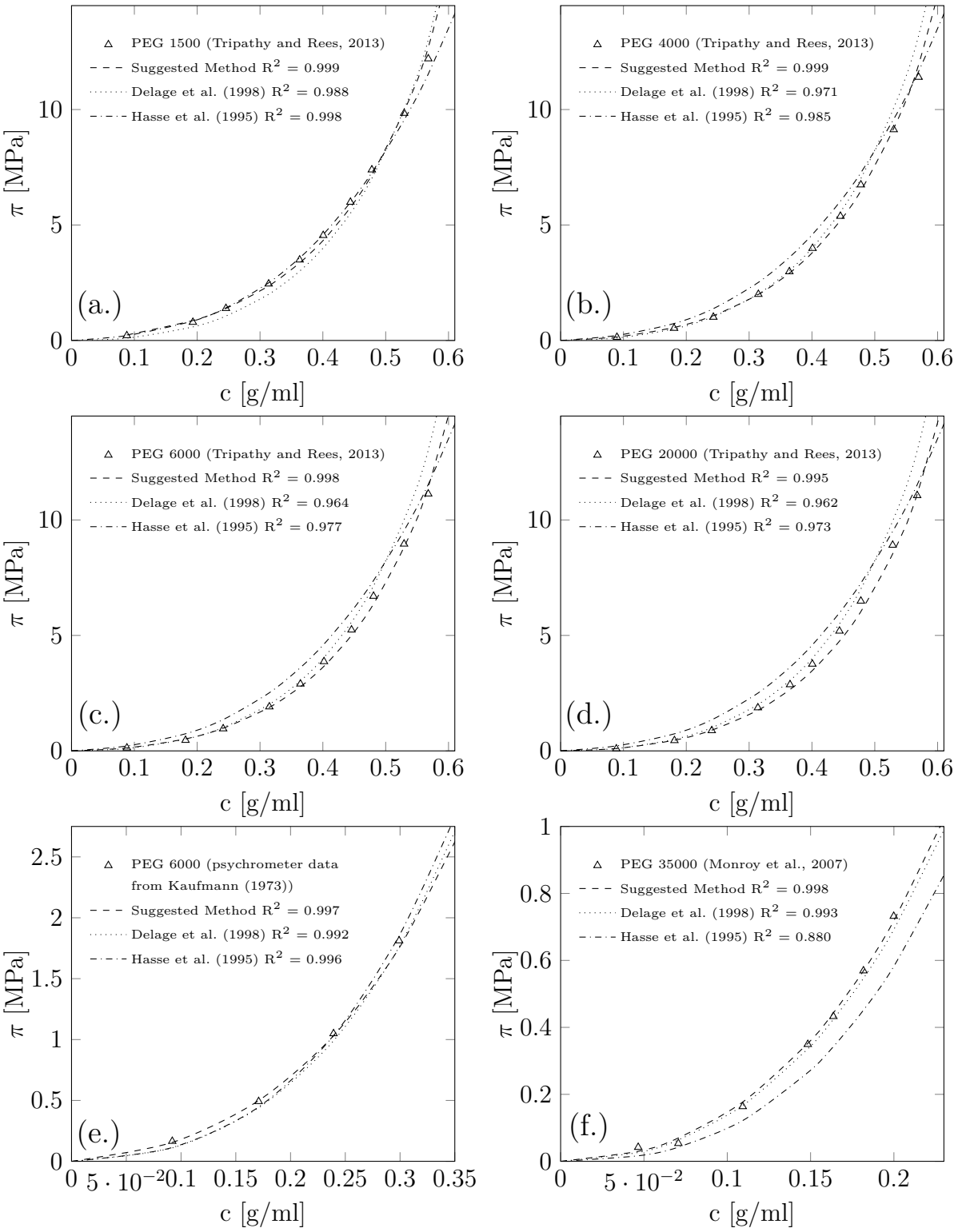

Figure 2.9: Comparisons of measured and calculated values of suction for different PEGs

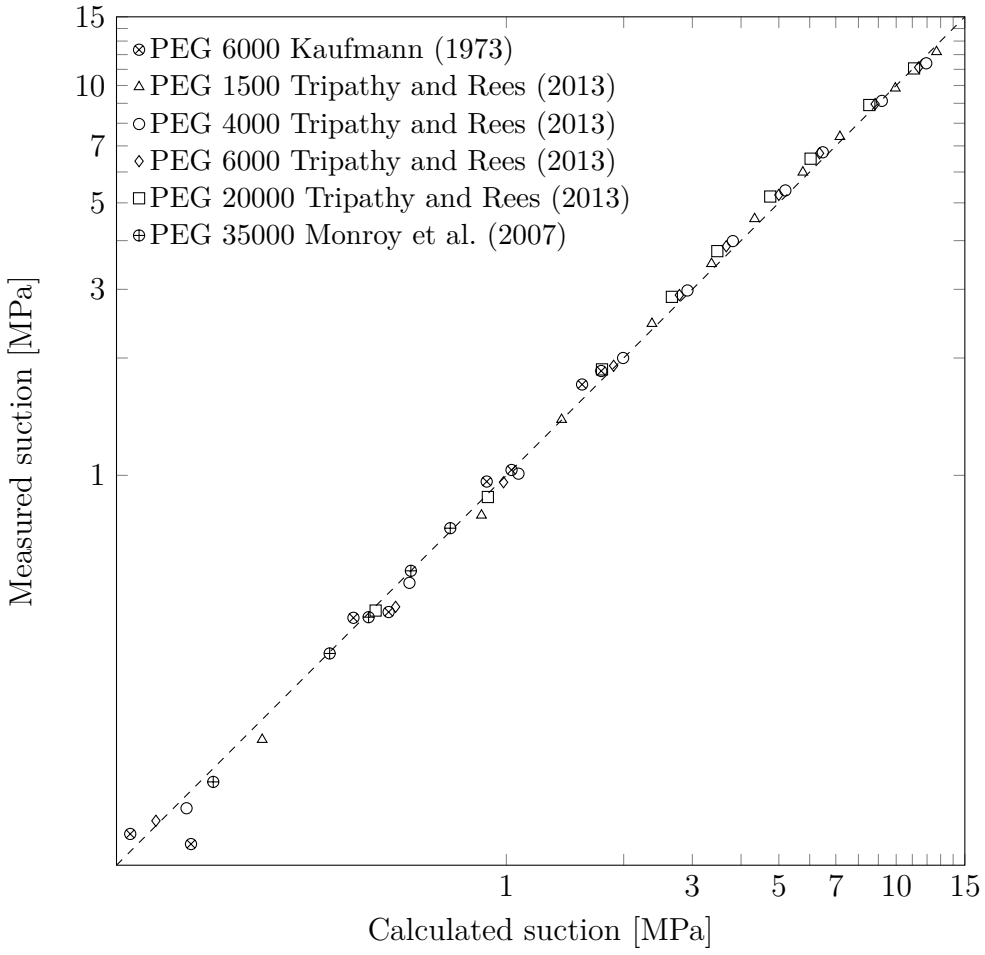

Figure 2.10: Comparisons of measured and calculated suctions using the suggested modified Flory-Huggins approach

range of concentration and for various PEGs. In particular the agreement is better at high concentrations and high suctions.

2.5 Viscosity of polymer solutions

In general, viscosity is a measure for the ability of a fluid to resist flow at a given shear rate. This resistance is caused by the internal friction of a fluid or, in other words, it is a measure for the energy dissipation in the liquid (Tanaka, 2011). A common method to determine viscosity is a test in a rotational viscosimeter. In this test, a fixed and a moveable plate separated by a layer of the studied fluid are moved against each other. The force needed to move the plate at a given shear rate $\dot{\gamma}$ [s^{-1}] divided by the area of the

plates is called shear stress τ [Pa]. The viscosity η [Pa·s] of a Newtonian fluid is defined by Equation (2.8).

$$\eta = \frac{\tau}{\dot{\gamma}} \qquad [Pa \cdot s] \tag{2.8}$$

For fluids with a constant viscosity, under constant temperature and pressure boundary conditions, τ proportionally increases or decreases with $\dot{\gamma}$. The shearing behaviour of such Newtonian fluids is demonstrated in a τ versus $\dot{\gamma}$ and η versus $\dot{\gamma}$-plot in Figure 2.11 (a.) and (b.), respectively. Most of the fluids found in geotechnical applications, e.g. water or salt solutions, can be idealised as incompressible Newtonian fluids with a constant viscosity value as the contained salt molecules are small.

The other kind of well-known fluids in geotechnical engineering are Bingham fluids. These type of fluids have a constant viscosity but a bingham yield stress. Therefore, plastic deformations only occur when the shear stress is larger than the yield stress. The Bingham yield stress is determined by linear extrapolation of experimentally determined shear stress-shear rate relationships to the y-axis intersection. Bentonite suspensions are typically idealised as Bingham fluids.

By contrast, polymer solutions are found with a non-linear shear stress - shear rate relationship, thus a shear rate dependent viscosity (Sochi, 2010). In general, two types of shear rate-dependent viscosity are distinguished: (i) pseudoplastic fluids and (ii) dilatant fluids. Pseudoplastic fluids show a decrease in viscosity with an increase of shear rate

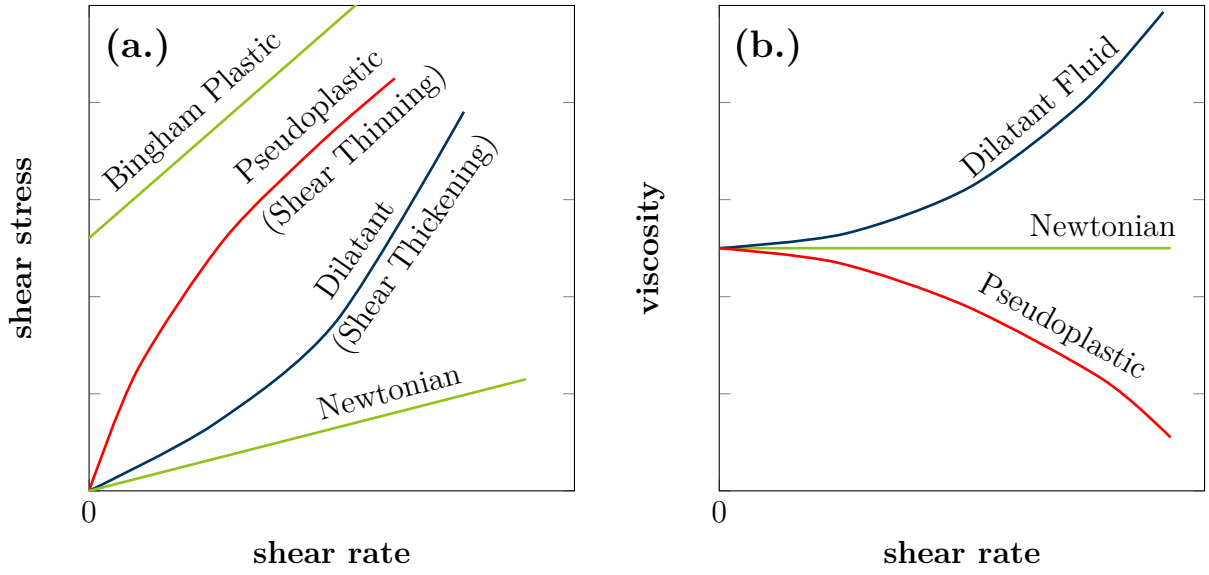

Figure 2.11: Shear stress (a.) and viscosisty (b.) against the shear rate for different fluid types

which is named shear-thinning. Dilatant fluids, conversely, show an increase in viscosity with shear rate, named shear-thickenning. However, since polymer solutions with dilatant behaviour are scarcely found, they have little relevance for the geotechnical practice. Hence, the subsequent considerations are limited to polymer solutions with idealised pseudoplastic behaviour.

Polymer solutions are commonly found with a 'Newton' plateau at very low shear rates (see Figure 2.11(b.)). The viscosity values obtained at this plateau are referred to as zero-shear viscosity, as it is postulated that there will be no significant change of viscosity when reducing the shear rate to zero. In this low energy environment, flexible polymer chains arrange themselves, depending on the polymer constitution, in a more or less coiled state and in a random arrangement. When the shear rate is increased beyond the Newton plateau specific shear rate, the previously described 'thinning' behaviour occurs and the viscosity decreases. In this shear regime, polymer chains stretch along the moving direction (Colby et al., 2007). The magnitude of elongation depends on the size, relaxation time and the endeavor of the polymer chains to stay in a coiled shape. In a fully stretched and aligned state, polymer chains have less 'friction' and thus, the viscosity decreases with increasing shear rate.

At very high shear rates, there is a theoretical second Newtonian plateau where viscosity becomes constant again. However, this plateau is practically impossible to reach. The high energy input which is needed to reach such a state causes rupture of the polymer chains (Sorbie, 1991; Al Hashmi et al., 2013) which in turn is causing an alteration of the molecular weight distribution and, thus, a change in viscosity (Yu et al., 1979). Thus, the viscosity - shear strain relationship of a polymer solution is only an integral consideration of the polymer interactions found at the molecular level. Several variables can be identified to affect this such as molecular weight, charge and relaxation time of the polymers, boundary conditions like temperature and shear rate and concentration of the polymer solution (Tanaka, 2011).

The behaviour of pseudoplastic fluids is of great importance for a growing number of geotechnical problems. Polymer solutions are increasingly used in deep excavations or tunnelling to replace bentonite suspensions as supporting fluid (Lam et al., 2015; Verst et al., 2022). Advantages compared to other bentonite-based supporting agents are chemical stability, better regeneration properties and environmental sustainability (Sorbie, 1991; Lam and Jefferis, 2018). The extreme viscosity of the polymer solution can significantly reduce the permeability of the soil, so that soils can become almost impermeable for a supporting fluid. This process is related to the shear-thinning behaviour of the polymer

solution. When a polymer solution penetrates a granular medium, friction increases with the polymer-soil interface and therefore with the depth of penetration. The flow velocity decreases with increasing friction. In the case of polymer solutions, the decrease in flow velocity leads to an increase in viscosity and thus to a further decrease in flow velocity.

A similar effect is observed in some modified clay liners. In this context, the effect is mainly explained by polymer gels clogging the pores between the aggregates, a process known as “macro-clogging” (Scalia et al., 2014). However, the polymers in a clay matrix are found to be significantly affected by the charge of the clay minerals (Chauveteau et al., 1984).

The impact of chain length and concentration of synthetic copolymers on the viscosity of polymer solutions and the permeability of sand and glass beads permeated with these solutions has been studied by Verst et al. (2022). Figure 2.12 shows the impact of chain lenght (L = long and S = short) and concentration (0.75 g/l and 1.5 g/l) on the viscosity of a polymer solution prepared with anionic polyacrylamide (PAM). The figure gives evidence that at small shear rates viscosity increases with concentration and chain length. However, at high shear rates, where polymerchains arrange in a more parallel manner, or ling chains become destroyed viscosity merely depends upon concentration.

When the concentration of the polymer solution is sufficiently high, polymer chains start to entangle (Colby et al., 2007; Lee and Schlautman, 2015). This regime where polymer chains interact due to geometric constrains is termed semi-diluted region. The concentration beyond where this regime starts is referred to as the ’overlap concentration’, which is connected to a significant increase in viscosity. Figure 2.13 (a.) shows the concentration dependence of the viscosity for a non-ionic polyacrylamide (PAM) (molecular weight = 18 Mg/mol) at various concentrations. Since the effect of entanglement is most evident at low shear rates, the concentration at which the polymers begin to overlap can be determined by analysing the viscosity at the first Newton plateau. The zero-shear specific viscosity is plotted against the concentration for different molecular weights in Figure 2.13 (b.). The specific viscosity η_{sp} is the viscosity of a solution normalised with respect to the viscosity of the pure solvent (η_0) according to Equation (2.9). The figure gives evidence for an overlap concentration of about 155 mg/l. At this point, a further increase of concentration is causing a drastic increase of viscosity caused by the increasing interactions between the polymer chains. The effect of overlap is less pronounced for the low molecular weights which can be reasoned by the impact of chain length on the viscosity at low shear rates (see Figure 2.12).

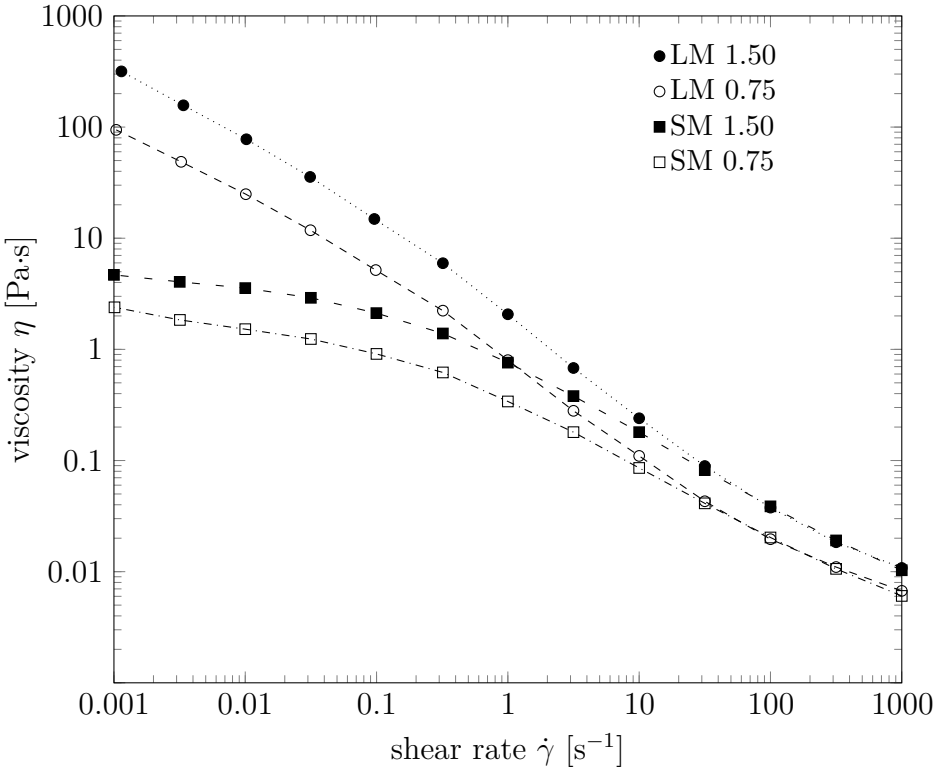

Figure 2.12: Viscosity of polyacrylamides determined with the rotational rheometer varying in molecular weight and concentration (Verst et al., 2022)

$$\eta_{sp} = \frac{\eta - \eta_0}{\eta_0} \tag{2.9}$$

Understanding of the mechanisms that govern the viscosity of polymer solutions is vital for capturing the adsorption morphology of polymers and charged surfaces, as in the case of modified clay. The shape of adsorbed polymer layers has an important impact on the macroscopic behaviour of modified clay (Fleer et al., 1988). For instance, the study presented by Lee and Schlautman (2015) demonstrated that exceeding the overlap concentration resulted not only in an increase in the viscosity of the polymer solution, but also in a decrease in the adsorption capacity of the polymers on kaolin. It has been discussed, that the polymer molecules remain entangled during adsorption which causes a complex and hardly controllable material behaviour accompanied with several difficulties.

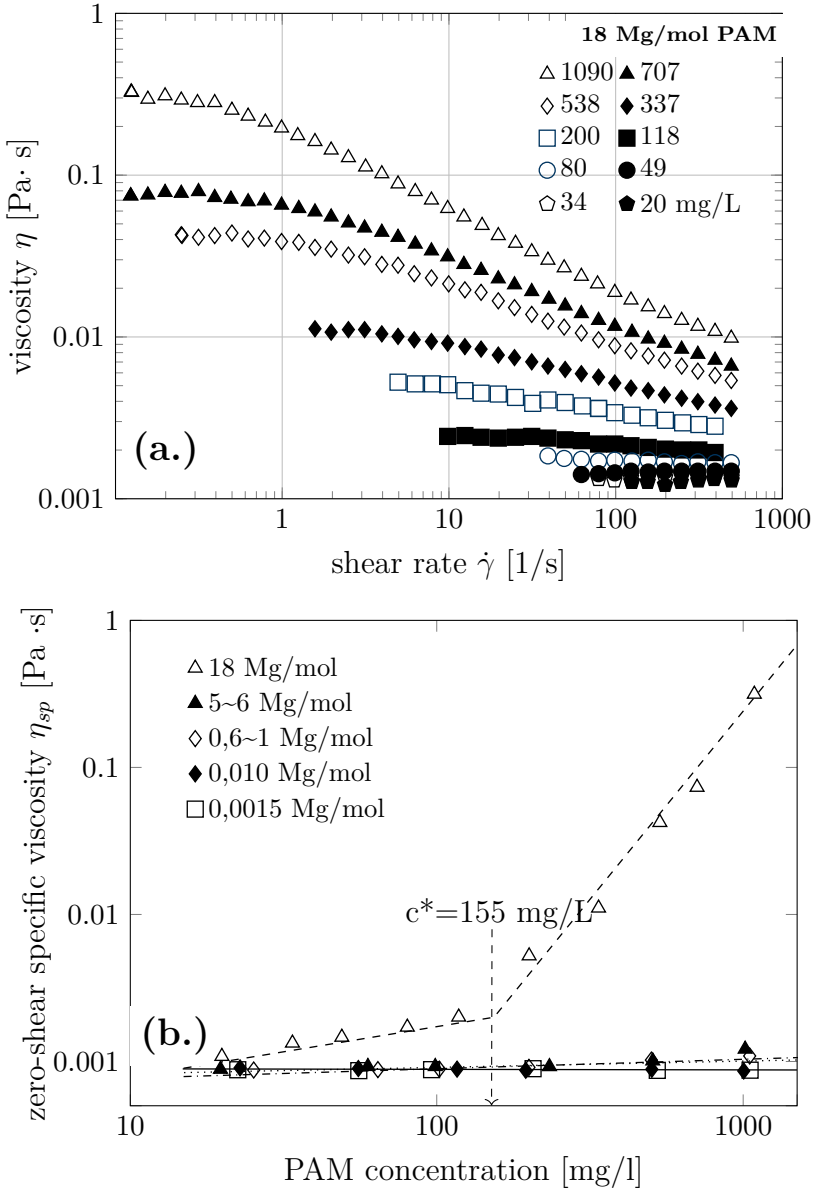

Figure 2.13: Viscosity of non-ionic polyacrylamides: (a.) viscosity versus shear-rate for different concentrations (b.), overlap concentration (c*) for various molecular weights modified from Lee and Schlautman (2015)

3 Clays and polymer-modified clays

The following chapter presents the basics of clays and polymer-modified clays. The chapter starts with a general definition of the term clay followed by an introduction into clay mineralogy and microfabric of fine grained soils. The second part of this chapter is dedicated to bentonite, since it was used in most of the experiments of the present work. Special focus is set on the sensitivity of bentonite to environmental conditions, which in many cases motivates the polymer modification. One subject presented is the influence of divalent salt solutions on the crack formation of a bentonite used in a gosynthetic clay liner (GCLs), which is based on the publication "Suction and crack propagation in GCLs subjected to drying and wetting in $CaCl_2$-solutions" (Lieske et al., 2020 (b.)). In the last part of this chapter, basic mechanisms of polymer-clay interaction are presented. Special attention is given to the charge properties of the respective polymers.

3.1 Mineralogical composition and fabric of clays

The term clay is generally understood as a natural, earthy, fine-grained material that exhibits plastic behaviour when mixed with a limited amount of water (Grim, 1953). In soil mechanics, soils with a liquid limit higher than 30 % and a combination of liquid limit and plasticity index localised above the A-Line in the Casagrande diagram are referred to as clays, see DIN EN ISO 17892-12 (2020). Moreover, clays or the clay-fraction of a soil are defined as soil constituents with a grain size smaller than 2 μm (Bergaya et al., 2006).

The ability of clays to bind water and to show plasticity is due to the high adsorption forces and the high specific surface area of the respective clay minerals. Clay minerals play a prominent role in the hydro-mechanical behaviour of soils, as they have a significant influence even when present in small quantities (Ochoa-Cornejo et al., 2020). The range of naturally occurring clay minerals is wide and different deposition conditions usually yield distinct differences in properties even if the mineralogical composition is similar. In

addition to the clay minerals evolved due to natural transformation processes, synthetic minerals (e.g. laponites) should also be listed. Although these have so far been of minor relevance for geotechnical construction practice, experimental studies show their potential to significantly change soil mechanical properties even in small quantities (Ochoa-Cornejo et al., 2020). Clays which are dominantly composed of a specific clay mineral have a special name, e.g. clay mainly composed of kaolinite is termed as kaolin or china clay whereas a bentonite's main fraction is the clay mineral montmorillonite (Bergaya et al., 2006).

Clay minerals belong to the family of phyllosilicates or sheet silicates (Mitchell et al., 2005). This kind of minerals consist, according to their name, of different layers. The single units of the sheets are the tetra- and octahedral elements shown in Figure 3.1 (a.) and 3.2 (a.), respectively. Each tetrahedron is composed of a cation which is coordinated at four oxygen atoms and is linked to adjacent tetrahedra by three common corners (the basal oxygen atoms). The central cation of the tetrahedron is commonly Si^{4+} why it is also known as silica sheet. However, Fe^{3+} and Al^{3+} are also potential central cations (Bergaya et al., 2006). Six tetrahedra connected by sharing the oxygens form a two-dimensional 'hexagonal' ring (Figure 3.1 (b.)). The connection of numerous of these rings results in a tetrahedral layer having a mesh pattern with large lateral dimensions as shown in Figure 3.1 (c.).

The octahedral unit is composed of six hydroxyl or oxygen atoms, typically coordinated with Al^{3+}, Fe^{3+}, Fe^{2+} or Mg^{2+} cations in the center (Bergaya et al., 2006). Depending on the charge of the central cation, the octahedrons are arranged in two different charge balanced formations. If the central cation is trivalent, the octahedrons are arranged in a ring where only 2 of 3 possible positions are occupied. This type of plate is called dioctahedral. Divalent octahedrons form sheets in which all (i.e. 3 of 3 possible) positions are occupied. This type of sheet is referred to as trioctahedral. The arrangement of octahedrons in such a state is shown in Figure 3.2 (b.) and (c.).

The plot of the tetrahedral sheet shows the configuration when connected to an octahedral sheet. The lateral dimension of the tetrahedral sheet is normally larger than that of the octahedral sheet. Therefore an adjustment of the arrangement is necessary in one or both sheets, which alters the layer structure from the ideal hexagonal symmetry (Bergaya et al., 2006).

Layered silicates are composed of combined octahedral and tetrahedral sheets, which are formed by sharing an oxygen atom. Clay minerals with the same sequence of octahedral and tetrahedral sheets are grouped according to their stacking. 1:1-layer minerals such as

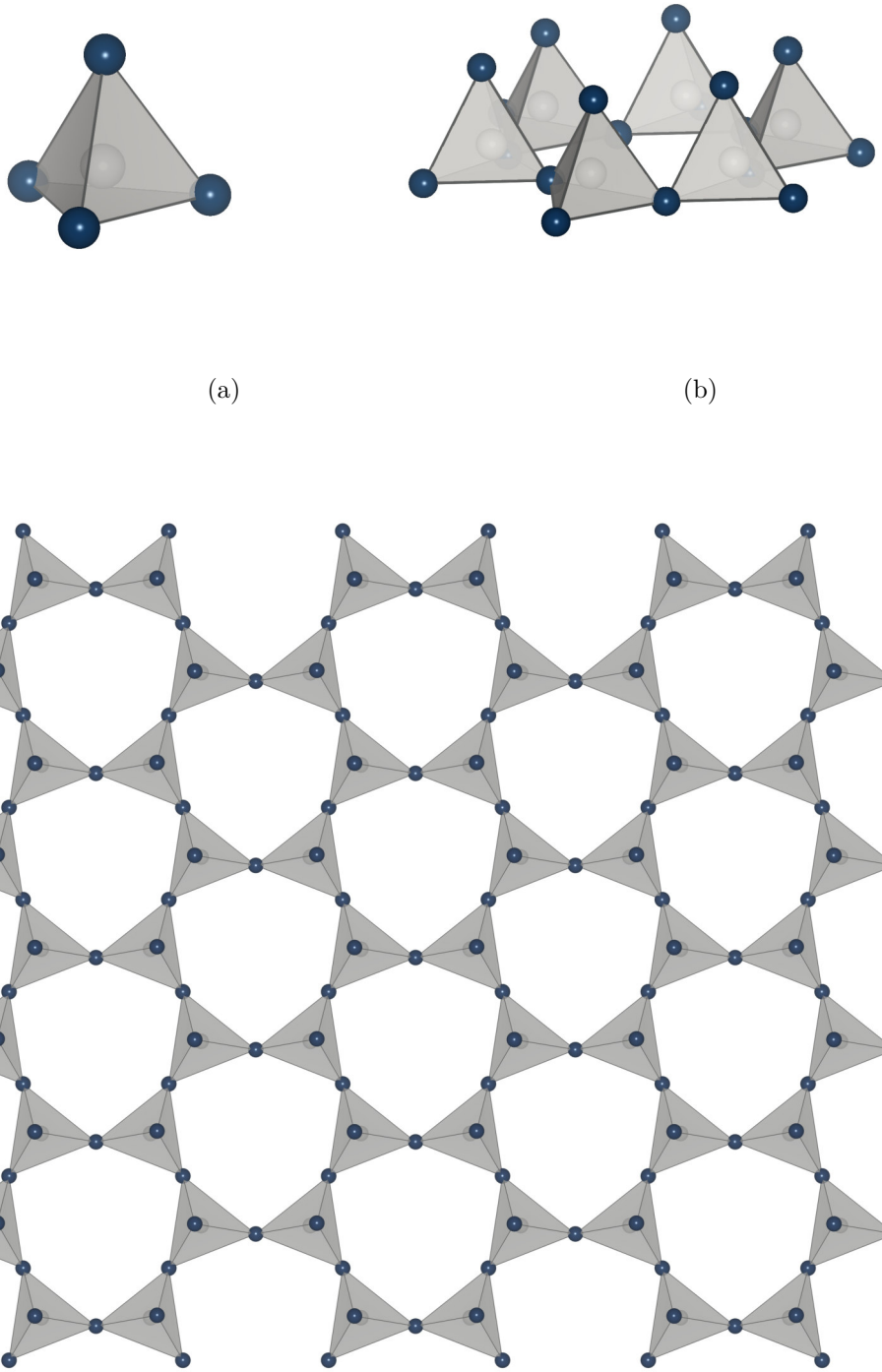

(a) (b)

(c)

Figure 3.1: Sketch of the composition of (a) the tetrahedron, (b) hexagonal ring composed of 6 connected tetrahedra, and (c) tetrahedral sheet with mesh pattern

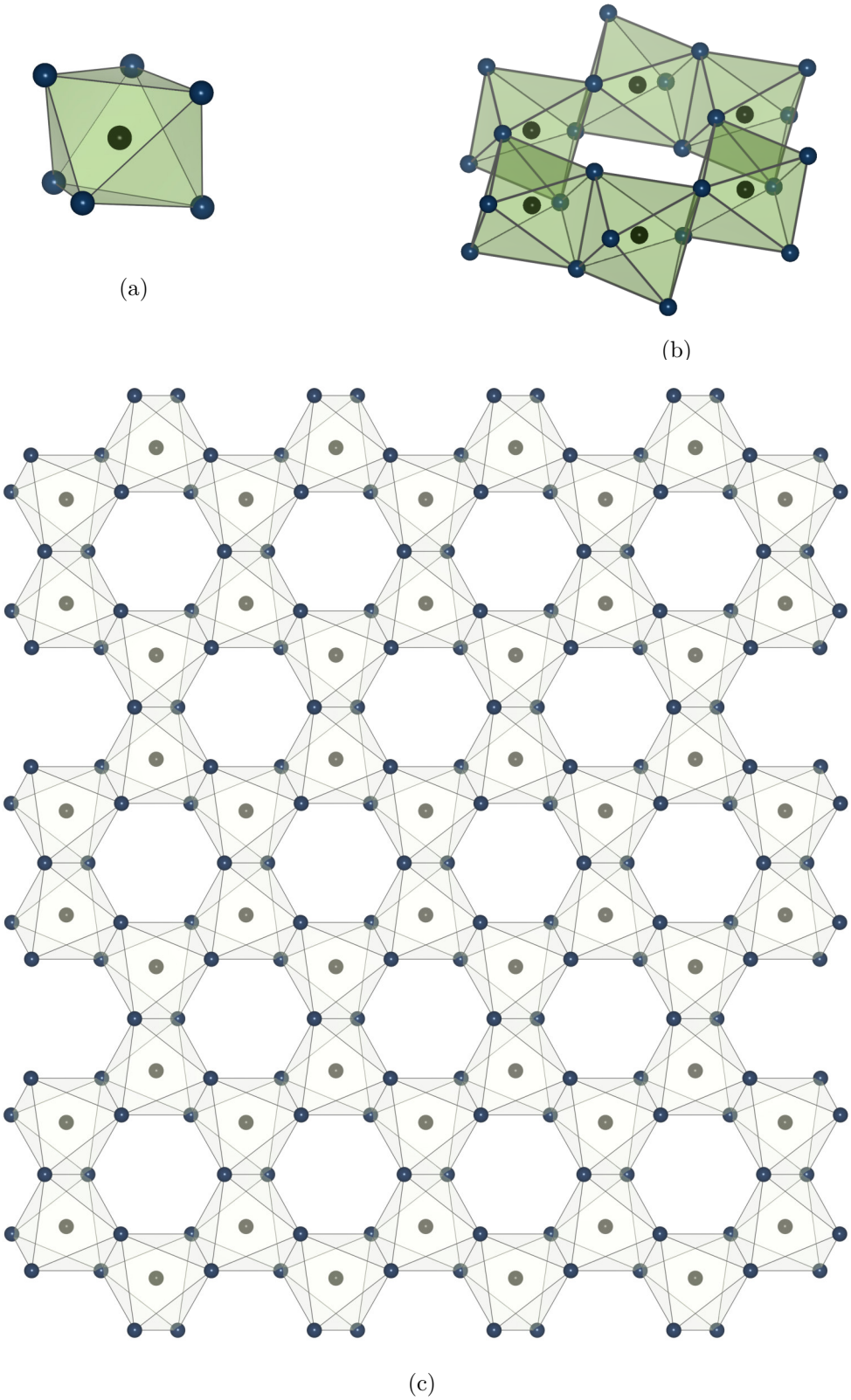

(a)

(b)

(c)

Figure 3.2: Sketch of the composition of (a) the octahedron, (b) six connected octahedra in a dioctahedral arrangement, and (c) octahedral sheet

kaolinite are composed of a tetrahedral and an octahedral sheet. 1:2-layer minerals consist of a trioctahedral or a dioctahedral sheet sandwiched between silica tetrahedral sheets. Smectite, vermiculite and illite belong to this group. The composition of an octahedral sheet sandwiched between tetrahedral sheets is shown in Figure 3.3. Chlorite is a special 2:1:1-mineral composed of a trioctahedral or a dioctahedral sheet sandwiched between tetrahedral silica sheets and a another octahedral sheet connecting the tetrahedral sheets of adjacent minerals. The formation of phyllosilicates by the combination of platy layers leads to minerals with a thickness significantly smaller than their lateral dimensions. The thickness of a 1:1-layer is about 0.7 nm and of a 2:1-layer about 1 nm. The lateral dimensions are usually several times larger, so that anisotropy is an important feature of clay minerals (Weber et al., 2014).

Layered silicates formed by charge-neutral octahedral and tetrahedral sheets are charge balanced (i.e. uncharged) minerals. However, due to isomorphic substitution of cations mainly in the octahedral sheet by cations of lower charge and due to imperfections in the mineral lattice, the cation occupancy differs from such ideal conditions. Clay minerals are therefore usually found with a net negative charge. Especially in the case of 2:1-layer silicates, the pronounced charge deficit plays a decisive role for the hydro-mechanical behavior. In the case of two-layer silicates, the charge is much less pronounced. The negative charge leads to the adsorption of cations on the mineral surface. However, these ions, known as exchangeable cations or cation coating, cannot entirely neutralise the negative charge due to the distance between source of the charge inside the lattice and the position of the cations on the surface.

The type of exchangeable cations depends on thermodynamic boundary conditions and can vary greatly. Furthermore, the exchange of cations is a dynamic process which is of importance in many geotechnical problems. The preferential adsorption of cations follows the Hofmeister or lyotropic series:

$$Al^{3+} > Ca^{2+} > Mg^{2+} > K^{+} > Na^{+}$$

The order of this series follows the mechanism that multivalent and small sized cations are attracted preferrably due to the increase in electrostatic attraction. However, by applying a chemical gradient, an ion exchange can take place in the opposite direction to the series. Bentonites used in suspensions to support trenches are often found as activated bentonites, i.e. they have been modified from a calcium bentonite to a sodium bentonite by the addition of soda. The gradient caused by a pronounced sodium ion excess leads to the exchange of calcium.

A measure for the ability of a clay to adsorb cations on its faces and edges is the cation exchange capacity (CEC). For clays with a low negative net charge (e.g. kaolinite) the value of the cation exchange capacity is in the range of 3 - 15 meq/100g and for clays with a high negative net charge (e.g. smectites) in the range of 80 - 180 meq/100g (Grim, 1953). The value of the CEC has been correlated to soil mechanical parameters of clay. Several researchers showed, that the liquid limit and the plasticity index of a clay increase with its CEC (Farrar and Coleman, 1967). The CEC has further been used as a measure for the amount of active clay minerals in a soil (von Blumenthal et al., 2021).

Micro- and macrofabric of clays

The smallest stable unit in a clay is a clay mineral which, as already discussed, consists of octahedral and tetrahedral sheets. However, the soil-mechanical behaviour of a clay cannot be interpreted by looking at the single clay layer. Due to attractive van der Waals forces acting between layers and ion-ion attraction between layers and exchangeable cations, smectite layers tend to arrange parallel (see Figure 3.3). The assemblage of parallel smectite layers is termed particle or quasicrystal. The latter term was introduced by Quirk and Aylmore (1971). Smectite particle size is a function of boundary conditions (e.g. water content, presence of ions, mechanical constrains to name but a few), since the interlayer (i.e. space between the layers in a particle) can be expanded by hydration of water or complex molecules (Bergaya et al., 2006). External forces such as stirring and shaking can shear particles apart. A breakdown of the smectite particles down to the level of the layers, however, is not likely in the frame of soil mechanical testing (Laird, 2006). In case of 1:1-layer silicates (e.g. kaolinite) the alignment of the layers in particles is stable due to strong hydrogen bonding between octahedral hydroxyls and tetrahedral oxygens. Interlayer expansion is therefore not relevant for 1:1-silicates.

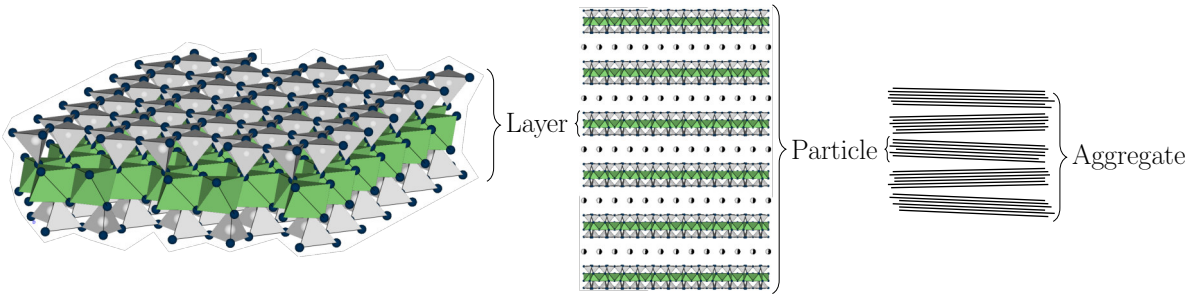

Figure 3.3: Definition of structural elements of a smectite: Layer, Particle and Aggregate

An assemblage of particles is termed aggregate. The aggregate shown in Figure 3.3 reveals a more or less parallel alignment of the particles. The spatial arrangement of particles in soils is termed fabric. Fabric can be found in a broad variety depending on the kind of deposition (e.g. sedimentation, compaction) and post-depositional influences of chemical and physical nature (e.g. drying, freezing, leaching) (Mitchell et al., 2005). As clay minerals feature a platy (anisotropic) shape, their soil mechanical behaviour is strongly linked to the fabric.

The different modes of particle arrangement can be described following the concept of van Olphen (1977), who defines two main categories: 'aggregated' and 'dispersed'. 'Aggregated' describes the parallel arrangement of clay particles. Depending on the arrangement of the aggregated units in the next larger scale (i.e. flocs) a further differentiation can be made in edge-to-edge, edge-to-face flocculation or a combination of both, where face refers to mineral surfaces and edge to the respective mineral sides. 'Dispersed' describes a fabric without parallel alignment of particles and flocculation in an edge-to-edge or edge-to-face arrangement. A special case is that of dispersed or aggregated minerals in a deflocculated state, where no association to the neighbour particles or aggregates can be observed. An overview of the different types of particle associations is given in Figure 3.4. Even though these categories were originally established for clay suspensions, they are widely used for the specification of clay fabric in a compacted state.

Natural clayey soils are commonly found as complex multi-level assemblage of aggregates (i.e. a combination of numerous particles) and larger mineral components (Collins and McGown, 1974; Lieske et al., 2021). In addition to fabric, bonding between particles, minerals and mineral assemblages has an important influence on the hydro-mechanical behaviour of clays. As the smallest elements of soil structure remain stable during remoulding or determination of the liquid limit, intrinsic behaviour of a soil becomes not solely a question of mineralogical constitution but also of structure, which is understood as the combined effect of fabric and bonding (Burland, 1990).

The structure of a clay is not only determined by its formation history but is also strongly affected by its mineralogy as evolution of structure and mineralogy are interlinked. Vice versa, the clay fabric significantly affects its hydro-mechanical behaviour and several attempts to dedicate specific soil mechanical features to fabric can be found in literature (Lambe, 1958; Olsen, 1960; Burland, 1990). For example, Lambe (1958) reasoned the different mechanical behaviour of clay samples that were compacted on the wet and dry side of the proctor maximum respectively, with an aggregated (dry side) and dispersed (wet side) fabric.

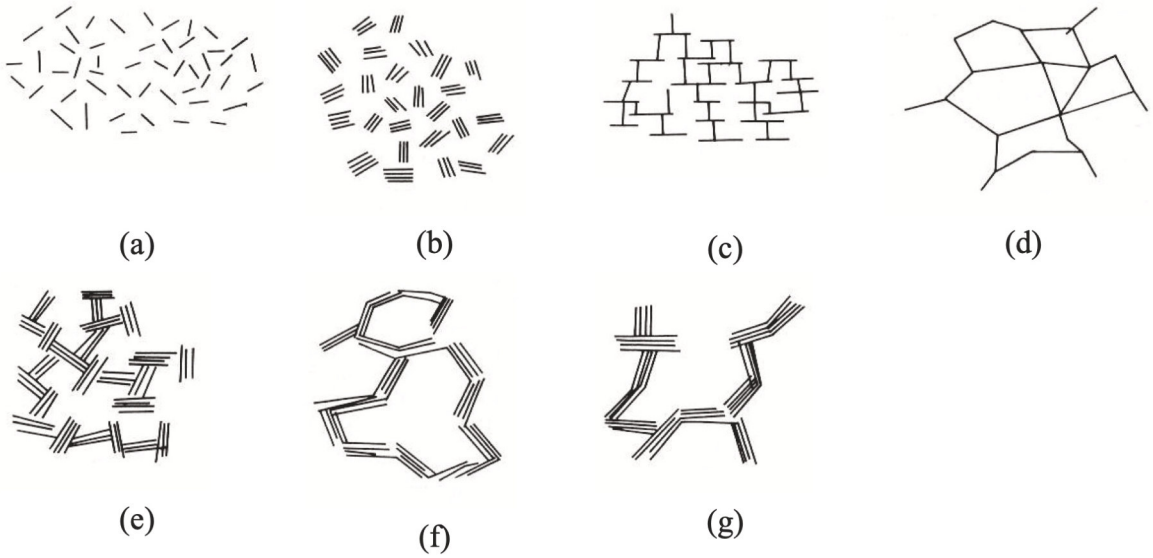

Figure 3.4: Types of clay particle associations according to van Olphen (1977): (a) dispersed; deflocculated, (b) aggregated; deflocculated, (c) dispersed edge-to-face flocculated, (d) dispersed edge-to-edge flocculated, (e) aggregated edge-to-face flocculated, (f) aggregated edge-to-edge flocculated, and (g) aggregated edge-to-face and edge-to-edge flocculated

The different levels of fabric and aggregation create distinct voids in between the mineral solids, which are filled with pore fluid or gas. Pores can be classified in micro- (generally < 2 nm), meso- (generally 2 - 50 nm) and macropores (generally > 50 nm) according to their size (Salles et al., 2009). Other definitions refer to the geometric arrangement of the pores rather than their size, so that a distinction is made between inter-aggregate and intra-aggregate pores (Gens and Alonso, 1992).

Figure 3.5 visualizes the geometric arrangement of clay components which are either (a) predominantly present as particles or (b) present as large aggregates. Different pores can be identified depending on their position. Inter-aggregate pores are located between large aggregates whereas intra-aggregate pores are embedded within aggregegates. It should be noted here, that in this context aggregate refers to large conglomerates of clay minerals or particles rather than describing the arrangement as it was done using the word 'aggregated' in Figure 3.4. The figure clearly shows the difference between inter- and intra-aggregate pores. Micropore is often synonymously used for intra-aggregate pore and macropore for inter-aggregate pore, respectively. Due to the interactions with water molecules resulting from the proximity to the clay surface and the small diameter of these pores, hydraulic flow as well as advective and diffusive transport mechanisms take place

very slowly in micro pores (Olsen, 1960; Mitchell et al., 2005). In the case of compacted bentonite, inter-aggregate pore space is reduced during saturation. As it will be discussed more in detail in the Section 3.1, hydration of smectite is causing the layers and therefore aggregates to expand. Dending on volumetric contrains, aggregates merge completely together and fill the inter-aggregate porespace (Musso et al., 2013).

Pore size distribution is commonly studied using mercury intrusion porosimetry (MIP) (Griffiths and Joshi, 1989; Romero et al., 1999; Burton et al., 2014). In this technique, an equivalent pore radius is back calculated from the pressure which is needed to inject mercury in a soil sample using the Washburn equation (Delage and Lefebvre, 1984). If the pore sizes of a soil sample are predominantly in a narrow band of equivalent diameters, the pore size distribution is described as unimodal. If there are two different dominant pore sizes (namely micro- and macropores), the pore size distribution is considered to be bimodal (Burton et al., 2014). The latter is often associated with an aggregated fabric, as the appearance of large pores is attributed to the formation of voids between the aggregates (see Figure 3.5). When soils consolidate as a result of mechanical stress, this is due to the decrease in pore volume and the increase in contact between soil components. The void space gradually decreases, starting with the largest pores, so that intra-aggregate pores remain unaffected over a wide range of stresses (Burton et al., 2014).

Clay-water interaction

Depending on the location of the water inside a clay fabric and its interaction with the mineral, three types of water can be distinguished in the clay matrix: structural water, adsorbed water and free water. Structural water in clays is part of the mineral lattice, as OH-groups coordinate to cations. At temperatures between 350-1000°C dehydroxylation as a result of a reaction between hydroxyls located in the octahedral sheet (Emmerich

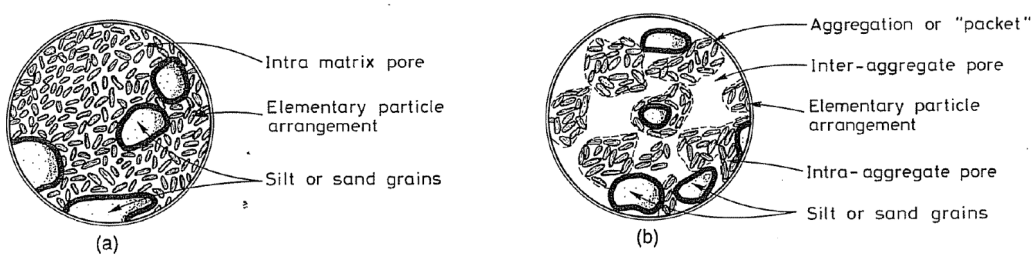

Figure 3.5: Fabric types (a) Clay predominantly present as individual particles (b) Clay particles form large aggregates (Gens and Alonso, 1992).

et al., 1999) causes the removal of structural water. It will not be released during the procedure to determine the water content (i.e. drying at 105 °C for 24 hours). The release of structural water from the lattice structure and the subsequent change in mineral properties is used for the production of geopolymers. By heating kaolin to 600 °C, the lattice water is released from kaolin and metakaolin is obtained. This pozzolanic active material is used as a binder and substitute for cement (Kakali et al., 2001).

Adsorbed water is associated by hydrogen bonding to the mineral surfaces caused by dipole-dipole attraction or by hydration of exchangeable cations caused by ion-dipole attraction. The different mechanisms are shown in Figure 3.6 (a) and (b), respectively. Due to the dipolar nature of H_2O, hydrogen bonds form between the water molecules and the tetrahedral oxygens or octahedral hydroxyls at the clay minerals surface. As illustrated in Figure 3.6, if the clay surface has a partial negative charge (i.e. oxygen), a water molecule aligns its positive partial charges towards the clay surface. However, if a hydroxyl (i.e. a negative partial charge on the mineral surface) is present, as in the case of 1:1 layer silicate, a water molecule directs its negative partial charges towards the clay surface (Mitchell et al., 2005). The hydration of particle outer surfaces is considered as the first hydration step of dry smectite minerals (Salles et al., 2009).

The exchangeable cations located on the layer surface of smectite, which are attracted by the negative charge of the mineral, are hydrated as a result of ion-dipole attraction. This hydration is a discrete process in which $0, 1, 2, 3$ or 4 layers of water can be attached to the interlayer cations. This process is inherently characterized by hysteresis (Laird, 1996; Montes-H et al., 2003). The repulsive forces between two adjacent clay surfaces gradually increase with relative humidity, while the attractive forces depend solely on the number of hydrate shells around the cations. When the relative humidity in a system is increased or decreased, the hydrate shell remains unaffected until the additional energy is high enough to jump to the next hydration level. The number of water layers around a cation between hydration levels is therefore higher when the water content is increased than when it is decreased (Laird, 2006). The above-mentioned hydration mechanisms are known as innercrystalline or simply crystalline swelling. This mechanism is particularly relevant at low water contents or high densities and can build up high swelling pressures in smectite if volumetric expansion is restricted (Madsen and Müller-Vonmoos, 1989). The crystalline swelling depends strongly on the type of interlayer cation.

By increasing the water content beyond the complete hydration of the clay surfaces and cations, a second swelling mechanism develops, which is termed osmotic swelling. The difference in concentration that arises from the clay surface towards the bulk fluid due

to adsorbed cations results in a chemical gradient. As the exchangeable cations are electrostatically attracted by the negative charge of the mineral, they cannot freely diffuse to compensate the gradient. Therefore water diffuses along the chemical gradient to "dilute" the concentration of cations near the surface (Madsen and Müller-Vonmoos, 1989). At the same time anions diffuse along the chemical gradient towards the mineral surface, but are repelled by the negative charge (van Olphen, 1977; Laird, 2006).

The penetration of water molecules to the cations, which moves the cations outwards from the surfaces, and at the same time coulombic attraction of the cations and the negative charged mineral surface, leads to the formation of a cloud of cations, anions and water molecules known as diffuse double layer (DDL) (see Figure 3.6). The term electrical or diffuse double layer raises from the (negative) particle charge and the equivalent amount of ionic charge from the counter-ions (cations). The maximum of electrical potential in the DDL is located directly at the clay surface. With increasing distance to the clay surface the potential is decreasing till reaching the chemical potential of the pore fluid.

Since the electrostatic attraction between cations and the negatively charged mineral surface prevents the chemical gradient inside the pore fluid to be equalised, the effect of this electrostatic interaction is often compared to that of a semi-permeable membrane. Using this concept, it becomes apparent that the pressure (R_{ddl}) acting at the central plane between two overlapping DDLs corresponds to the osmotic pressure (π), which can be calculated using the van't Hoff Equation (3.1),

$$R_{ddl} = \pi = kT \sum n_{ic} - n_{i0} = RT \sum c_{ic} - c_{i0} \tag{3.1}$$

where, k is the Boltzmann constant ($= 1.3810^{-23}$J/K), R is the gas constant ($= 8.314$ J/mol K) and T is the temperature (K). The concentrations n_{ic} and n_{i0} are given as ions per unit volume (m^{-3}) or c_{ic} and c_{i0} as molar concentration (mol/m^{-3}). The thickness of the DDL decreases with increasing salt concentration of the pore fluid, as the point at which the chemical potential in the DDL and the bulk are equal, is located closer at the clay surface. Equation (3.1) shows that an increase of the ion concentration in the bulk fluid therefore directly contributes to a reduction of the repulsive diffuse double layer forces.

Different approaches exist to calculate and predict the innercrystalline and the osmotic swelling of clays depending on material characteristics. Laird (1996) introduces an analytical model to calculate crystalline swelling of 3-sheet phyllosilicates. However, the modelling of osmotic swelling has gained much more attention in the field of soil mechanics, since its scope of validity meets the most frequently encountered boundary conditions.

Crystalline swelling is relevant at basal spacings between 1.0 and 2.2 nm, whereas osmotic swelling becomes relevant between 3.7 and 5.0 nm. The swelling between 2.2 and 3.7 nm can be considered as a transition range between the different swelling mechanisms (Laird, 1996).

Theoretical approaches to calculate the forces acting between two charged clay surfaces in the osmotic swelling range are usually based on the Poisson-Boltzmann Equation (3.2).

$$\frac{d^2\Psi}{dx^2} = \left(\frac{2n_0\nu e'}{\varepsilon}\right)\sinh\left(\frac{\nu e'\Psi}{kT}\right) \tag{3.2}$$

The electric potential Ψ (V) is calculated as a function of the distance x (m) to the clay surface, taken into account the valency of the ions ν (-), the bulk fluid equilibrium concentration n_0 (m^{-3}), the permittivity of the medium ε ($C^2/J^{-1}\,m^{-1}$) and the electron charge e' (C). The parameters k and T are the Boltzmann constant ($=1.3810^{-23}$J/K) and the temperature (K), respectively. Several attempts to calculate the swelling pressure or one-dimensional compression of swelling clays based on a theoretical calculation of DDL can be found in literature (Bolt, 1956; van Olphen, 1977; Sridharan and Jayadeva, 1982; Madsen and Müller-Vonmoos, 1989; Tripathy et al., 2004; Tripathy and Schanz, 2007; Baille, 2014; Haase, 2017).

Soils subjected to elevated temperatures and low relative humidity release water till the potential of the soil to retain water (soil suction) equates to the drying induced energy. The total change of the potential of soil-water μ_t given in Equation (3.3) consists of several components,

$$\Delta\mu_t = \Delta\mu_c + \Delta\mu_o + \Delta\mu_e + \Delta\mu_f \tag{3.3}$$

where μ_c is the potential resulting from capillary forces and negative pore water pressure, μ_o is the potential caused by dissolved solutes in the pore water and μ_e and μ_f are caused by short-range electric fields and van der Waal's fields, respectively. In soil mechanics the potentials arising from capillary forces, short-range electric fields and van der Waal's fields are summarised as matric suction ψ_{matric} and expressed in terms of a pressure potential. The osmotic potential is expressed as osmotic suction π (or ψ_o). The total suction (ψ_{total}) of a soil is regarded as the sum of two components according to Equation (3.4).

$$\psi_{total} = \psi_{matric} + \pi \tag{3.4}$$

The total suction ψ_{total} is a function of the relative humidity RH (-) and temperature T (K) and can be calculated by Kelvin's law given in Equation (3.5). The parameters ν_{wo}

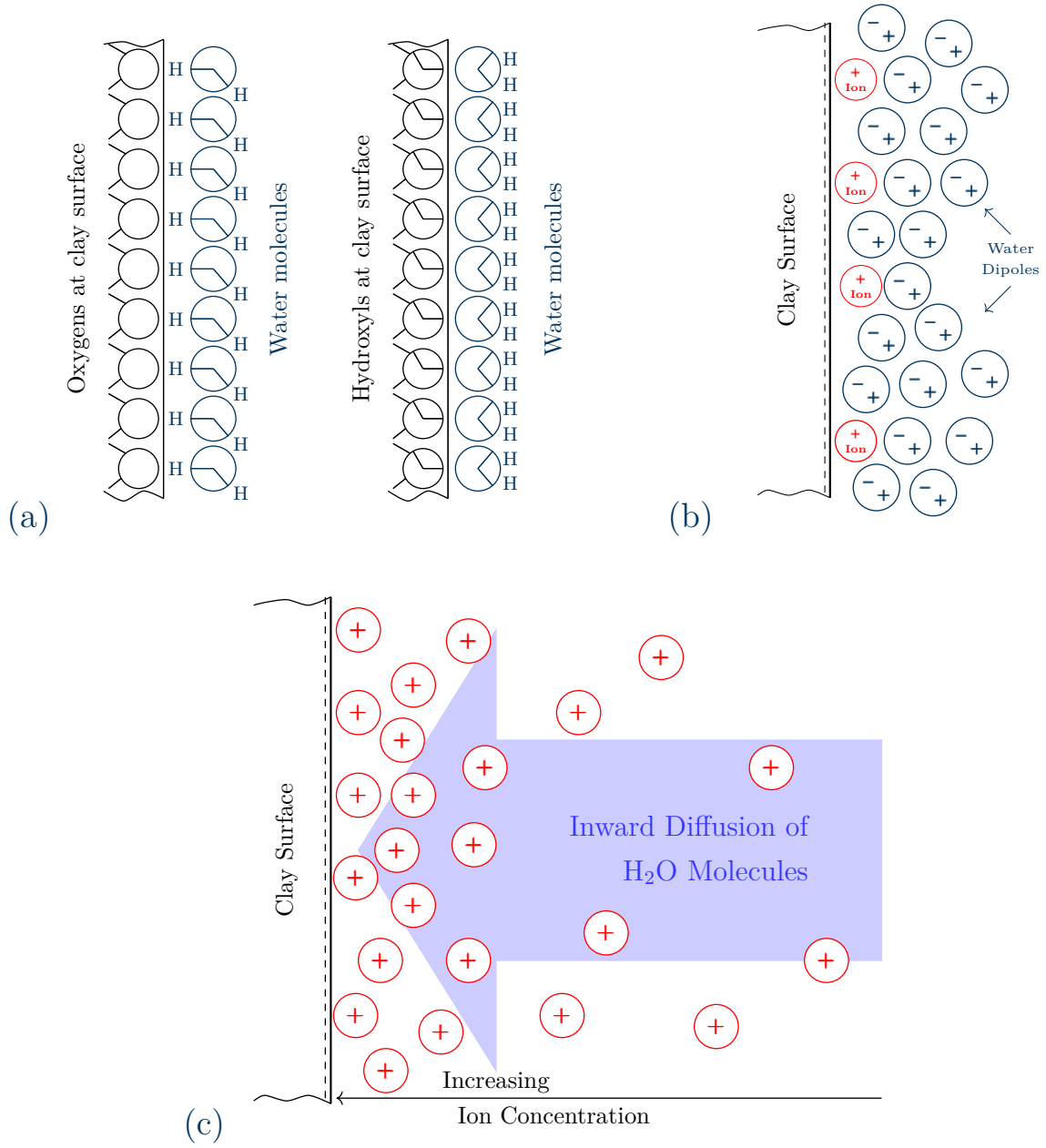

Figure 3.6: Fundamental mechanisms of inner-crystalline swelling: (a) hydration of clay surfaces, (b) hydration of exchangeable cations and, (c) osmotic swelling caused by diffusion of water molecules to the mineral surfaces driven by a chemical gradient (after Mitchell et al. (2005)).

and ω_v are the specific volume of water (m^3/kg) and the molecular mass of water vapour (kg/kmol), respectively, and R is the universal gas constant (J/mol K)).

$$\psi_{total} = -\frac{RT}{\nu_{wo}\omega_v}\ln(RH) \tag{3.5}$$

The equation shows that the magnitude of suction ψ_{total} acting on a soil at a given temperature increases when the relativ humidity decreases. Conversely, at a given relative humidity, the suction increases with temperature. The constitutive relationship between the water content of a soil in equilibrium with an external suction is called soil water characteristic curve (SWCC) or water retention curve, when referring to the drying path. Depending on the suction range, different water adsorption regimes are distinguished: capillary regime, adsorbed film regime and tightly film regime. Thereby, the first two are affected by fabric whereas the latter one mainly depends upon surface and interlayer hydration (Lu and Khorshidi, 2015).

Due to negative pore water pressure and thus an increase in effective stresses (Lu and Likos, 2006; Baille et al., 2014) the release of water from bentonites is commonly accompanied by a volumetric shrinkage process (Cornelis et al., 2006). The relationship between suction and density of a soil is called the shrinkage curve. Local reduction in volume due to drying induced shrinkage causes cracks on a larger scale when the suction induced stresses exceed the tensile strength of the soil. External influences causing suction can directly or indirectly result from climate-related factors, such as direct solar radiation. Heat generated by biological and chemical processes in waste has also been reported to be released from landfills or encapsulated nuclear waste. In addition, suction is also caused by competition for limited quantities of available water with the underlying soil layers (Acikel, Gates, Singh, Bouazza and Rowe, 2018).

In soil science, the volumetric shrinkage behaviour of a fully saturated structured soil subjected to drying is described in four different regimes (Miller et al., 1998; Mishra et al., 2019). The desaturation is starting with the release of water from large inter-aggregate pores and channels (e.g. from biological activity or geotextiles in case of geosynthetic clay liners), commonly causing only insignificant shrinkage and, thus, no cracks.

The second stage is named linear, normal or proportional shrinkage. More water is released from the inter-aggregate pores and the decrease in water volume is proportional to the decrease in total sample volume. This means that the inter-aggregate pores remain water saturated. Miller et al. (1998) studied the drying induced cracking of a compacted clay liner and found that the linear shrinkage is associated to the most pronounced development of drying induced cracks.

When the water content falls below a material specific value, residual shrinkage is observed. The onset of residual shrinkage is when air starts to enter the inter-aggregate pores and from this point the development of cracks with decreasing water content is less progressive. According to Miller et al. (1998), the residual drying did not cause a signif-

icant increase of cracks although the total value of matric suction was high. The final zero-shrinkage stage is reached, when further water content decrease is not associated with further pore volume reduction.

3.2 Bentonite: use and limitations of application in environmental geotechnics

Benonite is a highly plastic natural clay mixture, mainly composed of the 2:1-layer minerals of the smectite group, e.g. montmorillonite (see Figure 3.3). The clay is a product of volcanic action and large deposits of bentonite are available on all continents (e.g. Wyoming (USA), Milos (Greece)). Due to its net negative charge and resulting exchangeable cations, smectite minerals have a significant affinity to adsorb water. On the macroscopic scale this leads to low permeability (Petrov and Rowe, 1997), membrane behaviour (Bresler, 1973), and high swelling pressures when a volumetric expansion during hydration is prevented (Madsen and Müller-Vonmoos, 1989). For several geotechnical applications, such as technical barriers, bentonite has therefore established as an important construction material.

The negative charge of the particular smectite mineral (layer) is balanced by the adsorption of K^+, Na^+, Ca^{2+} or Li^+ cations (Laird, 2006; Salles et al., 2009). According to the dominant exchangeable cation, bentonites are named as calcium bentonites or sodium bentonites. A special case is activated bentonite, where the dominant exchangeable ions are transformed by a specific cation exchange. As the attractive forces acting between clay layers saturated with sodium are weak, such clays are found with pronounced double layer swelling and formation of stable suspensions, sometimes also named gel. Sodium-activated clays are therefore preferentially used in slurry supported trenches. Likewise, natural sodium bentonite is widely used for sealing applications. Vice versa, the exchange of sodium with the naturally thermodynamically preferred calcium significantly alters the material behaviour, accompanied by formation of large particles.

The hydro-mechanical behaviour of bentonite is a function of various boundary conditions as the material is sensitive to environmental conditions such as dissolved monovalent or divalent salt in the bulk fluid (Mesri and Olson, 1971; Petrov and Rowe, 1997; Jo et al., 2001; Kolstad et al., 2004), drying induced dewatering (Acikel, Gates, Singh, Bouazza and Rowe, 2018), and effects that arise from aggressive pH-values (Liu et al., 2015). For example, the presence of $CaCl_2$ in the bulk fluid of an expandable clay affects both

the physico-chemical adsorption as well as the soil structure. Thermodynamically driven cation exchange is causing aggregation as the electrostatic attraction between the $CaCl_2$ and the smectite layers is higher as in case of NaCl (Laird, 2006). The increase of $CaCl_2$-concentration in the bulk fluid reduces the osmotic gradient and therefore affects the osmotic component of the swelling (see also Section 3.1). On the macroscopic scale, the permeation of sodium bentonite with $CaCl_2$-solution is related to a change of hydraulic conductivity (Jo et al., 2001), a decrease of membrane behaviour (Bresler, 1973), and a decrease of self-healing capacity (Sivakumar Babu et al., 2001) of the bentonite.

In many cases, destructive boundary conditions are found which combine two or more of the influencing factors mentioned above. The combined impact of drying and subsequential wetting with divalent salt solutions (e.g. $CaCl_2$) is an example of this (De Camillis et al., 2016). Due to the high importance of barrier systems, much work has been devoted to understand the impact of divalent salt solutions on the hydro-mechanical behaviour of bentonite (Mesri and Olson, 1971; Petrov and Rowe, 1997; Thyagaraj and Salini, 2015; Thyagaraj and Julina, 2019) and the coupled impact of cation exchange and drying. In many cases, the sensitivity of bentonite for environmental influences is the motivation behind polymer modification (Daniels et al., 2003; Scalia et al., 2014; De Camillis et al., 2016; De Camillis et al., 2017).

Water retention and crack propagation of bentonite subjected to $CaCl_2$

For geotechnical applications, suction induced release of water and volumetric shrinkage pose challenges. In engineering practice, shrinkage was identified as a destructive factor for the integrity of GCLs, as cracks provide unrestricted flow-paths for leachate (Miller et al., 1998). Local volumetric strain caused by shrinkage triggers cracks on a larger scale. Propagation of cracks due to desiccation has been intensively studied in the recent years (Scherer, 1990; Colina and Roux, 2000; Tang et al., 2008; Peron et al., 2009; Lazarus and Pauchard, 2011; Shin and Santamarina, 2011; DeCarlo and Shokri, 2014; Schanz et al., 2016). In this context various factors were identified as relevant for the formation of cracks in clays. Roughly, they can be categorized as: i) material properties (e.g. grain size distribution, mineralogical composition, pore water chemistry), ii) boundary conditions during desiccation (suction stress, mechanical stress) and iii) geometric factors (e.g. layer thickness, size of the sample, sample base properties).

Lieske et al. (2020 (b.)) studied the cracking behaviour of commercially available geosynthetic clay liners (GCL) filled with a sodium bentonite. A GCL as shown in Figure 3.7 is a combination of a natural clayey filler and synthetic compounds which combines several of the above mentioned factors that influence crack propagation in a very specific way. For example, the fibres in the bentonite create a potential weak zone and at the same time cause a certain mechanical load by constraining swelling.

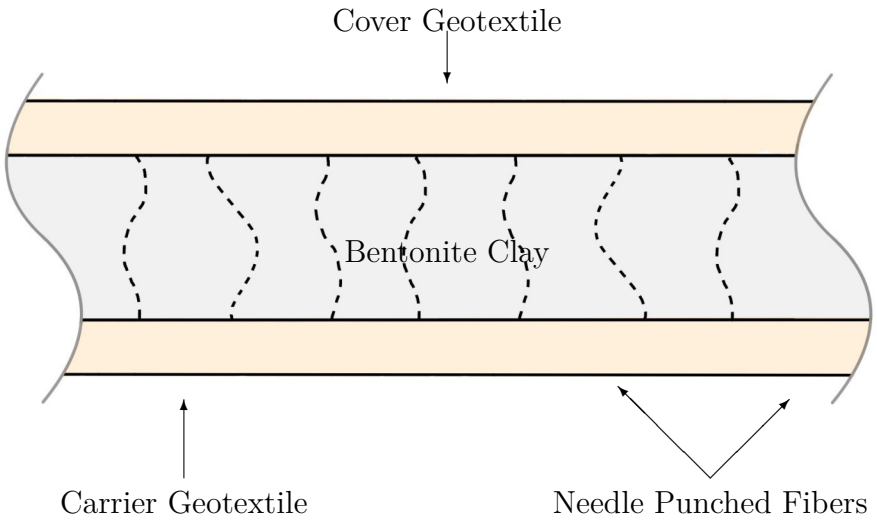

Figure 3.7: Schematic cross-section of a GCL

In the study, GCL specimens in a size of 42.5 cm × 30.5 cm were stepwise dried at 30°C and rewetted in deionised water, 0.05 mol/l and 0.5 mol/l $CaCl_2$-solution. An additional sample was prehydrated in deionised water and rewetted in a 0.05 mol/l $CaCl_2$-solution after the first drying interval. Crack evolution was studied by means of X-ray imaging. The evolution of cracks with progressive decrease of the water content and after rewetting is shown in Figure 3.8. The results clearly show the significant impact of the divalent salt on the cracking behaviour. The cracks in the sample saturated with deionised water were found with less but more pronounced cracks. However, the samples subjected to $CaCl_2$-solutions show very fine cracks but, in a higher quantity. The crack width decreased with increasing salt concentration, so that with a 0.5 mol $CaCl_2$ solution, cracks were no longer detectable with the used X-ray device.

The different crack evolution was reasoned by the impact of divalent salt on the microfabric. Cracks are generally believed to occur if the normal stress in a soil exceeds its tensile

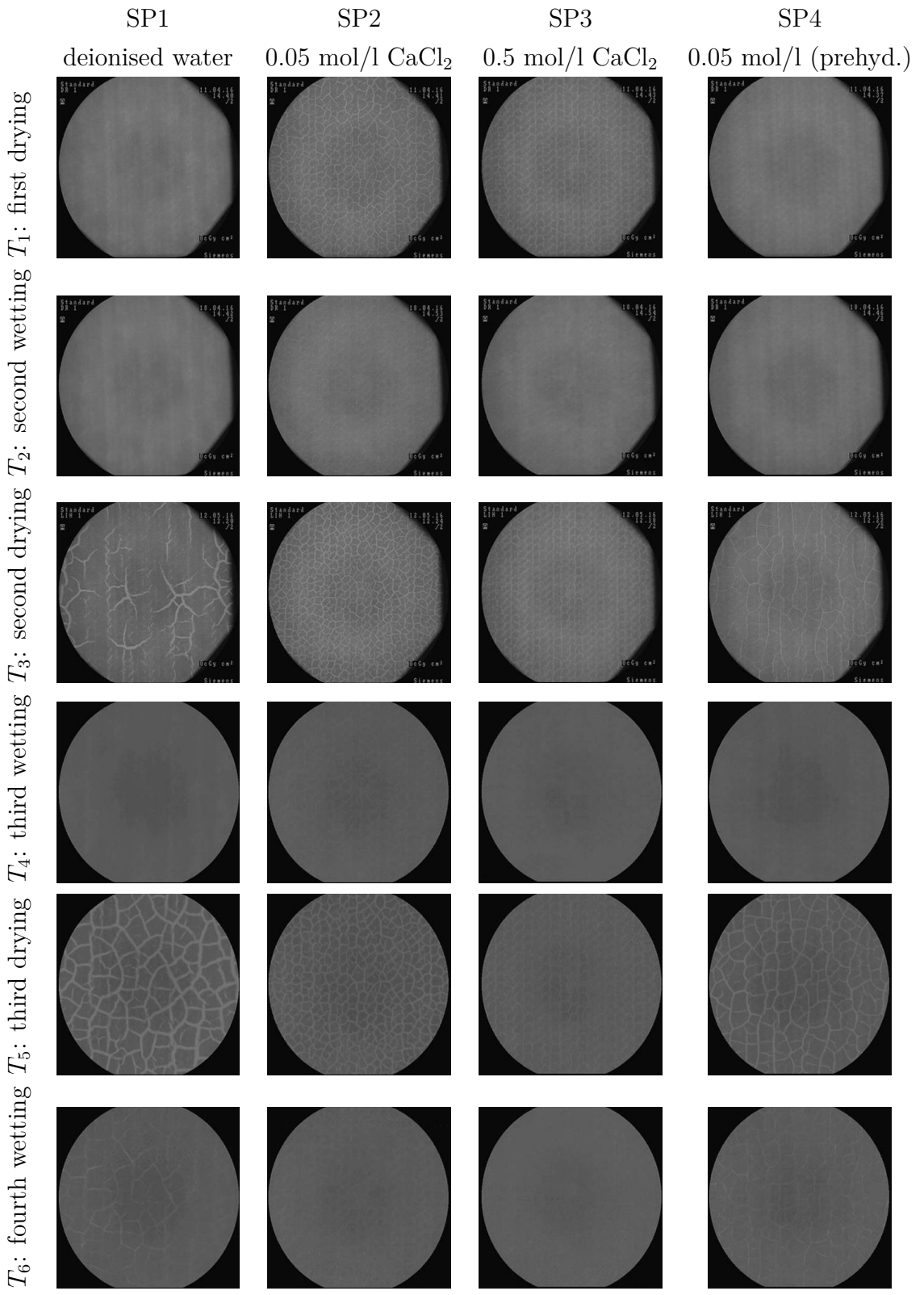

Figure 3.8: Crack patterns for SP1, SP2, SP3 and SP4 for different wetting and drying periodes (T_1-T_6). Note: X-ray device was replaced after second drying intervall

strength. Since the tensile strength of a soil is usually low and there are no standardised experimental techniques, it is rarely measured in soil mechanical studies. However, Zeh and Witt (2007) provided a set of experimental data of tensile strengths determined at different levels of suction and on samples compacted on the wet and dry side of the proctor curve and at the proctor optimum, respectively. The experimental results give evidence that tensile strength of a sample increases with suction. However, the magnitude of tensile strength follows the order of dry side of proctor $\leq$ proctor optimum $\leq$ wet side of the proctor at a given suction. Those observations give further evidence for the importance of fabric. Fine grained soils compacted on the wet side of the proctor maximum are found in a dispersed soil structure, whereas those compacted on the dry side are found in a more flocculated structure (Lambe, 1958). The results therefore reveal that soils with a unimodal distribution of small to medium pores are found with higher strength than those with a major number of large pores. Even though there are distinct differences between GCLs and proctor compacted soils, the bentonite in a GCL is also found in a bi-modal pore size distribution (Acikel, Gates, Singh, Bouazza, Fredlund and Rowe, 2018) and $CaCl_2$-solution has been identified to alter the fabric of bentonite to a more aggregated state (Thyagaraj and Salini, 2015).

Quantification of the cracks was performed by means of image analysis. The crack intensity factor (CIF) is defined as the ratio of the crack area divided by the total area. The relation between the CIFs of the different drying stages and their respective gravimetric water content is given in Figure 3.9, where the water content has been corrected by the mass of salt, that remains as solid after oven drying. The graph follows three different trends which are divided into initial shrinkage (dewatering of the geotextiles and large pores), followed by normal shrinkage and finally residual shrinkage. This trend is characterised by only minor influences of salt, as all points show only small deviations in the trends, making the CIF a function of gravimetric water content only. By contrast, the water retention behaviour of the bentonite in the GCL, and thus the water content, is significantly affected, as the presence of salt in the pore fluid increases the chemical potential and thus the osmotic component of the soil suction (Thyagaraj and Salini, 2015; Lu and Khorshidi, 2015). Furthermore, salt induced flocculation is accompanied by a change of capillary and hydration forces (Salles et al., 2009; Thyagaraj and Salini, 2015).

In addition, the time which is needed to release water from a GCL is directly affected by $CaCl_2$. Given that the duration of a drying event is limited, the rate at which water is released from the GCL is a key parameter for assessing crack propagation and the resilience of a GCL to regain its barrier properties after drying. The results of small-scale

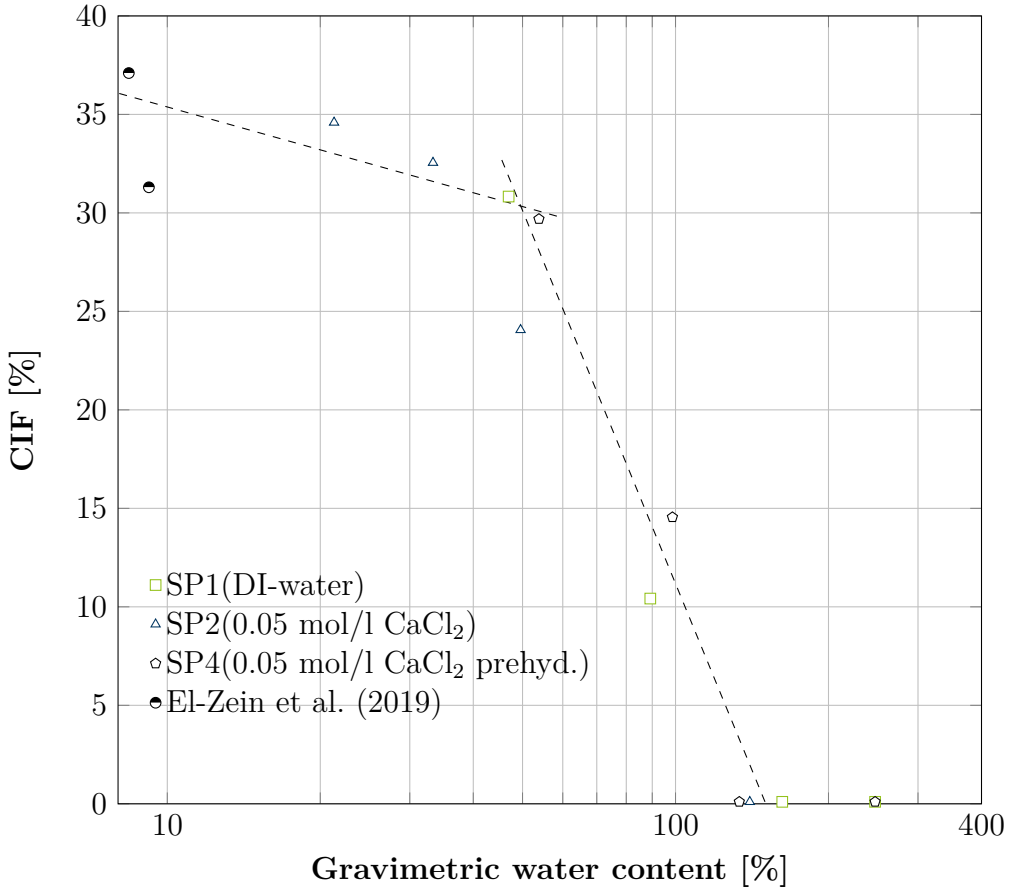

Figure 3.9: Measured crack intensity factor (CIF) against water content of the GCL

drying tests performed in constant volume micro-cells are plotted in Figure 3.10. The plot shows the evolution of the gravimetric water content with time at a constant suction of 20 MPa. All samples were saturated (at constant volume) prior to drying at 20 MPa. The data in Figure 3.10 shows that equilibrium water content was hardly reached for all samples after 20 days of drying. However, after 20 days the points of RB3 (0.50 mol/l) have crossed those of RB2 (0.05 mol/l) and RB4 (0.05 mol/l; prehyd.), indicating that the higher salt concentration yields a higher equilibrium water content.

The mentioned study shows the connection of fabric and physico-chemical forces acting on the mineral surfaces and the interlayer. At the same time, it gives insight into the sensitivity of bentonite to environmental conditions, as its hydro-mechanical behaviour is in turn strongly linked to physico-chemical forces.

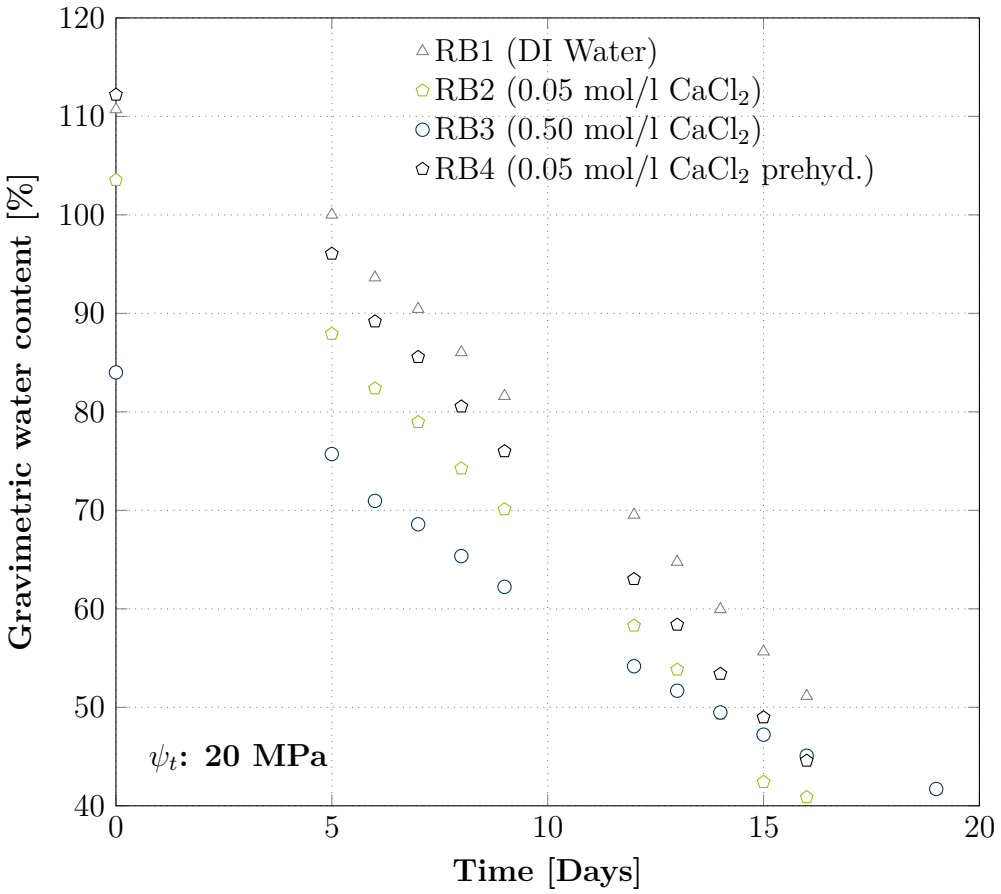

Figure 3.10: Evolution of gravimetric water content over time of the bentonite subjected to suction of 20 MPa (Lieske et al., 2020 (b.))

3.3 Polymer-enhanced clays

In geotechnical engineering, polymers are used to modify clays for the use in clay barriers and several approaches to modify smectite with respect to barrier applications excist (Di Emidio et al., 2017). One of the early polymer-enhanced barrier systems is 'trisoplast'. This mixture of mainly sand (89.1%) and a minor amount of clay and polymer (10.9%) is widely used in compacted clay liners. The material combines the high friction angle of sand with the low permeability of bentonite when located in the pores of the sand. The polymer which has been described to be similar to 'polyethylene' is believed to stabilise the bentonite particles by bridging (Schanz et al., 2004).

Di Emidio (2010) presents an approach to modify sodium bentonite by an addition of sodium CMC (see Chapter 2.3). The modification process, referred to as 'hyper-clay' treatment, involves the following steps: (1.) bentonite being dissolved in water to increase

the distance between the layers, (2.) mixing the bentonite suspension and the polymer solution and (3.) drying the mixture to bond the polymers to the clay surface. The latter is due to the few adsorption possibilities of a negatively charged polymer to a negatively charged clay. It has been shown that the treatment significantly improves the swelling and sealing properties of bentonite, even when exposed to salt solutions. Furthermore, it has been demonstrated that the water retention behaviour as well as the crack resistance during drying are improved (De Camillis et al., 2016). The improvement was attributed to the inclusion of polymers in the particle interlayer and thus to a more pronounced interlayer swelling.

In addition to approaches in which the improvement of the sealing performance is mainly reasoned by the modification of the clay minerals, the so-called bentonite polymer nanocomposites (BPN) and bentonite-polymer mixtures (B-P) should be mentioned (Scalia et al., 2014; Tian et al., 2016). In these materials, the effect of polymer has been attributed to the formation of viscous poreclogger in inter-aggregate pores and therefore in the main flow path of water during saturation. Due to this significant increase of viscosity caused by the polymer a decrease of permeability was achieved (Scalia et al., 2014; Tian et al., 2016).

Zumsteg et al. (2013) used polymer and foam to reduce the sticking potential of kaolinite for mechanised tunnelling applications. Zhang et al. (2020) demonstrated the potential of polymers to improve the cement treatment of hydraulically dredged mud by increasing the flocculation efficiency of the process and the mechanical strength of the treated material.

The previous example demonstrate the versatile potential of polymers to manipulate soil properties. In the following, an insight into the polymer-clay interaction is given. After a brief introduction to adsorption morphology and properties, the adsorption and modification of clays by polymers is specifically addressed. While there are a variety of parameters to characterise the polymers (as described in Section 2.2.2), the categorisation of the chapter follows the charge properties of the polymers and thus the possible interactions with the negative smectite surface.

3.3.1 Mechanisms of polymer-clay interaction

The attachment of polymer chains on charged smectite surfaces is widely accepted to occur in geometric arrangements that can be described by trains, loops and tails (Figure 3.11). Trains are polymer segments tightly bonded to the mineral surface, whereas loops are segments dangling from the surface but bonded by trains on both sides. Tails are free

polymer ends just fixed on one side. The arrangement of loops, tails and trains and the resulting constitution of the clay-water-interface strongly depends on the arrangement of polymer chains during adsorption (Fleer et al., 1988). In the case of charged polymers, the geometric arrangement of the charges on the mineral surface and in the polymer chain has a crucial effect (Steudel et al., 2020). The strong electrostatic interactions between the charges determine the location where the polymer chain attaches the smectite surface, thus it affects the adsorption morphology.

Entropic effects cause uncharged linear polymer chains in solution to arrange in dense coils and charged polymers in a more stretched geometry due to intra-chain repulsion (Fleer et al., 1988; Theng, 2012). Furthermore, the shape of polymer-coils depends upon boundary conditions such as pH-value, salinity, concentration, and temperature, which have a crucial effect on macroscopic properties and adsorption behaviour (Fleer et al., 1988; Roiter and Minko, 2005). Consequently coiled polymers are found to adsorb with a significant number of loops and tails while unfolded polymer chains occur with a high amount of trains (Fleer et al., 1988). Figure 3.12 shows the quantitative development of the proportions of loops, tails and trains with increasing number of molecules per volume and for different solvent qualities, where $\chi = 0$ is a good solvent (swollen state of the polymer coil) and $\chi = 0.5$ corresponds to a theta solvent, where the polymer is found in a less swollen state. This theoretical consideration of a polymer chain composed of 1000 monomer segments shows the importance of polymer coil size for the adsorption characteristics.

When the number of polymer segments per volume of the solvent is low (diluted regime) polymer chains do not have to compete for adsorption sides, so that they can adsorb in a flat way with major number of trains. However, as polymers in a theta solvent are found in a more coiled state than in a good solvent, they adsorb with a lower number

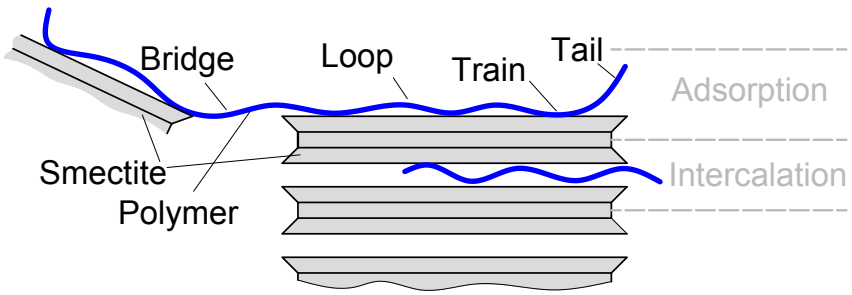

Figure 3.11: Adsorption, bridging and intercalation of polymers in a smectite (Lieske et al., 2022)

of trains in comparison to a fully swollen polymer chain. When increasing the number of polymers per volume of the solvent, inter chain interaction becomes more relevant and polymers starts to reduce their volume, as this is a thermodynamically preferential state. Therefore, differences caused by solvent quality become less relevant. Further, competition for adsorption sides decreases the space of possible adsorption and therefore of trains. As the number of tails (free-ends of polymer chains) increases with the number of adsorbed polymers, it is also associated with the increase of concentration. Polymer-clay interaction is therefore strongly connected to the composition of the raw materials and the boundary conditions during mixing (Fleer et al., 1988; Wilkinson et al., 2017, 2018).

The adsorption process and the resulting modification of surface properties is generally believed as irreversible, since simultaneous detachment of all adsorbed polymer segments is practically impossible (Ueda and Harada, 1968; Breen, 1999; Theng, 2012). This behaviour of polymers adsorbed on several points of a smectite surface is also described as 'octopus-effect'. Beside of adsorption on surfaces, intercalation into the interlayer of smectite particles (see Figure 3.11) was observed for several cationic polymers, accompanied by an increase of interlayer space (Theng, 2012). Some studies conducted on modification of smectite using anionic polymers show that intercalation does not take place (Theng, 2012) while other studies claim an intercalation (Di Emidio, 2010). Theng (2012) states, that intercalation of polymer chains having negatively charged segments is mainly caused by the intercalation of the non-ionic parts of the polymer chain whereas the anionic groups are repealed by the negatively charged clay surface.

Another important effect attributed to polymer-modification is bridging (see Figure 3.11). When a polymer chain is long enough to span the distance between adsorption sites located on different clay surfaces, polymer-bridging takes place. The probability of forming such a polymer bridge depends upon the distance between the clay solids and on the length of the individual polymer chains. In the case of linear polymers, the molecular weight of the polymer correlates to the chain length. However, as it has been discussed above, the total chain length of a polymer and its relevant dimension in solution are not essentially the same as linear flexible polymers are commonly found in a more or less coiled state, so that boundary conditions likewise affect the bridging probability (Theng, 2012). The impact of such polymer bridges might be compared to that of the bonds typically found in natural structured soils (Lieske et al., 2021). In contrast to these natural inter-particular cementations, polymer bridges are flexible and can induce properties that cannot be captured by common soil mechanical models.

The aforementioned mechanisms of polymer-clay interaction and the models of adsorption morphology require the availability of clay surfaces for the polymers. Several studies are therefore performed under extremely diluted conditions (Stutzmann and Siffert, 1977; Ueda and Harada, 1968; Denoyel et al., 1990; Theng, 2012).

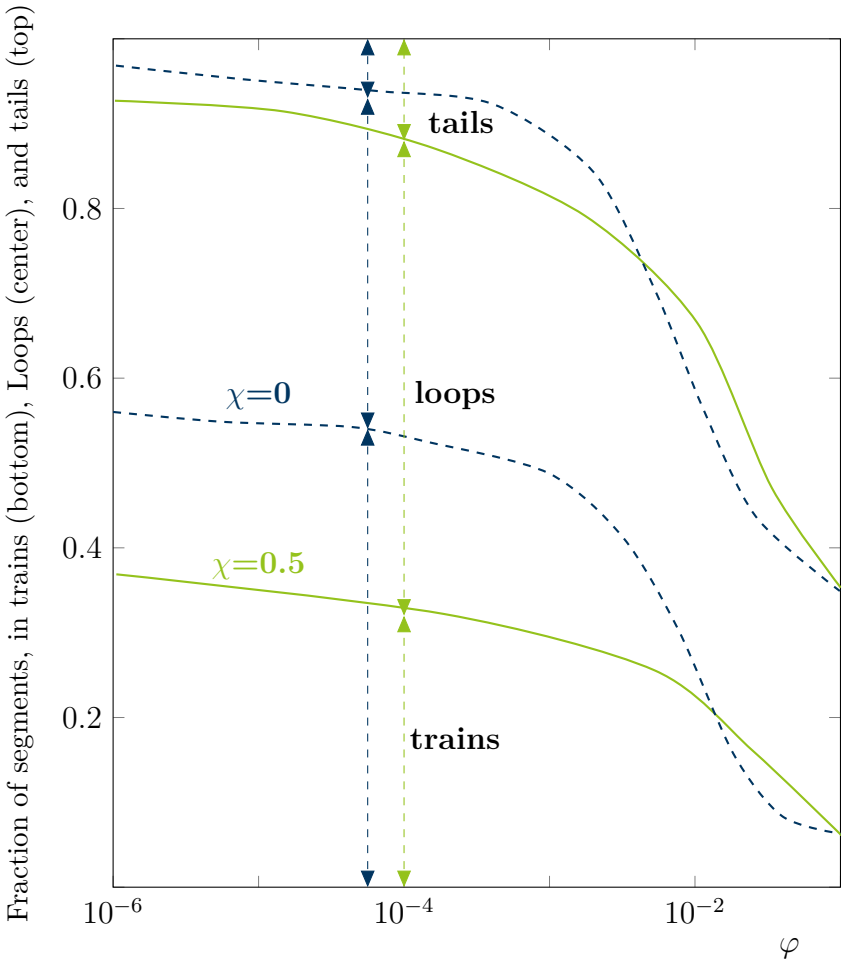

Figure 3.12: Fraction of segments, in trains (bottom), Loops (center), and tails (top) (modified from Fleer et al. (1988))

3.3.2 Interaction of cationic polymers with smectite

When brought in contact with smectites, cationic polymers (also referred to as polycations) interact via electrostatic (coulombic) attractions between the charged constituents of the polymer chain and the negatively charged basal surfaces of the smectite (Breen, 1999). Further, ion-dipole attraction between uncharged polar constituents of the polymer backbone and the exchangeable cations as well as hydrogen bonding between polar polymer-parts and water attracted by the cations might contribute to the adsorption of polycations on smectite surfaces (Deng, Dixon, White, Loeppert and Juo, 2006). The mode of adsorption of a cationic polymer on a smectite surface is shown in Figure 3.13 (a.).

Charged segments of the polymer irreversibly replace cations from the smectite surface as detachment of all bonds followed by a diffusion of the polymer from the clay surface is practically impossible. The consequence is a reduction of the number of exchangeable cations (Ueda and Harada, 1968; Breen, 1999).

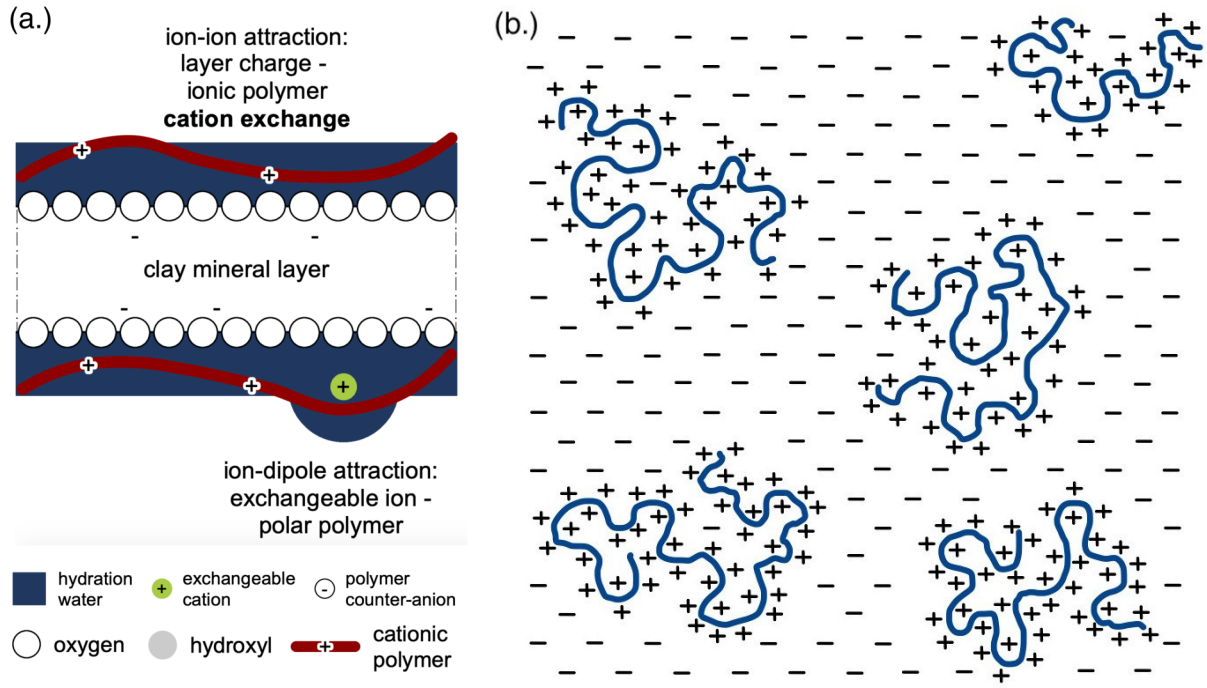

Figure 3.13: Adsorption of cationic polymers on smectite surfaces: (a.) Polymer-clay mechanisms (Haase, 2017), (b.) Adsorption of polymers in patches (modified after Bergaya et al. (2006)).

Relying on the observation of an increase in anion exchange capacity during cationic modification, Ueda and Harada (1968) indicated that non-adsorbed charged polymer segments can yield a surplus of positive charge in the smectite-polymer-water system and therefore induce a partial charge neutralisation or charge revision of the initially negatively charged clay surface after adsorption. Such excess charge may be caused by geometric effects, e.g. when the charge density in the polymer is higher than the charge density of the clay surface (Breen, 1999). Further, cationic polymers are believed to adsorb in localised patches rather than covering the whole surface of a charged mineral (Szilagyi et al., 2014). Figure 3.13 (b.) shows an idealised picture of polymer chains adsorbed in shape of a patch on a negatively charged smecite surface. In case of adsorbed polycations having a higher charge density than the clay surface a partial positive charge reversion of the clay surface is obtained. Unaltered clay surfaces remain negatively charged. The attraction of unaltered negatively charged and modified positively charged areas of adjacent clay minerals is termed patch flocculation (Bergaya et al., 2006). Patch flocculation is generally believed to be reversible and weaker than salt flocculation (Theng, 2012). Patch flocculation can be accompanied by steric effects, where patches of positive charge repeal each other.

In addition to the aforementioned mechanism of 'patch-flocculation', bridging is crucial for the understanding of macroscopic properties of modified clay (Chenu and Guérif, 1991; Theng, 2012). Due to their stretched shape, cationic polymers are more likely to be able to span the distance between two clay surfaces as polymers in a coiled conformation. The adsorption forces are strong, which is why cationic polymers are prone to shape strong interparticle bridges. From a colloid chemical point of view polymer briges are considered as additional attractive force as they prevent clay minerals to be seperated by swelling (Szilagyi et al., 2014). From a soil mechanical point of view polymer bridges might be understood as a repulsive force as they stabilise the soil structure and therefore increase compaction resistance.

The amendment of clays by the addition of cationic polymers is attributed to a significant increase in mechanical strength (Chenu and Guérif, 1991). Therefore, it is applied to increase the resistance against erosion (Inbar et al., 2015) and to increase stability when subjected to freeze and desiccation (Daniels et al., 2003). Beside these effects on the mechanical behaviour, flocculation induced flow paths and reduced diffuse double layer swelling are accompanied with an increase in permeability (Inyang and Bae, 2005; Di Emidio et al., 2017; Haase and Schanz, 2016). Therefore, the use of cationic polymers takes place only under special conditions, where mechanical strength might play a more important role than permeability i.e. in multi-barrier systems (Inyang and Bae, 2005).

3.3.3 Anionic polymers

In contrast to positively charged polymers, for negatively charged polymers there are only few possibilities to attach to the widely negatively charged smectite. The negatively charged polymers can interact with the positively charged edges of a smectite in terms of ion-ion-attraction. This mechanism, known as 'anion exchange' depends on the charge of the edges, variable depending on the pH-value (Laird, 1997). Further, Laird (1997) describes a mechanism which he termed 'cation bridging'. Local positive charges caused by cations adsorbed on the clay surface attract negatively charged polymer groups by local ion-ion attraction. This mechanism is solely attributed to multivalent exchangeable cations (Laird, 1997). The different modes of interaction between anionic polymers and 2:1-minerals is outlined in Figure 3.14.

However, despite or in particular for this reason, anionic polymers play a prominent role in the treatment of smectite and this group of polymers has probably most frequently been used to modify clays for barrier applications (Di Emidio et al., 2017). Due to interchain repulsion of the ionic groups, negatively charged polymers are mostly found in a more stretched geometry as their non-ionic counterparts. Further, as there are only few possibilities for adsorption on clays, negatively charged polymers are not widely bond. The polymer chains are dangling away from the clay surface and can therefore interact

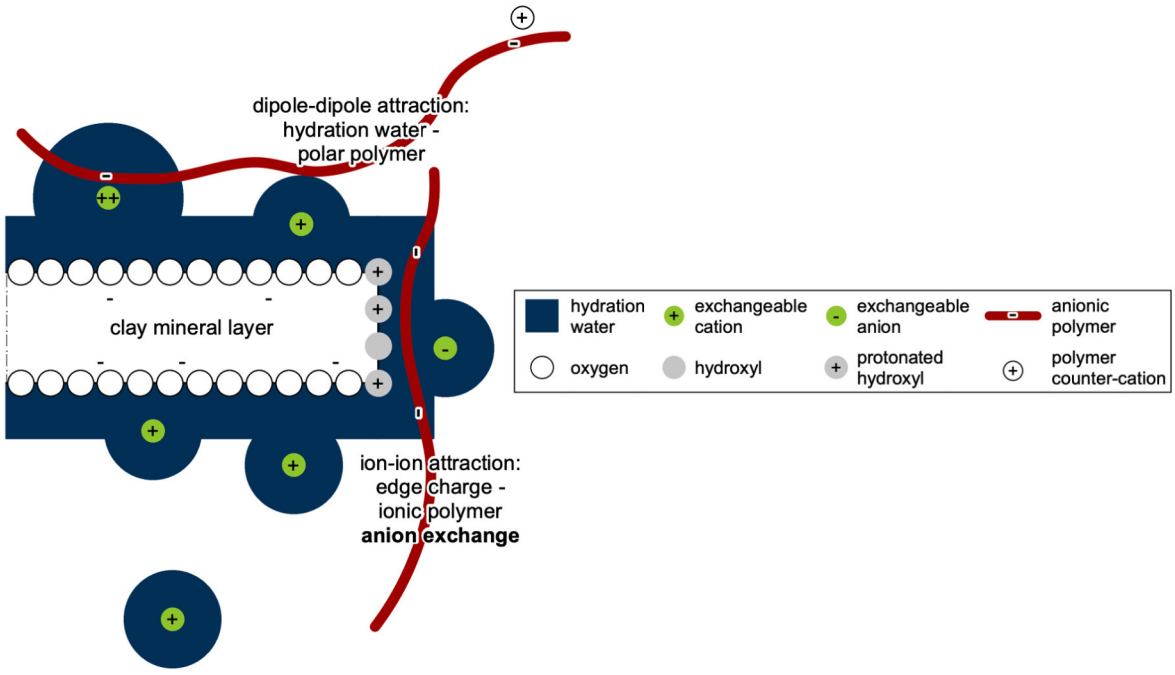

Figure 3.14: Adsorption of anionic polymers on smectite surfaces (Haase, 2017)

with the surfaces of other clay minerals. Theng (2012) proposed the picture of a 'ribbon-like structure' caused by an edge to edge flocculation. The charge density is consequently an important factor for polymer-clay interaction. Due to repulsion between the negative charge of the polymer chain and the clay surface, the possibility of a highly charged polymer to be adsorbed is lower than that of one with a lower charge density. Vice versa, with the decrease of charge density polymer chains are found in a less stretched geometry and the probability to be adsorbed on multiple clay-particles decreases (Theng, 2012).

In case of 'hyper-clay' treatment, the polymers are believed to be forced to be adsorbed on the mineral surface due to drying. The superior behaviour of clay treated in such a way in comparison to untreated clay is reasoned by the practically impossible cation exchange and the improved interlayer swelling, as the intercalated polymers increase the space between the clay layers caused by the surplus of negative charge (Di Emidio, 2010; Di Emidio et al., 2017). Following two different approaches to modify bentonite, Scalia et al. (2014) and Tian et al. (2016) discussed the 'clogging' of large pores as the mechanism causing the improved barrier properties of the modified clay. This effect is again made possible by the fact that there are only a few points of attachment between the polymers and the clay surface.

3.3.4 Non-ionic polymers

In contrast to their charged counterparts, non-ionic flexible polymers are commonly found in a more coiled geometry due to the absence of intra-chain repulsion of the charged groups. When inducing external energy (e.g. caused by shear or other tensile stresses), polymer chains change their conformation. However, when the energy is released, polymers rearrange again in their initial state. Since the driving force for the recoiling is an increase in entropy, such polymers are also called 'entropic spring' or the respective characteristic 'entropic elasticity' (Tanaka, 2011).

One of the important properties for polymer-clay interaction of this type of polymer is hydrophilic behaviour i.e. polarity. The polar groups of the polymer chain can either be attracted to a clay surface due to dipole-ion interaction between the exchangeable cations or by dipole-dipole interaction with water adsorbed on the clay surface and the hydration shells of the cations (Deng, Dixon, White, Loeppert and Juo, 2006; Theng, 2012). A general sketch of non-ionic polymer adsorption on a 2:1 clay mineral is demonstrated in Figure 3.15. As non-ionic groups are also present in ionic polymers, they can also contribute to clay-polymer-interaction (Deng, Dixon, White, Loeppert and Juo, 2006). The

aforementioned mechanisms of polymer-clay interaction are attributed to strong dipoles as present in case of polyacrylamides or polyvinyl alcohols (Theng, 2012). Weak dipoles or non-polar dipoles can only be adsorbed on smectites in the presence of additional surfactants.

Due to their generally more coiled arrangement in solution, non-ionic polymers are believed to adsorb with a pronounced number of loops. A theoretical approach to calculate osmotic swelling of smectite including the effect of adsorbed non-ionic polymers has been presented by Haase and Schanz (2016). In that study, a theoretical approach to consider the effects of non-ionic polymers on the potential distribution in the diffuse double layer, expressed by the Poisson-Boltzmann expression (see Equation (3.2)), has been adopted for platy charged surfaces as found in smectite. The modified Equation (3.6), which is based on the Flory-Huggins theory to describe the behaviour of polymers in solution has originally been proposed by Brooks (1973).

$$\frac{d^2\Psi}{dx^2} = \left(\frac{2n_0\nu e'}{\varepsilon}\right) \sinh\left(\frac{\nu e'\psi}{kT} - \beta(x)\right) \tag{3.6}$$

The parameter β which has been added to the original formulation, is definied as

$$\beta(x) = (\phi_p(x) - \phi_{pb}) \cdot (1 - \chi_{sp} + \chi_{ip} - \chi_{si}) \tag{3.7}$$

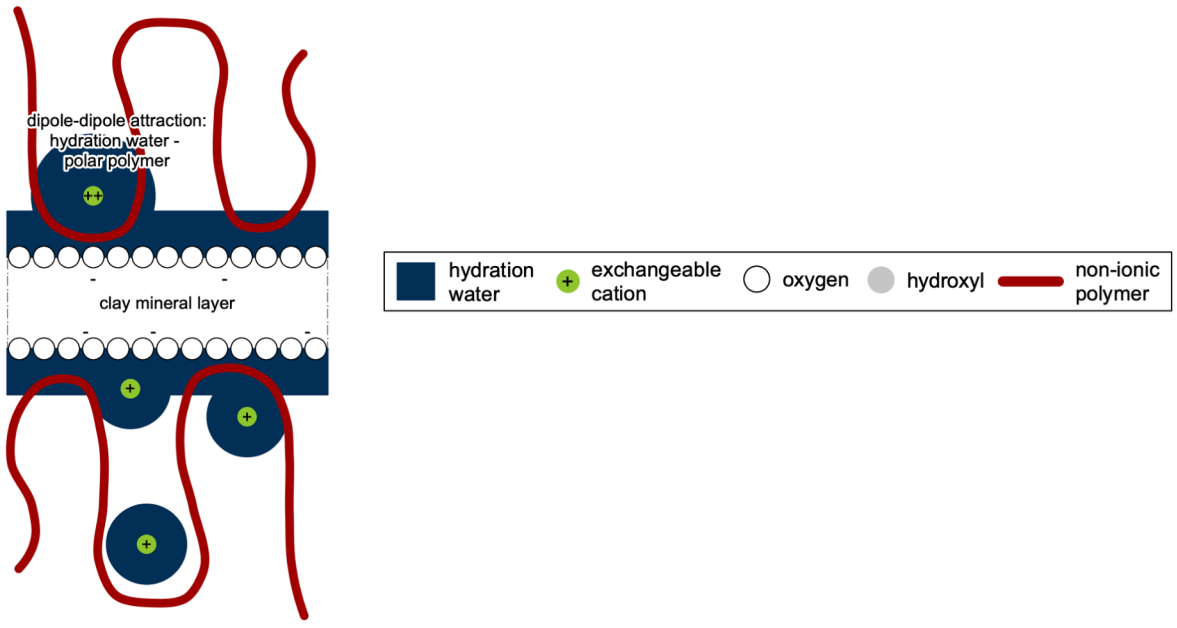

Figure 3.15: Adsorption of non-ionic polymers on smectite surfaces (Haase, 2017)

where ϕ_p (-) is the volume fraction occupied by the polymer and the subscript b refers to the bulk face. The interaction parameter χ has three components, where the subscribts s, p and i refer to the solvent, polymer and dissociation ions. Haase and Schanz (2016) used the Equation (3.6) to approximate the volumetric behaviour of bentonite, where the parameter β has been used as a fitting parameter. A determination of the interaction parameters in the context of geotechnical applications has not yet been carried out.

However, the work of Lee and Schlautman (2015) gives evidence that the arrangement of polymers in loops, tails and trains might not be valid in high concentration areas. Beyond overlap concentration mutual interference between polymers determine adsorption morphology so that the chains might be attached as interrelated polymer lumps rather than isolated chains. Likewise, Rao et al. (1993) found a decline in liquid limit after modification of a clay using a non-ionic polymer which he reasoned by impediment of swelling by polymer induced aggregation.

Beside the study of Haase (2017) which demonstrates that the modification of smectites using non-ionic polymers extended diffuse double layer swelling, other studies also demonstrated the beneficial impact on other barrier properties caused by the addition of non-ionic polymers. Inyang and Bae (2004) indicated the decrease of desiccation rate, which has been identified as a crucial factor for crack formation (Lieske et al., 2020 (b.)).

4 Materials and Methods

In the following chapter bentonite, polymers and the modification procedure are presented. Furthermore, the experimental methods to study the hydro-mechanical behaviour of the polymer modified smectite are described. The chapter begins with an overview of the research program. Afterwards, the properties of both the polymer and the bentonite as a raw material are presented, whereas the characteristics of the modified clay is presented in Chapter 5 and 6, respectively.

4.1 Research program

The aim of the current study was to outline how polymer properties affect the behaviour of modified bentonite, or more in detail: how does the basic polymer constitution influence the macroscopic properties of a bentonite modified with the respective polymer? It was convenient to use synthetic polymers based on acrylamide, as they are available in a significant variety of properties (molecular weight, type of charge, charge densities). The bentonite used in the current study was a sodium bentonite (MX80) which has been thoroughly investigated in numerous studies in literature with regard to its geotechnical and mineralogical properties.

The research program can be divided into two parts: the first part is dealing with the modification of bentonite using cationic and non-ionic polymers, varying polymer properties (e.g. molecular weight and charge density in case of cationic polymers). Due to their nature, these polymers can be adsorbed by bentonites and accordingly change the properties of the clay minerals by modifying surfaces and interlayers as well as by the formation of polymer bridges. Previous studies have shown, however, that anionic polyacrylamides can only be adsorbed to a very small extent using the intended modification procedure (Haase, 2017). However, due to their particular practical relevance, the second part of the thesis is devoted to anionic polymers. The experimental program was designed with a special emphasis on practical applications. An designedoverview of the tests conducted in the current study is given in Table 4.1.

Table 4.1: Overview of the experimental methods and variations employed in the current study

Polymer charge	Cationic	Non-ionic	Anionic
Clay		MX80	
Mixing method		Wet mixing	Dry mixing
Clay/polymer ratio		Adsorption max.	1 % /10%
Methods		Adsorption behavior Microstructural investigations Atterberg limits 1D-compression Unconfined water retention	Swelling Pressure Hydraulic conductivity
Variations	Charge density Molecular weight Post-Mixing treatment	Molecular weight Post-Mixing treatment	Mixing ratios

4.2 Materials

4.2.1 Polymer

Commercially available polymers provided by SNF (Andrezieux, France) were used in the current study. All the polymers used were initially present as white granules with a hygroscopic water content (geotechnical water content) in the range of 4 to 12 %. Figure 4.1 shows micrographs of the dry polymer obtained using a light microscope. The granules occur with a variability in sizes and shape. The individual polymer grains are translucent with a gleaming surface. When brought into solution all polymers show characteristic features of polymers in solution (e.g., a rapid increase in viscosity upon increase in concentration).

According to their charge properties, the polymer chains are homopolymers (non-ionic polymers) or copolymers (anionic and cationic polymers). The molecular configuration of the monomers incorporated in the polymers is shown in Figure 4.2. The polymer backbone of all polymers is formed by acrylamide (prop-2-enamide) monomers. To obtain a positive charge, the polymer chains of the cationic copolymers are a variation of acrylamide and methylated dimethylaminoethylacrylat ([2-(Acryloyloxy)ethyl]trimethylammonium chloride). The positive charge is balanced by chlorid ions. The negatively charged polymers are composed of acrylamid monomers and monomers of acrylic acid.

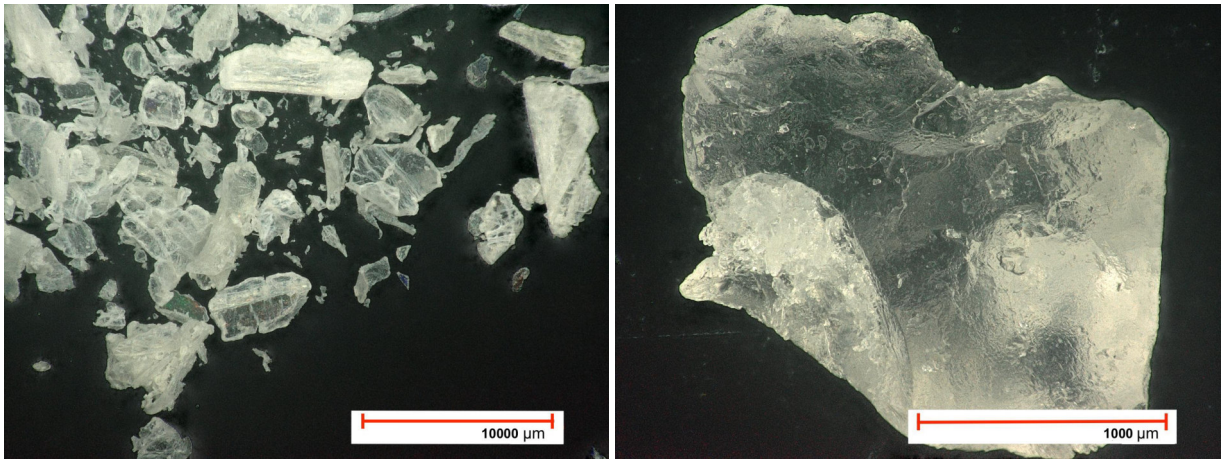

Figure 4.1: Micrographs of the dry polymer obtained using a light microscope

All the polymers employed are flexible chain polymers of linear structure, with varying molecular weight (Long [L], Medium [M], Short [S] and very Short [VS]) and ionicity (τ=40, τ=55). Three of the used polymers have the same charge density and solely differ in their average molecular weight, whereas the fourth polymer used has a higher charge density and a lower molecular weight. An overview of the polymers used and the abbreviations of the respective mixtures are listed in Table 4.2. Material that has been dried after mixing and processed into a powder is marked with a asterisk in the index.

One parameter that is varied in the study is the molecular weight. As it has been discussed in Chapter 2, the molecular weight correlates to the length of the chain in case of linear polymers. Due to the intrinsic polydispersity of the polymers, all molecular weights are given as bandwidth. It has been discussed in Chapter 2, that polymers are commonly found in a coiled state or globule like configuration depending on boundary conditions. The radius of gyration, a measure for the coil dimension is therefore commonly considered to quantify the size of a polymer in solution instead of the length of the fully stretched chain. Considering the uncoiled length of a polymer, however, is helpful in visualising the total dimensions of the respective macromolecule in comparison to a smectite mineral. This length is called the contour length and is calculated by multiplying the number of repeat units per polymer by the length of one repeat unit. Figure 4.3 gives an overview of the respective chains lengths in a theoretical, entirely stretched geometry. The length of a carbon-carbon bond was assumed to be 147 pm, and the number of bonds was calculated by dividing the molecular weight of the polymer by the molecular weight of the monomers.

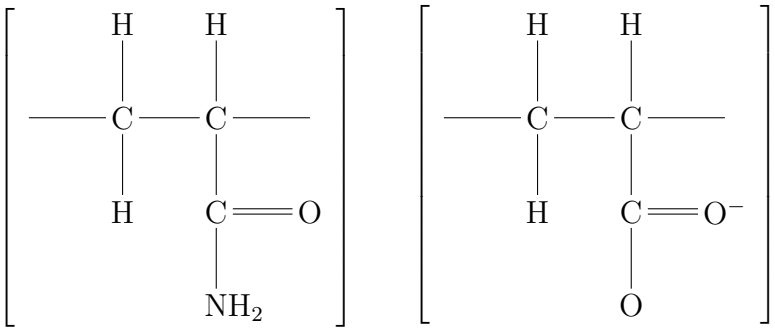

Acrylamide (non-ionic)

Acrylic acid (anionic)

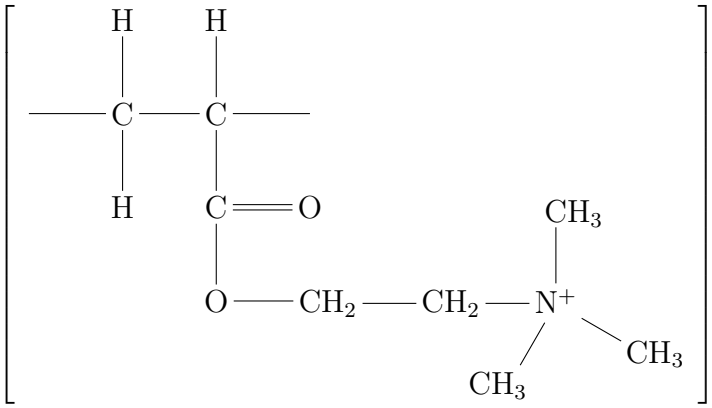

Methylated dimethylaminoethylacrylat (cationic)

Figure 4.2: Monomers of the polymers used in the study

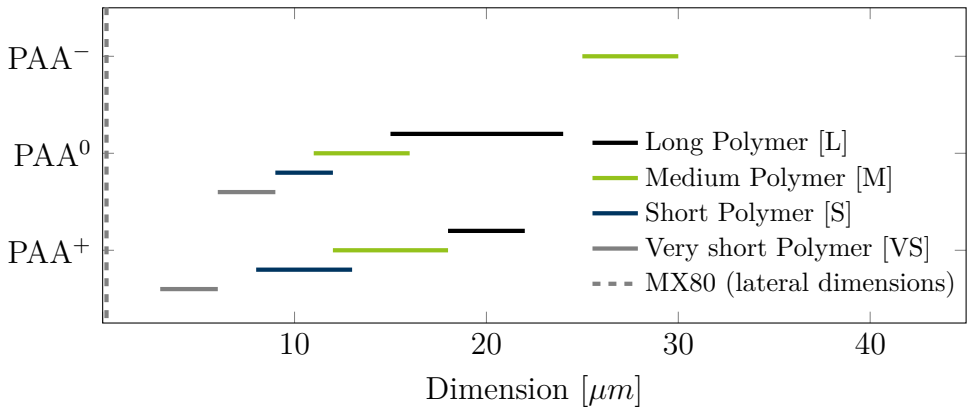

Figure 4.3: Dimensions of the anionic (PAA^-), the non-ionic (PAA^0) and the cationic (PAA^+) polymers in a fully uncoiled state

Name	Charge	Ionicity [%]	Mol. weight [Mg/mol]	abbr. mixture
FO4490VHM	cationic	40	9.5 - 12	$PAA^{+}_{L,\tau 40}$
FO4490SSH	cationic	40	7.0 - 9.5	$PAA^{+}_{M,\tau 40}$
FO4490	cationic	40	9.5 - 4.5	$PAA^{+}_{S,\tau 40}/PAA^{+}_{S*,\tau 40}$
FO4490MPM	cationic	55	1.8 - 3.1	$PAA^{+}_{VS,\tau 55}/PAA^{+}_{VS*,\tau 55}$
FA4490VHM	non-ionic	0	12 - 20	PAA^{0}_{L*}
FA4490SH	non-ionic	0	9.0 - 13	PAA^{0}_{M*}
FA4490	non-ionic	0	7.5 - 10	PAA^{0}_{S*}
FA4490BPM	non-ionic	0	5.0 - 7.0	PAA^{0}_{VS}/ PAA^{0}_{VS*}
AN945SH	anionic	40	13 - 17	$PAA^{-}_{M,\tau 40}$

Table 4.2: Overview of the polymers used in the current study

4.2.2 Bentonite

The bentonite used in the current study (MX80) is a commercially available material mined in Wyoming (USA) and is similar to the bentonite Volclay (Steudel et al., 2020). For this material a huge data set is available in the literature, as it is intended to be part of the nuclear waste disposal concept of some countries and has therefore been extensively studied (Delage et al., 2006; Salles et al., 2009; Tripathy et al., 2014; Haase, 2017; Cui, 2017).

The bentonite batch of MX80 used in the current study is found with a dioctahedral smectite content of 75 +/- 5 %. The exchangeable cations are dominated by sodium Na^{+}(62 %) with minor amounts of calcium Ca^{2+} (31 %), magnesium Mg^{2+} (5 %) and potassium K^{+} (2 %) (Steudel et al., 2020). The cation exchange capacity of the MX80 is determined to be 85 cmol(+)/kg. Given that the cation exchange capacity of the bentonite is mainly related to the smectite minerals, it can be normalised by the proportion of smectite minerals. This yields a cation exchange capacity of 113 cmol(+)/kg for the pure smectite (Steudel et al., 2020). The extensive review of experimental results on MX80 reported by Cui (2017) shows very similar specifications (e.g. 80 % smectite content), which gives evidence for a homogeneity of the deposit. The material has a liquid limit of 588 %, plastic limit of 37 % and a shrinkage limit of 14 % (Haase, 2017).

4.2.3 Formulation of polymer-bentonite mixtures

As discussed in detail in the last two chapters, the boundary conditions during formulation of clay-polymer-composites play a major role in the number of available adsorption spots, the morphology of adsorbed polymer and consequently the resulting soil structure (Fleer et al., 1988; Theng, 2012). Dispersed clay provides good availability of adsorption sites for the polymers and swollen interlayers facilitate possible intercalation. Diluted conditions reduce competition of the polymers for adsorption sites on the clay surfaces and polymer chains are commonly found in less coiled conditions due to low intra-chain interactions (Fleer et al., 1988; Theng, 2012). On the other hand, the dispersion of clay in large quantities requires a lot of technical effort and therefore dry mixing might be easier to be used for practical applications. For this reason, two different mixing methods were adopted to mix the different polymers with the bentonite (i.e. wet mixing and dry mixing). Further, the impact of post-mixing treatment (e.g. drying and grinding) was studied. The latter may be of practical importance, for example, when processing wet mixed material to a dry powder.

Wet-mixing was performed in case of cationic and non-ionic polymers in order to facilitate an optimal clay-polymer interaction. Sample preparation was conducted following the procedure presented in Haase (2017). As a first step, adsorption isotherms were established for the studied materials and mixing boundary conditions. Therefore bentonite was dispersed in deionised water. The bentonite was stirred for 12 hours using a mechanical agitator with a paddle at approximately 500 rpm. The ratio bentonite to liquid was chosen as 42 g Bentonite/ 1 l water (which corresponds to approximately $10 \cdot \mathrm{w}_l$). Small batches of bentonite suspension were subsequently mixed with polymer solutions of different concentrations for 12 hours. To analyse the amount of polymer bonded to the smectite, solids were separated by centrifugation for 30 minutes. The concentration of non-adsorbed polymers was determined from the measured concentration of organic carbon (TOC) in the supernatant. The adsorbed amount of polymer was then assumed to equate to the difference in initial concentration of the polymer solution and the concentration of the supernatant after centrifugation. By repeating the procedure for different concentrations and plotting the amount of adsorbed polymer q (mg/g) against the respective polymer concentration c_{eq} (mg/l) 'adsorption isotherms' are obtained. The isotherms were fitted using the Langmuir equation (4.1),

$$q = \frac{K \cdot q_{max} \cdot c_{eq}}{1 + K \cdot c_{eq}} \tag{4.1}$$

where K [-] is the Langmuir adsorption coefficient and q_{max} (mg/g) is the plateau of the fitting curve identifying the maximum adsorption capacity. The adsorption isotherms are discussed in more detail in the corresponding chapters.

The adsorption maxima were used to prepare the corresponding mixtures with the same preparation steps and mixing ratios. A batch of 5 litres bentonite suspension was prepared following the procedure mentioned above. The same volume of polymer solution was prepared with the concentration corresponding to the respective adsorption maximum.

The cationic polymers were mixed by adding 5 litres polymer solution to 5 litres bentonite suspension and stirring the mixtures for 12 hours with a blade paddle. The mixture was then centrifuged. Figure 4.4 (l.) shows the bentonite modified with cationic polymers (medium chain length) before centrifugation. Elongated agglomerates in the scale of millimetres to centimetres are visible. One series of experiments on cationic polymers are carried out on the material recovered from the centrifugate (i.e. $\mathrm{PAA}^{+}_{L,\tau 40}$, $PAA^{+}_{M,\tau 40}$, $PAA^{+}_{S,\tau 40}$, $PAA^{+}_{VS,\tau 40}$). Another series of tests was performed with centrifugate material subjected to post-mixing treatment. For this, the centrifugate material was dried at 40°C to constant mass and grinded using a roller crusher (Fritsch Pulverisette) to obtain granules with a diameter < 1 mm. The latter test series will be further labelled with an asterisk ($PAA^{+}_{S*,\tau 40}$, $PAA^{+}_{VS*,\tau 55}$).

The mixing procedure for the non-ionically modified bentonite was the same as that for the cationic polymers. However, since the shape of the coiled non-ionic polymers undergoes variations due to external shear stress, and thus also their adsorption morphology, a variation of the mixing energy was conducted. The mixture modified with the medium chain length polymer (PAA^{0}_{M}) was prepared with the same stirrer used to prepare the cationic polymer-clay mixtures, whereas PAA^{0}_{L} and PAA^{0}_{S} were mixed using a stirrer which eccentrically rotates and, thus, causes another shear regime during mixing. The material modified with non-ionic polymers is shown in Figure 4.4 (r.). The material is agglomerated to lumps of several centimetres to decimetres and shows a very high tensile strength. Thus, post-mixing treatment was applied to all non-ionically treated bentonite samples in order to obtain a material resembling to a soil which could be investigated using geotechnical methods. The material was dried carefully at 30-40°C and milled to a powder < 1 mm, similarly as for the cationic polymers.

The anionic polymer was mixed with the bentonite powder at hygroscopic water content without adding additional water. Therefore the bentonite was sieved to a powder < 1 mm and the respective amount of polymer was added and then mixed with a spoon before being compacted.

Figure 4.4: Mixtures of the (l.) cationically modified bentonite, and (r.) non-ionically modified bentonite before centrifugation

4.3 Experimental methods

4.3.1 Atterberg and shrinkage limits

Atterberg limits were determined using the Casagrande cup in accordance with DIN EN ISO 17892-12 (2020). The shrinkage limit was determined following the procedure proposed in DIN 18122-2 (2000). To prevent the formation of cracks, the desiccation rate was reduced. For this, a porcelain cup was placed upside down over the sample during drying and air exchange was only possible via a small gap on the side. The volume of the sample after the test was determined using the paraffin displacement method (DIN EN ISO 17892-2, 2015).

4.3.2 Onedimensional compression behaviour

Oedometer tests were carried out to investigate the impact of the different polymers, mixing and post-mixing treatments on the macroscopic properties, i.e. the compression/decompression behaviour of the corresponding polymer-clay mixtures. In order to

address specific characteristics attributed to modified bentonite three different oedometer devices were used: a standard oedometer according to DIN EN ISO 17892-5 (2017) (Figure 4.5 (a.) and (d.)), a high pressure oedometer (Figure 4.5 (b.) and (e.)) and an oedometer with a large sample size (Figure 4.5 (c.) and (f.)). All three oedometer devices allow for measuring vertical deformations at given vertical loads while horizontal sample deformations are restraint by the sample ring. In all the devices used, permanent drainage during the test is allowed through porous stones. Saturated filter papers were installed on both sides between the sample and the porous stone to prevent suffusion and clogging of the latter. The devices differ in loading capacity, i.e. maximum possible vertical stress and sample dimensions.

The standard oedometer shown in Figure 4.5 (a.) and (d.) has sample ring dimensions of 2 cm in height and 7 cm in diameter. The test material was brought to slurry conditions corresponding to a water content of $1.1 \cdot w_l$, and were then placed carefully in the oedometer ring using a spatula avoiding inhomogeneities and air voids. Subsequently to installation and before applying the load, the cylinder around the sample was filled with deionised water to ensure saturated sample conditions troughout the test. Stress was applied by a mechanically working load frame using dead loads. An initial loading by the dead weight of the upper end cap ($\sim$ 1.5 kPa) was applied to prevent the initially very soft material from being squeezed out.

The high pressure oedometer shown in Figure 4.5 (b.) and (e.) has a sample ring with in 2 cm height and 5 cm in diameter. The device is connected to a mechanical loading frame, which can apply forces up to 50 kN. The oedometer cell is thick-walled to limit deformation of the cell in high stress ranges (see Baille et al. (2010) for details). However, the installation of initially saturated samples is identical to the process described for the standard oedometer. After installation, the drainage was filled with deionised water on the top and bottom and a burette was connected to allow for drainage through the upper drainage system. The load is electronically controlled via a digital control unit. The vertical deformation is measured with an electronic displacement transducer mounted on the oedometer cell.

In addition, the large oedometer shown in Figure 4.5 (c.) and (f.) was used for a single experiment on the modified bentonite with non-ionic polymer with very short chain length (PAA^0_{VS}). The oedometer ring has a height of 8 cm and a diameter of 28 cm. The bottom is equipped with several small porous stones and at the top plate drainage is possible through a small gap between the top plate and the oedometer ring. The load is applied by dead loads at low stress levels and pneumatically controlled stresses at high stress levels.

The material to be tested was brought directly into the oedometer ring after centrifugation without altering the water content and without post-mixing treatment. The intention was to investigate the undisturbed structure of the material after the wet-mixing process.

Figure 4.5: The oedometer devices used in the current study (a.), (d.) standard oedometer, (b.), (e.) high pressure oedometer, (c.), (f.) large oedometer. Figures (d.),(e.),(f.) are total views of the devices including the loading frame, and (a.),(b.),(c.) are close-up views of the oedometer cells alone.

4.3.3 Microstructural investigations

The microfabric of the material was investigated using the Cryo-BIB-SEM technology (Broad Ion Beam polishing and Scanning Electron Microscopy under cryogenic conditions) as described in Schmatz et al. (2017). The material was obtained directly from the residues after centrifugation. In comparison to most conventional methods, using this technology the microfabric is not affected by water content related changes.

To prevent preparation-related alterations of the mirco fabric mainly by drying (Delage, 2010), the samples were rapidly frozen in slushed nitrogen. Large and damage-free cross-sections were cut into these samples using Cryo-BIB (Leica TIC3x). The sample was then removed from the liquid nitrogen and placed on a sample holder for subsequent surface preparation using an Ar-ion BIB polisher. After polishing, the pore fluid of the sample was completely sublimated by controlling the pressure and temperature in the chamber of the SEM (Zeiss Supra 55 SEM equipped with Leica VCT100). A large number of images are combined with a special mapping technique to produce high-quality cross-sections. A detailed description of the technique can be found in Desbois et al. (2013). Mapping was applied to assemble close-ups to a landscape mosaic showing a large overview of the fabric.

4.3.4 Unconfined shrinkage behaviour

The unconfined water retention behaviour was investigated using two different methods in order to cover a wide range of suctions. The osmotic method was used to apply suctions from 0.1 to 9 MPa and the vapor equilibrium method for the suction range of 4 to 345 MPa.

The osmotic method consists in using a polymer solution to apply suction through a chemical gradient. A semi-permeable membrane ensures that soil and polymer (PEG) solution are separated from each other, as both particles or molecules, respectively, are too large to move through them, while this is possible for the much smaller water molecules. It was theoretically shown that using the osmotic method the matric suction of the soil sample is controlled. This is true as long as the PEG-molecules are completely retained by the semi-permeable membrane, and the ions contained in the soil pore water can drain freely through the membrane. However, in Tripathy et al. (2014) it was shown that only few ions are drained, whereas a high percentage is retained, leading to an osmotic suction in the soil sample.

For the osmotic method, the material was brought in slurry conditions ($1.1 \cdot w_l$) and then filled into a large syringe. The tube-shaped semi-permeable membrane with a molecular weight cut-off (MWCO) value of 4000 was cut into 7 cm long pieces and closed at one side with a pressed brass sleeve. Subsequently, the material was filled into the membrane on the open side while avoiding trapped air voids. The still open side was then closed with a wire which was long enough to serve as a holder for the sample. The empty membrane, filled membrane and the sample after the osmotic test are shown in Figure 2.6. Suction was applied by hanging the sample into a Polyethylene glycol (PEG) solution. The concentrations of the PEG solution needed to obtain the desired suctions (i.e. 0.1, 0.3, 1, 3, 9 MPa) were determined following the approach of Lieske et al. (2020 (a.)). A chilled mirror hygrometer was later used to verify the actual suctions of the solution by determining the water activity.

Duplicate samples were tested with the PEG method at each test conditions. The sample was regularly taken from the PEG solution, cleaned from PEG residues and weighed to observe water content evolution. After reaching equilibrium, the samples were dismantled. One of the duplicate samples was oven dried to determine the water content and the other one was used for volume measurement, in accordance with (DIN EN ISO 17892-2, 2015). The samples were coated with paraffin and their volume was determined by immersion weighting. The determination of the volume was carried out to validate complete saturation of the samples, which is a precondition for back-calculating the void ratio from the water content.

Using the vapour equilibrium method, an external suction is applied by controlling the relative humidity under isothermal conditions (Delage et al., 1998; Leong et al., 2003). The total suction under isothermal conditions is calculated using Kelvin's equation (3.5). To apply suction, a saturated salt solution is placed in a closed container (desiccator) along with the sample to be tested, enabling an exchange of water via the vapour phase (Figure 4.7). During this process, the relative humidity depends on the type and concentration of the used salt. Since ions contained in the soil pore water will not evaporate into the atmosphere, but remain inside the soil, vapour equilibrium controls the total suction. When the water content of the soil sample reaches a constant value, the suction inside the sample is equal to the suction applied via salt solution. However, as the diffusion out of the sample and the transport through the vapour phase is slow, this method is time consuming.

To save time multiple samples were tested in parallel from identical initial conditions. The material ($1.1 \cdot w_l$) is installed in a plastic ring (height = 1.5 cm/ diameter = 5 cm)

Figure 4.6: Samples for osmotic method (a) empty membrane with brass sleeve, (b) sample at initial conditions inside the membrane, (c) sample after test with visible volumetric shrinkage induced by dewatering

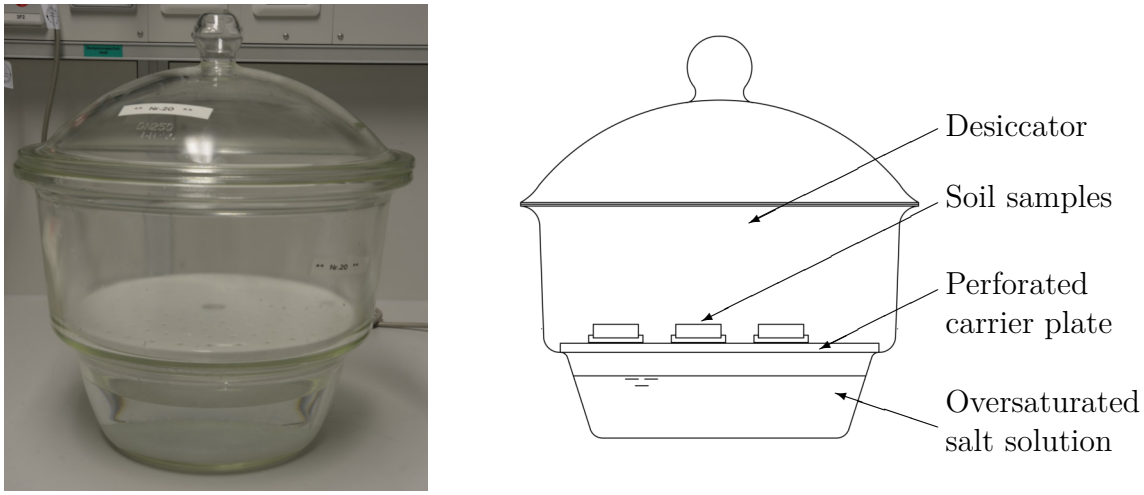

Figure 4.7: Setup of the vapor equilibrium technique (VET) (l.) photograph of a desiccator filled with salt solution at the bottom, and (r.) sketch of a dessicator with soil samples

with a suitable bottom plate. The rings were greased to prevent uneven shrinkage and cracking of the material caused by interactions between the soil and the sample holder. The samples were placed in desiccators with varying oversaturated salt solutions (suctions i.e. 4, 9, 40, 85, 153, 345 MPa) in order to control relative humidity, while temperature was kept constant (20°C).

For the wetting path, multiple samples were first subjected to the highest suction of 345 MPa. After reaching equilibrium they were moved to lower suctions (9, 21, 37, 83, 153 MPa) for rewetting. The actual water content was back-calculated from the changes in weight, while the volume of the sample was determined after the sample had reached equilibrium at the respective suction with kerosene according to the procedure described in Péron et al. (2007).

Both the relationships between void ratio and applied suction, known as shrinkage curve, and between gravimetric water content and applied suction (SWCC) were derived from the experiments. The experimental data points were best-fit to known mathematical functions describing the SWCC and shrinkage curve. The equations of Fredlund and Xing (1994) and Wijaya et al. (2015) were used for the fitting of the water retention curves in terms of degree of saturation and gravimetric water content, respectively. Equation (4.2) adopts the gravimetric water content (Wijaya et al., 2015),

$$w = w_s \left\{ \frac{1}{\ln[\exp(1) + (\psi/a)^n]} \right\}^m \frac{\ln[1 + (\psi/\psi_r)]}{\ln[1 + (10000000/\psi_r)]} \tag{4.2}$$

where a, n, m and ψ_r are curve-fitting parameters, w_s is the saturated gravimetric water content and ψ is the suction.

The shrinkage curves were fitted using Equation (4.3) (Wijaya et al., 2015). In this Equation the void ratio e (-) is a function of the gravimetric water content w (-), and the curve fitting parameters C_{sh}, a_{sh} and b_{sh}.

$$e(w) = a_{sh} \left[\frac{w^{C_{sh}}}{b_{sh}^{C_{sh}}} + 1 \right]^{1/C_{sh}} \tag{4.3}$$

The degree of saturation S was calculated according to Equation (4.4)

$$S(\psi) = \frac{w(\psi) \cdot G_s}{e(w)} \tag{4.4}$$

where G_s (-) is the specific gravity.

4.3.5 Multi-step permeameter

A new multi-step permeameter was developed to perform swelling pressure and permeability tests in one sequence. Furthermore, the device is equipped to study the membrane behaviour of clays. During design of the cells, special attention was paid to a salt resistant construction to enable tests with aggressive salt solution. Therefore, all connections, tubes and sample rings were made of plastic or high quality stainless steel. The device shown in Figure 4.8 is composed of two main components (1) the cell (Figure 4.8 (d.)), and (2) the panel (Figure 4.8 (c.)). The number in brackets in the following paragraph refer to the numbers of items on the legend in Figure 4.8.

The bottom plate (3) of the cell carries a porous stone (5) connected to two outlets (I, II), so that the lower drainage can be flushed, or fluid can be circulated. A pore water pressure transducer (4) is installed below the porous stone (5). The sample ring (2) has an inner diameter of 5 cm and a height of 5 cm. Sealing is ensured by an O-ring on the base plate below the sample ring. The sample height can be chosen freely between 5 and 30 mm. An outer ring (6) connects the sample ring and the bottom plate and has further screw holes to which the top plate is connected. The head construction (8) contains the upper drainage, which is equipped with a porous stone (7) and two outlets (III, VI) that again enable flushing of the drainge system and circulation of fluids. The fluid connections of the bottom and top porous stones can individually be connected directly or via a valve system (see Figure 4.8 (a.)) with each other or the hydraulic inlets of the panel (V,VI,VII). On top of the head construction a load cell (9) is mounted. This unit (7,8,9) is guided by the sample ring and sealed to the outside with O-rings. The top cap (10) which is connected to the outer ring is equipped with a big screw (11) and is kept in a fixed position to restrict vertical expansion of the sample. The screw serves as a counter bearing for the load cell and allows an exact positioning of the load cell. The screw can be used to allow a specific swell expansion of the sample.

The 'panel' is equipped with plexiglass tubes of different diameters which serve as reservoir (12), reference burette (17) and measuring burette (18). All burettes have a fluid supply on the lower side, which can flexibly be connected to either the valve system or directly to the drainage system of the cell. The measuring and the reference burettes are connected by a pore water differential pressure sensor (16). By keeping the water level in one of the burettes constant, the amount of water flowing into the other one can be measured by means of the change in differential pressure. Depending on the permeability of the soil, or the anticipated amount of water that need to be measured, the tube with the larger or smaller diameter can be used as a measuring burette. The upper side of the

reservoir burette is equipped with a digital air pressure sensor (13) and a manual pressure regulator (15), by which an air pressure can be manually applied to the water. The burette can also be operated at atmospheric pressure via a two-way connection (14). Both the units of measuring and reference burette use the same system for applying pressure. The data measured by the pore water pressure transducer in the cell, the load cell and the differential pressure transducer in the panel are externally recorded by a datalogger.

The current test setup allows for measurement of swelling pressure and permeability, and investigation of membrane behaviour, also known as osmotic efficiency. The swelling pressure is measured under constant volume conditions. For this, the screw (10) is adjusted, so that the top porous stone (6) is in contact with the sample and no heave of the sample is allowed. The sample is hydrated with a small hydraulic pressure (< 2 kPa) by connecting the water reservoir to the bottom porous stone. The force which develops during this hydration process is measured by the load cell. When testing the hydraulic conductivity a gradient is applied by increasing the air pressure on the water reservoir. In addition, pressure can be applied on the measuring burette as a back pressure, so small hydraulic gradients can be applied at high stress levels. The amount of fluid flown through the sample is measured by a change in differential pressure caused by an increasing water level in the measuring burette.

The membrane behaviour is measured by filling the measuring (17) and the reference burette (18) with different ionic fluids. The reference burette is connected to the bottom porous stone (5) and the measuring burette to the top porous stone (7), so that the sample is acting as a membrane. The differential pressure sensor is measuring the difference in the water level (osmotic pressure) which is caused by the flow of water from the lower (or non) ionic fluid to the higher ionic fluid.

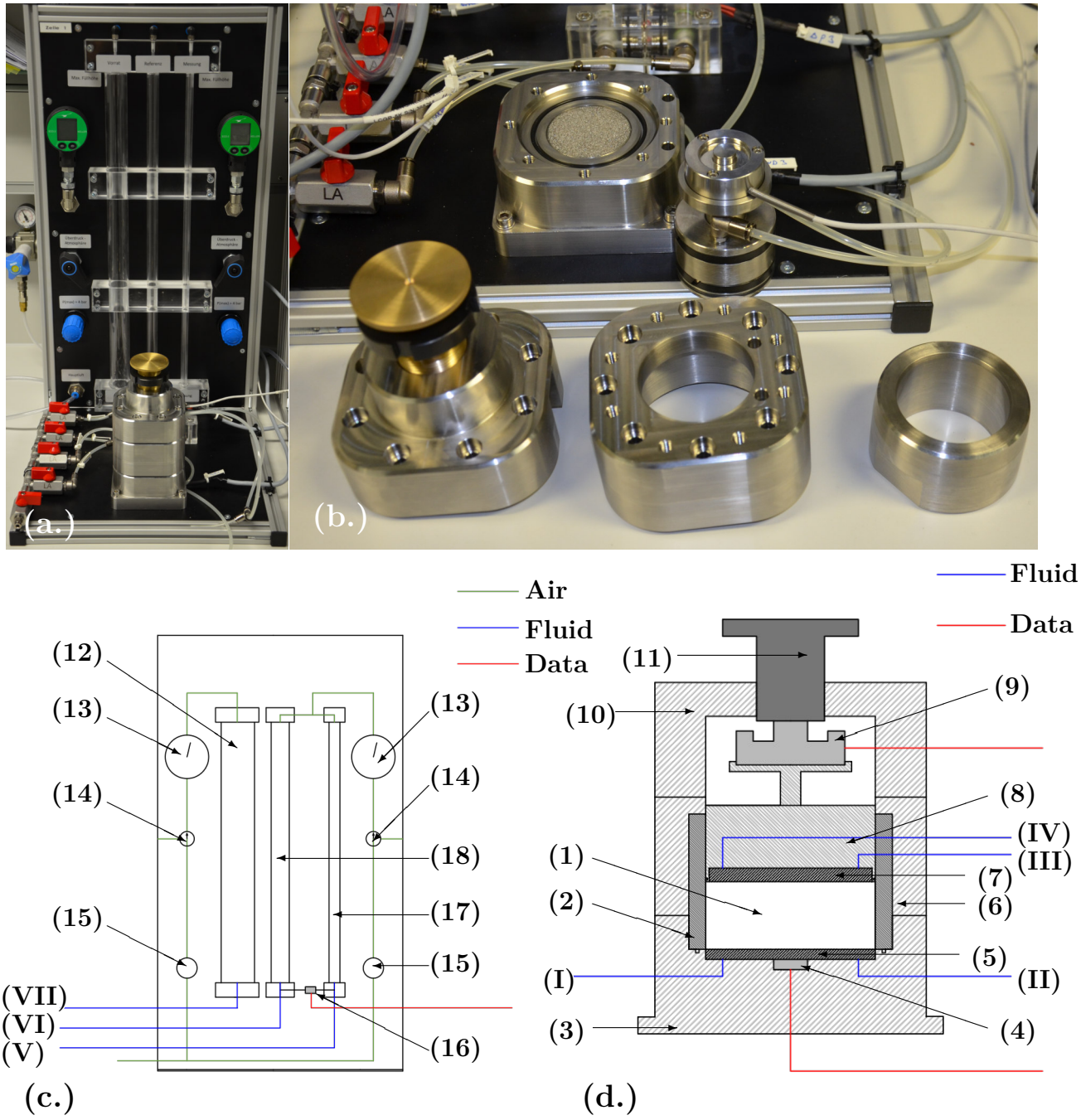

(1) sample, (2) sample ring, (3) bottom plate, (4) pore water pressure transducer, (5) bottom porous stone, (6) outer ring, (7) top porous stone, (8) steel body with drainage system and socle for load cell, (9) load cell, (10) top cap, (11) adjustment screw, (12) reservoir (13) digital air pressure sensor, (14) three-way-valve, (15) pressure regulator, (16) pore water differential tranceducer, (17) measuring burette, (18) reference burette

Figure 4.8: Multi-step permeameter: (a.) photograph of the fully assembled device including delta panel (b.) disassembled cell (c.) sketch of the delta panel (d.) sketch of the cell

5 Hydro-mechanical behaviour of polycationically modified bentonite

5.1 General

The following chapter is dedicated to the modification of bentonite using polycations. The results of the experimental programme introduced in Chapter 4 will be outlined, discussed and compared to literature results. The chapter will start with investigations addressing the polymer-clay interaction such as the adsorption behaviour, the microfabric, and the intercalation behaviour. Afterwards the soil mechanical index properties, the compression and decompression behaviour as well as the unconfined water retention behaviour of the different mixtures will be presented and compared to that of the pure bentonite. Part of this research was published in Lieske et al. (2022). Additional investigations performed in cooperation with the Competence Center for Material Moisture (KIT) to support the interpretation of the data on the microscale will be briefly introduced. The last part of the chapter will summarise the findings and discuss them with respect to their geotechnical relevance.

5.2 Adsorption, intercalation behaviour and cation exchange capacity

The amount of polymer which remains as a solid after centrifugation is plotted against the respective concentration of the polymer-solution in Figure 5.1. The resulting curve is known as adsorption isotherm. The adsorption isotherms of the bentonite modified with the polymer of long and medium chain length $PAA^{+}_{L,\tau 40}$ and $PAA^{+}_{M,\tau 40}$ follow a similar trend. By contrast, the short chained polymer $PAA^{+}_{S,\tau 40}$, shows a slightly higher maximum adsorption capacity. By the same token, the maximum amount of adsorbed polymer in

case of the short-chain polymer with the higher charge density ($PAA^{+}_{VS,\tau 55}$) is significantly lower than that of all other polymers.

The measured adsorption maxima reflect the mass of polymer retained as a solid in the centrifugate during centrifugation. However, the adsorption isotherm does not provide informations about the binding mechanism of the polymer to the clay. The amount of polymer in the solids is not equivalent to the polymer adsorbed onto a surface or intercalated into a smectite interlayer. Polymers can for instance be mechanically entrapped in aggregates as well. Therefore, it is not possible to assess from the adsorption maxima whether the polymer is intercalated or retained by other mechanisms. Since the material was not washed after centrifugation, non-adsorbed polymers are still being present in the pore fluid of the centrifugate.

Denoyel et al. (1990) showed that in case of polycations with a very low charge density ($\tau = 1\%$), the adsorption capacity decreases with chain length. Different observations were made in the current study, where no strong correlation between molecular weight and adsorption maximum exists for $\tau = 40\%$. The adsorption of polycations is generally believed to occur in patches with only minor possibilities to rearrangement due to strong electrostatic interaction of the charges of the polymer and the smectite (Breen, 1999; Bergaya et al., 2006). Provided that the shape of the patches on a smectite surface will be round according to the coiled conformation of the polymer in solution (Figure 3.13 (b.)), spaces between neighbored patches will remain free or will be less effectively covered. The surface coverage will increase with decreasing patch size, as small patches

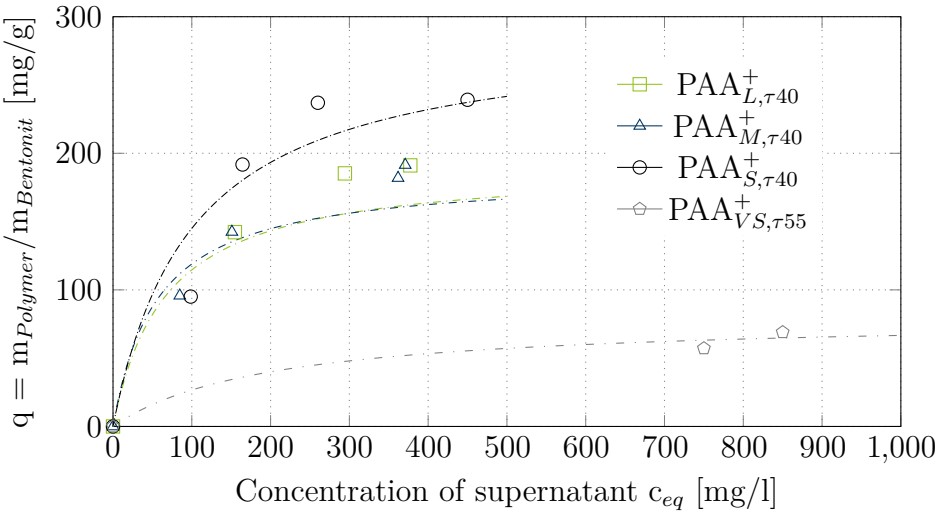

Figure 5.1: Adsorption isotherms of the MX80 modified with cationic polymers

are more flexible to be arranged in a compact way. Since the size of a polymer-coil correlates to its molecular weight, the maximum adsorption capacity likewise does. This can be compared to the maximum and minimum density of non-cohesive soils where the volume of pores (here analogue to the free spaces between the patches) decreases with grain size, assuming non-ideally round grains. This idealised picture helps to capture why the maximum adsorption capacity decreases with increasing coil size (i.e., molecular weight) for small charge densities.

At high charge densities ($\tau > 15\%$) the intra-chain repulsion causes the polymer to stretch and to be more rigid, which in general reduces the adsorption capacity (Breen, 1999). Therefore, the maximum amount of surface coverage as well as the maxima of the adsorption isotherms decrease with increasing charge density (Denoyel et al., 1990). This is in good agreement with the results of $PAA^{+}_{VS,\tau 55}$, which appears to have a lower adsorption maximum in comparison to the other polymers with a lower charge density.

However, the ionicity of the polymers with the lower charge density ($PAA^{+}_{S,\tau 40}$,$PAA^{+}_{M,\tau 40}$ and $PAA^{+}_{L,\tau 40}$) is identical. Effects caused by repulsion between and within the chain can likewise be assumed to be of an equivalent magnitude. Beside the molecular weight and resulting patch size and the charge density, viscosity is a third factor affecting adsorption behaviour. Typically, the viscosity of linear chain polymers decreases with decreasing chain length (Verst et al., 2022). Denoyel et al. (1990) discussed that mixing conditions might affect the adsorption, as high viscosity and intensive flocculation limit accessibility of polymers to surfaces. The slightly higher value of the adsorption maximum of the short chained polymer might therefore be a result of the mixability, which might be lower after exceeding a certain viscosity (Steudel et al., 2020). As viscosity arises a limiting factor in polymer-clay interaction, it becomes apparent that the course of the adsorption isotherms reflects the accessibility of polymers to respective adsorption spots. Therefore, the course of an adsorption isotherm needs to be considered with care. In fact, adsorption isotherms approach a plateau reflecting that a further increase in mixing concentrations will not affect the adsorbance. However, considering polymer-clay mixtures, due to the increasing viscosity, the adsorption decreases again at high concentrations.

An important interaction between polymers and clay is intercalation. This process describes the penetration of polymer chains into the interlayers of the clay particles. Intercalation is evaluated by determining the distance between the smectite layers using the XRD-analysis (Steudel et al., 2020). In this technique, an X-ray beam is directed at a sample and the diffraction of the reflected X-rays is measured. The X-ray diffraction pattern obtained in this way is evaluated using the Rietfeld analyses. To avoid interfer-

ences by water during the measurement, the samples are dried and prepared as a powder before the examination. Figure 5.2 shows the result of an XRD-analysis conducted on the unmodified MX80 and the modified bentonites $PAA^{+}_{VS*,\tau 55}$ and the $PAA^{+}_{S*,\tau 40}$.

The distance between the individual layers can be derived from the first basal reflection (001) of the smectite. The size of the interlayer of the unaltered MX80 is 0.113 nm, which is slightly higher than the value given for a sodium bentonite in Madsen and Müller-Vonmoos (1989) (i.e. 0.05 - 0.09 nm). However, the value is in a reasonable range for a non-hydrated smectite.

The 001 reflection showed an expansion after the treatment with polymer for both the $PAA^{+}_{VS*,\tau 55}$ and the $PAA^{+}_{S*,\tau 40}$. The larger interlayer distance for the modified bentonite proved that the polymer has intercalated into the interlayer of the smectite. The interlayer distance of the $PAA^{+}_{VS*,\tau 55}$ is 0.127 nm which corresponds to the distance of a sodium bentonite hydrated with 6 H_2O molecules per ion (Madsen and Müller-Vonmoos,

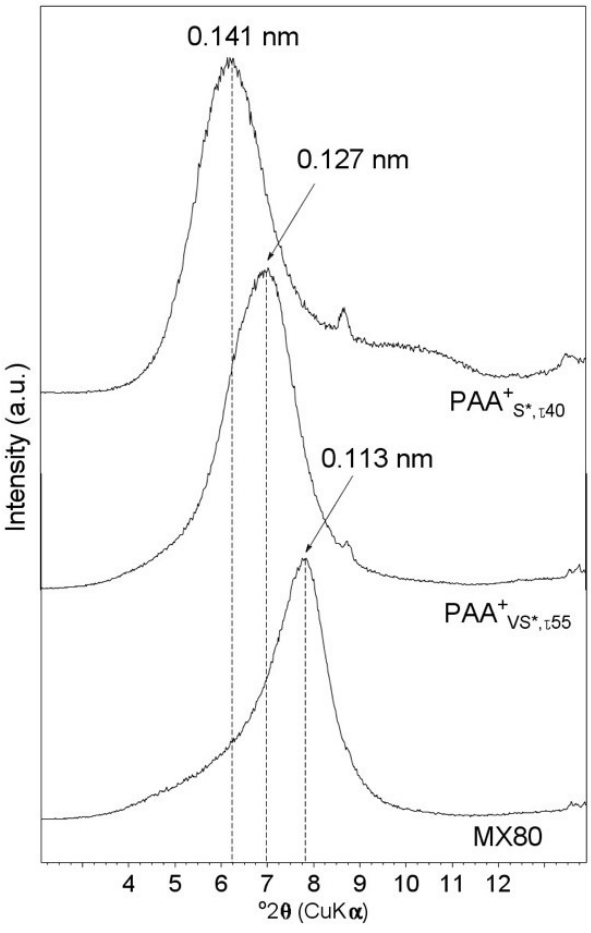

Figure 5.2: XRD pattern of the oriented samples - first basal (001) reflections

1989). The distance obtained for the $PAA^{+}_{S*,\tau 40}$ is 0.141 nm, which corresponds to 12 H_2O molecules per ion (Madsen and Müller-Vonmoos, 1989). The expansion of the 001 reflection is lower for $PAA^{+}_{VS*,\tau 55}$ compared to the sample $PAA^{+}_{S*,\tau 40}$. The different expansion proved that the charge of the polymer influenced the intercalation process. However, from this XRD-measurement, it remains unclear what causes the different expansions. Both polymers intercalate in a flat orientation of the polymer as the length of the sidechain is close to 1 nm.

The adsorption of cationic polymers on smectite surface occurs as a cation exchange process (Ueda and Harada, 1968). However, dipol-dipol and dipol-ion attraction between the uncharged parts of the polymer chain and the exchangeable cations of the smectite and their hydration shells play a further role in adsorption of non-ionic polymers. In contrast to the naturally occurring exchangeable cations, however, polymers are adsorbed irreversibly. This can be explained by the number of adsorption spots. Even if individual bonds between polymer and clay can be released, a simultaneous detachment of all charges

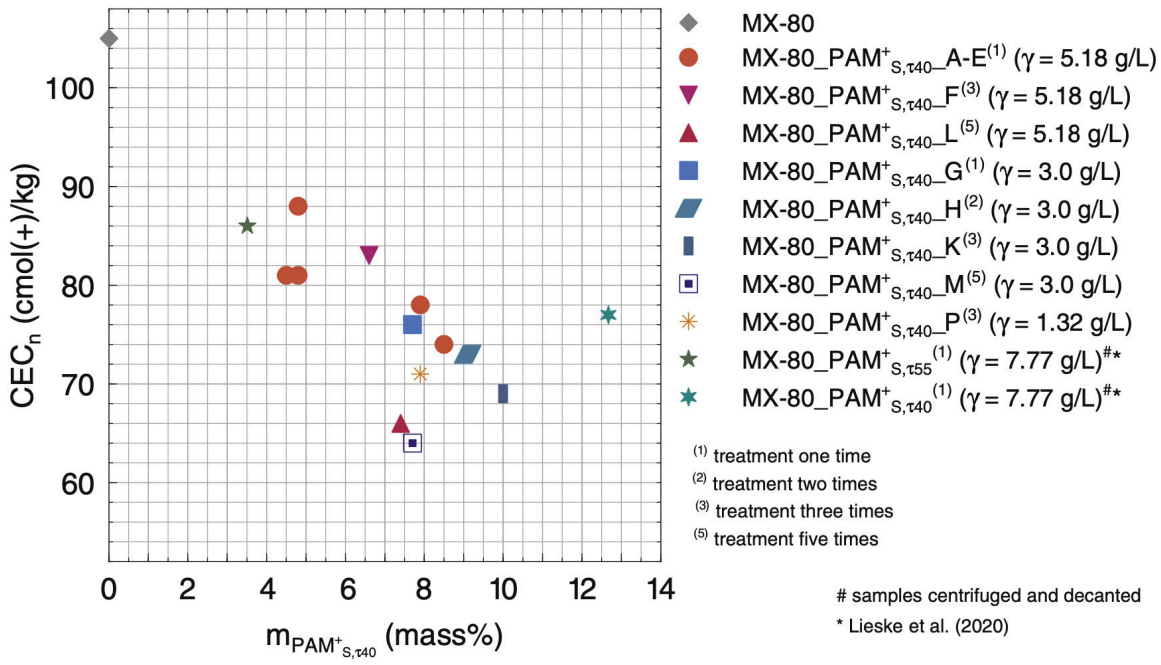

Figure 5.3: Decrease of cation exchange capacity (CEC) versus mass of polymer in a $PAA^{+}_{S,\tau 40}$ and a $PAA^{+}_{S,\tau 55}$ composite, from Steudel et al. (2020)

of the polymer chain from the clay surface is almost impossible. The replacement of natural cations such as sodium, calcium or potassium by cationic polymers consequently reduces the measurable cation exchange capacity (Ueda and Harada, 1968). Steudel et al. (2020) studied the evolution of the cation exchange capacity with uptake of cationic polyacrylamides using the Cu-trien method (Meier and Kahr, 1999) with special focus to the impact of the mixing (intercalation) conditions. The amount of polymer in the mixture was determined by means of thermal analyses.

The cation exchange capacity of pure MX80 and modified MX80 with differently concentrated and differently treated cationic polyacrylamide solutions are shown in Figure 5.3. The samples were obtained by treating a bentonite solution with polymer solutions with a given concentration (γ). Some of the solutions were mixed one time with a fresh polymer solution while others were subjected to multiple treatments.

The results of the study showed that the cation exchange capacity effectively decreased with the increasing mass of polymers in the mixture. With 4 % adsorbed polymers with a charge density $\tau = 40\,\%$, the CEC is reduced to 88 cmol/kg, which corresponds to a reduction of 17 percent compared to bentonite normalised to its smectite content. The lowest CEC was 69 cmol/kg obtained at 10 % polymers in the mixture which corresponds to a reduction of 34 % of the initial CEC.

The authors stated that multiple treatments do not have a significant effect on the CEC, but viscosity does. The CEC of the smectite treated three times with a polymer solution with a concentration of 3.0 g/l is therefore lower than that of the smectite treated three times with a concentration of 5.18 g/l. The $PAA^{+}_{S,\tau 40}$ treated once with $\gamma = 7.77\,\mathrm{g/l}$ shows the highest amount of polymer, however, the corresponding CEC is far beyond the trendline. This shift might be caused by polymer entrapped in the solids but not bond due to cation exchange or intercalation. Steudel et al. (2020) claimed that about 3 % additional polymer may be present in the sample if it is not washed several times after mixing.

A calculation of the coverage of the clay surfaces resulting from the adsorption shows that only 4.5 - 10 % of the charges were neutralised by the polymers. Thus the reduction of CEC of about 34 % cannot be explained by the exchange of cations by polymers alone. Therefore, the occlusion of the interlayers by the polymers and thus the prevention of the intercalation of Cu-trien molecules was considered as another mechanism explaining the reduced cation exchange capacity.

The higher charge density of the polymer ($PAA^{+}_{S,\tau 55}$) does not cause a significant deviation from the overall trend. However, it should be noted that, again, the sample was not

washed after mixing and so the amount of adsorbed or intercalated polymer might be lower than the total one and thus the point would be shifted to the left of the trend line for the $PAA^{+}_{S,\tau 40}$. Consequently, a greater impact on the CEC was achieved by adding smaller amounts of polymers. Moreover, the results indicate that the distance between the individual charges need to match those of the charges on the clay surface to be effectively neutralised.

5.3 Microfabric

Figure 5.4 (a.) to (c.) show images of the microfabric of $PAA^{+}_{M,\tau 40}$ in different magnifications. The large landscape given in Figure 5.4 (a.) shows conglomerates of different sizes up to 100 microns. The large assemblages of smectite correspond to the large fibrous structures which are visible for the blank eye (see Figure 4.4). The shape of these conglomerates is dictated by the way of mixing resulting in an elongated shape when using a blade paddle. However, the durability of the flocs during the mixing process is limited. As it has been observed in shearing experiments not all polymer chains withstand the shearing induced energy and thus break (Yu et al., 1979). It can therefore be reasonably expected that many of the smaller flocs seen in Figure 5.4 (a.) are the result of the fragmentation of larger ones sheared apart during mixing. A complex arrangement of inter-aggregate pores is located in between different sized flocs. The close-ups given in Figure 5.4 (b.) and 5.4 (c.) show further a heterogenous distribution of intra-aggregate pores.

At a closer look to the micrograph with the highest magnification given in Figure 5.4 (c.) some throats of polymeric hydrogels can be seen in between the clay platelets which corresponds to the observation in Steudel et al. (2020), that there is a surplus of polymer which would probably be removed during washing. To this end it remains unclear how this additional polymer affects the behaviour of the material.

It has been discussed before that it is unlikely that simple stirring can disperse clay to the level of a single layer. Therefore, the smallest occuring structures are particles made of few layers or small aggregates. The arrangement of the smallest recognisable unit is occurring in a honey-comb fabric of particles connected on their edges. This arrangement corresponds to the dispersed, edge-to-edge and partially edge-to-face flocculated fabric shown in Figure 3.4 (d). Palomino and Santamarina (2005) summarised effects that arise from particle size, mineralogy, structural charge, fluid interactions and its effect on DDL formation, pH and ionicity, particle geometry and the resulting particle-particle

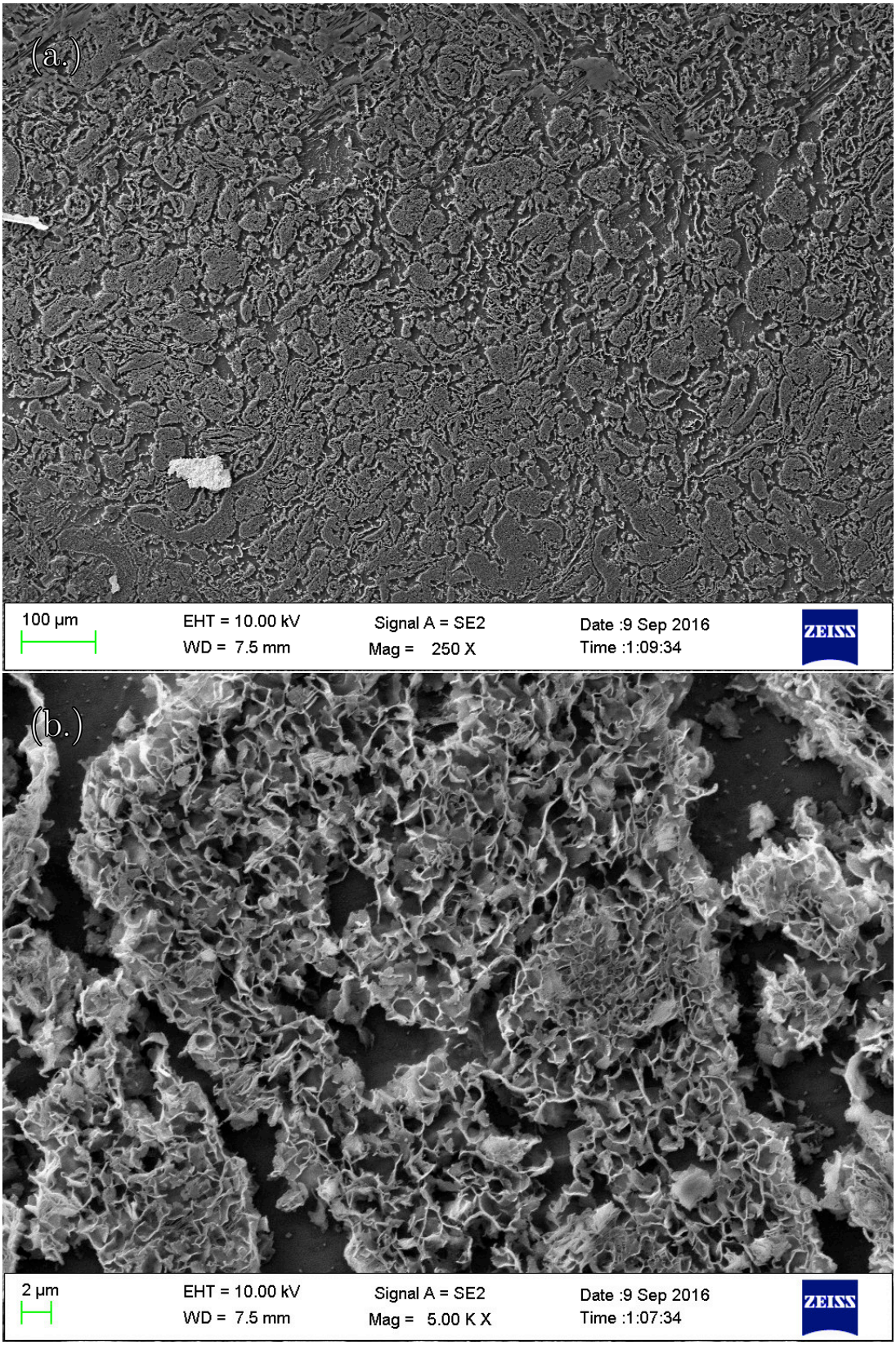
(a.)
100 µm
EHT = 10.00 kV
WD = 7.5 mm
Signal A = SE2
Mag = 250 X
Date :9 Sep 2016
Time :1:09:34
ZEISS
(b.)
2 µm
EHT = 10.00 kV
WD = 7.5 mm
Signal A = SE2
Mag = 5.00 K X
Date :9 Sep 2016
Time :1:07:34
ZEISS

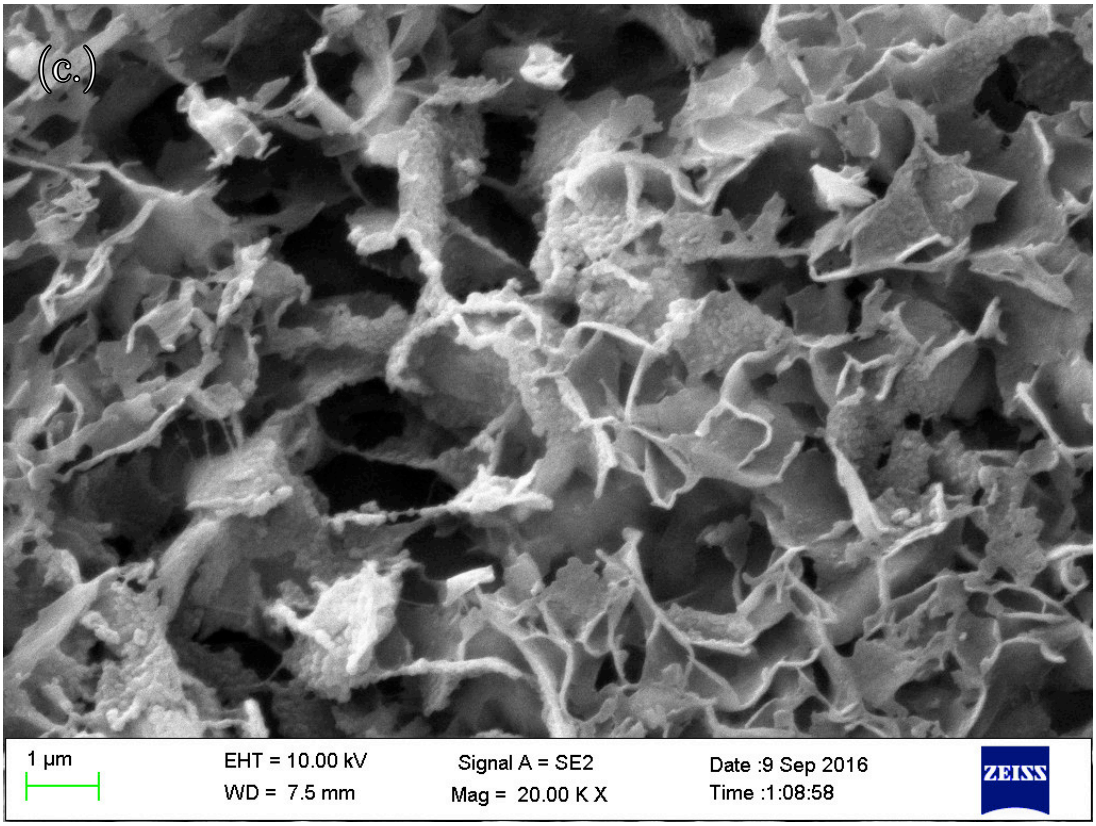

Figure 5.4: Microfabric of $PAA^{+}_{M/\tau 40}$

interaction as the governing parameters for clay fabric formation. As the adsorption of cationic polymers is a fast and instantaneous reaction this honeycomb fabric can be understood as the preserved dispersed fabric from the initial contact of bentonite with the polymers in solution which in turn is a complex interplay affected by polymer, smectite, the respective concentration and mixing conditions.

5.4 Index properties

Liquid limit, plastic limit and shrinkage limit of the unmodified bentonite and the different mixtures are shown in Table 5.1, respectively. Moreover, the liquid limit is plotted against the plasticity index in terms of a Casagrande diagram in Figure 5.5. The liquid limit shows a clear trend to decrease with decreasing chain length for the material modified with the lower charge density. In comparison to the natural bentonite no clear trend could be observed. The material modified with the highest molecular weight has a slightly higher liquid limit than the pure MX80, while the other polymers yield a reduction of the liquid limit. It is striking that this trend is independent of the different adsorption maxima

and, thus, amount of polymer in the mixture. This observation is in accordance with literature, where a significant change in the clay properties was obtained even by adding small amounts of polymer (Inbar et al., 2015; Razakamanantsoa et al., 2014). However, a further increase of the amount of added polymer is commonly associated with less pronounced changes in material behaviour (Rao et al., 1993).

This behaviour reflects the complex polymer-clay interaction on the different scales which might cause contrary effects on the macro scale. Charge neutralisation and patch-flocculation limit adsorption of water by hydration of cations and, thus, cause a reduction of the overall ability to bind water followed by a reduction of the liquid limit. Such effects are attributed to surface modification of the minerals. By contrast, steric effects (i.e. geometric incompatibility of polymer patches), bridging, and formation of large conglomerates supports a open porous fabric. The latter two mechanisms support the uptake of water due to strutural effects and therefore increase the ability to hold water without changing from the solid to the liquid state like it is known for quick clays (Delage and Lefebvre, 1984).

Moreover, the formation of large conglomerates has impact on the mechanical properties of the material and therefore affects the liquid limit in a second way. The determination of liquid limit in the Casagrande cup is considered as a dynamic shear test and the corresponding water content as that at which the soil has an undrained shear strength of 6 kPa (Mitchell et al., 2005). Shear resistance increases with the size of the aggregates, as more energy is needed to move them against each other.

The strong correlation between liquid limit and molecular weight at given charge density can directly be related to structural effects attributed to the different molecular weights. The ability of a polymer to adsorbe on multiple surfaces increases with molecular weight and, thus, also the size of conglomerates. The comparison between MX80 and the mixtures obtained by modification with polymers with a charge density $\tau = 40\,\%$ shows that structural effects might overcome effects that arise from surface modification. The material modified with the highest molecular weight has a higher liquid limit than the unmodified material even though the surface modification causes a reduction of the liquid limit.

This picture of structure that supports a high liquid limit and surface modification that forster reduction of the liquid limit also gives a reason for the observation, that the material whose structure was partially destroyed by drying and grinding prior to testing has a significantly lower liquid limit compared to the mixtures which did not undergo such a treatment (Figure 5.5). A direct comparision between the different charge densities is not possible because charge will affect both surface modification and structure (Breen,

Table 5.1: Liquid limit, plastic limit, plasticity index and shrinkage limit for the different mixtures

Material	Liquid limit [%]	Plastic limit [%]	Plasticity index [%]	Shrinkage limit [%]	Specific density [-]
MX80[1]	588	37.0	551.0	14	2.65
$PAA^{+}_{L/\tau 40}$	633	122.9	510.1	10	2.37
$PAA^{+}_{M/\tau 40}$	543	108.6	434.4	9	2.32
$PAA^{+}_{S/\tau 40}$	461	98.7	362.3	10	2.25
$PAA^{+}_{S^*/\tau 40}$	168	80.8	87.2	-	
$PAA^{+}_{VS/\tau 55}$	544	63.0	481	7	2.49
$PAA^{+}_{VS^*/\tau 55}$	301	47.0	254	-	

[1] Data From Haase (2017) * Material has been dried and grinded prior to testing

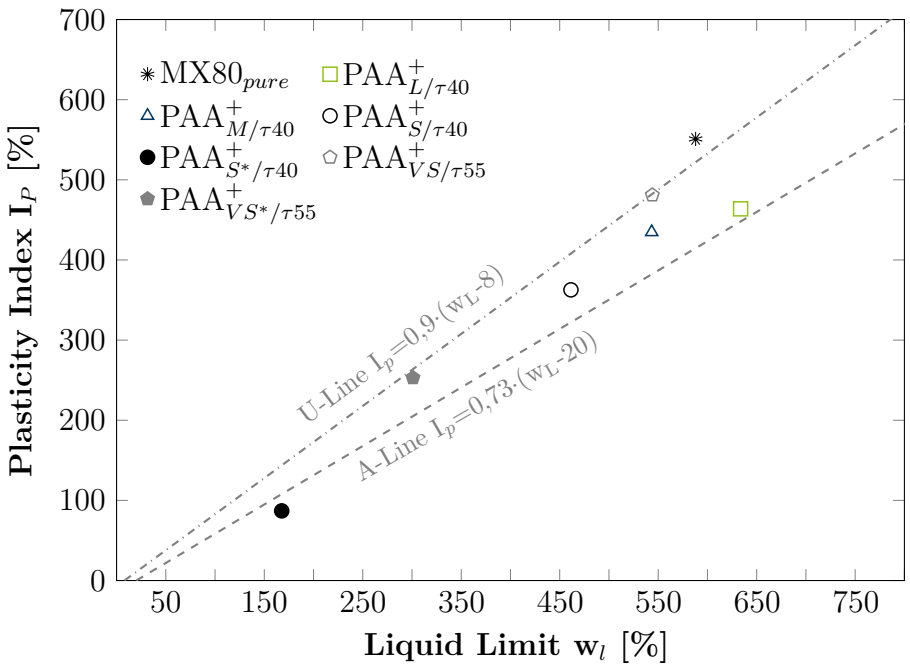

Figure 5.5: Classification of MX80 and polycationically modified MX80 in the plasticity chart

1999). However, a decline in liquid limit after drying and grinding is observed for both studied charge densities indicating the relevance of such post-mixing treatment for the material behaviour.

Similarily to the liquid limit a correlation between plastic limit and chain length can be observed (Table 5.1). As the plastic limit reflects the point at which water stops acting as a continuum, it is related to the air entry value (Haigh et al., 2013). An aggregated and flocculated fabric yields large macropores which are associated with a low capillary suction and, thus, a higher plastic limit. The previously assumed correlation between chain length and aggregate size is therefore supported by observations made on the plastic limit.

Shrinkage limit has been observed to be independent of molecular weight for the same cationicity and to be slightly smaller for the material modified with the high charge density. In comparison to the natural material, a lower shrinkage limit is reached. As demonstrated in Sridharan and Prakash (1998) the shrinkage limit is rather a 'packing phenomena' than a function of surface properties. One possible explanation for the lower shrinkage limit is the flexibility and small size of the polymers which were considered as solids in the current frame and allow a denser packing of the solids. It has yet not been studied how polymer chains change their behaviour upon reduction of water content or heating, however, the release of water during drying might cause coiling of polymer chains due to an increase in water potential. Another reason for the lower shrinkage limit is a potential change of polymer shape which induce an additional attractive force and thus, a compaction.

5.5 One-dimensional compression behaviour

The one-dimensional compression behaviour of $PAA^{+}_{L,\tau40}$, $PAA^{+}_{S,\tau40}$, $PAA^{+}_{S*,\tau40}$, $PAA^{+}_{VS,\tau40}$ and of the unmodified MX80 from Haase (2017) are compared in Figure 5.6. It can be clearly recognised that the behaviour of the pure MX80 is qualitatively different from that of the MX80-polymer mixtures. Both, the compression and decompression index of the pure MX80 are significantly larger ($C_c = 6.46$ and $C_s = 1.95$) than those of the mixtures ($C_c = 0.42$ – 1.90 and $C_s = 0.10$ to 0.31).

During virgin compression both bentonites modified with the polymers of same charge density ($PAA^{+}_{L,\tau40}$, $PAA^{+}_{S,\tau40}$) show a comparable compression index while the material modified with the higher charge density ($PAA^{+}_{VS,\tau55}$) reveals a slightly stiffer behaviour. This difference is more pronounced for the material dried and grinded prior to testing

($PAA^{+}_{S*,\tau 40}$). However, at a vertical stress of 1600 kPa, all curves of the materials subjected this stress merge in one point.

The hydro-mechanical behaviour of plastic soils is mainly determined by interaction of the mineralogical constitutes. Therefore, semi-empirical approaches such as the correlation of compression properties with plasticity properties are widely established in geotechnical engineering (Burland, 1990; Mitchell et al., 2005; Tiwari and Ajmera, 2012). Plasticity, or more in detail, the liquid limit reflects the ability of a material to hold water without loosing its strength. Two basic micromechanical features can be identified to be responsible for the plastictiy on the macroscale i.e. inter-particle interactions (such as friction) and the ability to hold water (i.e. porosity and physico-chemical adsorption of water). As these are essentially the mechanisms that govern the compression and decompression behavior of soil, an interrelation becomes apparent. Equations (5.1) and (5.2) correlate the compression index and the decompression index with the plasticity index (I_p) (Mitchell et al., 2005).

$$C_c = \frac{I_p}{74} \tag{5.1}$$

$$C_s = \frac{I_p}{370} \tag{5.2}$$

The results obtained from the one-dimensional compression tests and the values calculated using Equation (5.1) and (5.2) are compared in Figure 5.7. The results show that the correlation gives a quite good estimation for both compression and decompression index in case of natural MX80 and for the modified MX80 subjected to post-mixing treatment. However, for all the mixtures which were not dried and grinded before testing the experimental values were significantly smaller than those obtained from the correlation. Even though the correlations in Equations (5.1) and (5.2) were determined empirically and such correlations are found with different expressions by different researchers, the general relationship of an increase in C_c with I_p is generally accepted. However, the C_c-I_p data of the modified MX80 do not show this correlation at all. It can therefore be concluded, that relevant mechanisms dictating the plasticity properties are significantly altered during compression or do not play a significant role. This is supported by the observation, that the behaviour during unloading is similar for all modified materials, whether or not they were grinded before testing.

One of the basic assumptions for constitutive relationships and correlations in soil mechanics is that the smallest relevant units (e.g., aggregates) of the soil are stable, i.e. do not undergo fundamental changes during testing. The used correlations (Equation 5.1

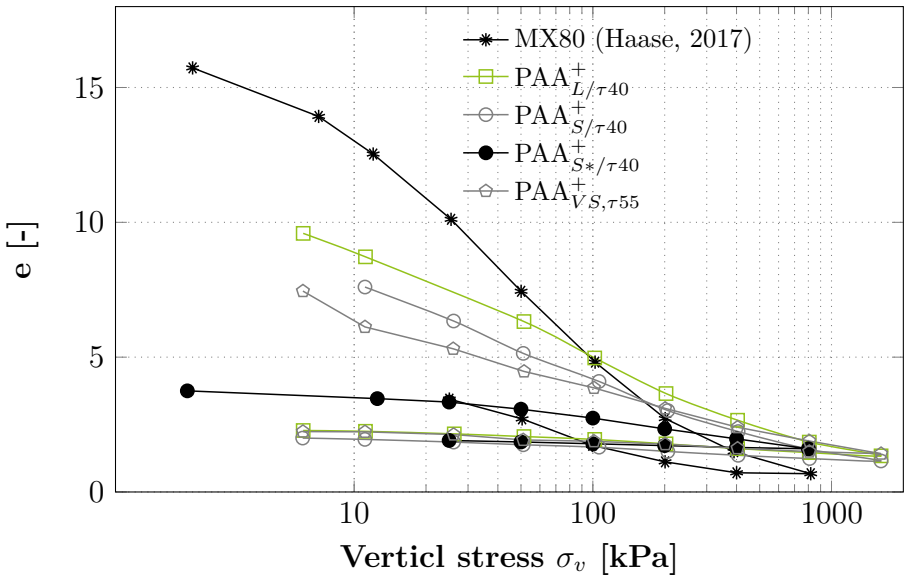

Figure 5.6: One-dimensional compression behaviour of MX80 and the various polymer-modified MX80

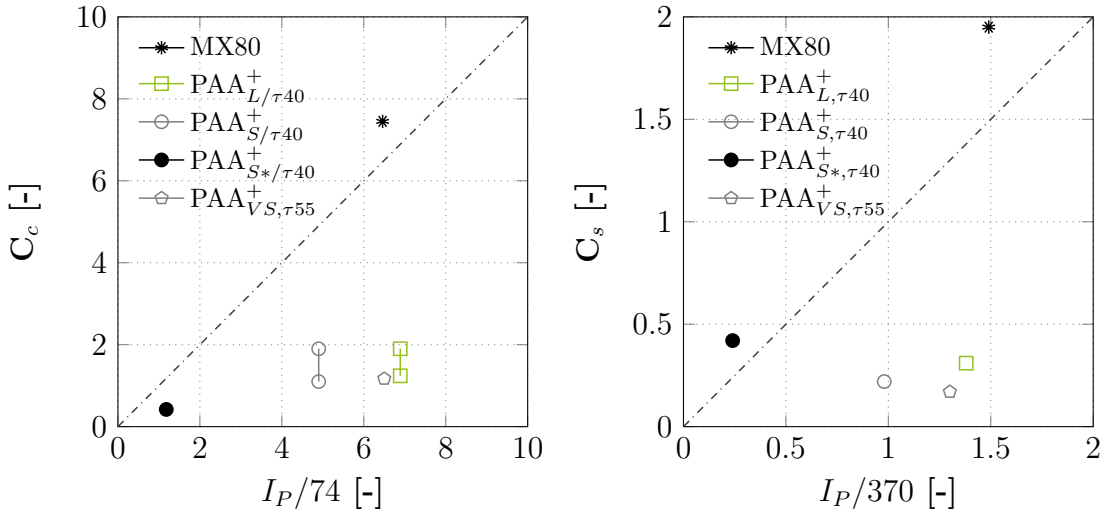

Figure 5.7: Compression and decompression index of MX80 and the various polymer-modified MX80

and 5.2) were derived for remoulded soils. Remoulding describes the removal of inter-particle bonding and effects that arise from geological history (e.g. preconsolidation) by mechanical mixing at a water content above the liquid limit (Burland, 1990). However, further treatment such as drying causes a further degree of disturbance on the level of microfabric which is accompanied by fundamental alterations of material properties like liquid limit and compressibility. The strong deviations from well established relationships shown in Figure 5.7 give evidence that the mechanisms underlying plasticity and those governing compression behaviour of cationically modified smectite are significantly different from the unmodified one. This is further supported by the C_s-value obtained from the oedometer test, which is similar for all modified samples independent of post-mixing treatment. This observation suggests that the post-mixing treatment (drying and grinding) has a similar effect as the extensive compression i.e., alteration of the smallest relevant unit and therefore, that the smallest relevant unit is not stable.

Even though under moderate stress conditions such effects are less relevant for most common soils, polymer chains are an artificial new component in the soil matrix forming polymer bridges. A likely explanation for the alteration of microfabric is the mechanically induced tear-off of polymer bridges between bentonite particles. Mechanical degradation of polymer-chains was demonstrated in literature, for instance caused by shear forces (Yu et al., 1979). During compression, rearrangement of the bentonite matrix stresses polymer bridges that limit the degree of freedom for reorientation of the bentonite constitutes. Therefore, the C_c-values of the mixtures without grinding were found to be smaller than for the pure MX80. At a given stress, the polymer bridges can tear. Such a behaviour of chain tear-off might be compared to the destructuration of natural structured soils, where breakage of inter-particular connectors is accompanied with a significant and irreversible loss of macroscopic strength properties (Delage, 2010; Lieske et al., 2021). However, in contrast to such rigid and brittle connectors found in natural soils (e.g. iron oxides), the connection by polymer bridges is flexible, and therefore no clear yield stress is found as for structured soils.

During compression positively charged patches of adsorbed polymer and unaltered negatively charged parts of the smectite surface attract each other, causing a face-to-face attraction, but not in a well-ordered way. This mechanism is known as patch-flocculation (Bergaya et al., 2006; Szilagyi et al., 2014). The adsorption of cationic polymers is far away from total coverage of the smectite surface (Theng, 2012). External loads cause the modified and unmodified clay surfaces to approach each other and overcome partial repulsion caused by geometric imperfections. The structures flocculated in this way remain

stable due to strong bonding of cationic patches from different smectite surfaces.

Moreover cationic polymers neutralise negative charges by permanent adsorption and further bridging the interlayer by mutual adsorption of the functional group on surfaces and therefore limit interlayer swelling (Suter et al., 2011). However, such neutralisation requires a geometric match between the charge distances on the clay surface and those in the polymer chains, indicating an influence of the chain length on the compression and decompression behaviour.

5.6 Unconfined water retention behaviour

The experimental data of the unconfined suction-controlled water retention and shrinkage behaviour of $PAA^{+}_{L,\tau 40}$ and $PAA^{+}_{S,\tau 40}$ is compared to that of unmodified bentonite presented in Tripathy et al. (2014) in Figure 5.8. Further, tests on $PAA^{+}_{S*,\tau 40}$ are shown for suction values < 9 MPa to demonstrate the impact of drying and grinding on the water retention behaviour. The experimental data and the best fit curves using the Fredlund and Xing (1994) Equations (4.2), (4.3) and (4.4), (adopted in Wijaya et al., 2015) are plotted in terms of water content w, void ratio e and degree of saturation S_r over suction (Figure 5.8 (a.), (c.) and (d.)). Moreover, the shrinkage curve (water content over void ratio) is plotted (Figure 5.8 (b.)).

The comparison of the modified material and the natural MX80 shows that for suctions lower than 10 MPa, both the water content and the void ratio of the modified material are higher than those of the natural MX80. For suction ranges higher than 10 MPa, this proportion changes for the void ratio as well as for the water content. This observation is in agreement with the shrinkage limit which was found to be significantly lower for the modified material ($w_s = 9 - 10$ %) in comparison to the natural MX80 ($w_s = 14$ %).

The volumetric behaviour and the water retention behaviour of $PAA^{+}_{L,\tau 40}$ and $PAA^{+}_{S,\tau 40}$ shows slight differences. This is most obvious for suction ranges < 3 MPa, where the water retention behaviour is predominantly determined by the larger pores. The material modified with longer polymer chains $PAA^{+}_{L,\tau 40}$ has a higher water content and consequently a higher void ratio at suctions in the range below the air entry value as compared to $PAA^{+}_{S,\tau 40}$ with shorter chains for a given suction. However, these differences become smaller with increasing suction and therefore increasing density. The post-mixing treatment of sample $PAA^{+}_{S^*,\tau 40}$ induced an alteration of fabric leading to a distinct effect on the water retention properties. This is consistent with the similar strong effect of

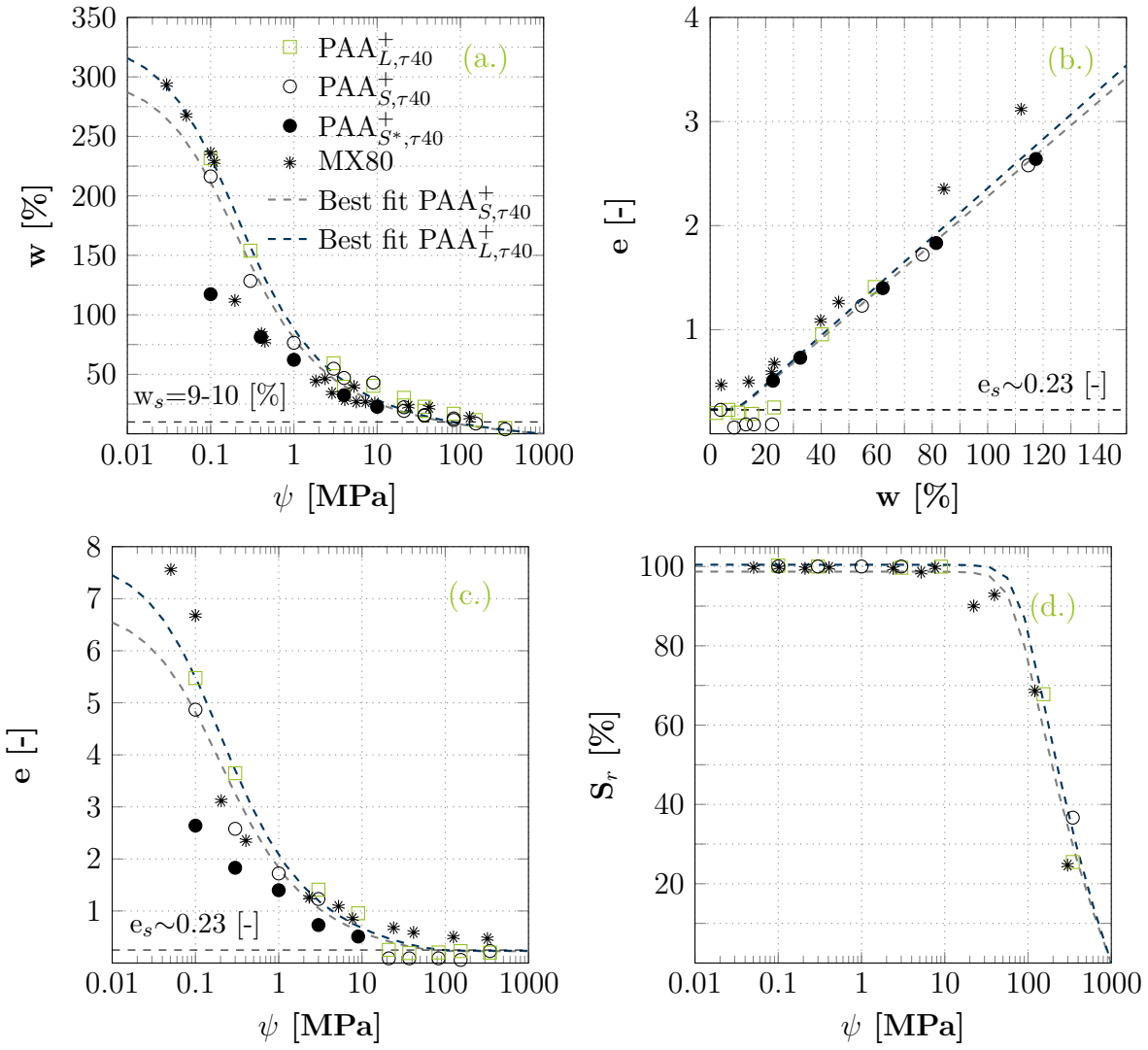

Figure 5.8: Desorption behaviour of the modified and natural MX80 (a.) gravimetric water content versus suction, (b.) void ratio versus water content, (c.) void ratio versus suction, and (d.) degree of saturation versus suction

post-mixing drying and grinding on the Atterberg limits and the behaviour observed in one-dimensional compression tests.

The unconfined suction-controlled shrinkage behaviour of the material can be attributed to similar mechanisms found to dictate the compression behaviour: polymer bridges support an open porous fabric and therefore act as an additional repulsive force whereas adsorption of cationic groups neutralises negative charges, and therefore can be identified as attractive (or reduced repulsive) forces. In addition, non-adsorbed polymer parts such as loops, and tails cause steric repulsion. Such free polymer parts are able to in-

crease the chemical potential of the pore fluid and therefore the osmotic component of suction (Lieske et al., 2020 (a.)). However, during compression, the polymer chains are stressed and when the external forces overcome the repulsive forces, this leads to patch flocculation.

Figure 5.9 shows relationships between the relative humidity and the respective water content of the different composites $PAA^{+}_{S,\tau 40}$, $PAA^{+}_{M,\tau 40}$ and $PAA^{+}_{L,\tau 40}$ compared to that of pure MX80 from Montes-H et al. (2003). For the low water content and adsorption dominated regime of soil water retention the water content is typically studied in terms of water vapour sorption isotherms (Lu and Khorshidi, 2015) and therefore the data shown in Figure 5.8 (a.) has been replotted. The water content at high suctions is believed to be independent of soil fabric and merely represent the surface characteristics of a soil. It should be noted here, that the curve shows the desorption and adsorption behaviour starting from slurry conditions whereas typical literature values start from a dried state (Lu and Khorshidi, 2015). Moreover, the dehydration path does not reach fully desaturation (RH = 0 %). The diagram can therefore not directly be compared with traditional vapour-sorption diagrams, but it provides an indication of the different influences of chain length on the surface properties of the clay. At relative humidities < 86 % (~ 21 MPa suction at 20°C) the amount of adsorbed water of the different composites decreases with the molecular weight. Khorshidi and Lu (2017) showed the strong correlation between CEC as a measure for mineralogical composition and the ability to adsorb water at low RH. It was shown that the affinity for water is decreasing with the CEC. The lower adsorption of water at a given relative humidity can therefore be taken as an evidence for a lower CEC in case of $PAA^{+}_{S,\tau 40}$ by short polymers. This observation is in good accordance with the lower adsorption capacity of the $PAA^{+}_{M,\tau 40}$ and $PAA^{+}_{L,\tau 40}$ in comparison to $PAA^{+}_{S,\tau 40}$, reasoned by a higher degree of cation replacement by the short chained polymers. However, this comparison showed that $PAA^{+}_{M,\tau 40}$ seems to be more effective than $PAA^{+}_{L,\tau 40}$ in cation replacement, although the adsorption maxima are in a similar range.

5.7 Fouling

In some samples kept after the tests, significant fouling of the composites was noticed. After opening the containers in which the samples were stored in a wet state for 2 - 3 months, a distinct odor development was perceived indicating a degradation accompanied by a release of ammonium. Similarly, the samples dehydrated with VET and consequently stored rather dry showed a thin layer of growth on the surface.

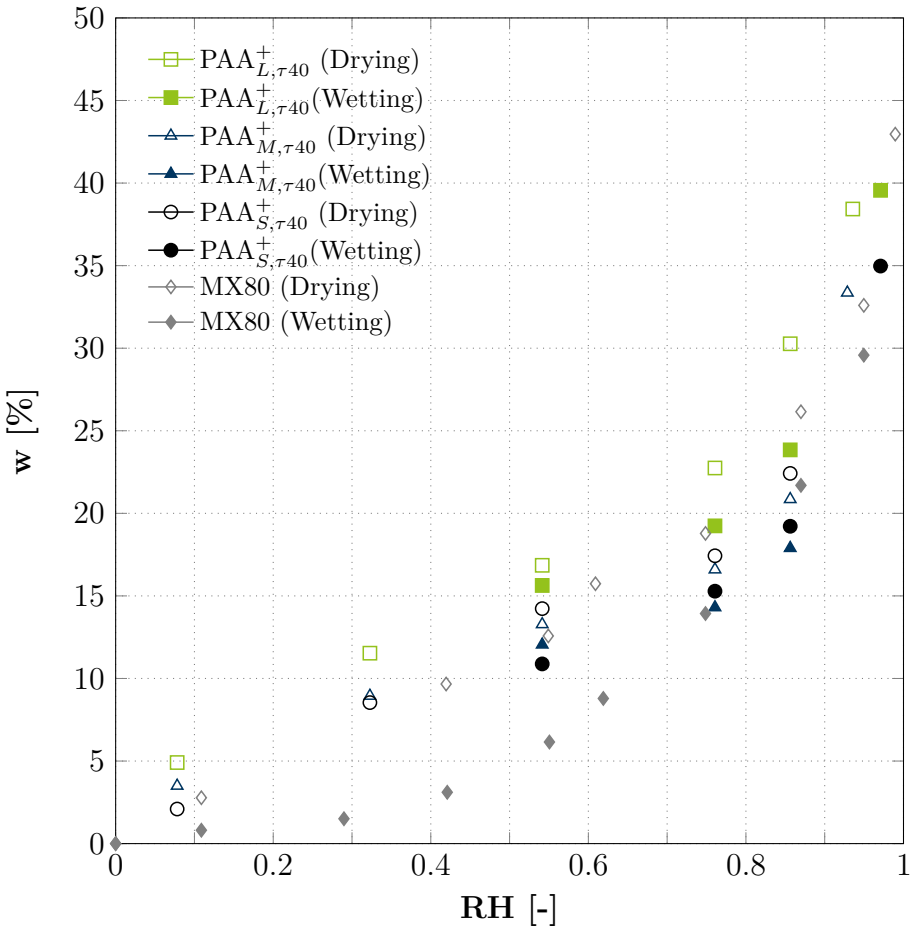

Figure 5.9: Water vapour sorption isotherms for PAA$^+_{L,\tau40}$,PAA$^+_{M,\tau40}$ and PAA$^+_{S,\tau40}$

Figure 5.10 shows the three different samples PAA$^+_{S,\tau40}$ (left), PAA$^+_{M,\tau40}$ (middle) and PAA$^+_{L,\tau40}$ (right) dewatered in the same desiccator at 328 MPa suction. Obvious biological activities can be recognized on the surface of the samples, which are differently pronounced depending on the polymer used. It is significant to note that a different picture of biological catabolism can be observed for the different molecular weights. The surface of PAA$^+_{S,\tau40}$ shows a dense, grey and thick layer of overgrowth, while PAA$^+_{L,\tau40}$ has a very light and relatively flat layer of overgrowth. This observation indicates that the molecular weight can have an influence on the degradability of the composites, which is particularly important for long-term applications. However, this process of degradation needs further investigation as it has not been studied yet.

Figure 5.10: $PAA^{+}_{S,\tau 40}$ (left), $PAA^{+}_{M,\tau 40}$ (middle) and $PAA^{+}_{L,\tau 40}$ (right) samples after desaturation at a suction of 328 MPa

5.8 Conclusion

In this chapter the influence of polymer constitution (i.e., molecular weight and charge density) on the hydro-mechanical behaviour of cationically modified bentonite was studied. Cationic polymers are preferentially used to increase mechanical strength and structural integrity by linking soil constitutes by bridging. At the same token this kind of polymers potentially neutralise negative charges by irreversibly replacing exchangeable cations of the smectite and therefore reduce diffuse double layer swelling, whereas intercalation of cationic polymers causes a permanent expansion of the interlayer.

The experimental results (XRD-results and CEC-measurements, see Steudel et al. (2020)) have proved that only a part of the polymers is intercalated into the interlayer whereas another part of the polymers is adsorbed on external clay aggregate surfaces leading to bridge-formation or is entrapped in pores.

The results of the tests performed to address the macroscale showed the influcene of the molecular weight on the index properties. Likewise, an influence on the compression-decompression behaviour as well as the unconfined suction-controlled shrinkage behaviour was found which was, however, less pronounced. The influence of the different molecular weights were related to differences in fabric for the low suction range whereas differences in water sorption behaviour at low relative humidities are related to different abilities to alter surface properties.

High mechanical stresses caused by suction, applied load or grinding led to a significant change in the material properties. This was reasoned by a breakdown of the initially

open porous structure caused by mechanical degradation of polymer bridges and patch flocculation, when stress induced forces overcome steric repulsions.

The findings of this study suggest that effects induced by polymer modification can significantly alter during mechanical loading or post-mixing treatment by drying and grinding, which has to be considered particularly with respect to possible production steps and with regard to alteration of the initial properties in long-term applications. This effect may be more important for wet modified clays, where the initial open-pored fabric is formed after mixing and destroyed by subsequent drying and grinding.

The study shows that the macroscopic behaviour of polymer solutions and the polymer-clay interaction are directly influenced by the boundary conditions during preparation which is directly related to the molecular weight of the used polymer. At a given concentration, the viscosity of the polymer solutions, osmotic pressure and adsorption behaviour change significantly with the molecular weight (Lieske et al., 2020 (a.); Verst et al., 2022). For the implementation of polymer modification on the engineering relevant scale, the molecular weight provides therefore a parameter for optimization with regard of the technological process. It needs further to be taken into account that all the polymers examined in the study were rather long. The impact of the molecular weight may be more pronounced below certain molecule sizes.

6 Hydro-mechanical behaviour of non-ionically modified bentonite

6.1 General

In the following chapter, the experimental investigations on bentonite modified with non-ionic polymer are presented and discussed. The chapter opens with adsorption properties and the microfabric of the modified clay. Subsequently, the macroscopic properties of the material are addressed, i.e. the index properties, the one-dimensional compression behaviour and the unconfined shrinkage behaviour. In the last part of this chapter the micro- and macroscopic properties are summarised. The focus of this chapter is set on the impact of molecular weight on the hydro-mechanical behaviour of non-ionically modified bentonite. Moreover, the impact of mixing and post-mix processes is adressed with respect to their potential to control soil mechanical properties.

6.2 Adsorption behaviour and morphology

The adsorption isotherms of the PAA^0_L, PAA^0_M, PAA^0_S and PAA^0_{VS} are plotted in Figure 6.1. The maximal adsorption capacity of PAA^0_M, PAA^0_S and PAA^0_{VS} is in a similar range. In contrast, the polymer with the longest chain length (i.e. highest molecular weight) has a significantly lower maximum adsorption capacity of about 50 % of that of the other polymers. It should be noted that, similarly to cationically modified bentonite, the amount of polymer bonded by surface adsorption or intercalation is lower than the amount indicated by the adsorption isotherms. This is due to polymer being entrapped in aggregates rather than being adsorbed, a phenomenon termed as 'pore adsorption' (Schamp and Huylebroeck, 1973). The adsorption maxima of PAA^0_M, PAA^0_S and PAA^0_{VS} are in a similar range to that of their cationic counterparts as it has been observed in Haase (2017) for sodium bentonite. However, the adsorption mechanisms and the effect

of the non-ionic polymers on smectite surfaces and fabric are different from those of the cationic polymers. Due to the absence of Columbic attraction between the negatively charged smectite layers and the polymer, non-ionic polymers are adsorbed via dipol-dipol attraction, whereas the adsorption of charged polymers is strongly determined by the electrostatic forces. Moreover, the non-ionic polymers are present in rather coiled state, while the ionic polymers are present in a rather stretched form.

A study on the influence of the molecular weight on the adsorption behaviour of non-ionic polyacrylamides presented by Schamp and Huylebroeck (1973) showed that in case of sodium bentonite, the adsorption maximum increases with the molecular weight of the polymer. However, comparing the results of the current study and the study performed by Schamp and Huylebroeck (1973) two major differences can be observed. The overall adsorption capacity of PAA^0_M , PAA^0_S and PAA^0_{VS} is less than 20 % and that of PAA^0_L is even less than 10 % of that obtained in Schamp and Huylebroeck (1973). Moreover, in contrast to Schamp and Huylebroeck (1973) the adsorption capacity decreases with the molecular weight, at least for the PAA^0_L. These differences can be attributed on the one hand to the bentonite used, as it is not homo-ionic, but contains both monovalent sodium and divalent calcium as exchangeable ions. As stated by Laird (2006) mixed-ionic exchangeable cations are mostly occurring in separated homo-ionic particles. In other words, some smectite surfaces or interlayers contain only calcium, while other areas are mainly covered by sodium. Due to the high attractive forces acting in case of the divalent calcium, the calcium saturated particles of such a bentonite are more stable than the monovalent sodium saturated particles and therefore show a different behaviour.

In various studies it was shown, that bentonites with mixed-valence exchangable cations show a very different behaviour as compared to their homo-ionic counterparts (Salles et al., 2009). As the adsorption of non-ionic polymers strongly depends upon the available surfaces, it follows that the maximum adsorption capacity decreases in the order smectite > illite > kaolinite (Deng, Dixon and White, 2006; Haase, 2017). Although the intercalation of polymer in the interlayer of Ca^{2+} saturated smectite has been repeatedly demonstrated (Theng, 2012), the amount of polymer retained in the interlayer is not in the magnitude of the quantity adsorbed on the external surfaces. Therefore, it is in good agreement with these studies that a bentonite with Na/Ca-mixed layers has larger particles and thus less available surfaces for adsorption.

The other difference between the current study and Schamp and Huylebroeck (1973) is the concentration of the polymer solutions and bentonite suspension at which maximum adsorption capacity was determined. As it has been discussed in Chapter 2.2, the mor-

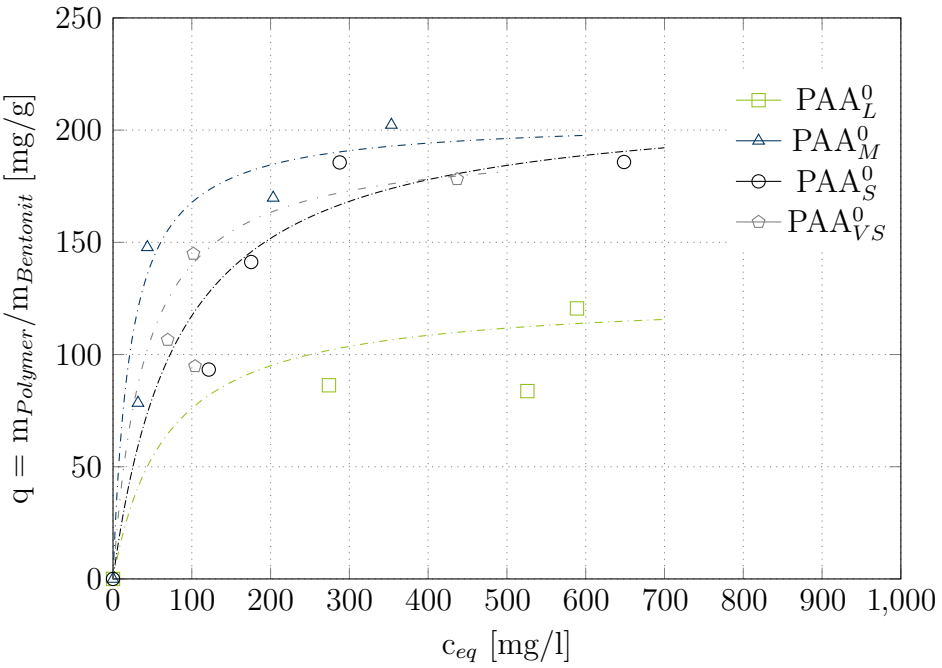

Figure 6.1: Adsorption isotherms

phology of polymer chains strongly depends upon intra- and interaction of the chains as well as solvent quality. This interaction becomes typically evident in the shear thinning behaviour upon shear as shown for the used non-ionic polyacrylamide with a chain length of 9 - $13 \cdot 10^6$ g/mol in Figure 6.2. The relationship of viscosity versus shear rate was obtained using a conventional rotational rheometer at different concentrations. The higher the concentration the more pronounced the shear-thinning, that means the decrease of viscosity with increasing shear rate, due to more potential interaction of the polymer coils (Verst et al., 2022).

The most pronounced change in the behaviour of polymer solutions is attributed to the point where the available space in a solution is equal to the space occupied by the single polymer coils and coils begin to overlap. Lee and Schlautman (2015) showed that for concentrations greater than the concentration at which the polymer coils begin to overlap (overlap concentration c*), a substantial difference in the polymer-clay interaction becomes apparent in macroscopic properties. In this concentration regime polymer chains entangle and polymers are adsorbed as an entangled bulk rather than as isolated chains. Likewise, Schamp and Huylebroeck (1973), observed a critical concentration at which polymer chains can no longer be regarded as isolated chains but where interactions between the chains dominate the behaviour of a polymer solution. Lee and Schlautman

(2015) determined the overlap concentration of non-ionic polyacrylamides at 155 mg/l in a 0.01 M NaCl solution for a molecular weight of $18 \cdot 10^6$ g/mol. The overlap was assigned to a significant change in the viscosity at zero shear (η_0) i.e., the viscosity at the Newton plateau. The critical concentration observed by Schamp and Huylebroeck (1973) and the overlap concentration c* determined by Lee and Schlautman (2015) are plotted as a function of the molecular weight M in Figure 6.3. The plot gives evidence for a unique relationship between overlap concentration and molcular weight, showing that the overlap concentration is decreasing with decreasing molecular weight.

The low concentrations required to achieve the overlap concentration are due to the relatively large volume of a polymer coil. The large individual volume occupied by a single polymer coil is visualised through the relationship between molecular weight and radius of gyration shown in Figure 6.4. The experimental results of Ball et al. (1984) showed that there is a linear increase in the radius of gyration with molecular weight in a double logarithmic scale. The plot also shows the mean value of the molecular bandwidth for the polymers used. The plot highlights the significant differences in the volumes occupied by the single polymer chains.

The initial concentrations used to prepare the mixtures are shown in Figure 6.3. It can be seen that all the solutions used are well above the overlap concentration and strong intermolecular interactions are therefore to be anticipated between the polymers. In contrast, studies on polymer-clay interactions in the field of colloid science are usually conducted at concentrations near or below the overlap concentration, and so it is in Schamp and Huylebroeck (1973). The strong interaction between the polymers at the high concentrations used in the current study promotes the picture of an adsorption morphology present as a coating of interacting polymer chains rather than as isolated chains that individually absorb at the smectite surface. The clay minerals act as cross-linkers that bind the polymer chains, which is similar to the procedure used in the production of nano-composites where the clay mineral acts as a filler. This high concentration when mixing polymer and bentonite causes the interactions between the clay surface and the polymer as well as to significant interactions between the polymers. Consequently, external factors that influence the interaction between polymers (e.g. shear) play a role in the preparation of the polymer-clay mixtures.

This can be illustrated on the basis of the size of the polymer chains. The coil of a non-ionic polymer with a moleclar weight of $1.7 \cdot 10^7$ g/mol has a radius of gyration of about 440 nm. The absolute length of the same but absolutely stretched polymer, however, is 21 μm. These variable sizes of the polymer compared to the size of a smectite mineral of

2 μm demonstrate the variability of a polymer chain and ability to attach to different clay surfaces depending on the boundary conditions. When the size or shape of a polymer coil is altered by external influences, this results in different polymer-clay associations and thus fabrics (Mpofu et al., 2004). This is pronounced in case of non-ionic polymers due to the weak attraction of the surfaces and the rather coiled morphology of the polymers, and, further for wet mixed materials, as all components have a comparatively high degree of variability when dissolved in water. At the same token, the evolution of fabric during mixing is a dynamic process: flocs are sheared apart and then merge with other flocs combining to larger flocs (Mpofu et al., 2004). With increasing number of attached polymers, the stability of flocs increases whereas the number of non-adsorbed polymers decrease.

A hypothesis why PAA_L^0 does not follow the trend of an adsorption maximum increasing with molecular weight observed in Schamp and Huylebroeck (1973) might be found in the size of the molecules. The comparison of the influence of different molecular weights on the viscosity in Lee and Schlautman (2015) (see Figure 2.13) reveals that polymers with a molecular weight below $6 \cdot 10^6$ g/mol show a rather moderate increase of viscosity beyond overlap concentration, whereas a significant increase in viscosity beyond the overlap concentration was observed for the polymer with a molecular weight of $18 \cdot 10^6$ g/mol. This increase in viscosity reflects strong interaction at the molecular level which is obviously more pronounced for large molecules. Vice versa, more energy is therefore needed to bring long chained polymers in motion. Especially after exceeding the overlap, it seems plausible that with similar mixing energy, the longer-chained polymer is more difficult to be intermixed with the clay. Due to the significantly lower molecular weights of the polymers ($< 10^6$ g/mol) and concentrations investigated in Schamp and Huylebroeck (1973), these effects might therefore be of lesser relevance in that study. Furthermore, the ability to form aggregates increases with the concentration of the clay because of the smaller distance between the minerals and longer polymer chains due to their larger capacity to bridge the distance between two clay minerals. Deng, Dixon, White, Loeppert and Juo (2006) noted that the formation of aggregates can restrict the access to the surfaces within the aggregate. It can therefore be concluded that boundary conditions that promote flocculation, such as high molecular weights and high concentrations, tend to cause lower adsorption maxima.

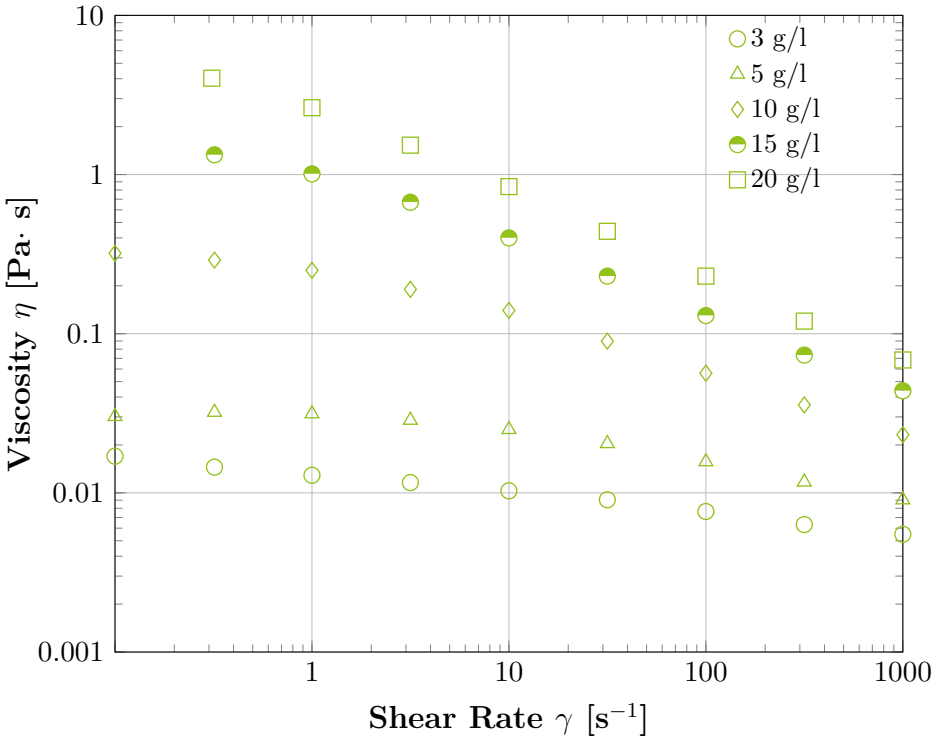

Figure 6.2: Viscosity of the pure polymer solution used to prepare PAA^0_M

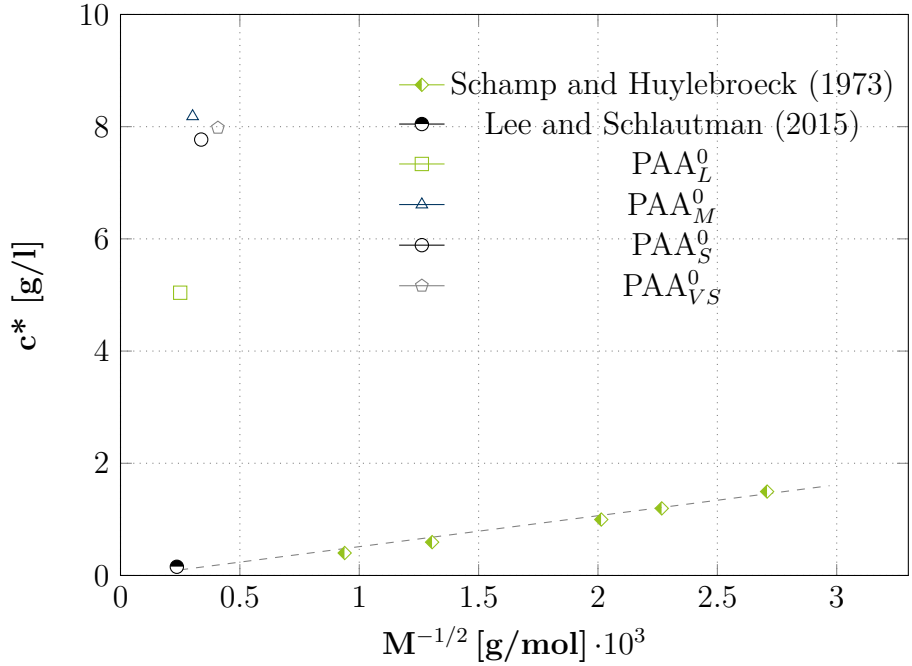

Figure 6.3: Overlap concentration as a function of polymer molecular weight

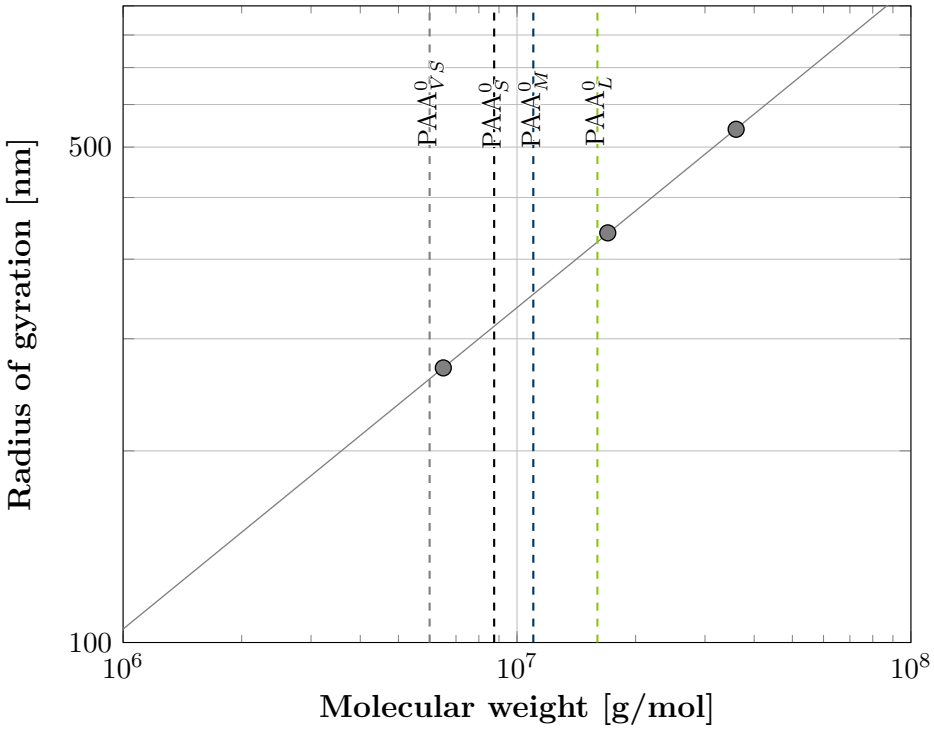

Figure 6.4: Radius of gyration versus molecular weight of a non-ionic polyacrylamide solved in water. The grey dots represent the experimental results from Ball et al. (1984). The dashed lines show the molecular weight of the polymers used in the current study.

6.3 Microfabric

For the investigations on microfabric, bentonite and polymer were mixed in small quantities (i.e. 30 ml bentonite suspension and 30 ml polymer solution) following the mixing procedure applied to determine the adsorption isotherms. The material studied was obtained directly from the centrifugate. The microfabric of PAA^0_M which has been studied after cryo-BIB treatment and that of PAA^0_L studied at RH $< 80\,\%$ in an ESEM without prior treatment are shown at different magnifications in Figures 6.5 and 6.6, respectively.

The micrograph of the PAA^0_M in Figure 6.5 (a.) and (b.) shows an artificial fabric which is hardly recognized as a clay-based microfabric or a natural soil fabric. The close-up in Figure 6.5 (b.) shows a net-like architecture with a very open porous fabric. A disperse edge-to-edge flocculated fabric (Figure 3.4 (d)), corresponds most closely to the fabric visible in Figure 6.5 (a.). The thin wall-like elements that compose this fabric are sometimes present in a length that clearly exceeds 2 μm. As smectite minerals are

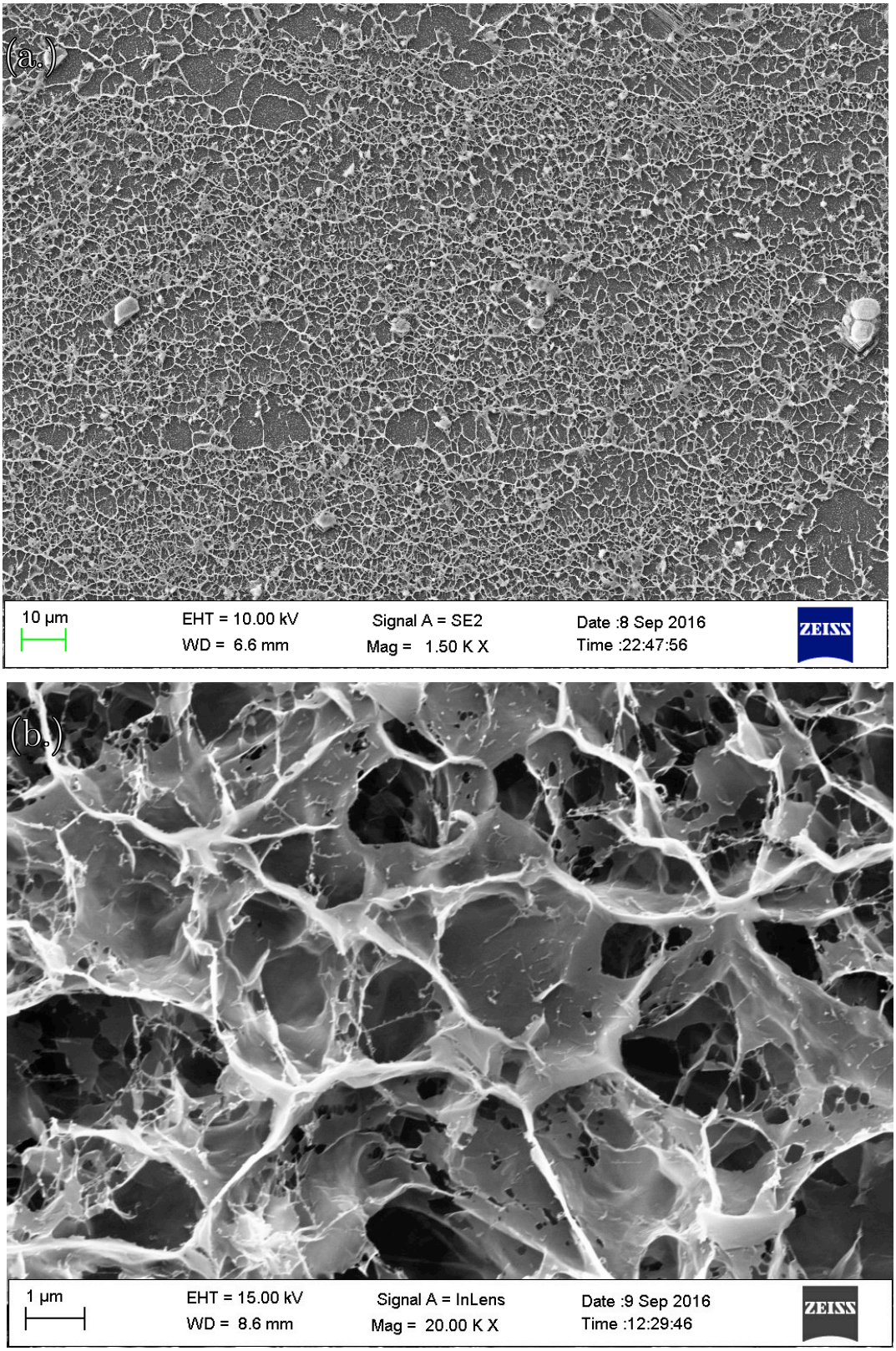

Figure 6.5: Microfabric of PAA^{0}_{M} centrifugate in different magnifications studied using an ESEM after cryo-BIB preparation

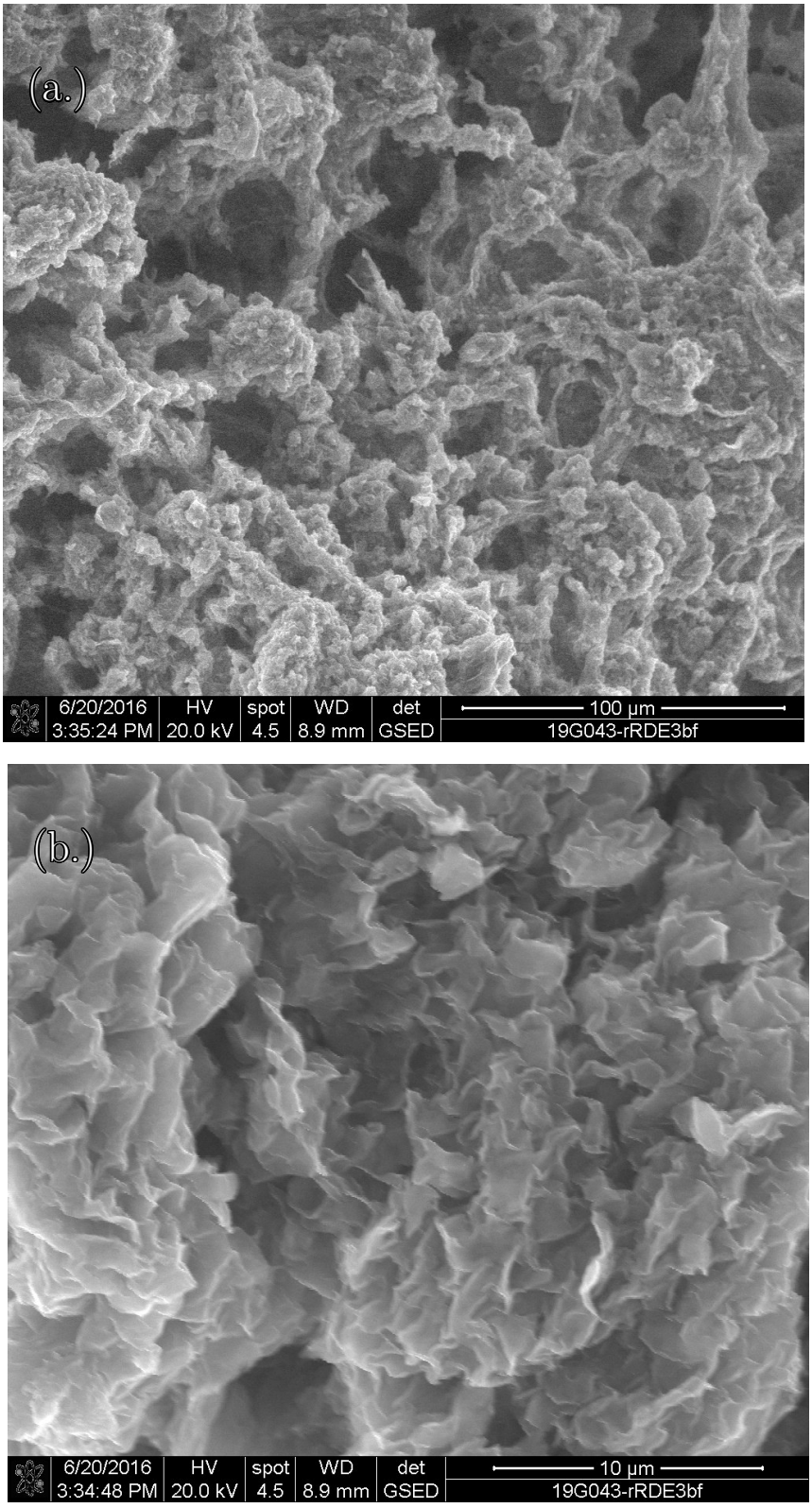

Figure 6.6: Microfabric of PAA_L^0 centrifugate in different magnifications studied in an ESEM at a RH $< 80\%$

typically present in lateral dimensions of 1 - 2 μm (Grim, 1953), it can be expected that several minerals are arranged side by side in a wormlike arrangement. However, in contrast to the cationically modified smectite (Figure 5.4), the mineral phase is rather difficult to be identified. The minerals appear to have a gel-like coating and there are polymer threads crossing the large pores between the walls. The large landscape shown in Figure 6.5 (b.) shows that there is a certain variability of the pores ranging between 3 μm up to >10 μm.

The fabric of the PAA^0_M given in Figure 6.5 (a.) shows the typical micro-architecture known for polymer gels. Such networks can be found in several natural and technical applications. Cuadros (2017) found similar fabric in a cryo-SEM experiment conducted on a biofilm grown on a mineral surface, where a biofilm present as extracellular polymeric substances (EPS) consist of 50- 90 % polysaccharides. Moreover, researchers found such structures in cross-linked polymer gels (Dragan, 2014) and polymer-hybrid structures such as nanocomposites (Sheng et al., 2017). Although the polymer content in PAA^0_M is significantly lower compared to that of the previously mentioned applications, it is obvious that the polymer dominates the architecture of the microfabric in both cases. These observations are confirmed by the microfabric shown in Mpofu et al. (2004), which is also very open-porous and similar to that shown in Figure 6.5, although the polymer to clay ratio was lower than in the current study (500 g/ton solid).

Figure 6.7 shows an idealised schematic of the fabric of the PAA^0_M given in Figure 6.5 (b.). The smallest relevant unit of the clay is on the level of particles, as the mixing energy is not high enough to disintegrate the clay to the level of a sheet. Hydrogen bonds between NH_2 and O groups of adjacent acrylamid chains and entanglement yield polymer threads, composed of several polymer chains. Adsorption of multiple polymer chains on a particular particle yields a cross-link, i.e. a connection of several polymer chains to a branched 3D fabric. This microfabric is generally termed a phase-separated structure or intercalated structure, depending on if intercalation takes place (Ray and Okamoto, 2003; Palomino, 2010).

The PAA^0_L studied at RH < 80 % shows pronounced differences to PAA^0_M, were the initial fabric has been preserved by rapid freezing. The close-up shown in Figure (b.) 6.6 (note the different magnification) does not show the mesh like arrangement but looks more like a continuous mass. The less magnified image in Figure 6.6 (a.) shows very large pores. The arrangement of the soil constitutes appears as aggregates, some of them are relatively spherical, connected by elongated aggregates in the order of 20 - 30 μm. The occurrence of globular agglomerates after modification of sodium bentonite with alkylamine was

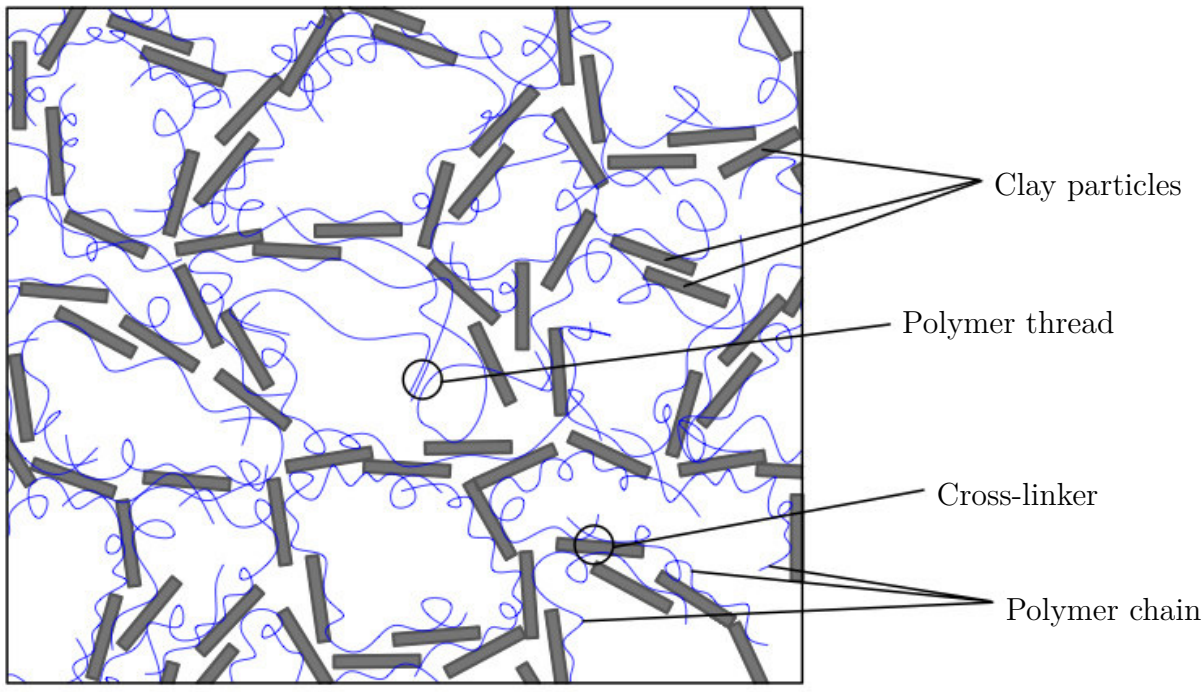

Figure 6.7: Schematic of the PAA^0 microfabric based on a phase-separated structure

also observed in Xie et al. (2017). Similar to the alkylamine used in Xie et al. (2017), the functional group of the polyaclyamide used in the current study is a primary amine. Haase (2017) studied the same composite of non-ionic polyacrylamide and MX80 (PAA^0_M), at a relative humidity of 77.6 % and observed a similar picture of the microfabric. However, the micropores were a little less pronounced which again underlines the sensitivity for even small modifications in the mixing procedure.

The comparison of the investigations on microfabric of Haase (2017) and those in the present study shows that the clear difference between the microfabrics shown in Figures 6.5 and 6.6 cannot be attributed to different polymer chain length. The differences are the result of a dewatering induced adjustment of the fabric. The network shown in Figure 6.5 (a.) collapses and forms more compact but still disperse aggregates (Ning et al., 2014). However, due to the rather weak attraction of the polymers to the clay surface a certain rearrangement is possible without rupture of the polymer chains (Takeno and Nakamura, 2019). The zoomed microfabric shown in Figure 6.6 (b.) indicates that this collapse cause the opening of new large macropores.

6.4 Index properties

The plasticity properties and the shrinkage limit of the different mixtures are shown in Table 6.1 and in the Casagrande plasticity chart in Figure 6.8, respectively. The liquid limit of all composites is lower than that of the unmodified MX80. The trend of the liquid limit, however, neither shows a clear correlation with the polymer chain length nor with the adsorption maximum. PAA^0_{M*} and PAA^0_{VS*} have almost the same liquid limit although they have significantly different molecular weights. The same applies to PAA^0_{L*} and PAA^0_{S*}. For the latter two polymers there are significant differences in the polymer-concentration during mixing, as the adsorption maximum of PAA^0_{L*} is only slightly more than half of the maximum of PAA^0_{S*}. In contrast to the molecular weight and the amount of added polymer, a clear correlation exists between the liquid limit and the mixing method. PAA^0_{L*} and PAA^0_{S*} were stirred with the eccentric rotating whisk, while PAA^0_{M*} and PAA^0_{VS*} were mixed with the paddle stirrer according to the procedure used for the formulation of cationic mixtures.

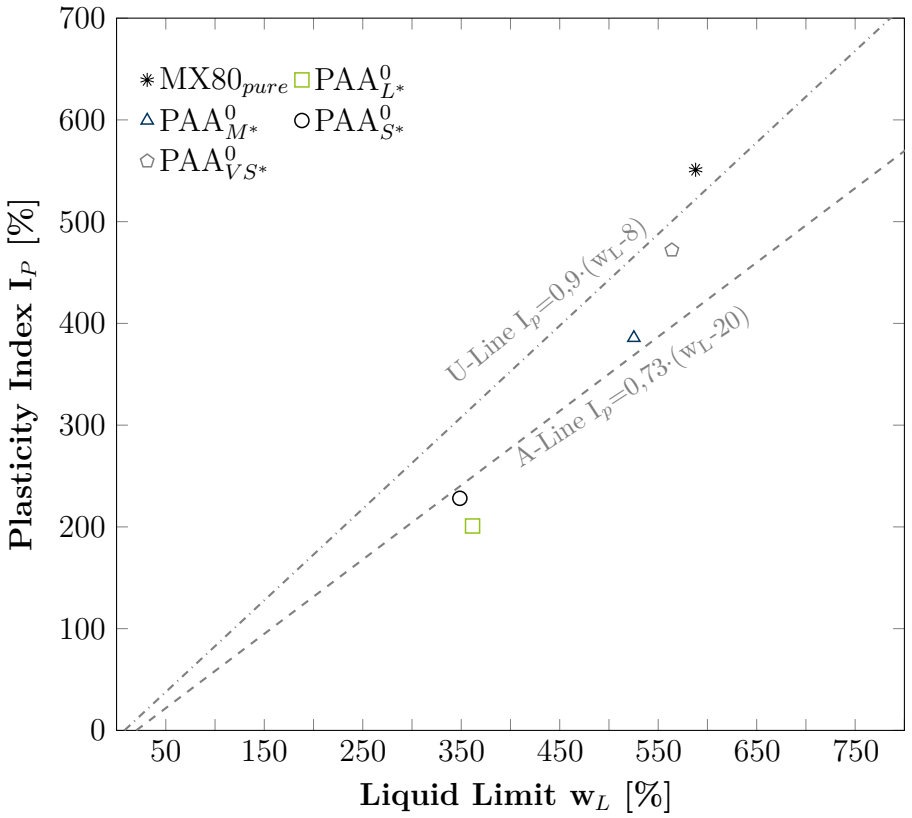

Figure 6.8: Classification of MX80 and polymer-modified MX80 in the plasticity chart

Table 6.1: Plasticity properties and shrinkage limit for the different mixtures

Material	Liquid limit [%]	Plastic limit [%]	Plasticity index [%]	Shrinkage limit [%]	Specific density [-]
MX80[1]	588	37.0	551.0	14	2.65
$PAA^0_{L^*}$	361.5	160.6	200.9	7.34	2.37
$PAA^0_{M^*}$	525.3	139.5	385.8	4.45	2.31
$PAA^0_{S^*}$	348.6	120.5	228.1	6.35	2.31
$PAA^0_{VS^*}$	563.9	91.9	472.0	-	2.27

[1] Data From Haase (2017) * Material has been dried and grinded prior to testing

The liquid limit of all composites is lower than that of the unmodified MX80. However, it needs to be considered that the water content was calculated based on the dry mass of the mixture including the weight of the polymer solids. Taking into account that the proportion of polymers is > 10 % (the exact value is uncertain), this yields a liquid limit (based on the pure clay content) for $PAA^0_{M^*}$ and $PAA^0_{VS^*}$ that is higher than that of natural clay. This observation is in accordance with Haase (2017), where the adsorption of non-ionic polymers was associated with an extended diffuse double layer swelling and thus a higher ability of the clay minerals to bind water. By contrast, the liquid limit of $PAA^0_{L^*}$ and $PAA^0_{S^*}$ is lower than the value of the unmodified material. Likewise, Rao et al. (1993) reported a significant reduction of the liquid limit after modification of a bentonite with a non-ionic polysaccharide. Sridharan and Prakash (1998) reasoned the effect of the polymer to induce aggregation of the smectite minerals and therefore to curtail the available surface area (or particle splitting) and diffuse double layer swelling. In this sense, a possible reason for the reduction of the liquid limit is the formation of polymer bridges, which act as an additional attractive force and consequentially limit the diverge of overlapping diffuse double layer during water adsorption or even their development. Considering that the morphology of microfabric is highly affected by boundary conditions during mixing, it becomes obvious why the mixing procedure has such an important effect on the ability to hold water.

Although polymer bridges are also present in $PAA^0_{M^*}$ and $PAA^0_{VS^*}$, their arrangement and the resulting microfabric facilitates higher ability to retain water without loosing its strength. The hydro-mechanical behaviour and in particular the plasticity properties

of smectite are governed by its surface properties but also by its fabric. As discussed in Section 6.3, non-ionic polymers can cause the formation of a fabric exhibiting features not common in natural soils. The different plasticity properties can therefore be attributed to the different energies used during mixing, which appear to have resulted in a different fabric. A study conducted by Mpofu et al. (2004) showed, that external effects that yield a reduction of polymer coil size during mixing will significantly alter microfabric of polymer-clay mixtures. A small hydrodynamic radius of polymers during mixing was found to cause an initially very open porous fabric which was easily destroyed. By contrast, a small hydrodynamic radius was causing a more compact and very stable open porous fabric.

Such different microfabrics are a potential reasoning for the different plasticity properties related to different mixing energies and therefore polymer coil dimensions. However, the impact of complex shearing scenarios on the coil size of polymers is still not entirely clear and therefore it is not possible to dedicate a shearing energy to a specific fabric. Moreover, it is unclear whether the different liquid limits are solely caused by different microfabric or also due to different surface modifications. This is because the mixing process and the resulting polymer morphology influences both the adsorption at the surface and the bridging between the particles. However, with regard to the influence on the liquid limit, polymer bridges can be attributed to opposite effects. If polymer bridges hold particles together and prevent the formation of a diffuse double layer, they cause a reduction of the liquid limit (Sridharan and Prakash, 1998). If polymer bridges support very open porous structures that allow a distance beyond the thickness of the diffuse double layer to develop, then this can cause larger liquid limits (Lieske et al., 2022).

The results show, that the difference in liquid limit between $PAA^0_{S^*}$ and $PAA^0_{L^*}$ is low, even though the mixing ratio between polymer and clay is different. This observation indicates, that lower uptake of polymer will not fundamentally change the material behaviour. Various studies proved that the most significant effects were achieved through the addition of small amounts of polymers, while a further increase of polymer was less relevant. Rao et al. (1993) reported, that the addition of 3 percent polymer reduced the liquid limit by half, while a further increase to 10 percent polymer in the mixture caused only a slight additional change in the liquid limit. Similarly, Otsubo (1993) indicated strong bridging of non-ionic polymers based on viscosity measurements, although the concentration of the polymer was low during mixing.

The concept of different microstructures as a consequence of different mixing energies is further supported by the shrinkage limits, which are almost identical for $PAA^0_{L^*}$ and

$PAA^0_{S^*}$, with their values being slightly above the value of $PAA^0_{M^*}$. The shrinkage limit is a function of the densest possible packing and is relatively independent of surface properties (Sridharan and Prakash, 1998). From the observation that the mobility of the matrix in the case of $PAA^0_{L^*}$ and $PAA^0_{S^*}$ is more restricted by the bridging which acts as an additional attractive force than in the case of $PAA^0_{M^*}$, it follows that a denser arrangement is possible in the case of the latter.

The plastic limit of the modified material is significantly higher than that of the natural material. In contrast to the liquid limit, the plastic limit decreases with the molecular weight. The plastic limit corresponds to the water content of a sample when cracks occur during the rolling out test. As the cracks are filled with air, the plastic limit is generally believed to correspond to the air entry value. From a micromechanically point of view cracks occur when the frictional forces exceed the capillary stresses and therefore a further reduction of the water content cannot reduce the pore volume equivalently. Taking into account that also in the case of the plastic limit the polymer bridges act as an additional stabilisation of the clay matrix, it becomes evident that the ability of the material to deform equivalent to the capillary stress is exceeded faster than in the case of the non-modified material. Furthermore, due to steric effects, the adsorbed polymers hinder an orderly formation of particles during drying (Jasmund and Lagaly, 1993).

6.5 One-dimensional compression behaviour

Oedometer tests were carried out to investigate the influence of the non-ionic polymer modification on the one-dimensional compression behaviour of the MX80. The centrifugate of the PAA^0 mixtures was found to exist as a ductile elastic mass (see Figure 4.4) which requires further treatment prior to testing. Similarly to the index tests, the elastic mass was dried and grinded and subsequently again mixed with water to obtain the target water content. Only one sample PAA^0_{VS} was tested without post-mixing treatment. In that case the elastic mass was tested in the large oedometer. An overview of the preparation steps and used oedometer devices is given in Table 6.2.

The void ratio over effective vertical stress is plotted in Figure 6.9 for the pure MX80, $PAA^0_{L^*}$, $PAA^0_{S^*}$, $PAA^0_{VS^*}$, and PAA^0_{VS}, respectively. The virgin compression lines of the composites $PAA^0_{S^*}$ and $PAA^0_{L^*}$ are clearly positioned below the curve of the MX80 over wide stress ranges. By contrast, the compression line of $PAA^0_{VS^*}$ exceeds the curve of MX80 starting at about 55 kPa and shows a distinctly higher resistance against deformation. Like the liquid limit, the relative position of the compression curves correspond to

Table 6.2: Post-mixing treatment, initial conditions and oedometer devices used to study the different PAA^0

Material	Post-mixing treatment	initial conditions	Oedometer device
PAA^0_{L*}	drying + grinding	1.1 w_L	standard
PAA^0_{S*}	drying + grinding	1.1 w_L	standard
PAA^0_{VS*}	drying + grinding	1.1 w_L	standard
PAA^0_{VS}	none	centrifugate	large

the mixing boundary conditions. However, a comparison of PAA^0_{S*} and PAA^0_{L*} shows that the virgin compression line of PAA^0_{S*} ($C_c = 3.4$) is slightly steeper than that of PAA^0_{L*} ($C_c = 2.7$), mixed at similar boundary conditions.

The direct comparison of PAA^0_{VS} and PAA^0_{VS*} shown in Figure 6.9 indicates a substantial alteration of the material behaviour caused by drying and grinding. PAA^0_{VS}, the material that has not been dried before the compression test, shows a much softer behaviour ($C_c = 3.1$) than PAA^0_{VS*} ($C_c = 4.5$) and the virgin compression line remains below the curve of the MX80 over the whole range of tested stresses. The investigations conducted on microfabric shown in Figure 6.6 (a.) and (b.) indicate a local collapse of the polymer induced mesh and the formation of large aggregates by drying. The PAA^0_{VS} can therefore be assumed with a microfabric represented by the mesh-like arrangement in Figure 6.5 while PAA^0_{VS*} possesses a more aggregated fabric as shown in Figure 6.6. The compression behaviour of PAA^0_{VS} reflects the progressive collapse of the open porous net-like fabric where polymers have a certain flexibility in contrast to PAA^0_{VS*}. However, at the same token the dried material has a much higher porosity during compression over the whole range of tested stresses.

It is remarkable, however, that drying causes a rearrangement of fabric even after compression in case of PAA^0_{VS}. Figure 6.10 shows the PAA^0_{VS} sample from the oedometer after drying at 105°C overnight. The material shows a distinct but irregular expansion (see Figure 6.10 (a.) + (b.)). A probable explanation for the atypical behaviour of the modified material suggests the deformation of the polymer chains when dried (Mpofu et al., 2004). This phenomenon, which could be described as drying deformation, can also be observed in the sample of PAA^0_{VS} shown in Figure 6.10 (a.) + (b.), where drying after compression was accompanied by an unusual expansion.

The comparison of the compression and decompression indices from the oedometer tests

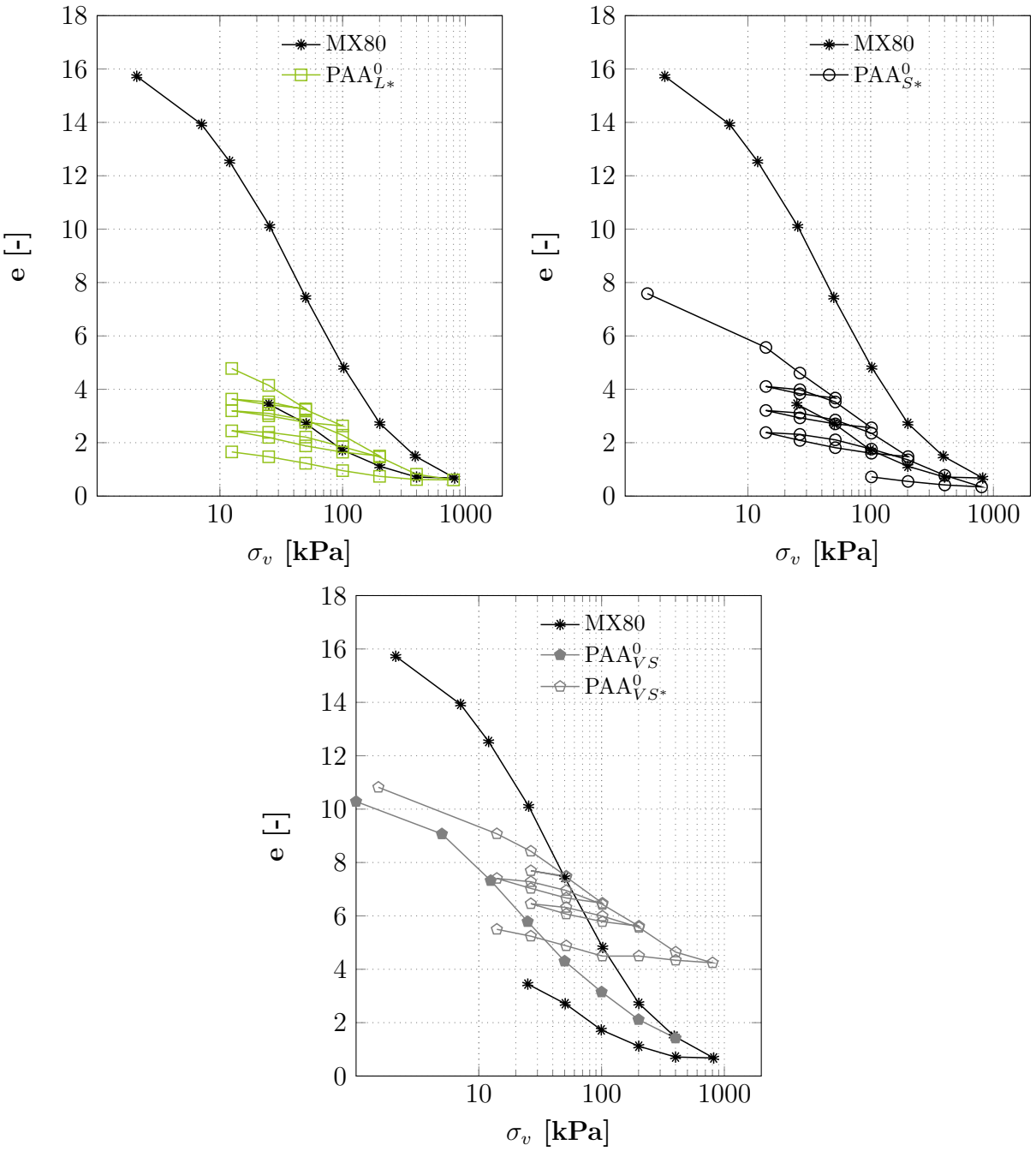

Figure 6.9: Vertical compression behaviour of MX80 and the various polymer-modified MX80

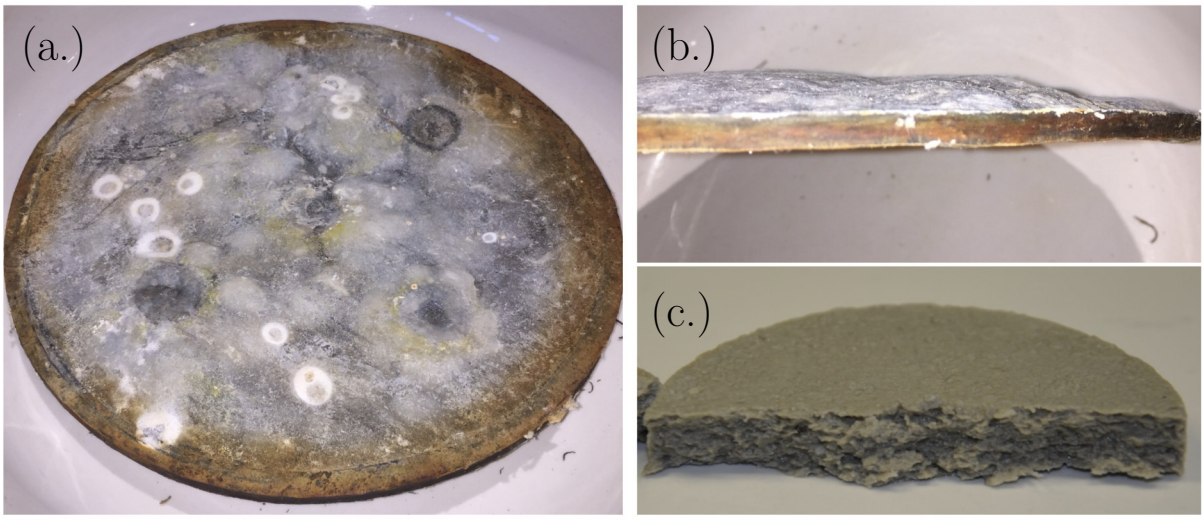

Figure 6.10: Photographs of the PAA^0_{VS} after one-dimensional compression in the large-oedometer: (a.) top view, (b.) side view (c.) Photograph of the $PAA^0_{L^*}$ after one-dimensional compression test

and the empirical correlations according to Equations (5.1) and (5.2) are shown in Figure 6.11. With the exception of $PAA^0_{VS^*}$, all compression and decompression indices from the oedometer data do approximately fit the empirical correlations. This indicates that the smallest relevant unit (i.e. aggregate) of the material is not fundamentally altered due to mechanical stresses, after being subjected to post-mixing treatment. Figure 6.10 (c.) shows the specimen $PAA^0_{L^*}$ after dismantling from the oedometer. Unmodified bentonites commonly show a gel-like consistency when fully saturated. By contrast, in the case of modified material $PAA^0_{L^*}$, the shape of the initial aggregates is clearly apparent. This underlines the stability of the aggregates, but also the limited ability to merge into a homogeneous mass due to a restricted mobility caused by the polymer bridges. Unlike PAA^0_{S*} and PAA^0_{L*} , PAA^0_{VS*} became a tough cohesive mass during the compression test. This characteristic of the mass implies that there was additional linkage of the mineral assemblages during compression. Vice versa, this additional linkage requires free polymeric portions that can be attached to surfaces. During compression, such unattached polymer parts initially cause a steric repulsion and thus account for the higher stiffness of the material.

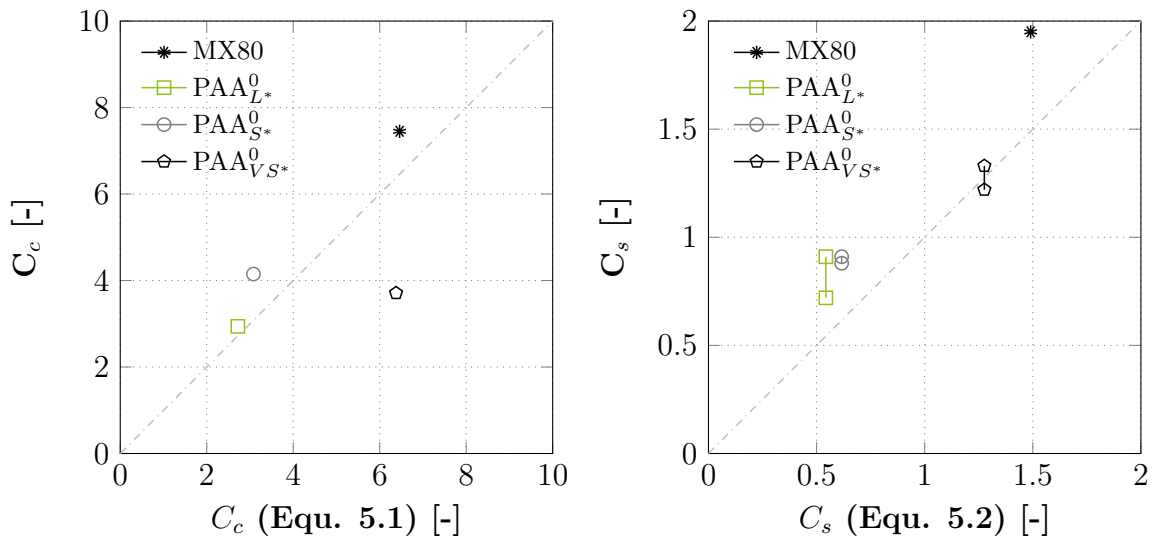

Figure 6.11: Compression and decompression indices of MX80 and the various polymer-modified MX80

6.6 Unconfined water retention behaviour

The unconfined suction-controlled water retention and shrinkage behaviour of PAA^0_{S*}, PAA^0_{M*} and PAA^0_{L*} is compared to that of unmodified bentonite presented in Tripathy et al. (2014) in Figure 5.8. The experimental data and the best fit based on the adopted Fredlung & Xing equation given in Equations (4.2), (4.3) and (4.4) (Wijaya et al., 2015) are plotted in terms of water content w, void ratio e and degree of saturation S_r over suction (Figure 5.8 (a.), (c.) and (d.)). Moreover, the shrinkage curve (water content over void ratio) is shown in Figure 5.8 (b.). It was assumed, that the water content at a suction of 1000 MPa is zero.

Similar to the compression behaviour and the index properties, the water retention properties show a strong dependence on the mixing method rather than on the chain length or molecular weight of the polymers used. The dehydration tests demonstrated that PAA^0_{M*} has a higher ability to resist dehydration and suction induced shrinkage than PAA^0_{S*} and PAA^0_{L*} in the low suction range. Furthermore, from the best-fit in the S_r over suction plot, a significantly higher air entry value of the PAA^0_{M*} can be seen. The strong scattering of the experimentally determined saturation levels is related to the very small sample volumes after drying and the resulting sensitivity of the measurements for even small measurement errors (Christ et al., 2022).

However, with increasing suction the differences between PAA^0_{S*}, PAA^0_{M*} and PAA^0_{L*}

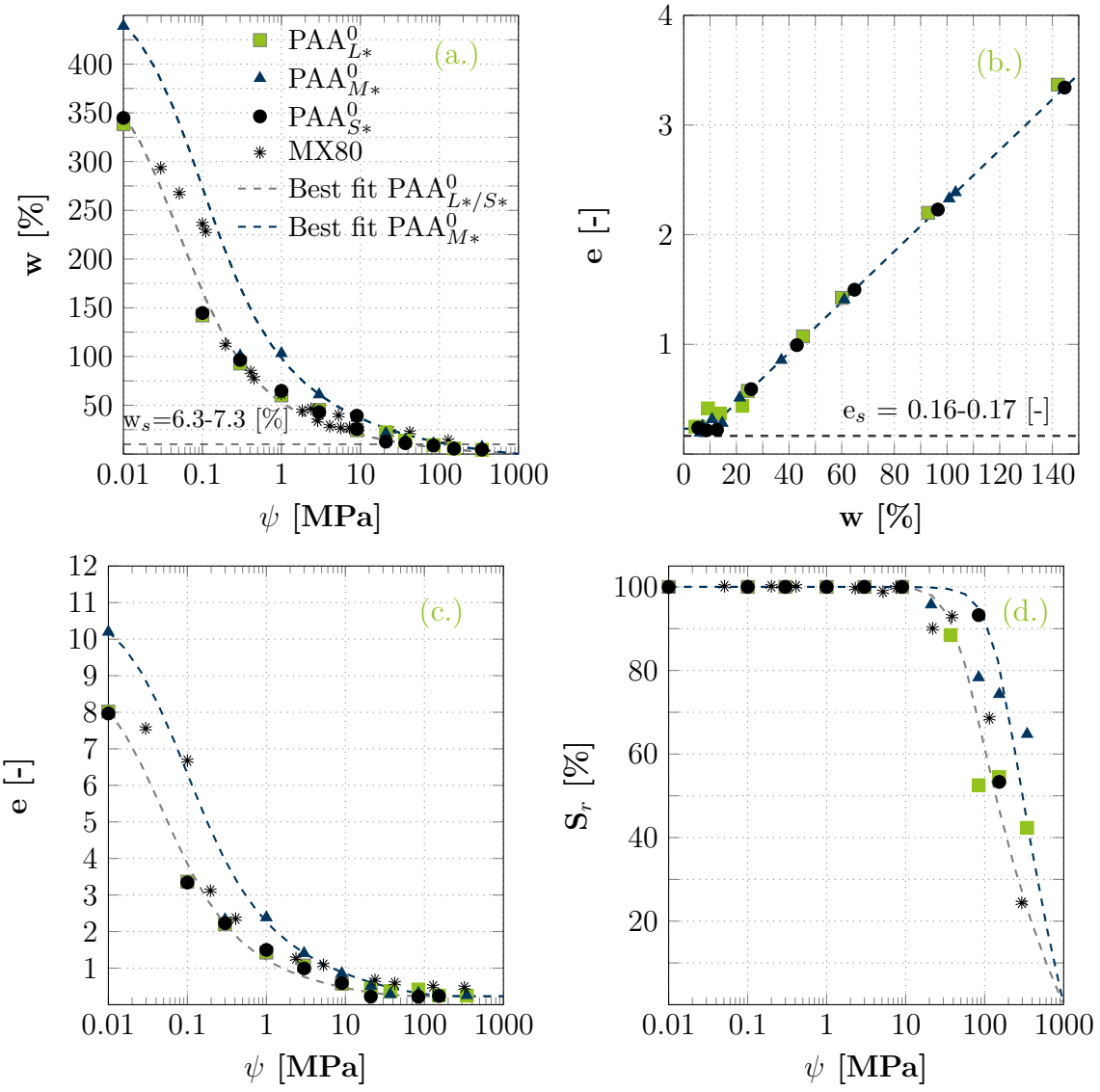

Figure 6.12: Desorption behaviour of the modified and natural MX80: Gravimetric water content versus suction (a.), void ratio versus water content (b.), void ratio versus suction (c.) and degree of saturation versus suction (d.)

become smaller. The water retention curves of the different mixtures in Figure 6.12 (a.) are virtually aligned from a suction stress of about 40 MPa. However, the degree of saturation S_r of PAA^0_M in Figure 6.12 (d.) is located above that of PAA$^0_{S*}$ and PAA$^0_{L*}$ even at relatively high suction ranges (10-345 MPa). These differences might be attributed to differences in water adsorption behaviour or in the shrinkage behaviour as both affect the degree of saturation. Different shrinkage limits give evidence for the latter one. At very high suctions or low relative humidities, the retention of water is exclusively controlled by

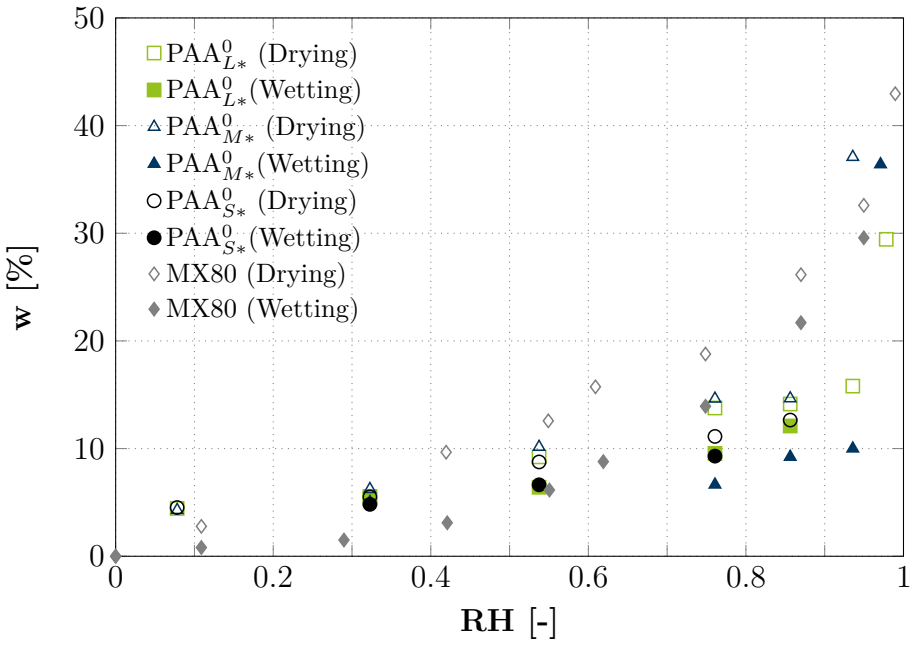

Figure 6.13: Water vapour sorption isotherms for PAA$^0_{L*}$,PAA$^0_{M*}$ and PAA$^0_{S*}$

hydration of the surfaces, interlayers and exchangeable cations (Lu and Khorshidi, 2015). Effects that arise from microfabric such as capillarity are significant for low suction stress ranges. The water vapor sorption isotherms of the PAA$^0_{L*}$, PAA$^0_{M*}$ and PAA$^0_{S*}$ compared to that of MX80 obtained from Montes-H et al. (2003) are shown in Figure 6.13. The plot gives evidence, that the different desaturation behaviour is due to structural effects rather than different adsorption morphologies since at very low relative humidities the water sorption curves of the modified materials merge. In the RH $<$ 30 % range, however, the modified clay is above the natural MX80, which clearly shows the effect of the polymer on water adsorption in the tighlty adsorbed water regime.

In contrast to the clear differences observed up to suctions of 10 MPa (appr. RH = 93 %, T = 20°C), the difference between the different composites in the range of humidity from 85 to 30 % is rather small. In this suction range, hysteresis can be observed which is highest for PAA$^0_{M*}$ caused by a lower water uptake upon rewetting. At very low relative humidities all measured values are identical. The differences and similarities between water retention properties in different suction stress ranges allow conclusions to be drawn about different levels of modification. The minimal differences at low relative humidities reveal that modification of the surfaces and interlayers by the non-ionic polymer is not measurably influenced by molecular weight. The differences observed on the macroscale could therefore be predominantly attributed to variations in the fabric conditioned by the

different mixing methods that influence the constrains of polymer-clay interaction rather than their adsorption morphology. However, this discussion must also be understood under the precondition that it is not yet clear to what extent polymer-modified soils can be interpreted in the same way as non-modified soils. This may be particularly controversial in the partially saturated range, as it is for instance not clear in which range of water contents a polymer bridge is flexible and when it is rigid.

From the S_r over ψ diagram in Figure 6.12 it becomes evident that the PAA^0_M has a higher air entry value than the PAA^0_S and PAA^0_L. Given that the air entry value is the point at which the repulsive and frictional forces of the soil matrix become greater than the stress induced by the suction stress, it appears that the system with the larger flexibility will reach this point at a higher value of suction than a more rigid system. This observation is in good agreement with the rationale that in the case of PAA^0_M, the polymers are arranged in a way that concede greater structural flexibility and consequently a lower shrinkage limit.

6.7 Conclusion

In this chapter, the influence of molecular weight on the hydro-mechanical behaviour of bentonite modified with non-ionic polymers was addressed. This type of polymer is less common than its ionic counterparts for the modification of soil properties in geotechnical engineering. In contrast to ionic polymers, non-ionic polymers are found in a much more coiled geometry due to the absence of intra-chain repulsion. Furthermore, there are only weak attractions between the polar groups of the polymer chain and the smectite minerals. Previous studies showed that the adsorption of non-ionic polymers on the one hand potentially increases diffuse double layer swelling. In contrast, extensive bridging was found to hinder the accessibility of the surfaces and thus impede the swelling properties of the material.

The investigation of the adsorption characteristics showed, that the adsorption capacity of 3 of the 4 polymers was independent of molecular weight within the limits of measurement accuracy. However, for the highest molecular weight, the adsorption capacity was found to be significantly lower than the other ones. Based on the observation that all mixtures were prepared beyond the concentration at which the polymer chains strongly interact with each other (overlap concentration), it is suggested that the adsorption morphology occurs in a "coating" of the mineral surfaces rather than in isolated chains in a morphology of loop tails and trains. Investigations carried out on the level of microfabric using cryo-bib

prepared samples showed a fabric with a net-like architecture typically known for polymer gels, nano- and microcomposites. This arrangement, being characteristic for polymeric structures, demonstrated that the microfabric of the mxtures, although the main part consisted of smectite minerals, was strongly formed by the polymers.

In contrast to the more stretched ionic polymers, non-ionic polymer coils brought into motion are likely to change their shape. To investigate the significance of this effect on the material behaviour, a variation of the mixing conditions was carried out in addition to the variation of the molecular weights. Comparing the plasticity properties of materials with different molecular weight mixed with the same procedure give evidence for a rather moderate impact of the molecular weight. By contrast, different mixing procedures were found to cause a pronounced different plasticity properties and shrinkage limit. These differences were reasoned by different microfabrics. Depending on the flexibility of the respective polymer bridges and the accessibility of surfaces the polymers cause an increase or decrease of liquid limit, plastic limit and shrinkage limit.

Similarly, the compression behaviour and water retention properties showed a clear dependence on the mixing method, while the influence of the molecular weight was less pronounced. A deeper examination of the water retention properties at high suction stresses suggested that the effects resulting from surface modification by polymer addition are similar for all polymers used and that the differences in water retention behaviour are therefore more attributable to effects which arise from microfabric. An investigation by means of one-dimensional compression tests showed that the post-mixing drying and grinding causes an increase of stiffness. This influence of drying can be attributed to additional bonding of polymers in the dehydrated state. In contrast to the clay modified with cationic polymers, the dried material modified with non-ionic polymers maintained a distinct plasticity. This was due to the fact that the non-ionic polymers are deformed elastically to a large extent due to their coiled shape.

The current investigation has revealed that non-ionic polymers can have very divergent impacts on the hydro-mechanical behaviour of clay. Depending on the boundary conditions during production, the desired effect can vary significantly. In the current investigation the effect of the mixing process was much more pronounced than that of variations in the amount added or polymer chain length. However, it was also discussed that there is interrelation between molecular weight and overlap concentration which might play an important role in less concentrated conditions.

7 Hydro-mechanical behaviour of anionically modified bentonite

7.1 General

This chapter deals with the modification of bentonite with anionic polymers. In geotechnical practice, this group of polymers has major relevance when dealing with modified clays. In some cases, it was possible to bind anionic polymers to the mineral phase of the bentonite and subsequently treat it as a new, improved mineral (Di Emidio et al., 2017). By contrast, Haase (2017) showed that the adsorption capacity of the MX80 used in combination with anionic polyacrylamide is practically non-existent. However, several approaches to modify bentonites for the use in barriers rely on the modification of the pore fluid rather than modifying the mineral characteristics. Considering this, dispersion in water to provide as many interaction surfaces as possible is not necessary.

This chapter will investigate how the amount of polymer added affects the hydro-mechanical properties of an MX80 under constant volume and low-density conditions. In contrast to the modification of MX80 using cationic and non-ionic polymers, samples were prepared by dry mixing. Multi-step tests were carried out in the newly developed membrane cell presented in Chapter 3. In the first part of this Chapter, the swelling pressure of the unmodified and modified MX80 is considered and then compared with literature data and the study by Haase (2017), in which constant volume swelling pressure tests were performed on anionic modified bentonite with proctor density. In the second part of the chapter, the influence of polymer addition on permeability of the material is studied with DI-water and $CaCl_2$ solution.

7.2 Swelling pressure

Constant volume swelling pressure tests were performed in the 'membrane cell'. The hydration was conducted via the lower drainage where the pressure during hydration was about 1 to 3 kPa, according to the water level in the water reservoir. The dry density of the unmodified MX80 was 0.75 [g/cm^3]. This value corresponds to an expected swelling pressure in the range of 80 - 200 kPa and is in a similar order of magnitude as the initial porosity in the experiments described by Di Emidio (2010). This low density was used to represent the boundary conditions of a GCL under low overburden stress.

Dry mixing was performed by mixing the target amounts of clay and polymer using a spatula. The amount of polymer added is given as a mass percent of the bentonite weight, so that the total amount of material is dry 100 % bentonite + x % dry polymer. In this respect, two ways of considering the global density of the mixture are possible. On one hand, the polymer can be considered as a solid, which means that the addition of polymers leads to a higher density of the mixture. On the other hand, the polymers can also be attributed to the liquid phase, which implies an identical dry density of the MX80 in all three experiments. In the current tests, the second approach was followed. The density of the bentonite was kept constant and the polymer was considered to be in solution even though the global density increases with the amount of added polymer. This is in contrast to the consideration of cationic and non-ionic polymers, were polymers were considered as solids, due to the higher potential for adsorption and intercalation.

Figure 7.1 shows the evolution of the swelling pressure over time for MX80, MX80 + 1% $PAA^-_{M,\tau 40}$ and MX80 + 10% $PAA^-_{M,\tau 40}$. The evolution of swelling pressure of both mixtures containing polymer is characterised by a relatively flat increase in the beginning followed by a sharp rise in the swelling pressure up to the maximum. This can be explained by the relatively low density. In the case of watering with liquid water (not via the vapour phase), a swollen, relatively water-impermeable layer forms immediately on contact with water, which is why the subsequent hydration of the material is rather slow. This initial hydration only leads to an expansion of a small layer while the rest of the sample is hydrated subsequently. Since the total density is low, the non-hydrated part of the sample is compressed by this expansion and no significant swelling pressure is observed.

Figure 7.2 shows the final swelling pressure over dry density for the tests perfomed in comparison to data from literature. The grey hatch represents a typical bandwidth of swelling pressures observed for natural MX80 documented in the literature. Since MX80 is typically used as a highly compacted buffer material in nuclear waste repositories, there

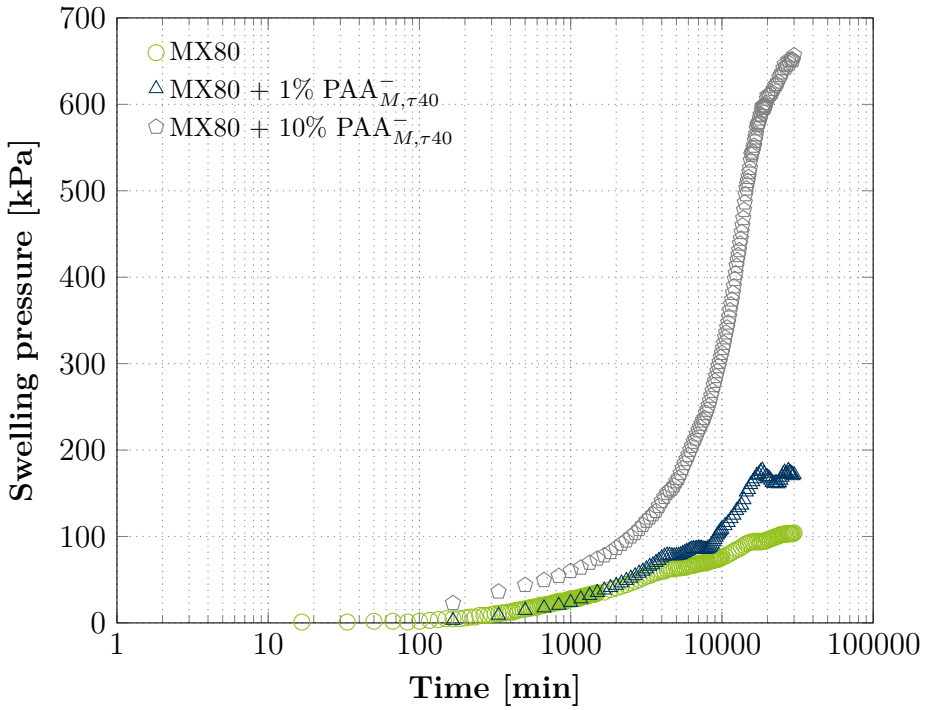

Figure 7.1: Swelling pressure of the pure MX80 and after addition of 1 and 10 % anionic polymer

is a large data basis in the medium and high density range. The rather low density chosen for the study, as it is relevant for the use in GCLs, has not been investigated so far on this material and is therefore poorly covered by the diagram. The variations in swelling pressure magnitues are attributed to different sample geometries, variations in the test setup (e.g. rigidity of the devices, precision and arrangement of the load cells) or to the material itself (e.g. compaction method, initial water content, mineralogical composition, type of cations).

Both, the unmodified material tested in the current study as well as the one tested in the work of Haase (2017) lie in the lower range of typically observed values of swelling pressure. The diagram indicates the distinct influence of the anionic polymer in case of 10 % polymer. The addition of 1% anionic polymer leads to an increase of the swelling pressure located on the upper limit of the typical range of measured values. However, the addition of 10 % polymer causes an increase of swelling pressure corresponding to that of pure MX80 at a density of 1 - 1.25 g/cm^3. A comparison with the data from Haase (2017) obtained at a higher density shows a less pronounced increase in swelling pressure after addition of 1% anionic polyacrylamide by dry mixing.

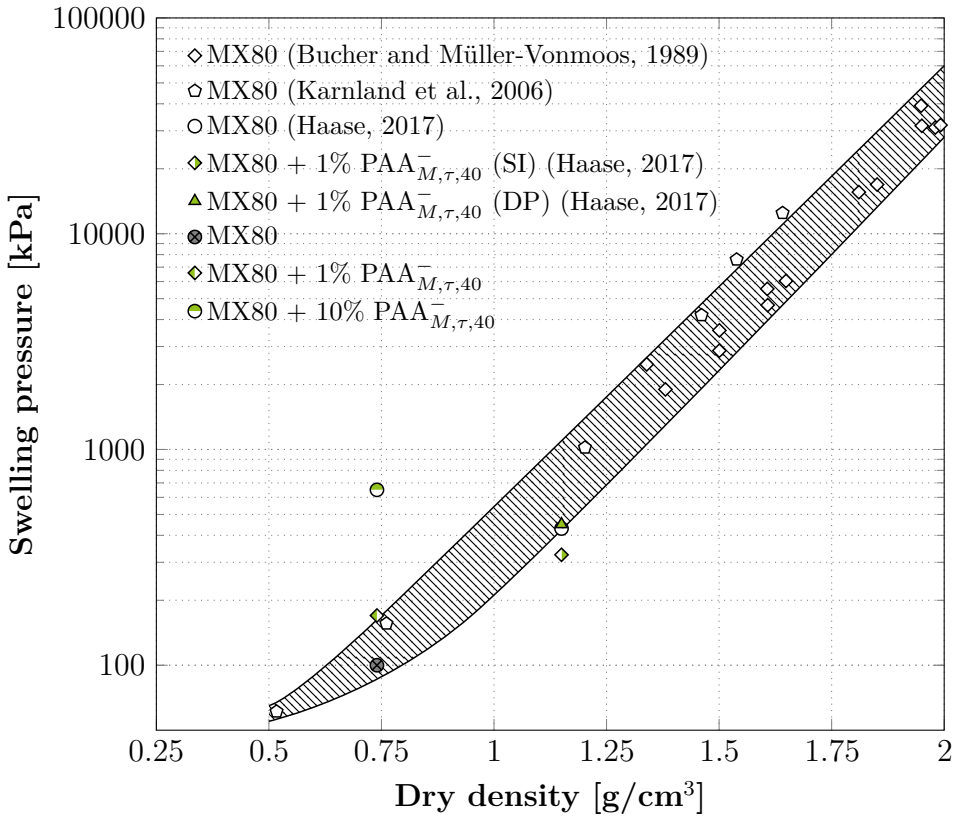

Figure 7.2: Swelling pressure - dry density relation of MX80 and the various polymer-MX80 mixtures

7.3 Permeability

The evolution of the hydraulic conductivity over time determined with deionised (DI) water and 0.05 mol/l $CaCl_2$ solution is plotted in Figure 7.3. The permeability tests were directly started after the swelling pressure tests reached equilibrium by increasing the air pressure on the water reservoir to obtain a pressure gradient of 100 kPa. The unmodified MX80 has a hydraulic conductivity of 4 - $5{\cdot}10^{-12}$ m/s when permeated with DI water. The initial lower conductivity is related to a not fully saturated state of the sample and the device at the end of the swelling pressure test. Entrapped air causes a reduction in the hydraulically effective cross section. After about 2 weeks, however, the coefficient of permeability approaches a constant level. The comparison between the tests conducted in the current study and a typical range of hydraulic conductivities of MX80 reported in the literature is shown in Figure 7.4. The results obtained with the newly developed device are within a typical range for MX80. The permeation with a 0.05 mol/l $CaCl_2$

solution started after 97 days of permeation with DI water caused an increase of the hydraulic conductivity to $9 \cdot 10^{-12}$ m/s within 40 days of permeation. The addition of 1 % of anionic polymer by dry mixing causes the reduction of the permeability coefficient from 4 - $5 \cdot 10^{-12}$ m/s in the unmodified state to $1.3 \cdot 10^{-12}$ m/s. During permeation with 0.05 mol/l $CaCl_2$ the hydraulic conductivity increases to $2 \cdot 10^{-12}$ m/s. The addition of 10 % of anionic polymer is associated to a further reduction of the permeability coefficient to 3 - $4 \cdot 10^{-13}$ m/s. During permeation with 0.05 mol/l $CaCl_2$ the hydraulic conductivity even decreases to 2 - $3 \cdot 10^{-13}$ m/s. In both tests, elution of the polymer was observed, visible by an alteration of the fluid in the measuring burette.

The relationship between the hydraulic conductivity k [m/s] and the intrinsic permeability K [m^2] is given by Equation (7.1), where μ is the viscosity (Pa $\cdot$ s) and γ is the unit weight of the pore fluid (N/m^3). The intrinsic permeability is independent of fluid properties and describes the hydraulically relevant cross section.

$$K = k_h \cdot \left(\frac{\mu}{\gamma}\right) \qquad [m^2] \tag{7.1}$$

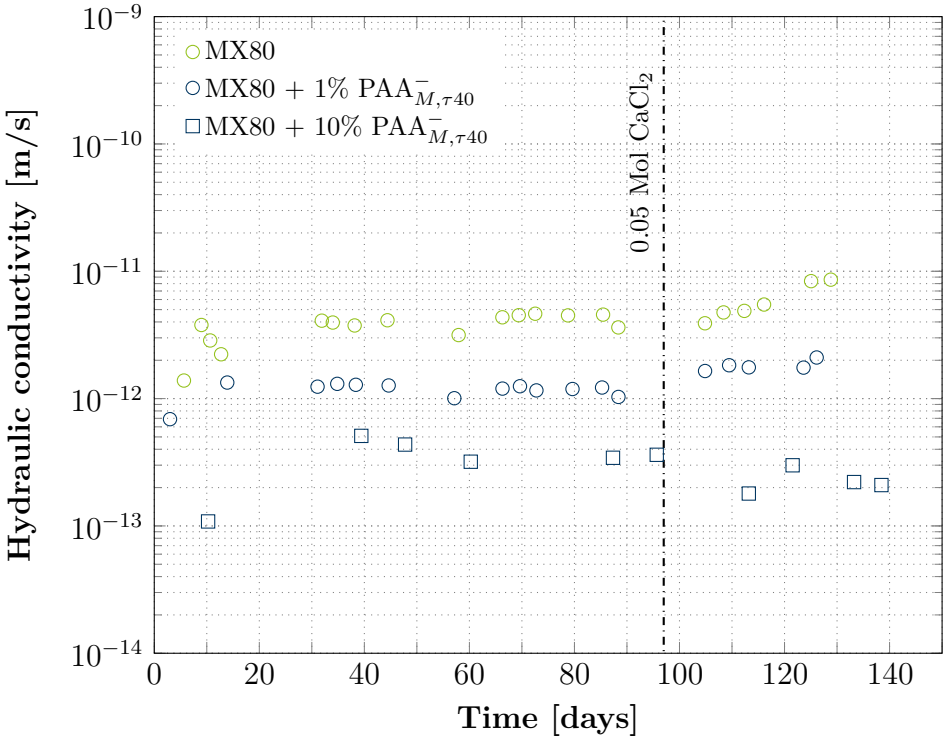

Figure 7.3: Permeability of MX80 and two polymer-modified MX80 over time for DI-Water (0-98 days) and 0.05 Mol $CaCl_2$ (99-140 days)

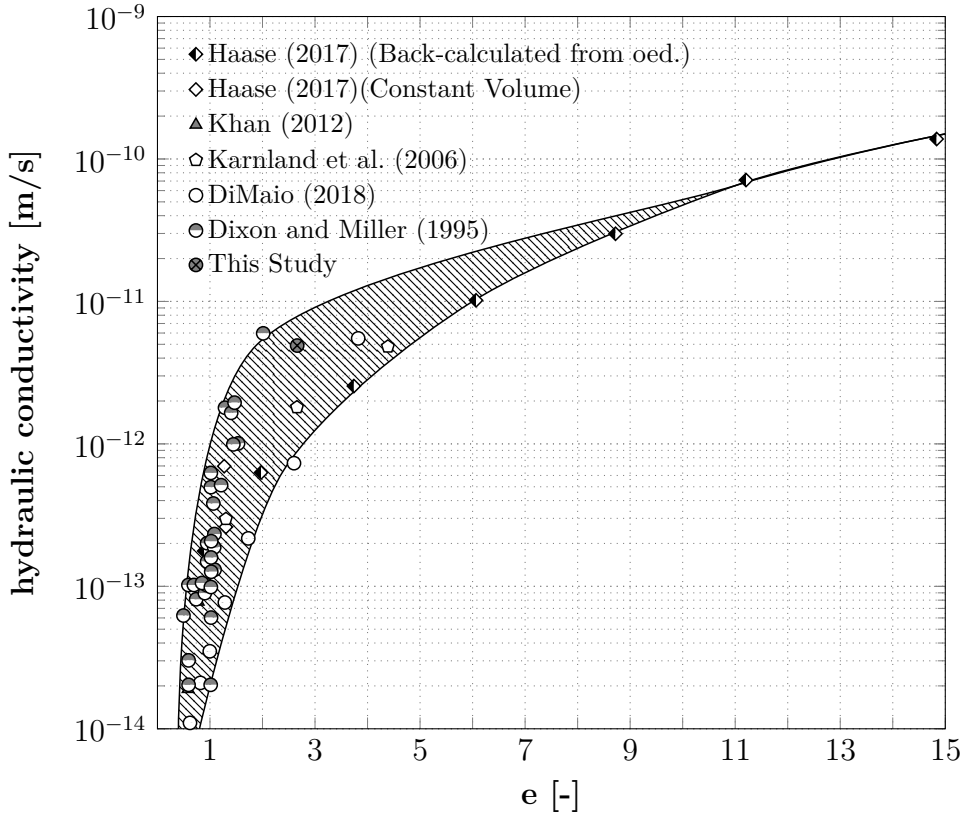

Figure 7.4: Void ratio over permeability of MX80

The experimentally determined hydraulic conductivity of MX80 results in a permeability K of $5.1 \cdot 10^{-19}$[m^2] when permeated with DI-water. Provided that the polymer after dry mixing primarily effects the pore fluid properties by clogging and the influence on the microfabric is small, then K remains constant indepent of the presence of polymer. From the permeability test, an apparent viscosity can be determined by rearranging the equation 7.1, as is typically done in models for predicting the penetration behaviour of polymeric liquids (Verst et al., 2022). The apparent viscosity of the pore fluid is 0.0025 Pa·s for 1 % polymer and 0.025 Pa·s in the case of 10% added polymer. The apparent viscosity of dry mixed MX80-polyacrylamide composites at proctor density calculated from experiments presented in Haase (2017) is 0.0012 Pa s.

The apparent viscosity obtained from the tests is slightly higher than that of water (0.001005 Pa s at 20°C). However, the shear-thinning characteristic of polymers in solution induces a significant increase in viscosity especially at low shear rates. In a pore, the shear stress correlates to the flow velocity (Verst et al., 2022). The flow velocity in clay is quite low and so the shear rate is. The expected viscosity lies in the range of the

lower Newtonian plateau. The low apparent viscosity calculated for the MX80 polymer mixture thus indicates that the polymers do not increase the viscosity uniformly in all hydraulically active pores.

This observation is moreover supported by the presence of polymer 'spots' as shown in Figure 7.5. A uniform distribution of polymer in such a low viscosity would lead to a relatively high mobility of the polymer and thus a very fast leaching of the polymer by advective transport. The sample shows a high proportion of remaining polymer even after permeation for 5 months. Likewise, the sample with initially 1 % polymer was found with polymer threads during disassembling. These observations support the picture of local spots of highly concentrated polymer solution embedded in the clay matrix.

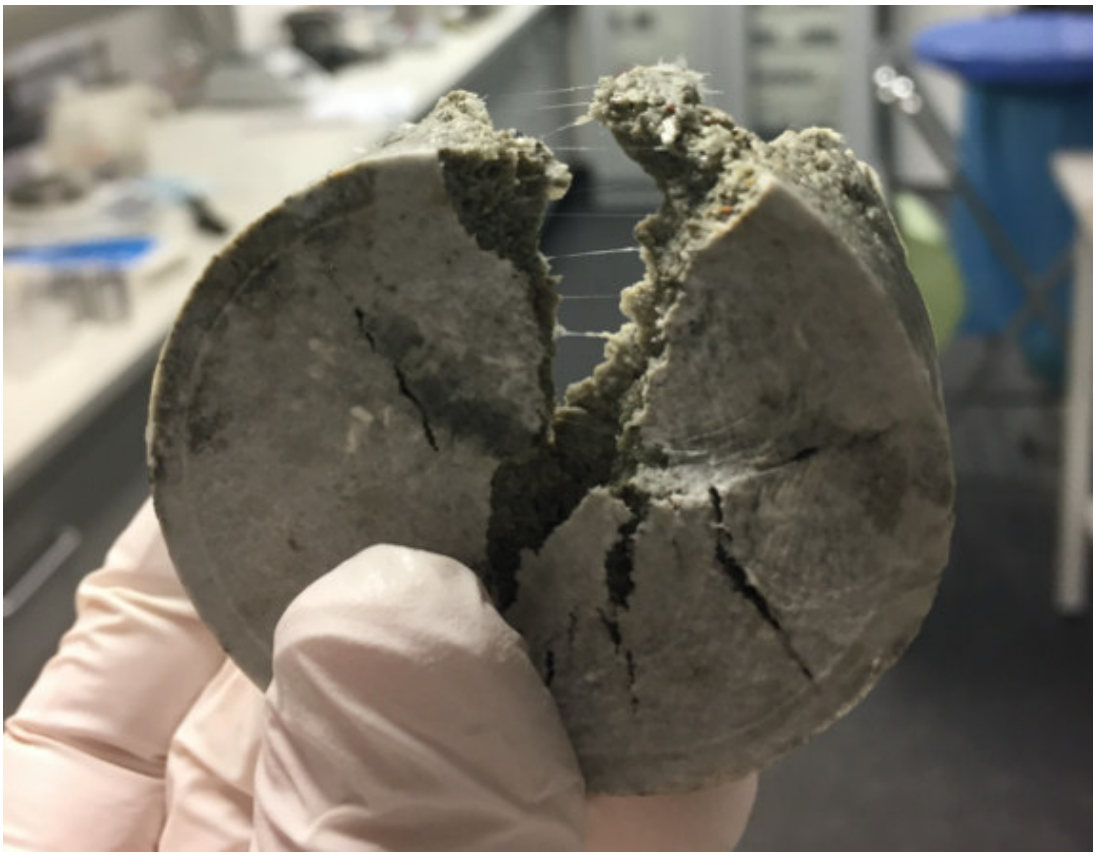

Figure 7.5: Dismantled MX80 sample with initially 10% of anionic polymer after the permeability test

7.4 Discussion

The swelling pressure tests conducted on the dry-mixed MX80 + $PAA^{-}_{\tau,40}$ samples show higher swelling pressure than the MX80 tested without polymer. This observation contradicts some studies where anionic polymers were used to inhibit swelling (Inyang et al., 2007). Furthermore, following the classical DDL theory a decrease in swelling pressure due to the presence of negatively charged polymer in the pore fluid is expected. The presence of dissolved ions and thus the increase in the chemical potential of the bulk fluid leads to a decrease in the gradient and thus to a decrease in osmotic swelling.

The explanation of these apparently contradictory findings provides a more detailed insight into the underlying mechanisms. Water-soluble polymers swell when water is added. The driving mechanism is osmosis, whereby the osmotic pressure of a polymer solution does not become zero even in the fully saturated state (Lieske et al., 2020 (a.)). When the polymer solution is restricted in swelling due to geometric constraints, a swelling pressure builds up (Bhattacharyya et al., 2020). This process can lead to the development of swelling pressure even in soils that actually do not contain expandable minerals, such as sand and silt (Misiewicz et al., 2020).

The dry mixing process used for the preparation of the samples promotes a heterogeneous distribution of polymers and thus spots of highly concentrated polymer solutions, whereas other parts of the soil matrix remain initially unaffected. Figure 7.6 shows an idealised model of the soil fabric to account for the observations made in the experimental program. The soil exists as a complex mixture of three different phases, given the absence of a gas phase due to fully saturated conditions. The soil solids (i.e. clay) are present in an aggregated fabric and therefore with a bimodal pore size distribution. The inter-aggregate pores are filled with immobile water (dark blue) due to strong interactions between clay surfaces and interlayers and the water phase. Water transport along a hydraulic gradient takes place mainly in the macropores between the aggregates (light blue). Large pores between the clay aggregates are plugged by polymer clumps (light gray) that transform into highly viscous gels during hydration (Tian et al., 2019).

Swelling of the polymer leads to competition for the space available for the clay to swell and thus to an increase in clay density at a given volume. However, as the swelling pressure of polymer solutions is directly connected to osmotic pressure it could apparently not occur in very diluted conditions. The behavior of a polymer-clay mixture in which polymer is strongly attached to the mineral phase or the polymer is dispersed in the pore fluid is therefore significantly different from that in which a highly concentrated polymer is

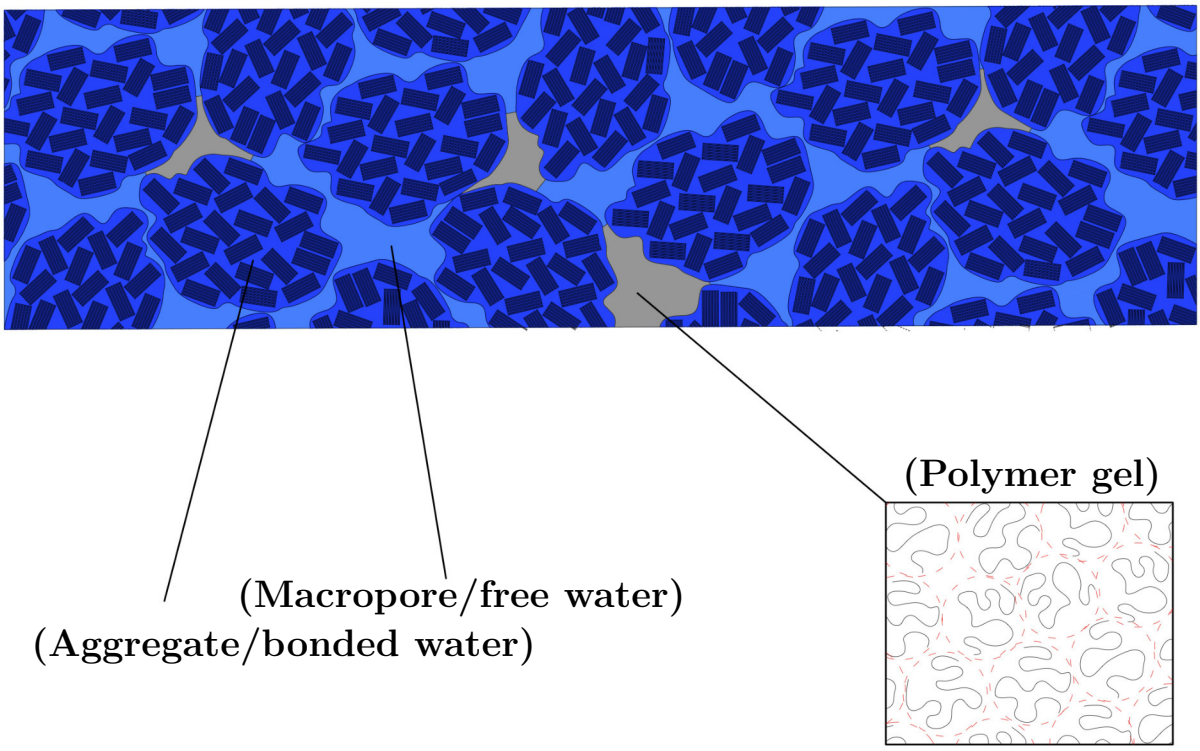

Figure 7.6: Idealisation of an aggregated clay matrix containing polymer solution

present. This is confirmed by the experiments of Haase (2017), where a 1%-$PAA^{-}_{M,\tau 40}$ - MX80 mixture had a higher swelling pressure than the unmodified MX80 after dry mixing, while the wet-mixed 1%-$PAA^{-}_{M,\tau 40}$ - MX80 mixture developed a lower swelling pressure.

The model sketched in Figure 7.6 also accounts for the observations made in the conductivity tests. The addition of polymer causes some of the macropores to become hydraulically inactive due to a significant increase of viscosity, whereas other macropores where just little or no polymers are present remain hydraulically active. In this model flow of polymers from hydraulically inactive macropores to active flow paths is due to diffusive flux driven by chemical gradients. This process is very slow and allows the effect of polymer to be maintained over a long period. Moreover, different retention mechanisms related to the pore structure and polymer-clay interactions supporting polymer gel stability (Sorbie, 1991).

This model of heterogeneous distribution of polymer in the clay matrix also accounts for the lower sensitivity of the modified material for permeation with $CaCl_2$. Upon wetting of clay under constant volume conditions, volumetric expansion of aggregates reduces the size of macropores and therefore preferential flow paths. Osmotic swelling is commonly associated with larger volumetric expansion as innercrystalline swelling. It is therefore

vital for the reduction of hydraulically active flow paths. The effect of increasing hydraulic conductivity when compacted prehydrated clay is permeated with salt solutions is caused by the reduction of chemical gradient that arises from the diffuse double layer to the bulk fluid and therefore the reduction of the osmotic swelling, accompanied by an increase of the intra-aggregate macropores.

Considering that the pores blocked by the polymer are hydraulically inactive, penetration of salt solution into these pores is very slow and the previously described effect mainly occurs in the part of the pores that is hydraulically active. This reasons the significantly less pronounced increase in permeability upon penetration with saline fluid for MX80 with 1% anionic polymer. For the material with 10% anionic polymer, the influence of the salt is hardly measurable, which in turn can be explained by the lower proportion of hydraulically active pores. At this point, however, it should be mentioned that dissolved ions significantly reduce the viscosity of polymer solutions, as the intra-chain repulsion is reduced (Sorbie, 1991). It can therefore be assumed that with long-term effects of salt, ions diffuse into the polymer solution.

7.5 Conclusion

In this chapter, the influence of anionic polyacrylamide on the hydro-mechanical properties of bentonite was assessed. In contrast to the studies on cationically and non-ionically modified bentonite, the mixtures were obtained by dry mixing. This was motivated on the one hand by the fact that previous studies showed that there is practically no adsorption of anionic polyacrylamide on the MX80. On the other hand dry mixing is of higher importance in terms of practical applications. The material was studied by means of multi-step testing, where constant volume swelling pressure tests were followed by permeability tests with DI-water and 0.05 mol/l $CaCl_2$-solutions.

First tests to validate the newly developed equipment were conducted using pure MX80. The results of both the experimentally observed swelling pressure as well as the hydraulic conductivity lie in a reasonable range in comparison to literature values. The addition of 1% and 10% anionic polymer to the MX80 leads to a significant increase in swelling pressure compared to the unmodified material.

Likewise, permeability tests show a significant impact of polymer. The addition of 1% polyacrylamide reduces the hydraulic conductivity when permeated with water from 4-5 $\cdot 10^{-12}$ [m/s] to 1.3 $\cdot 10^{-12}$ [m/s]. The effect of 10% polyacrylamide was even more

pronounced causing a reduction to 3 - 4 $\cdot 10^{-13}$ m/s. During permeation with 0.05 mol/l $CaCl_2$ the hydraulic conductivity even decreases to 2 - 3 $\cdot 10^{-13}$ m/s. A model of a clay microfabric which contains polymer gels as an additional phase was discussed. In this model a heterogeneously distributed highly concentrated polymer solution cloggs part of the hydraulic relevant macropores. Beside the increased swelling pressure and the reduced hydraulic conductivity, this model is also able to explain why the hydraulic conductivity of the polymer-clay mixtures was quite stable during the tests even though polymer elution was observed. The less pronounced increase of the hydraulic conductivity after permeation with $CaCl_2$ was consequently reasoned by an insensitivity of the macropores clogged by the polymer. This explanation was supported by the observation, that the sensitivity was practically absent in case of 10% added polyacrylamide where the number of clogged pores is high.

8 Conclusion and Outlook

8.1 General

Water-soluble polymers are used in geotechnical engineering to modify the hydro-mechanical properties of soils and pore fluids. According to technical possibilities, polymers are produced from a variety of different raw materials and they differ significantly in constitution, e.g. charge properties and molecular weights. The current thesis was motivated by the lack of systematic studies on the relevance of physical and chemical parameters of polymers on the behaviour of modified clay at microscopic and macroscopic scale. While in a preceding work the effect of general type of polymer charge (cationic, non-ionic, anionic) on different clay types was investigated, the present study focuses on effects of polymer chain length, charge density and of mixing and post-mixing methods on the soil mechanical behaviour.

The first part of this work was a theoretical study on the impact of polymer constitution on the behaviour of polymers in solution. The intra- and interactions of polymer chains, which are directly influenced by concentration and polymer composition, have a significant impact on macroscopic properties of polymeric solutions, such as osmotic pressure and viscosity. In this frame, a new approach to calculate suction of polymer solutions based on a modified Flory-Huggins equation was introduced with special emphasis to the polymer named polyethylen glycol (PEG) which is widely used in experimental unsaturated soil mechanics to control soil suction (Lieske et al., 2020 (a.)).

The second part of the theoretical work was dealing with fundamentals of clay mineralogy and structure. Special emphasis was put on bentonite clay, as it has major relevance for geotechnical applications. The behaviour of bentonite exposed to aggressive environmental influences was discussed on the basis of a study on the shrinkage of bentonite in a geosynthetic clay liner subjected to wetting and drying cycles in $CaCl_2$-solutions (Lieske et al., 2020 (b.)). The sensitivity of bentonite for environmental conditions motivates polymer modification in many cases. Based on the individual considerations of

polymer and bentonite, the modification of clay surfaces with polymers was subsequently discussed. The following sections summarise the results of the study on the influence of polymer properties according to their charge properties based on the experiments carried out in the current study.

8.2 Impact of polymer-constitution on the behaviour of smectite modified with polycations

The investigations to address the impact of the molecular weight on bentonite modified with cationic polymer were carried out on four different wet mixed polyacrylamid-MX80-composites. Charged polymers are found in a stretched confirmation due to intra-chain repulsion and electrostatic interactions between polymer and mineral surface strongly determines adsorption morphology. The used polyacrylamide had a charge density $\tau = 40\,\%$ and solely varied with respect to the molecular weight. In addition, tests were carried out on a mixture containing polymers with higher charge density ($\tau = 55\,\%$) and wet-mixed samples that have been subjected to drying and grinding after mixing. The mixtures were prepared with a mixing ratio based on the maximum adsorption capacity. The experimental program included an examination of Atterberg limits, microfabric, adsorption and intercalation behaviour as well as the hydro-mechanical properties of the composite (compression tests and water retention tests).

The results reveal that extensive bridging of the adsorbed polymers causes an open porous fabric, where the positive charges of the polymer balance negative charges of the clay by cation exchange. Intercalation of the polymers into the mineral interlayer was proven for both charge densities. The adsorption maxima showed a dependence on the molecular weight. However, even though the mixtures were prepared with different amounts of added polymer due to different adsorption maxima, the differences in hydro-mechanical behaviour of the mixtures were not significant.

The Atterberg limits showed a certain correlation to the molecular weight which was discussed in the context of a higher probability of long polymer chains to build bridges over longer distance. Therefore the correlation between Atterberg limits and chain length was mainly attributed to geometric factors (i.e. fabric). However, during compression the differences become smaller. The failure of well-established correlations between Atterberg limits and compression behaviour to describe the behaviour of clay-polymer mixtures was attributed to an alteration of the smallest relevant units (i.e. aggregates) during

compression. The compression behaviour and the unconfined water retention behaviour of the polymers with a charge density $\tau = 40$ % showed a rather small dependence on the molecular weight. In contrast, the polymer with a charge density $\tau = 55$ % caused a significant increase of stiffness, even though the adsorption capacity was less than 50% of the different polymers with lower charge density.

The aforementioned importance of fabric was confirmed by the study on effects of post-mixing treatment by drying and grinding. While the polymer bridges support an open porous fabric, the drying and grinding destroys bridges so that effects that arise from the modified surfaces dominate the hydro-mechanical behaviour. This was accompanied by a significant decrease of liquid limit, increase of stiffness and lower ability to retain water when subjected to suction.

The influence of the molecular weight on the hydro-mechanical properties observed in the present study was rather small compared to the influence of post-mixing treatment. The influence of the molecular weight was mainly attributed to a different number of polymer bridges, as the ability to build bridges at given mixing conditions decreases with decreasing molecular weight. By contrast, the impact of charge density was found to be more pronounced.

8.3 Impact of polymer-constitution on the behaviour of smectite modified with non-ionic polymers

The impact of molecular weight in case of non-ionic polymers was investigated on four different composites, obtained by wet mixing of polyacrylamide and MX80. The mixing ratios were chosen corresponding to the concentration at adsorption maximum determined from adsorption isotherms. The testing program of the non-ionic composites comprised Atterberg limits, compression and decompression behaviour in oedometer tests, unconfined water retention behaviour and investigation of mircofabric.

Non-ionic polymers are typically found in a coiled geometry when brought in solution. Special features dedicated to their molecular configuration were addressed by a variation of mixing energy through variation of mixing tools (rotational stirring and eccentric stirring). The bentonite-polymer mixtures obtained from wet-mixing formed an extremely cohesive mass which required a post-mixing treatment by drying and grinding in order to obtain a granular material being suitable for the use in the planned soil mechanical experiments. A single one-dimensional compression test on the cohesive mass obtained after wet mixing

(without drying and grinding) required the use of a large oedometer to address the impact of post-mixing treatment.

The results of the investigation conducted on microfabric revealed an architecture strongly dominated by the polymer. The fabric of the composite obtained from wet-mixing investigated on cryo-BIB treated samples showed strong similarities to that of extra-cellular polymeric substances (EPS) but is rather different from typical soil fabric. The polymers appear in the form of a surface coating rather than as individual polymer chains. These observations give evidence for fabric dominated by polymers even though found in a minor proportion in the mixtures.

The index properties of the composites showed a correlation with molecular weight, but this was less pronounced than the correlation with mixing conditions. This is due to the rather coiled shape of the non-ionic polymer chains in solution and the weak interaction between the polymers and the mineral surfaces. The coiled geometry of the polymer chains is highly affected by external shear energy and therefore the polymer-clay interaction is.

During one-dimensional compression the polymer-modified material behaved significantly stiffer than the natural bentonite, which was attributed to the limited flexibility of the clay matrix caused by extensive bridging of the polymers. Post-mixing treatment by drying caused an increase in stiffness, with the total void ratio of the treated material remaining higher than that of the fresh wet-mixed one. This behaviour was attributed to additional bonding effects induced by drying, a material feature which is beyond the classical soil mechanical behaviour. The behaviour observed in both the oedometer tests and the water retention tests confirmed the dominating effect of mixing method and post-mixing treatment and a less pronounced influence of molecular weight.

8.4 Impact of anionic polymers on the behaviour of bentonite

The influence of anionic polymers on the hydro-mechanical behaviour of bentonite was investigated by means of multi-step tests, with a first stage of swelling pressure measurement followed by subsequent permeability tests. For permeability testing the samples were initially permeated with deionized water and after 97 days using 0.05 mol/l $CaCl_2$-solution. A specially developed test apparatus was used for this purpose. The samples were obtained by dry mixing of bentonite with 1% and 10% polyacrylamide, respectively.

The addition of anionic polymers was found to significantly increase the swelling pressure, reduce the permeability, and cause a lower sensitivity of the permeability to $CaCl_2$-solution. The back calculation of an apparent viscosity and theoretical considerations of the effect of polymers on swelling properties of clays revealed that the observations made could not be reasoned by the presence of polymers alone. A model was proposed to consider the fully saturated mixtures as a three-phase material, where a highly concentrated polymer gel is acting as an individual phase. The effect of the polymer gel was attributed to an increase in clay density and a clogging of the pores relevant for hydraulic flow.

8.5 Recommendations for further studies

Development of a polymer-characterisation system for geotechnical purposes

The presented investigations showed that physical and chemical characteristics of polymers used have major impact on properties of polymer solutions and polymer-modified smectite. Since methods from polymer chemistry for the identification of polymer properties are complex and involve techniques beyond the know-how of geotechnical laboratories they are hardly employed in geotechnical practice. In practice, the choice of appropriate polymers for a given application is currently based on trial-and-error and individual experiences of contractors. Therefore, the development of a basic method for characterising polymers that can be easily applied in geotechnical laboratories is recommended as an important step towards a more systematic approach for categorisation of polymers and polymer-modified soils in geotechnical and geoenvironmental engineering. A potential approach to systematization is the determination of viscosity, which is directly related to polymer properties such as chain length. From the sensitivity of this macroscopic property of a polymer solution to salt, conclusions can be drawn about the charge properties. For the adaptation of a simple experiment, however, a comprehensive data basis and adaptation of polymer-chemical fundamentals is necessary.

Degradation of polymers during their service time

Degradation of polymers implicates a steady alteration of their properties caused by changes to molar mass, molar mass distribution and composition of the polymer. In general, degradation of polymers is caused by mechanical, chemical or biological actions.

Some degradation by-products like acrylamide monomers are known to be toxic for humans. In this study, the effect of post-mixing treatment by drying and grinding was clearly illustrated in case of bentonite modified with cationic polymers. Further, biological activity was observed in case of the cationic polymers, which is an indicator for biological degradation mechanisms occuring in the modified clays.

However, it remains yet unclear which degradation mechanisms play a role under geotechnically relevant boundary conditions and to which extend they effect the material behaviour. It follows that further research is needed to understand which degradation mechanisms are relevant, how they affect the material behaviour and how they can be controlled.

Systematic variation of mixing conditions and polymer to clay ratios

The mixing procedure used in the current study was adapted to achieve an optimal polymer-clay interaction. Therefore, in case of cationic and non-ionic polymers both the clay and the polymer were mixed in solution to facilitate high accessibility of the polymers to the clay surfaces. The mixing ratio of polymer and clay was based on the adsorption maximum. The intention behind this was to achieve a pronounced effect of polymer-modification. The approach was appropriate to outline the basic mechanisms of polymer-clay interaction. However, the study also deepened the understanding for the sensitivity to boundary conditions and showed that the results can not be readily adopted to other geotechnical problems. Further more, it was demonstrated that the concentration of the polymer solutions was too high to reach a maximum of polymer-clay interaction.

The chosen polymer concentration corresponding to the adsorption maximum is relatively high with regard to geotechnical applications where mostly polymer contents of less than 10 percent are used. These high concentrations may cause secondary effects, such as the entanglement of polymer chains. For some mixtures the question arises, to what extent the modified material can still be described by soil mechanical approaches, because for example elastic polymer bridges cause properties that do not occur in normal soils. This was clearly shown in the case of the non-ionic polymers, where the extreme cross-linking of the soil components leads to a tough cohesive material.

In addition, for some applications dry mixing with subsequent hydration in a compacted state may be more relevant than the wet-mixing performed in the current study. In view of this background, the need for a further systematic investigation with regard to the mixing conditions arises. The transition phase between the presence of the individual polymer

and minerals and the polymer-clay composite is the key to identifying the influence of the boundary conditions and the polymer properties on the hydro-mechanical behaviour of the composite. In detail, the importance of the overlap concentration, i.e. the concentration above which the interaction between the polymer molecules increases significantly, should be investigated more closely with regard to the ability of clay and polymer to interact. Furthermore, it was discussed in Chapter 7.5 that the presence of concentrated polymer solutions ('spots') leads to different macroscopic properties than a uniform distribution of polymers in the pore fluid. The concentration at which a polymer solution no longer exists as a separate phase but as part of the pore fluid has not yet been identified.

Bibliography

Acikel, A., Gates, W., Singh, R., Bouazza, A., Fredlund, D. and Rowe, R. (2018), 'Time-dependent unsaturated behaviour of geosynthetic clay liners', *Canadian Geotechnical Journal* **55**(12), 1824–1836.

Acikel, A., Gates, W., Singh, R., Bouazza, A. and Rowe, R. (2018), 'Insufficient initial hydration of gcls from some subgrades: factors and causes', *Geotextiles and Geomembranes* **46**(6), 770–781.

Al Hashmi, A., Al Maamari, R., Al Shabibi, I., Mansoor, A., Zaitoun, A. and Al Sharji, H. (2013), 'Rheology and mechanical degradation of high-molecular-weight partially hydrolyzed polyacrylamide during flow through capillaries', *Journal of Petroleum Science and Engineering* **105**, 100–106.

Anderson, R., Ratcliffe, I., Greenwell, H., Williams, P., Cliffe, S. and Coveney, P. (2010), 'Clay swelling — a challenge in the oilfield', *Earth-Science Reviews* **98**(3), 201 – 216.

Ashmawy, A. K., El-Hajji, D., Sotelo, N. and Muhammad, N. (2002), 'Hydraulic performance of untreated and polymer-treated bentonite in inorganic landfill leachates', *Clays and Clay Minerals* **50**(5), 546–552.

Baille, W. (2014), Hydro-mechanical behaviour of clays: significance of mineralogy, PhD thesis, Ruhr-Universität Bochum Lehrstuhl für Grundbau, Boden-und Felsmechanik.

Baille, W., Tripathy, S. and Schanz, T. (2010), 'Swelling pressures and one-dimensional compressibility behaviour of bentonite at large pressures', *Applied Clay Science* **48**(3), 324–333.

Baille, W., Tripathy, S. and Schanz, T. (2014), 'Effective stress in clays of various mineralogy', *Vadose Zone journal* **13**(5).

Ball, J., Pitts, M. et al. (1984), Effect of varying polyacrylamide molecular weight on tertiary oil recovery from porous media of varying permeability, *in* 'SPE Enhanced Oil Recovery Symposium', Society of Petroleum Engineers.

Bergaya, F., Theng, B. K. and Lagaly, G. (2006), *Handbook of Clay Science*, Elsevier.

Bhattacharyya, A., O'Bryan, C., Ni, Y., Morley, C. D., Taylor, C. R. and Angelini, T. E. (2020), 'Hydrogel compression and polymer osmotic pressure', *Biotribology* **22**, 100125.

Bolt, G. H. (1956), 'Physico-chemical analysis of the compressibility of pure clays', *Géotechnique* **6**(2), 86–93.

Breen, C. (1999), 'The characterisation and use of polycation-exchanged bentonites', *Applied Clay Science* **15**(1), 187 – 219.

Bresler, E. (1973), 'Anion exclusion and coupling effects in nonsteady transport through unsaturated soils: I. theory 1', *Soil Science Society of America Journal* **37**(5), 663–669.

Brooks, D. (1973), 'The effect of neutral polymers on the electrokinetic potential of cells and other charged particles: Ii. a model for the effect of adsorbed polymer on the diffuse double layer', *Journal of colloid and interface science* **43**(3), 687–699.

Bucher, F. and Müller-Vonmoos, M. (1989), 'Bentonite as a containment barrier for the disposal of highly radioactive wastes', *Applied Clay Science* **4**(2), 157–177.

Burland, J. B. (1990), 'On the compressibility and shear strength of natural clays', *Géotechnique* **40**(3), 329–378.

Burton, G., Sheng, D. and Campbell, C. (2014), 'Bimodal pore size distribution of a high-plasticity compacted clay', *Géotechnique Letters* **4**(2), 88–93.

Casassa, E. F. (1972), 'Thermodynamics interactions in dilute polymer solutions: the virial coefficients', *Pure Appl. Chem.* **31**(1-2).

Chang, I. and Cho, G.-C. (2019), 'Shear strength behavior and parameters of microbial gellan gum-treated soils: from sand to clay', *Acta Geotechnica* **14**(2), 361–375.

Chang, I., Jeon, M. and Cho, G.-C. (2015), 'Application of microbial biopolymers as an alternative construction binder for earth buildings in underdeveloped countries', *International Journal of Polymer Science* **2015**.

Chauveteau, G., Tirrell, M. and Omari, A. (1984), 'Concentration dependence of the effective viscosity of polymer solutions in small pores with repulsive or attractive walls', *Journal of Colloid and Interface Science* **100**(1), 41–54.

Chenu, C. and Guérif, J. (1991), 'Mechanical strength of clay minerals as influenced by an adsorbed polysaccharide', *Soil Science Society of America Journal* **55**(4), 1076–1080.

Christ, F., Lieske, W., Herz, C. and Wichtmann, T. (2022), 'Evaluation of the penetration behaviour of viscous fluids into porous media in the context of volume determination', *Geotechnical testing journal* **45**(4).

Colby, R. H., Boris, D., Krause, W. and Dou, S. (2007), 'Shear thinning of unentangled flexible polymer liquids', *Rheologica acta* **46**(5), 569–575.

Colina, H. and Roux, S. (2000), 'Experimental model of cracking induced by drying shrinkage', *The European Physical Journal E* **1**(2), 189–194.

Collins, K. and McGown, A. (1974), 'The form and function of microfabric features in a variety of natural soils', *Géotechnique* **24**(2), 223–254.

Cornelis, W., Corluy, J., Medina, H., Díaz, J., Hartmann, R., Meirvenne, M. V. and Ruiz, M. (2006), 'Measuring and modelling the soil shrinkage characteristic curve', *Geoderma* **137**(1), 179 – 191.

Cuadros, J. (2017), 'Clay minerals interaction with microorganisms: a review', *Clay Minerals* **52**(2), 235–261.

Cui, Y.-J. (2017), 'On the hydro-mechanical behaviour of mx80 bentonite-based materials', *Journal of Rock Mechanics and Geotechnical Engineering* **9**(3), 565 – 574.

Cuisinier, O. and Masrouri, F. (2005), 'Influence de sollicitations hydriques et mécaniques complexes sur le comportement d'un sol gonflant compacté', *Canadian Geotechnical Journal* **42**(3), 731–741.

Daniels, J. L. and Inyang, H. I. (2004), 'Contaminant barrier material textural response to interaction with aqueous polymers', *Journal of materials in civil engineering* **16**(3), 265–275.

Daniels, J. L., Inyang, H. I. and Iskandar, I. K. (2003), 'Durability of boston blue clay in waste containment applications', *Journal of Materials in Civil Engineering* **15**(2), 144–152.

De Camillis, M., Di Emidio, G., Bezuijen, A., Verastegui Flores, D., Van Stappen, J. and Cnudde, V. (2017), 'Effect of wet-dry cycles on polymer treated bentonite in seawater: swelling ability, hydraulic conductivity and crack analysis', *Applied Clay Science* **142**, 52 – 59. Modified Clays for Barriers.

De Camillis, M., Emidio, G. D., Bezuijen, A. and Verástegui-Flores, R. D. (2016), 'Hydraulic conductivity and swelling ability of a polymer modified bentonite subjected to wet–dry cycles in seawater', *Geotextiles and Geomembranes* **44**(5), 739 – 747. Developments in Geosynthetics for Environmental Protection.

DeCarlo, K. F. and Shokri, N. (2014), 'Effects of substrate on cracking patterns and dynamics in desiccating clay layers', *Water Resources Research* **50**(4), 3039–3051.

Delage, P. (2010), 'A microstructure approach to the sensitivity and compressibility of some eastern canada sensitive clays', *Géotechnique* **60**(5), 353–368.

Delage, P. and Cui, Y. J. (2008), 'An evaluation of the osmotic method of controlling suction', *Geomechanics and Geoengineering : An International Journal* **3**(1), 1–11.

Delage, P., Howat, M. and Cui, Y. (1998), 'The relationship between suction an welling properties in heaving compacted unsaturated clay', *Eng. Geol.* **50**, 31 – 48.

Delage, P. and Lefebvre, G. (1984), 'Study of the structure of a sensitive champlain clay and of its evolution during consolidation', *Canadian Geotechnical Journal* **21**(1), 21–35.

Delage, P., Marcial, D., Cui, Y. and Ruiz, X. (2006), 'Ageing effects in a compacted bentonite: a microstructure approach', *Géotechnique* **56**(5), 291–304.

Deng, Y., Dixon, J. B. and White, G. N. (2006), 'Adsorption of polyacrylamide on smectite, illite, and kaolinite', *Soil Science Society of America Journal* **70**(1), 297–304.

Deng, Y., Dixon, J. B., White, G. N., Loeppert, R. H. and Juo, A. S. (2006), 'Bonding between polyacrylamide and smectite', *Colloids and Surfaces A: Physicochemical and Engineering Aspects* **281**(1), 82 – 91.

Denoyel, R., G, D., Lafuma, F. and Audbert, R. (1990), 'Adsorption of cationic polyelectrolytes onto montmorillonite and silica: microcalorimetric study of their conformation.', *Journal of colloid and interface science* **139**(3), 281–290.

Desbois, G., Urai, J., Perez-Willard, F., Radi, Z., Offern, S., Burkart, I., Kukla, P. and Wollenberg, U. (2013), 'Argon broad ion beam tomography in a cryogenic scanning electron microscope: a novel tool for the investigation of representative microstructures in sedimentary rocks containing pore fluid', *Journal of Microscopy* **249**(3), 215–235.

Di Emidio, G. (2010), Hydraulic and chemico-osmotic performance of polymer treated clays, PhD thesis, Ghent University.

Di Emidio, G., Verastegui-Flores, R. D., Mazzieri, F. and Dominijanni, A. (2017), 'Modified clays for barriers: a review', *Innovative Infrastructure Solutions* **2**(1), 47.

DiMaio, C. (2018), *Chemo-Mechanical Coupling in Clays: From Nano-scale to Engineering Applications: Proceedings of the Workshop, Maratea, 38-30 June 2001*, Routledge.

DIN 18122-2 (2000), 'Soil - investigation and testing - part 2: Determination of the shrinkage limit'.

DIN EN ISO 17892-12 (2020), 'Geotechnical investigation and testing - laboratory testing of soil - part 12: Determination of liquid and plastic limits'.

DIN EN ISO 17892-2 (2015), 'Geotechnical investigation and testing - laboratory testing of soil - part 2: Determination of bulk density'.

DIN EN ISO 17892-5 (2017), 'Geotechnical investigation and testing - laboratory testing of soil - part 5: Incremental loading oedometer test'.

Dineen, K. and Burland, J. (1995), A new approach to osmotically controlled oedometer testing, *in* 'Proceedings of the first international conference on unsaturated soils Unsat' 95 2', Balkema, pp. 459–465.

Dixon, D. and Miller, S. (1995), Comparison of the mineralogical composition, physical, swelling and hydraulic properties of untreated sodium bentonites from canada, the united states and japan, Technical report, Atomic Energy of Canada Ltd.

Dobrynin, A. V. and Rubinstein, M. (2005), 'Theory of polyelectrolytes in solutions and at surfaces', *Progress in Polymer Science* **30**(11), 1049–1118.

Doppalapudi, S., Jain, A., Khan, W. and Domb, A. J. (2014), 'Biodegradable polymers—an overview', *Polymers for Advanced Technologies* **25**(5), 427–435.

Dragan, E. S. (2014), 'Design and applications of interpenetrating polymer network hydrogels. a review', *Chemical Engineering Journal* **243**, 572–590.

Edil, T. B. (2007), A review of environmental impacts and environmental applications of shredded scrap tires, *in* 'Proceedings of international workshop on lightweight geomaterials, Tokyo, Japan', pp. 3–18.

El-Zein, A., Yu, B. and Ghavam-Nasiri, A. (2019), Insights into desiccation and self-healing of bentonite in geosynthetic clay liners under thermal loads, *in* 'E3S Web of Conferences', Vol. 92, EDP Sciences, p. 03006.

Emmerich, K., Madsen, F. T. and Kahr, G. (1999), 'Dehydroxylation behavior of heat-treated and steam-treated homoionic cis-vacant montmorillonites', *Clays and Clay Minerals* **47**(5), 591–604.

Farrar, D. M. and Coleman, J. D. (1967), 'The correlation of surface area with other properties of nineteen british clay soils', *Journal of Soil Science* **18**(1), 118–124.

Fleer, G., Scheutjens, J. and Cohen Stuart, M. (1988), 'Theoretical Progress in Polymer Adsorption, Steric Stabilization and Flocculation', *Colloids and Surfaces* **31**, 1–29.

Fleureau, J.-M., Kheirbek-Saoud, S., Soemitro, R. and Taibi, S. (1993), 'Behavior of clayey soils on drying-wetting paths', *Canadian Geotechnical Journal* **30**, 287–296.

Fleureau, J.-M., Verbrugge, J.-C., Huergo, P. J., Correia, A. G. and Kheirbek-Saoud, S. (2002), 'Aspects of the behaviour of compacted clayey soils on drying and wetting paths', *Canadian Geotechnical Journal* **39**, 1341–1357.

Fredlund, D. and Xing, A. (1994), 'Equations for the soil-water characteristic curve', *Canadian Geotechnical Journal* **31**(4), 521–532.

Gens, A. and Alonso, E. (1992), 'A framework for the behaviour of unsaturated expansive clays', *Canadian Geotechnical Journal* **29**(6), 1013–1032.

Gregory, J. and Barany, S. (2011), 'Adsorption and flocculation by polymers and polymer mixtures', *Advances in colloid and interface science* **169**(1), 1–12.

Griffiths, F. J. and Joshi, R. C. (1989), 'Change in pore size distribution due to consolidation of clays', *Géotechnique* **39**(1), 159–167.

Grim, R. E. (1953), *Clay mineralogy*, McGraw-Hill Book Company, Inc.

Haase, H. (2017), Multiscale analysis of clay-polymer composites for geoenvironmental applications, PhD thesis, Ruhr-Universität Bochum.

Haase, H. and Schanz, T. (2015), 'Hydro-mechanical properties of calcigel-polyacrylamide composites', *Clays Minerals* **50**, 377–389.

Haase, H. and Schanz, T. (2016), 'Compressibility and saturated hydraulic permeability of clay-polymer composites - experimental and theoretical analysis', *Applied Clay Science* **130**, 62–75.

Haigh, S., Vardanega, P. and Bolton, M. (2013), 'The plastic limit of clays', *Géotechnique* **63**(6), 435–440.

Hasse, H., Kany, H., Tintinger, R. and Maurer, G. (1995), 'Osmotic Virial Coefficients of Aqueous Poly(ethy1ene glycol) from Laser-Light Scattering and Isopiestic Measurements', *Macromolecules* **28**, 3540–3552.

Heerten, G. (2012), 'Reduction of climate-damaging gases in geotechnical engineering practice using geosynthetics', *Geotextiles and Geomembranes* **30**, 43–49.

Inbar, A., Ben-Hur, M., Sternberg, M. and Lado, M. (2015), 'Using polyacrylamide to mitigate post-fire soil erosion', *Geoderma* **239**, 107–114.

Inyang, H. I. and Bae, S. (2004), 'Estimation of polyethylene oxide polymer train and loop densities on contaminant barrier materials', *Journal of Environmental Engineering* **130**(8), 896–905.

Inyang, H. I. and Bae, S. (2005), 'Polyacrylamide sorption opportunity on interlayer and external pore surfaces of contaminant barrier clays', *Chemosphere* **58**(1), 19–31.

Inyang, H. I., Bae, S., Mbamalu, G. and Park, S.-W. (2007), 'Aqueous polymer effects on volumetric swelling of na-montmorillonite', *Journal of Materials in Civil Engineering* **19**(1), 84–90.

Israelachvili, J. N. (2015), *Intermolecular and surface forces*, Academic press.

Jasmund, K. and Lagaly, G. (1993), *Tonminerale und Tone: Struktur, Eigenschaften, Anwendungen und Einsatz in Industrie und Umwelt*, Springer-Verlag.

Jefferis, S. and Lam, C. (2013), Polymer support fluids: use and misuse of innovative fluids in geotechnical works, *in* 'Proceedings of the 18th international conference on soil mechanics and geotechnical engineering, Paris', Vol. 4, pp. 3219–3222.

Jo, H. Y., Katsumi, T., Benson, C. H. and Edil, T. B. (2001), 'Hydraulic conductivity and swelling of nonprehydrated gcls permeated with single-species salt solutions', *Journal of Geotechnical and Geoenvironmental Engineering* **127**(7), 557–567.

Kakali, G., Perraki, T., Tsivilis, S. and Badogiannis, E. (2001), 'Thermal treatment of kaolin: the effect of mineralogy on the pozzolanic activity', *Applied clay science* **20**(1-2), 73–80.

Kang, X. and Bate, B. (2016), 'Shear wave velocity and its anisotropy of polymer modified high-volume class-f fly ash–kaolinite mixtures', *Journal of Geotechnical and Geoenvironmental Engineering* **142**(12), 04016068.

Karnland, O., Olsson, S. and Nilsson, U. (2006), Mineralogy and sealing properties of various bentonites and smectite-rich clay materials, Technical report, Swedish Nuclear Fuel and Waste Management Co.

Kassiff, G. and Ben Shalom, A. (1971), 'Experimental Relationship Between Swell Pressure and Suction', *Géotechnique* **21**(3), 245–255.

Kaufmann, M. R. (1973), 'The Osmotic Potential of Polyethylene Glycol 60001', *Plant Physiol.* **51**, 914–916.

Khan, M. I. (2012), Hydraulic Conductivity of Moderate and Highly Dense Expansive Clays Highly Dense Expansive Clays, PhD thesis, Ruhr-Universität Bochum.

Khorshidi, M. and Lu, N. (2017), 'Determination of cation exchange capacity from soil water retention curve', *Journal of Engineering Mechanics* **143**(6), 04017023.

Kolstad, D. C., Benson, C. H. and Edil, T. B. (2004), 'Hydraulic conductivity and swell of nonprehydrated geosynthetic clay liners permeated with multispecies inorganic solutions', *Journal of Geotechnical and Geoenvironmental Engineering* **130**(12), 1236–1249.

Lagerwerff, J., Ogata, G. and Eagle, H. E. (1961), 'Control of Osmotic Pressure of Culture Solutions with Polyethylene Glycol', *Science* **133**(3463), 1486–1487.

Laird, D. A. (1996), 'Model for crystalline swelling of 2:1 phyllosilicates', *Clays and Clay Minerals* **44**(4), 553–559.

Laird, D. A. (1997), 'Bonding between polyacrylamide and clay mineral surfaces', *Soil science* **162**(11), 826–832.

Laird, D. A. (2006), 'Influence of layer charge on swelling of smectites', *Applied clay science* **34**(1-4), 74–87.

Lam, C. and Jefferis, S. (2018), *Polymer support fluids in civil engineering*, ICE Publishing, London.

Lam, C., Jefferis, S. A., Suckling, T. P. and Troughton, V. M. (2015), 'Effects of polymer and bentonite support fluids on the performance of bored piles', *Soils and Foundations* **55**(6), 1487 – 1500.

Lambe, T. W. (1958), 'The structure of compacted clay', *Journal of the Soil Mechanics and Foundations Division* **84**(2), 1–34.

Lazarus, V. and Pauchard, L. (2011), 'From craquelures to spiral crack patterns: influence of layer thickness on the crack patterns induced by desiccation', *Soft Matter* **7**, 2552–2559.

Lee, B. J. and Schlautman, M. A. (2015), 'Effects of polymer molecular weight on adsorption and flocculation in aqueous kaolinite suspensions dosed with nonionic polyacrylamides', *Water* **7**(11), 5896–5909.

Lee, S., Chung, M., Park, H. M., Song, K.-I. and Chang, I. (2019), 'Xanthan gum biopolymer as soil-stabilization binder for road construction using local soil in sri lanka', *Journal of Materials in Civil Engineering* **31**(11), 06019012.

Leong, E.-C., Tripathy, S. and Rahardjo, H. (2003), 'Total suction measurement of unsaturated soils with a device using the chilled-mirror dew-point technique', *Géotechnique* **53**(2), 173–182.

Lieske , W., Christ, F., Baille, W., Di Emidio, G. and Wichtmann, T. (2020 (b.)), 'Suction and crack propagation in GCLs subjected to drying and wetting in $CaCl_2$-solutions', *Geotextiles and Geomembranes* **48**(6), 973–982.

Lieske, W., Baille, W., Schmatz, J., Kaufhold, S. and Dohrmann, R. (2021), 'Characterisation of natural and remoulded onsøy clay with focus on the influence of mica', *Engineering Geology* **295**, 106378.

Lieske, W., Steudel, A., Di Emidio, G. and Baille, W. (2022), 'Influence of constitution and mixture treatment of cationic polymers on modified bentonite', *Environmental Geotechnics* **9**(6), 412–420.

Lieske, W., Tripathy, S., Baille, W. and Schanz, T. (2020 (a.)), 'An alternative approach for determining suction of polyethylene glycols for soil testing', *Géotechnique Letters* **10**(1), 45–49.

Liu, Y., Bouazza, A., Gates, W. and Rowe, R. (2015), 'Hydraulic performance of geosynthetic clay liners to sulfuric acid solutions', *Geotextiles and Geomembranes* **43**(1), 14 – 23.

Lu, D., Xiao, C. and Xu, S. (2009), 'Starch-based completely biodegradable polymer materials', *Express polymer letters* **3**(6), 366–375.

Lu, N. and Khorshidi, M. (2015), 'Mechanisms for soil-water retention and hysteresis at high suction range', *Journal of Geotechnical and Geoenvironmental Engineering* **141**(8), 04015032.

Lu, N. and Likos, W. J. (2006), 'Suction stress characteristic curve for unsaturated soil', *Journal of Geotechnical and Geoenvironmental Engineering* **132**(2), 131–142.

Madsen, F. T. and Müller-Vonmoos, M. (1989), 'The swelling behaviour of clays', *Applied Clay Science* **4**(2), 143 – 156.

Mamedov, A., Wagner, L., Huang, C., Norton, L. and Levy, G. (2010), 'Polyacrylamide effects on aggregate and structure stability of soils with different clay mineralogy', *Soil Science Society of America Journal* **74**(5), 1720–1732.

Mazzieri, F., Di Emidio, G. and Van Impe, P. O. (2010), 'Diffusion of calcium chloride in a modified bentonite: Impact on osmotic efficiency and hydraulic conductivity', *Clays and Clay Minerals* **58**(3), 351–363.

Meier, L. and Kahr, G. (1999), 'Determination of the cation exchange capacity (cec) of clay minerals using the complexes of copper(ii) ion with triethylenetetramine and tetraethylenepentamine', *Clays and Clays Minerals* **47**(3), 386–388.

Mesri, G. and Olson, R. E. (1971), 'Mechanisms controlling the permeability of clays', *Clays and Clay Minerals* **19**(3), 151–158.

Miller, C. J., Mi, H. and Yesiller, N. (1998), 'Experimental analysis of desiccation crack propagation in clay liners 1', *JAWRA Journal of the American Water Resources Association* **34**(3), 677–686.

Mishra, P. N., Scheuermann, A., Bore, T. and Li, L. (2019), 'Salinity effects on soil shrinkage characteristic curves of fine-grained geomaterials', *Journal of Rock Mechanics and Geotechnical Engineering* **11**(1), 181–191.

Misiewicz, J., Głogowski, A., Lejcuś, K. and Marczak, D. (2020), 'The characteristics of swelling pressure for superabsorbent polymer and soil mixtures', *Materials* **13**(22), 5071.

Mitchell, J. K., Soga, K. et al. (2005), *Fundamentals of soil behavior*, Vol. 3, John Wiley & Sons New York.

Money, N. P. (1989), 'Osmotic pressure of aqueous polyethylene glycols', *Plant Physiology* **91**(2), 766–769.

Monroy, R., Ridley, A., Dineen, K. and Zdravkovic, L. (2007), 'The Suitability of the Osmotic Technique for the Long-term Testing of Partly Saturated Soils', *Geotechnical Testing Journal* **30**(3), 220–226.

Montes-H, G., Duplay, J., Martinez, L., Geraud, Y. and Rousset-Tournier, B. (2003), 'Influence of interlayer cations on the water sorption and swelling–shrinkage of mx80 bentonite', *Applied Clay Science* **23**(5-6), 309–321.

Mpofu, P., Addai-Mensah, J. and Ralston, J. (2004), 'Temperature influence of nonionic polyethylene oxide and anionic polyacrylamide on flocculation and dewatering behavior of kaolinite dispersions', *Journal of Colloid and Interface Science* **271**(1), 145 – 156.

Muguda, S., Booth, S. J., Hughes, P. N., Augarde, C. E., Perlot, C., Bruno, A. W. and Gallipoli, D. (2017), 'Mechanical properties of biopolymer-stabilised soil-based construction materials', *Géotechnique Letters* **7**(4), 309–314.

Munk, P., Aminabhavi, T. M., Williams, P., Hoffman, D. E. and Chmelir, M. (1980), 'Some solution properties of polyacrylamide', *Macromolecules* **13**(4), 871–876.

Musso, G., Romero, E. and Vecchia, G. (2013), 'Double-structure effects on the chemo-hydro-mechanical behaviour of a compacted active clay', *Géotechnique* **63**(3), 206–220.

Ning, J., Li, G. and Haraguchi, K. (2014), 'Effects of polymer concentration on structure and properties of zwitterionic nanocomposite gels', *Macromolecular Chemistry and Physics* **215**(3), 235–244.

Ochoa-Cornejo, F., Bobet, A., Johnston, C., Santagata, M. and Sinfield, J. V. (2020), 'Dynamic properties of a sand–nanoclay composite', *Géotechnique* **70**(3), 210–225.

Olsen, H. W. (1960), 'Hydraulic flow through saturated clays', *Clays and Clay Minerals* **9**(1), 131–161.

Orofino, T. A. and Flory, P. J. (1957), 'Relationship of the Second Virial Coefficient to Polymer Chain Dimensions and Interaction Parameters', *J. Chem. Phys.* **26**(5), 1067.

Otsubo, Y. (1993), 'Size effects on the shear-thickening behavior of suspensions flocculated by polymer bridging', *Journal of Rheology* **37**(5), 799–809.

Palomino, A. M. (2010), 'Polymer-enhanced geomaterials for use in geoenvironmental applications', *The First US-India Workshop on Global Geoenvironmental Engineering Challenges New Delhi, India* .

Palomino, A. M. and Santamarina, J. C. (2005), 'Fabric map for kaolinite: effects of ph and ionic concentration on behavior', *Clays and Clay minerals* **53**(3), 211–223.

Peck, A. and Rabbidge, R. (1968), 'Design and performance of an osmotic tensiometer for measuring capillary potential', *Soil Science* **33**(2), 196–202.

Péron, H., Hueckel, T. and Laloui, L. (2007), 'An improved volume measurement for determining soil water retention curves', *Geotechnical Testing Journal* **30**(1), 1–8.

Peron, H., Hueckel, T., Laloui, L. and Hu, L. B. (2009), 'Fundamentals of desiccation cracking of fine-grained soils: experimental characterisation and mechanisms identification', *Canadian Geotechnical Journal* **46**(10), 1177–1201.

Petrov, R. J. and Rowe, R. K. (1997), 'Geosynthetic clay liner (gcl) - chemical compatibility by hydraulic conductivity testing and factors impacting its performance', *Canadian Geotechnical Journal* **34**(6), 863–885.

Prambauer, M., Wendeler, C., Weitzenböck, J. and Burgstaller, C. (2019), 'Biodegradable geotextiles – an overview of existing and potential materials', *Geotextiles and Geomembranes* **47**(1), 48–59.

Pusch, R. and Yong, R. N. (2006), *Microstructure of smectite clays and engineering performance*, CRC Press.

Quirk, J. and Aylmore, L. (1971), 'Domains and quasi-crystalline regions in clay systems', *Soil Science Society of America Journal* **35**(4), 652–654.

Rao, S. M., Sridharan, A. and Shenoy, M. (1993), 'Influence of starch polysaccharide on the remoulded properties of two indian clay samples', *Canadian Geotechnical Journal* **30**(3), 550–553.

Ray, S. S. and Okamoto, M. (2003), 'Polymer/layered silicate nanocomposites: a review from preparation to processing', *Progress in polymer science* **28**(11), 1539–1641.

Razakamanantsoa, A., Djeran-Maigre, I. and Barast, G. (2014), 'Characterisation of bentonite polymer for bottom liner use', *Environmental Geotechnics* **3**(1), 28–35.

Roiter, Y. and Minko, S. (2005), 'Afm single molecule experiments at the solid-liquid interface: In situ conformation of adsorbed flexible polyelectrolyte chains', *Journal of the American Chemical Society* **127**(45), 15688–15689.

Romero, E., Gens, A. and Lloret, A. (1999), 'Water permeability, water retention and microstructure of unsaturated compacted boom clay', *Engineering Geology* **54**(1), 117–127.

Salles, F., Douillard, J.-M., Denoyel, R., Bildstein, O., Jullien, M., Beurroies, I. and Van Damme, H. (2009), 'Hydration sequence of swelling clays: evolutions of specific surface area and hydration energy', *Journal of colloid and interface science* **333**(2), 510—522.

Scalia, J., Benson, C. H., Bohnhoff, G. L., Edil, T. B. and Shackelford, C. D. (2014), 'Long-term hydraulic conductivity of a bentonite-polymer composite permeated with aggressive inorganic solutions', *Journal of Geotechnical and Geoenvironmental Engineering* **140**(3), 04013025.

Schamp, N. and Huylebroeck, J. (1973), 'Adsorption of polymers on clays', *Journal of Polymer Science: Polymer Symposia* **42**(2), 553–562.

Schanz, T., Agus, S. and Tscheschlo, G. (2004), 'Hydraulisch-mechanische Eigenschaften einer polymerverbesserten Sand-Bentonit-Mischung beim Einsatz im Deponiebau', *Geotechnik* pp. 344–355.

Schanz, T., Datcheva, M., Haase, H. and Marty, D. (2016), 'Analysis of desiccation crack patterns for quantitative interpretation of fossil tracks', *Dinosaur Tracks: The Next Steps* p. 367.

Schenning, J. A. (2004), Hydraulic performance of polymer modified bentonite, Masters-thesis, University of South Florida.

Scherer, G. W. (1990), 'Theory of drying', *Journal of the American Ceramic Society* **73**(1), 3–14.

Schmatz, J., Klaver, J., Jiang, M. and Urai, J. L. (2017), 'Nanoscale morphology of brine/oil/mineral contacts in connected pores of carbonate reservoirs: Insights on wettability from cryo-bib-sem', *SPE Journal* **22**(05), 1374–1384.

Sheng, X., Zhang, L. and Wu, H. (2017), 'Generation of polymer nanocomposites through shear-driven aggregation of binary colloids', *Polymers* **9**(11), 619.

Shin, H. and Santamarina, J. C. (2011), 'Desiccation cracks in saturated fine-grained soils: particle-level phenomena and effective-stress analysis', *Géotechnique* **61**(11), 961–972.

Sivakumar Babu, G., Sporer, H., Zanzinger, H. and Gartung, E. (2001), 'Self-healing properties of geosynthetic clay liners', *Geosynthetics International* **8**(5), 461–470.

Slatter, E. E., Jungnickel, C. A., Smith, D. W. and Allman, M. A. (2000), Investigation of suction generation in apparatus employing osmotic methods, *in* Toll and Leong, eds, 'Unsaturated Soils for Asia', Balkema, pp. 297–302.

Smith, E. A., Prues, S. L. and Oehme, F. W. (1997), 'Environmental degradation of polyacrylamides', *Ecotoxicology and environmental safety* **37**(1), 76–91.

Sochi, T. (2010), 'Non-newtonian flow in porous media', *Polymer* **51**(22), 5007 – 5023.

Sorbie, K. S. (1991), *Polymer-improved oil recovery*, Springer Science & Business Media.

Sridharan, A. and Jayadeva, M. S. (1982), 'Double layer theory and compressibility of clays', *Géotechnique* **32**(2), 133–144.

Sridharan, A. and Prakash, K. (1998), 'Mechanism controlling the shrinkage limit of soils', *Geotechnical Testing Journal* **21**(3), 240–250.

Steudel, A., Friedrich, F., Boháč, P., Lieske, W., Baille, W., König, D., Schuhmann, R. and Emmerich, K. (2020), 'Equimolar cation exchange of polyacrylamide in smectite', *Applied Clay Science* **188**, 105501.

Steuter, A. A., Mozafar, A. and Goodin, J. R. (1981), 'Water potential of aqueous polyethylene glycols', *Plant Physiology* **67**(1), 64–67.

Stutzmann, T. and Siffert, B. (1977), 'Contribution to the adsorption mechanism of acetamide and polyacrylamide on to clays', *Clays and Clay Minerals* **25**(6), 392–406.

Suter, J., Coveney, P., Anderson, R., Greenwell, H. and Cliffe, S. (2011), 'Rule based design of clay-swelling inhibitors', *Energy & Environmental Science* **4**(11), 4572–4586.

Szilagyi, I., Trefalt, G., Tiraferri, A., Maroni, P. and Borkovec, M. (2014), 'Polyelectrolyte adsorption, interparticle forces, and colloidal aggregation', *Soft Matter* **10**(15), 2479–2502.

Takeno, H. and Nakamura, A. (2019), 'Effects of molecular mass of polymer on mechanical properties of clay/poly (ethylene oxide) blend hydrogels, and comparison between them and clay/sodium polyacrylate blend hydrogels', *Colloid and Polymer Science* **297**, 641–649.

Tanaka, F. (2011), *Polymer Physics: Applications to Molecular Association and Thermoreversible Gelation*, Cambridge University Press.

Tang, C., Shi, B., Liu, C., Zhao, L. and Wang, B. (2008), 'Influencing factors of geometrical structure of surface shrinkage cracks in clayey soils', *Engineering Geology* **101**(3), 204 – 217.

Teraoka, I. (2002), *Polymer solutions - An Introduction to Physical Properties*, Vol. 3, Wiley.

Theng, B. K. G. (2012), *Formation and properties of clay-polymer complexes*, Elsevier.

Thomareisa, A. S. and Chatziantoniou, S. (2011), 'Evaluation of the consistency of low-fat mayonnaise by squeezing flow viscometry', *Procedia Food Science* **1**, 1997–2002. 11th International Congress on Engineering and Food (ICEF11).

Thyagaraj, T. and Julina, M. (2019), 'Effect of pore fluid and wet-dry cycles on structure and hydraulic conductivity of clay', *Géotechnique Letters* **9**(4), 1–7.

Thyagaraj, T. and Salini, U. (2015), 'Effect of pore fluid osmotic suction on matric and total suctions of compacted clay', *Géotechnique* **65**(11), 952–960.

Tian, K., Benson, C. H. and Likos, W. J. (2016), 'Hydraulic conductivity of geosynthetic clay liners to low-level radioactive waste leachate', *Journal of Geotechnical and Geoenvironmental Engineering* **142**(8), 04016037.

Tian, K., Likos, W. J. and Benson, C. H. (2019), 'Polymer elution and hydraulic conductivity of bentonite–polymer composite geosynthetic clay liners', *Journal of Geotechnical and Geoenvironmental Engineering* **145**(10), 04019071.

Tiwari, B. and Ajmera, B. (2012), 'New correlation equations for compression index of remolded clays', *Journal of Geotechnical and Geoenvironmental Engineering* **138**(6), 757–762.

Tripathy, S. and Rees, S. W. (2013), 'Suction of some polyethylene glycols commonly used for unsaturated soil testing', *Geotechnical Testing Journal* **36**(5), 768–780.

Tripathy, S. and Schanz, T. (2007), 'Compressibility behaviour of clays at large pressures', *Canadian Geotechnical Journal* **44**(3), 355–362.

Tripathy, S., Sridharan, A. and Schanz, T. (2004), 'Swelling pressures of compacted bentonites from diffuse double layer theory', *Canadian Geotechnical Journal* **41**(3), 437–450.

Tripathy, S., Tadza, M. Y. M. and Thomas, H. R. (2011), 'On the intrusion of polyethylene glycol during osmotic tests', *Géotech. Lett.* **1**(3), 47–51.

Tripathy, S., Tadza, Y. M. and Thomas, H. R. (2014), 'Soil-water characteristic curves of clays', *Canadian Geotechnical Journal* **51**(8), 869–883.

Ueda, T. and Harada, S. (1968), 'Adsorption of cationic polysulfone on bentonite', *Journal of Applied Polymer Science* **12**(11), 2395–2401.

van Olphen, H. (1977), *An introduction to clay colloid chemistry, for clay technologists, geologists, and soil scientists.*, Wiley.

Verst, R., Lieske, W., Baille, W., Pulsfort, M. and Wichtmann, T. (2022), 'On the applicability of viscosity-based capillary bundle concepts to predict the penetration behaviour of polymer solutions into sand', *Acta Geotechnica* **17**, 497–510.

von Blumenthal, A., Lieske, W., König, D. and Wichtmann, T. (2021), 'Quantification of the bentonite content in diaphragm wall filter cakes based on a related cation exchange capacity value', *Geotechnical Testing Journal* **44**(6).

Ward, T. C. (1981), 'Molecular weight and molecular weight distributions in synthetic polymers', *Journal of Chemical Education* **58**(11), p 867.

Weber, C., Heuser, M. and Stanjek, H. (2014), 'A collection of aspect ratios of common clay minerals determined from conductometric titrations', *Clay Minerals* **49**(3), 495–498.

Wijaya, M., Leong, E. and Rahardjo, H. (2015), 'Effect of shrinkage on air-entry value of soils', *Soils and Foundations* **55**(1), 166 – 180.

Wilkinson, N., Metaxas, A., Brichetto, E., Wickramaratne, S., Reineke, T. M. and Dutcher, C. S. (2017), 'Ionic strength dependence of aggregate size and morphology on polymer-clay flocculation', *Colloids and Surfaces A: Physicochemical and Engineering Aspects* **529**, 1037–1046.

Wilkinson, N., Metaxas, A., Quinney, C., Wickramaratne, S., Reineke, T. M. and Dutcher, C. S. (2018), 'ph dependence of bentonite aggregate size and morphology on polymer-clay flocculation', *Colloids and Surfaces A: Physicochemical and Engineering Aspects* **537**, 281–286.

Williams, J. and Shaykewich, C. (1969), 'An evaluation of polyethylene glycol (P.E.G.) 6000 and P.E.G. 20 000 in the osmotic control of soil water matric potential', *Canadian Journal of Soil Science* **49**, 397–401.

Xie, G., Luo, P., Deng, M., Su, J., Wang, Z., Gong, R., Xie, J., Deng, S. and Duan, Q. (2017), 'Investigation of the inhibition mechanism of the number of primary amine groups of alkylamines on the swelling of bentonite', *Applied Clay Science* **136**, 43–50.

Yong, R. N. and Mourato, D. (1990), 'Influence of polysaccharides on kaolinite structure and properties in la kaolinite–water system', *Canadian Geotechnical Journal* **27**(6), 774–788.

Yu, J., Zakin, J. and Patterson, G. (1979), 'Mechanical degradation of high molecular weight polymers in dilute solution', *Journal of Applied Polymer Science* **23**(8), 2493–2512.

Zeh, R. M. and Witt, K. J. (2007), The tensile strength of compacted clays as affected by suction and soil structure, *in* T. Schanz, ed., 'Experimental Unsaturated Soil Mechanics', Springer Berlin Heidelberg, Berlin, Heidelberg, pp. 219–226.

Zhang, R.-J., Zheng, Y.-l., Zheng, J.-J., Dong, C.-q. and Lu, Z. (2020), 'Flocculation–solidification combined method for treatment of hydraulically dredged mud at extra high water content', *Acta Geotechnica* **15**, 1685–1698.

Zumsteg, R., Plötze, M. and Puzrin, A. (2014), Reduction of the clogging potential of clays: new chemical applications and novel quantification approaches, *in* 'Bio-and Chemo-Mechanical Processes in Geotechnical Engineering: Géotechnique Symposium in Print 2013', ICE Publishing, pp. 44–54.

Zumsteg, R., Plötze, M. and Puzrin, A. M. (2013), 'Effects of dispersing foams and polymers on the mechanical behaviour of clay pastes', *Géotechnique* **63**(11), 920–933.

Zur (1966), 'Osmotic control of soil water matric potential', *Soil Science* **102**(6), 394 –398.

Schriftenreihe des Instituts für Grundbau, Wasserwesen und Verkehrswesen der Ruhr-Universität Bochum

Herausgeber: H.L. Jessberger

1 (1979) **Hans Ludwig Jessberger**
Grundbau und Bodenmechanik an der Ruhr-Universität Bochum

2 (1978) **Joachim Klein**
Nichtlineares Kriechen von künstlich gefrorenem Emschermergel

3 (1979) **Heinz-Joachim Gödecke**
Die Dynamische Intensivverdichtung wenig wasserdurchlässiger Böden

4 (1979) **Poul V. Lade**
Three Dimensional Stress-Strain Behaviour and Modeling of Soils

5 (1979) **Roland Pusch**
Creep of soils

6 (1979) **Norbert Diekmann**
Zeitabhängiges, nichtlineares Spannungs-Verformungsverhalten von gefrorenem Schluff unter triaxialer Belastung

7 (1979) **Rudolf Dörr**
Zeitabhängiges Setzungsverhalten von Gründungen in Schnee, Firn und Eis der Antarktis am Beispiel der deutschen Georg-von-Neumayer- und Filchner-Station

8 (1984) **Ulrich Güttler**
Beurteilung des Steifigkeits- und Nachverdichtungsverhaltens von ungebundenen Mineralstoffen

9 (1986) **Peter Jordan**
Einfluss der Belastungsfrequenz und der partiellen Entwässerungs-möglichkeiten auf die Verflüssigung von Feinsand

10 (1986) **Eugen Makowski**
Modellierung der künstlichen Bodenvereisung im grundwasserdurchströmten Untergrund mit der Methode der finiten Elemente

11 (1986) **Reinhard A. Beine**
Verdichtungswirkung der Fallmasse auf Lastausbreitung in nichtbindigem Boden bei der Dynamischen Intensivverdichtung

12 (1986) **Wolfgang Ebel**
Einfluss des Spannungspfades auf das Spannungs-Verformungsverhalten von gefrorenem Schluff im Hinblick auf die Berechnung von Gefrierschächten

13 (1987) **Uwe Stoffers**
Berechnungen und Zentrifugen-Modellversuche zur Verformungsabhängigkeit der Ausbaubeanspruchung von Tunnelausbauten in Lockergestein

14 (1988) **Gerhard Thiel**
Steifigkeit und Dämpfung von wassergesättigtem Feinsand unter Erdbebenbelastung

15 (1991) **Mahmud Thaher**
Tragverhalten von Pfahl-Platten-Gründungen im bindigen Baugrund,
Berechnungsmodelle und Zentrifugen-Modellversuche

Schriftenreihe des Instituts für Grundbau der Ruhr-Universität Bochum

Herausgeber: H.L. Jessberger

16 (1992) **Rainer Scherbeck**

Geotechnisches Verhalten mineralischer Deponieabdichtungsschichten
bei ungleichförmiger Verformungswirkung

17 (1992) **Martin M. Bizialiele**
Torsional Cyclic Loading Response of a Single Pile in Sand

18 (1993) **Michael Kotthaus**
Zum Tragverhalten von horizontal belasteten Pfahlreihen aus langen Pfählen in Sand

19 (1993) **Ulrich Mann**
Stofftransport durch mineralische Deponieabdichtungen:
Versuchsmethodik und Berechnungsverfahren

20 (1992) **Festschrift anlässlich des 60. Geburtstages von**
Prof. Dr.-Ing. H. L. Jessberger
20 Jahre Grundbau und Bodenmechanik an der Ruhr-Universität Bochum

21 (1993) **Stephan Demmert**
Analyse des Emissionsverhaltens einer Kombinationsabdichtung im Rahmen der
Risikobetrachtung von Abfalldeponien

22 (1994) **Diethard König**
Beanspruchung von Tunnel- und Schachtausbauten in kohäsionslosem Lockergestein
unter Berücksichtigung der Verformung im Boden

23 (1995) **Thomas Neteler**
Bewertungsmodell für die nutzungsbezogene Auswahl von Verfahren zur Altlastensanierung

24 (1995) **Ralph Kockel**
Scherfestigkeit von Mischabfall im Hinblick auf die Standsicherheit von Deponien

25 (1996) **Jan Laue**
Zur Setzung von Flachfundamenten auf Sand unter wiederholten Lastereignissen

26 (1996) **Gunnar Heibrock**
Zur Rissbildung durch Austrocknung in mineralischen Abdichtungsschichten
an der Basis von Deponien

27 (1996) **Thomas Siemer**
Zentrifugen-Modellversuche zur dynamischen Wechselwirkung zwischen Bauwerken
und Baugrund infolge stoßartiger Belastung

28 (1996) **Viswanadham V. S. Bhamidipati**
Geosynthetic Reinforced Mineral Sealing Layers of Landfills

29 (1997) **Frank Trappmann**
Abschätzung von technischem Risiko und Energiebedarf bei Sanierungsmaßnahmen für Altlasten

30 (1997) **André Schürmann**
Zum Erddruck auf unverankerte flexible Verbauwände

31 (1997) **Jessberger, H. L. (Herausgeber)**
Environment Geotechnics, Report of ISSMGE Technical Committee TC 5 on Environmental Geotechnics

Schriftenreihe des Institutes für Grundbau und Bodenmechanik der Ruhr-Universität Bochum

Herausgeber: Th. Triantafyllidis

32 (2000) **Triantafyllidis, Th. (Herausgeber)**
Boden unter fast zyklischer Belastung: Erfahrung und Forschungsergebnisse (Workshop)

33 (2002) **Christof Gehle**
Bruch- und Scherverhalten von Gesteinstrennflächen mit dazwischenliegenden Materialbrücken

34 (2003) **Andrzej Niemunis**
Extended hypoplastic models for soils

35 (2004) **Christiane Hof**
Über das Verpressankertragverhalten unter kalklösendem Kohlensäureangriff

36 (2004) **René Schäfer**
Einfluss der Herstellungsmethode auf das Verformungsverhalten von Schlitzwänden in weichen bindigen Böden

37 (2005) **Henning Wolf**
Zur Scherfugenbänderung granularer Materialien unter Extensionsbeanspruchung

38 (2005) **Torsten Wichtmann**
Explicit accumulation model for non-cohesive soils under cyclic loading

39 (2008) **Christoph M. Loreck**
Die Entwicklung des Frischbetondruckes bei der Herstellung von Schlitzwänden

40 (2008) **Igor Arsic**
Über die Bettung von Rohrleitungen in Flüssigböden

41 (2009) **Anna Arwanitaki**
Über das Kontaktverhalten zwischen einer Zweiphasenschlitzwand und nichtbindigen Böden

Schriftenreihe des Lehrstuhls für Grundbau, Boden- und Felsmechanik der Ruhr-Universität Bochum

Herausgeber: T. Schanz

42 (2009) **Yvonne Lins**
Hydro-Mechanical Properties of Partially Saturated Sand

43 (2010) **Tom Schanz (Herausgeber)**
Geotechnische Herausforderungen beim Umbau des Emscher-Systems,
Beiträge zum RuhrGeo Tag 2010

44 (2010) **Jamal Alabdullah**
Testing Unsaturated Soil for Plane Strain Conditions: A New Double-Wall Biaxial Device

45 (2011) **Lars Röchter**
Systeme paralleler Scherbänder unter Extension im ebenen Verformungszustand

46 (2011) **Yasir Al-Badran**
Volumetric Yielding Behavior of Unsaturated Fine-Grained Soils

47 (2011) **Usque ad finem**
Selected research papers

48 (2012) **Muhammad Ibrar Khan**
Hydraulic Conductivity of Moderate and Highly Dense Expansive Clays

49 (2014) **Long Nguyen-Tuan**
Coupled Thermo-Hydro-Mechanical Analysis: Experimental and Back Analysis

50 (2014) **Tom Schanz (Herausgeber)**
Ende des Steinkohlenbergbaus im Ruhrrevier: Realität und Perspektiven für die Geotechnik, Beiträge zum RuhrGeo Tag 2014

51 (2014) **Usque ad finem**
Selected research papers

52 (2014) **Houman Soleimani Fard**
Study on the Hydro-Mechanical Behaviour of Fiber Reinforced Fine Grained Soils with Application to the Preservation of Historical Monuments

53 (2014) **Wiebke Baille**
Hydro-Mechanical Behavior of Clays - Significance of Mineralogy

54 (2014) **Qasim Abdulkarem Jassim Al-Obaidi**
Hydro-Mechanical Behavior of Collapsible Soils

55 (2015) **Veselin Zarev**
Model Identification for the Adaption of Numerical Simulation Models - Application to Mechanized Shield Tunneling

56 (2015) **Meisam Goudarzy**
Micro and Macro Mechanical Assessment of Small and Intermediate Strain Properties of Granular Material

57 (2016) **Oliver Detert**
Analyse einer selbstregulierenden interaktiven Membrangründung für Schüttkörper auf geringtragfähigen Böden

58 (2016) **Yang Yang**
Analyses of Heat Transfer and Temperature-induced Behaviour in Geotechnics

59 (2016) **Alborz Pourzargar**
Application of suction stress concept to partially saturated compacted soils

60 (2017) **Hanna Haase**
Multiscale analysis of clay-polymer composites for Geoenvironmental applications

61 (2017) **Kavan Khaledi**
Constitutive modeling of rock salt with application to energy storage caverns

62 (2017) **Nina Silvia Müthing**
On the consolidation behavior of fine-grained soils under cyclic loading

63 (2017) **Elham Mahmoudi**
Probabilistic analysis of a rock salt cavern with application to energy storage systems

64 (2017) **Negar Rahemi**
Evaluation of liquefaction behavior of sandy soils using critical state soil mechanics and instability concept

65 (2018) **Chenyang Zhao**
A contribution to modeling of mechanized tunnel excavation

66 (2018) **Tom Schanz (Herausgeber)**
Innovationen im Spezialtiefbau und in der Umweltgeotechnik,
Beiträge zum RuhrGeo Tag 2018

67 (2019) **Linzhi Lang**
Hydro-Mechanical Behaviour of Bentonite-Based Materials Used for
Disposal of Radioactive Wastes

68 (2019) **Usama Al-Anbaki**
Hydraulic Interaction of Soil and Nonwoven Geotextiles under Unsaturated Conditions

69 (2019) **Abhishek Rawat**
Coupled Hydro-mechanical Behavior of a Compacted Bentonite-Sand Mixture: Experimental and Numerical Investigations

Schriftenreihe des Lehrstuhls für Bodenmechanik, Grundbau und Umweltgeotechnik der Ruhr-Universität Bochum

Herausgeber: T. Wichtmann

70 (2019) **Mahmoud Qarmout**
Tunnel face stability using Kinematical Element Method (KEM)

71 (2021) **Raoul Hölter**
Optimal Experimental Design in Geotechnical Engineering

72 (2022) **Wolfgang Lieske**
Impact of polymer constitution on the hydro-mechanical behaviour of modified bentonite